

CHARACTERIZATION OF ARCHAEOLOGICALLY
SIGNIFICANT OBSIDIAN SOURCES IN OREGON
BY NEUTRON ACTIVATION ANALYSIS

A Thesis
presented to
the Faculty of the Graduate School
University of Missouri-Columbia

In Partial Fulfillment
of the Requirements for the Degree
Master of Science

by
JESSICA ANN AMBROZ

Dr. Michael Glascock, Thesis Supervisor

DECEMBER 1997

© copyright by Jessica A. Ambroz 1997
All Rights Reserved

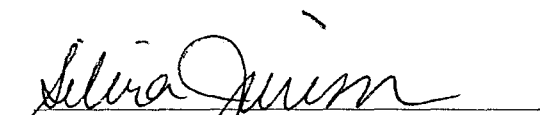
The undersigned, appointed by the Dean of the Graduate School, have examined the thesis entitled

CHARACTERIZATION OF ARCHAEOLOGICALLY
SIGNIFICANT OBSIDIAN SOURCES IN OREGON

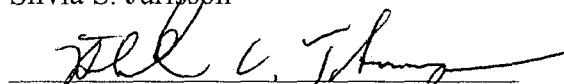
presented by Jessica Ann Ambroz

a candidate for the degree of Master of Science

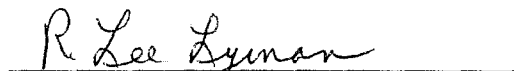
and hereby certify that in their opinion it is worthy of acceptance.




Silvia S. Jurisson



Richard C. Thompson



R. Lee Lyman



Michael D. Glascock



Hector Neff

ACKNOWLEDGEMENTS

First and foremost I would like to thank the University of Missouri Chemistry Department for allowing me to undertake this interdisciplinary project. Without their approval this thesis would never even have been started.

Secondly, I would like to thank Dr. Michael D. Glascock, my principle advisor, and Dr. Hector Neff for inviting me to join the Archaeometry Group at the Missouri University Research Reactor and for finding such an interesting project for me to work on. Both of them were always there to answer my many questions and always willing to help me out. Mike and Hector also donated considerable editorial time once the writing began. Others in the Archaeometry Group were also helpful by assisting in the hundreds of sample irradiations, especially Julie Farnum and Danielle Parks.

The Missouri University Research Reactor provided reactor and p-tube time as well as a place to perform all the sample preparation. Support for the graduate student was provided by the NSF (grant SBR 9503035) as was funding for sample collection, irradiation, and analysis.

A special thank you to Craig Skinner who not only provided many samples but was a wonderful guide to the back-roads of Oregon during my sample collection trip. He helped locate obscure references as well as providing editorial assistance. It couldn't have been done without him!

John Zancanella contributed the artifacts from the Robins Spring site and kindly allowed me to take a small piece for analysis.

Others I should thank, but in no particular order.... Stephen Stanton, the geology librarian: I never would have survived GeoRef without him. My parents and my sisters, especially my mom, because they refused to let me quit. Julie, Danielle, Jessica, Rachel, and Maria: they provided much relief from insanity in an insane world. And finally, most of all, John, Elvira, and Chicken Little: they always knew how to make me feel better.

ABSTRACT

Six hundred sixty-two obsidian samples from sources in Oregon were characterized by instrumental neutron activation analysis (INAA) in order to establish the number of geochemical groups present. Neutron irradiations were performed at the Missouri University Research Reactor (MURR) and gamma-ray spectra were measured with high-purity germanium (HPGe) detectors to determine absolute concentrations for 27 elements.

Thirty-six different geochemical groups were formed. Four groups were found in the Malheur National Forest area of Grant County. Six groups were found in Harney County, three of them near the town of Burns. Three correlated groups, part of an extensive ash-flow tuff, were found in the Ochoco National Forest area of Harney County. Seven groups were found at Glass Buttes, Lake County where x-ray fluorescence (XRF) showed only six groups. Nine groups were found in Lake County. Four groups were found in Newberry Caldera. Previously, based on XRF, it was thought that only two groups existed. A single chemical group was identified in Klamath County. Two chemical groups were found in Lane County.

Most of the above chemical groups were successfully separated using an abbreviated-INAA procedure (only the elements Na, Mn, and Ba). Only in the Ochoco National Forest was the procedure unsuccessful.

Use of the database on an archaeological problem was demonstrated by analyzing thirty-one artifacts from the Robins Spring site, on Glass Buttes, by the procedures in this study. The results indicate the artifacts were made from several of the obsidian sources on Glass Buttes as well as Yreka Butte, a source near Glass Buttes.

LIST OF TABLES

Table	Page
1.1 Age Progression Across Harney Basin	11
3.1 Oregon Obsidian Sources and Their Locations	58
3.2 Nuclear Parameters Used in Analysis	67
3.3 Elemental Concentrations of Standards	68
4.1 Statistics for Whitewater Ridge Obsidian	75
4.2 Statistics for Wolf Creek Obsidian	76
4.3 Statistics for Parish Cabin Campground A Obsidian	77
4.4 Statistics for Parish Cabin Campground B Obsidian	78
4.5 Statistics for Burns Area Obsidian	89
4.6 Statistics for Burns-Rimrock Obsidian	90
4.7 Statistics for Dog Hill Obsidian	91
4.8 Statistics for Riley Obsidian	92
4.9 Statistics for Chickahominy Reservoir Obsidian	93
4.10 Statistics for Venator Obsidian	94
4.11 Statistics for Buck Springs Obsidian	107
4.12 Statistics for Delintment Lake A Obsidian	108
4.13 Statistics for Delintment Lake B Obsidian	109
4.14 Statistics for Glass Buttes A Obsidian	123
4.15 Statistics for Glass Buttes B Obsidian	124

4.16	Statistics for Glass Buttes C Obsidian	125
4.17	Statistics for Glass Buttes D Obsidian	126
4.18	Statistics for Glass Buttes E Obsidian	127
4.19	Statistics for Glass Buttes F Obsidian	128
4.20	Statistics for Glass Buttes G Obsidian	129
4.21	Statistics for Yreka Butte Obsidian	139
4.22	Statistics for Brooks Canyon Obsidian	140
4.23	Statistics for Quartz Mountain Obsidian	141
4.24	Statistics for Cougar Mountain Obsidian	142
4.25	Statistics for Horse Mountain Obsidian	143
4.26	Statistics for Silver Lake Obsidian	144
4.27	Statistics for Hager Mountain Obsidian	145
4.28	Statistics for Tucker Hill Obsidian	146
4.29	Statistics for Surveyor Spring Obsidian	147
4.30	Statistics for Big Obsidian Flow Obsidian	157
4.31	Statistics for Buried Obsidian Flow Obsidian	158
4.32	Statistics for East Lake Obsidian Flows Obsidian	159
4.33	Statistics for Game Hut Obsidian Flow Obsidian	160
4.34	Statistics for Deer Creek Obsidian	168
4.35	Statistics for Inman Creek A Obsidian	169
4.36	Statistics for Inman Creek B Obsidian	170

5.1	Posterior Classification Matrix of Regional Groups Using Long Elements	176
5.1	Posterior Classification Matrix of Regional Groups Using Short Elements	179

LIST OF FIGURES

Figure	Page
1.1 Geologic Time Chart	3
1.2 Map of Physiographic Provinces in Oregon	4
1.3 Map of Miocene and Older Cenozoic Ash-flow Tuffs in Oregon	6
1.4 Map of Early and Middle Pliocene Ash-flow Tuffs in Oregon	8
1.5 Map of Late Pliocene, Pleistocene, and Holocene Ash-flow Tuffs in Oregon	9
1.6 Map of Physiographic Provinces of Oregon Showing Brothers Fault Zone and Isochrons of Age Progression	10
2.1 Obsidian Zones in Domes and Flows	19
2.2 World Map Showing Distribution of Obsidian	24
2.3 Depiction of the Structure of Glass	27
2.4 Depiction of Aluminum Bonding in Glass	29
2.5 Chemical Classification of Volcanic Rocks	31
3.1 Activation of a Nucleus by a Neutron	52
3.2 Neutron Energy vs Neutron Flux	53
3.3 Gamma Spectrum from Short Count	63
3.4 Gamma Spectrum from Middle Count	65
3.5 Gamma Spectrum from Long Count	66
4.1a Map of Grant County, Oregon	73
4.1b Map of Obsidian Collection Areas in the Malheur National Forest	74

4.2a	Th vs. Eu for Obsidian from the Malheur National Forest	79
4.2b	Eu vs. Rb for Obsidian from the Malheur National Forest	79
4.3a	Th vs. Eu for Obsidian from the Malheur National Forest showing possible linear trend through samples	82
4.3b	Fe vs. Rb for Obsidian from the Malheur National Forest showing possible linear trend through samples	83
4.3c	Hf vs. Rb for Obsidian from the Malheur National Forest showing lack of a linear trend through samples	83
4.4a	Mn vs. Na for Obsidian from the Malheur National Forest	84
4.4b	Ba vs. Mn for Obsidian from the Malheur National Forest	84
4.5a	Map of Harney County, Oregon	86
4.5b	Map of Obsidian Collection Areas Around Burns, Oregon	87
4.6a	Hf vs. Eu for Obsidian from Harney County	95
4.6b	Fe vs. Cs for Obsidian from Harney County	95
4.7	Plot Showing Obsidian Samples from Burns-Willow Flat Projected Against Ellipses from the Ochoco National Forest	97
4.8a	Mn vs. Na for Obsidian from Harney County	98
4.8a	Ba vs. Mn for Obsidian from Harney County	98
4.9	Diagram Showing Zones of an Ash-flow Tuff	101
4.10	Isopach Map Showing Distribution of Rattlesnake Formation	103
4.11a	Map of Harney County, Oregon	105
4.11b	Map of Obsidian Collection Sites in the Ochoco National Forest	106
4.12a	Th vs. Cs for Obsidian from the Ochoco National Forest	111

4.12b	Hf vs. Rb for Obsidian from the Ochoco National Forest	111
4.13a	Fe vs. Ta for Obsidian from the Ochoco National Forest Showing Possible Linearity	112
4.13b	Fe vs. Zr for Obsidian from the Ochoco National Forest Showing Possible Linearity	112
4.13c	Fe vs. Lu for Obsidian from the Ochoco National Forest Showing Possible Linearity	113
4.13d	Fe vs. Eu for Obsidian from the Ochoco National Forest Showing Possible Linearity	113
4.14a	Mn vs. Na for Obsidian from the Ochoco National Forest	115
4.14b	Ba vs. Mn for Obsidian from the Ochoco National Forest	115
4.15	Map of Lake County, Oregon	118
4.16a	Cs vs. Eu for Obsidian from Glass Buttes	121
4.16b	Rb vs. Th for Obsidian from Glass Buttes	121
4.17	Map Showing Obsidian Collection Sites Around Glass Buttes	122
4.18	Sr vs. Rb for Obsidian from Glass Buttes from XRF Data	130
4.19a	Mn vs. Na for Obsidian from Glass Buttes	133
4.19b	Ba vs. Na for Obsidian from Glass Buttes	133
4.20	Map of Lake County, Oregon	136
4.21a	Eu vs. Rb for Obsidian from Lake County	148
4.21b	Cs vs. Fe for Obsidian from Lake County	148
4.22a	Mn vs. Na for Obsidian from Lake County	149
4.22b	Ba vs. Mn for Obsidian from Lake County	149

4.23	Map of Deschutes County, Oregon	151
4.24	Map of Newberry Caldera	152
4.25a	Cs vs. Fe for Obsidian from Newberry Caldera	161
4.25b	Rb vs. Fe for Obsidian from Newberry Caldera	161
4.26	Mn vs. Na for Obsidian from Newberry Caldera	163
4.27	Map of Klamath County, Oregon	165
4.28	Map of Lane County, Oregon	166
4.29a	Hf vs. Fe for Obsidian from Klamath and Lane Counties	171
4.29b	Ce vs. Cs for Obsidian from Klamath and Lane Counties	171
4.30	Mn vs. Na for Obsidian from Klamath and Lane Counties	172
5.1	Cs vs. Hf Showing Separation of All Obsidian Chemical Groups Analyzed in this Study Using Long Elements	177
5.2	Cs vs. Sc Showing Separation of All Obsidian Chemical Groups Analyzed in this Study Using Long Elements	178
5.3	Mn vs. Na Showing Separation of All Obsidian Chemical Groups Analyzed in this Study Using Short Elements	181
5.4	Ba vs. Mn Showing Separation of All Obsidian Chemical Groups Analyzed in this Study Using Short Elements	182
5.5	Cs vs. Eu Showing Projection of Obsidian Artifacts from the Robins Spring Site Against Ellipses from Glass Buttes	184
5.6	Mn vs. Na Showing Projection of Obsidian Artifacts from the Robins Spring Site Against Ellipses from Glass Buttes	186

TABLE OF CONTENTS

ACKNOWLEDGMENTS	ii
ABSTRACT	iii
LIST OF TABLES	iv
LIST OF FIGURES	vii
Chapter	
1. INTRODUCTION	1
Geological History of Oregon	2
Previous Work in Oregon	12
Research Goals	13
2. BACKGROUND	15
Formation and Emplacement	17
Primary vs. Secondary Deposits	20
Location of Obsidian	21
Geological Environment	21
Geographical Environment	22
Characteristics of Obsidian	23
Chemistry of Obsidian	23
Obsidian as Glass	25
Properties of Obsidian	33
Hydration of Obsidian	35

Previous Methods Used to Examine Obsidian	38
Physical Methods	38
Spectrographic Methods	40
X-ray Fluorescence	43
Neutron Activation Analysis	47
3. MATERIALS AND METHODS	51
Laboratory Methods Employed at MURR	57
4. RESULTS AND DISCUSSION	69
Malheur National Forest	72
Introduction	72
Results and Discussion	72
Harney County	85
Introduction	85
Results and Discussion	88
Ochoco National Forest	100
Introduction	100
Results and Discussion	104
Glass Buttes	117
Introduction	117
Results and Discussion	120
Lake County	135
Introduction	135

Results and Discussion	138
Newberry Volcano	150
Introduction	150
Results and Discussion	155
Miscellaneous	164
Introduction	164
Results and Discussion	167
5. APPLICATIONS	173
An Artifactual Case Study	183
Introduction	183
Results and Discussion	183
6. CONCLUSIONS	187
BIBLIOGRAPHY	190

CHAPTER 1 INTRODUCTION

Obsidian is a volcanic glass. A small proportion forms when highly viscous lava erupts and is cooled rapidly against water, air or colder rock (Bouska *et al.*, 1993; Hughes and Smith, 1993). Thick flows of obsidian form when a siliceous lava is cooled below its crystallization temperature as it rises. The lava lacks the energy to move atoms into an orderly pattern (i.e., a crystalline solid) and it becomes a supercooled liquid, i.e., glass (Bakken, 1977).

Due to its glassy properties, obsidian was widely used by prehistoric peoples for several millennia to produce tools, jewelry, weapons and other objects such as bowls and mirrors. As Ericson *et al.* (1975; p. 129) have stated, “[p]rehistorically, obsidian, having the importance of modern steel, was much sought after and widely traded.” Today obsidian is sought out not only by people interested in flintknapping or jewelry making but also by archaeologists interested in investigating prehistoric human behavior.

Geologists, geochemists, and archaeologists are all interested in obsidian. Geologists and geochemists find obsidian interesting because its physical and chemical properties can be used to interpret igneous and metamorphic processes. Archaeologists find obsidian suitable for provenance studies because its unique physical and chemical properties permit the placement of artifacts in time and space (Hughes and Smith, 1993). Oregon is an ideal region for geochemists and archaeologists to study obsidian because its geologic processes generated huge amounts of volcanic activity, including the formation of large deposits of obsidian. These deposits of obsidian were erupted within larger, trending geologic areas and were exploited extensively for several thousand years

by the prehistoric people who lived in the region.

The main goal of this thesis is to establish a database of obsidian source analyses that can be used in the future by archaeologists seeking to understand prehistoric interaction in the Pacific Northwest. First, however, some geological background is necessary.

Geological History of Oregon

Throughout the geologic history of the Cenozoic Era (see Figure 1.1), the northwestern United States, especially Oregon, was dominated by significant amounts of volcanism. The limits and types of volcanism can be defined both spatially and temporally. There were four main physiographic provinces of Cenozoic volcanism: the Cascades, the Columbia Plateau, the Oregon Plateau, and the Snake River Plain (Figure 1.2). Although the geology of Oregon was influenced by three of these provinces, it was dominated by the Oregon Plateau. Oregon was thus covered by volumes of bimodal tholeiitic and alkalic basalt-rhyolitic volcanism. Both Hart and Carlson (1987) and Carlson and Hart (1987) provide excellent reviews of the geology of Oregon as outlined below.

The Oregon Plateau is the northernmost expression of the Basin and Range province. Its features include both north-northeast trending normal faults and a series of west-northwest trending right lateral strike-slip fault zones with tens of kilometers of offset caused by the generally east-west extension of the plateau. It is bordered on the west by Paleozoic to Mesozoic rocks of the northern Klamath Mountains and the Cenozoic calc-alkaline volcanic rocks of the Cascade chain. The northern border is defined by the Paleozoic to Mesozoic terrains of the Blue Mountains and the Olympic-

EON	ERA	PERIOD	EPOCH	APPROX. AGE (Ma)	
Phanerozoic	Cenozoic	Quaternary		Holocene	0.010 1.7 5 24 38 55 66
				Pleistocene	
		Tertiary	Neogene Subperiod	Pliocene	
				Miocene	
			Paleogene Subperiod	Oligocene	
				Eocene	
				Paleocene	
	Mesozoic	Cretaceous		Late	96 138 205 ~240
				Early	
		Jurassic		Late	
				Middle	
				Early	
				Late	
	Triassic		Middle	~240	
			Early		
	Paleozoic	Permian		Late	290
				Early	
		Carboniferous Periods	Pennsylvanian	Late	~330
				Middle	
			Mississippian	Early	
Late					
Devonian		Early	360		
		Late			
Silurian		Middle	410		
		Early			
Ordovician		Late	435		
		Middle			
Cambrian		Early	500		
		Late			
Proterozoic			Early	~570	
			Middle	900	
			Late	1600	
Archean			Late	2500	
			Middle	3000	
			Early	3400	
pre-Archean		(3800?)		4550	

Figure 1.1: Geologic time chart. (Adapted from Diggles et al., 1988)

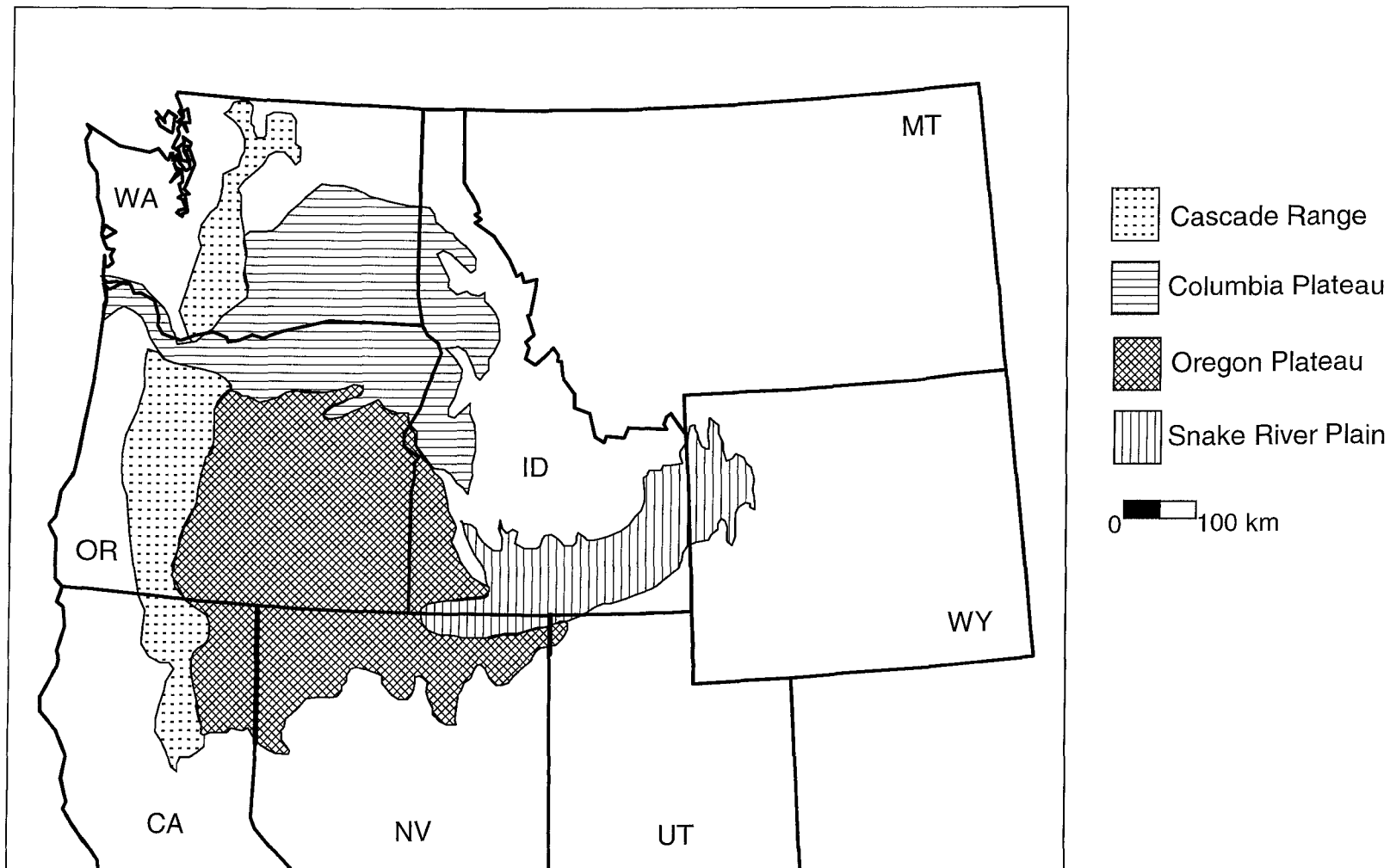


Figure 1.2: Extent of the four main physiographic provinces of the northwestern United States dominated by Cenozoic volcanism. (Adapted from Hart and Carlson, 1987)

Wallowa lineament and is covered by Columbia River basalts. The Orevada rift defines the southern boundary and the Oregon-Nevada lineament is the eastern boundary.

In the mid-Eocene to the early Miocene (50-20 million years ago), the volcanic evolution within the northwestern United States was fairly coherent between all the provinces. The oldest volcanism took place during the late Eocene to early Miocene and consisted of calc-alkalic and intermediate to silicic rocks. About 17-18 million years ago, voluminous eruptions of iron- and incompatible-element enriched basalts occurred. Basaltic eruptions peaked at approximately 15-17 million years ago, though some basaltic volcanism continued up to 11 million years ago. During the interval between 17 and 15 million years ago, bimodal basaltic and silicic volcanism began in the southeastern Oregon Plateau and continued into the Holocene. This was due to regional extension and/or a major crustal thermal disturbance. By about 10 million years ago, a major shift of tectonic and magmatic character caused the loci of the silicic eruptions to migrate west-northwest following the fault zones, specifically the Oregon-Nevada lineament. Eruption of incompatible-element poor, high-alumina olivine, normative tholeiitic (HAOT) basalts started about 10.5 million years ago. The last large modification of volcanism occurred about 2 million years ago when alkaline basalts erupted north of the Orevada rift zone.

A large amount of the silicic material that erupted in Oregon was in the form of hot, high-density suspensions of material in volcanic gas. Such deposits occurred over vast areas and are termed ash-flow tuff sheets (Walker, 1970). The ash-flow tuffs of the Eocene, Oligocene, and Miocene were of small to moderate volume, e.g., the Clarno and John Day Formations (Figure 1.3). Large volume ash-flow tuffs erupted in the early to

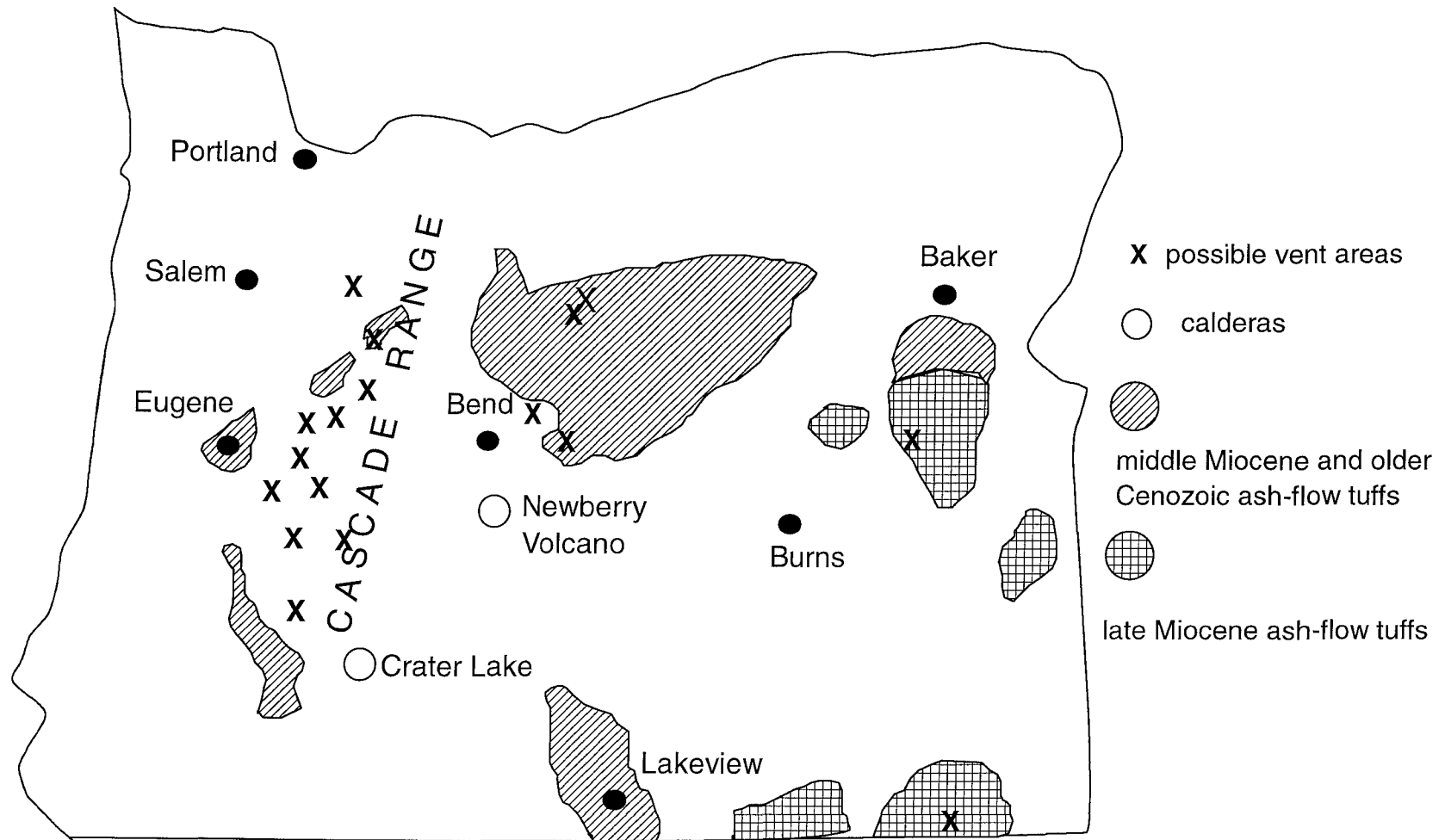


Figure 1.3: Approximate outcrop areas of Miocene and older Cenozoic ash-flow tuffs in Oregon. (Adapted from Walker, 1970)

middle Pliocene. These tuffs are exposed extensively in the Harney Basin and are thickest and most continuous in areas around Glass Buttes, especially three units exposed along Highway 395 near the town of Burns (Figure 1.4). The most recent ash flow tuffs erupted during the late Pliocene, the Pleistocene, and the Holocene. These tuffs were of relatively small volume and erupted near the Cascade Range, including those from Crater Lake and Newberry Volcano (Walker, 1970) [Figure 1.5].

The High Lava Plains, as defined by Dicken (1950), is a physiographic province within the Oregon Plateau. The High Lava Plains, extending from the Harney Basin to Newberry Volcano, constitutes a volcanic upland approximately 260 km long and several tens of kilometers wide (Walker, 1974). One of its principal features is the Brothers Fault Zone, a west-northwest trending zone of en echelon normal faults. Along this trend there is a progressive decrease in the age of silicic rocks from the Harney Basin to Newberry Volcano (Figure 1.6). The age decrease begins in the eastern Harney Basin at Duck Butte (Table 1.1).

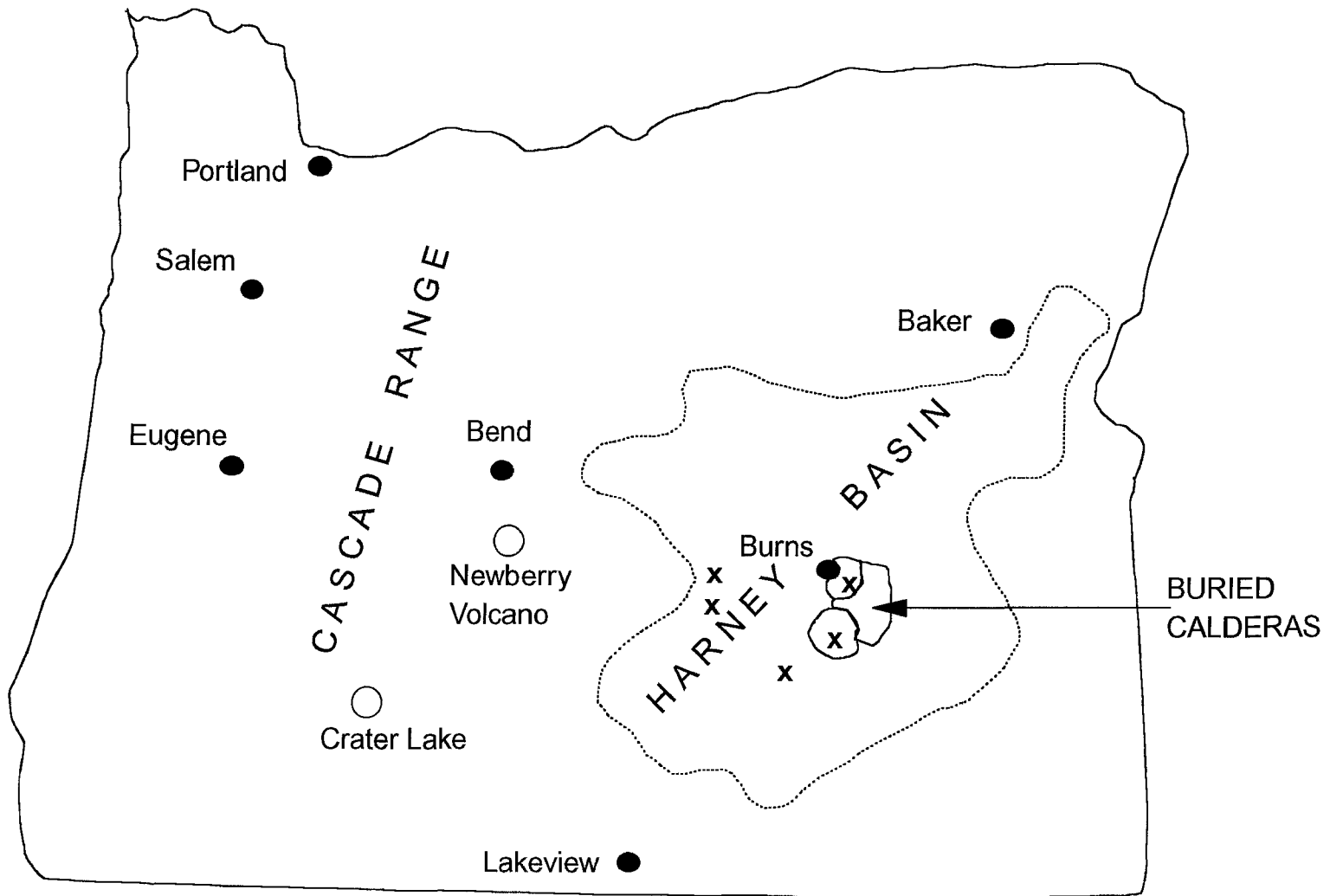


Figure 1.4: Approximate outcrop area of early and middle Pliocene ash-flow tuffs in Oregon. X's denote possible vent areas. (Adapted from Walker, 1970)

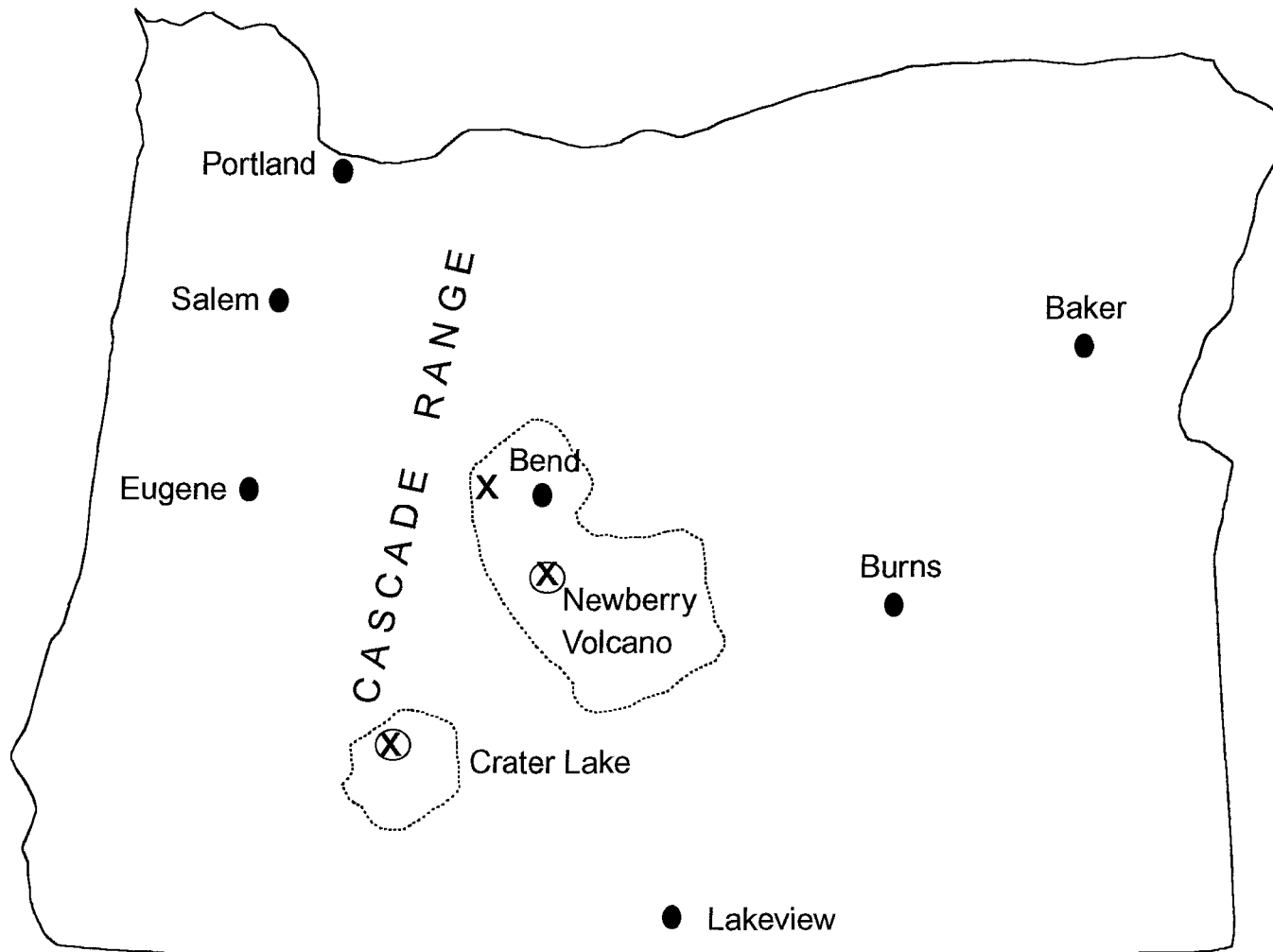


Figure 1.5: Approximate outcrop areas of late Pliocene, Pleistocene, and Holocene ash-flow tuffs in Oregon. X's denote vent areas. (Adapted from Walker, 1970)

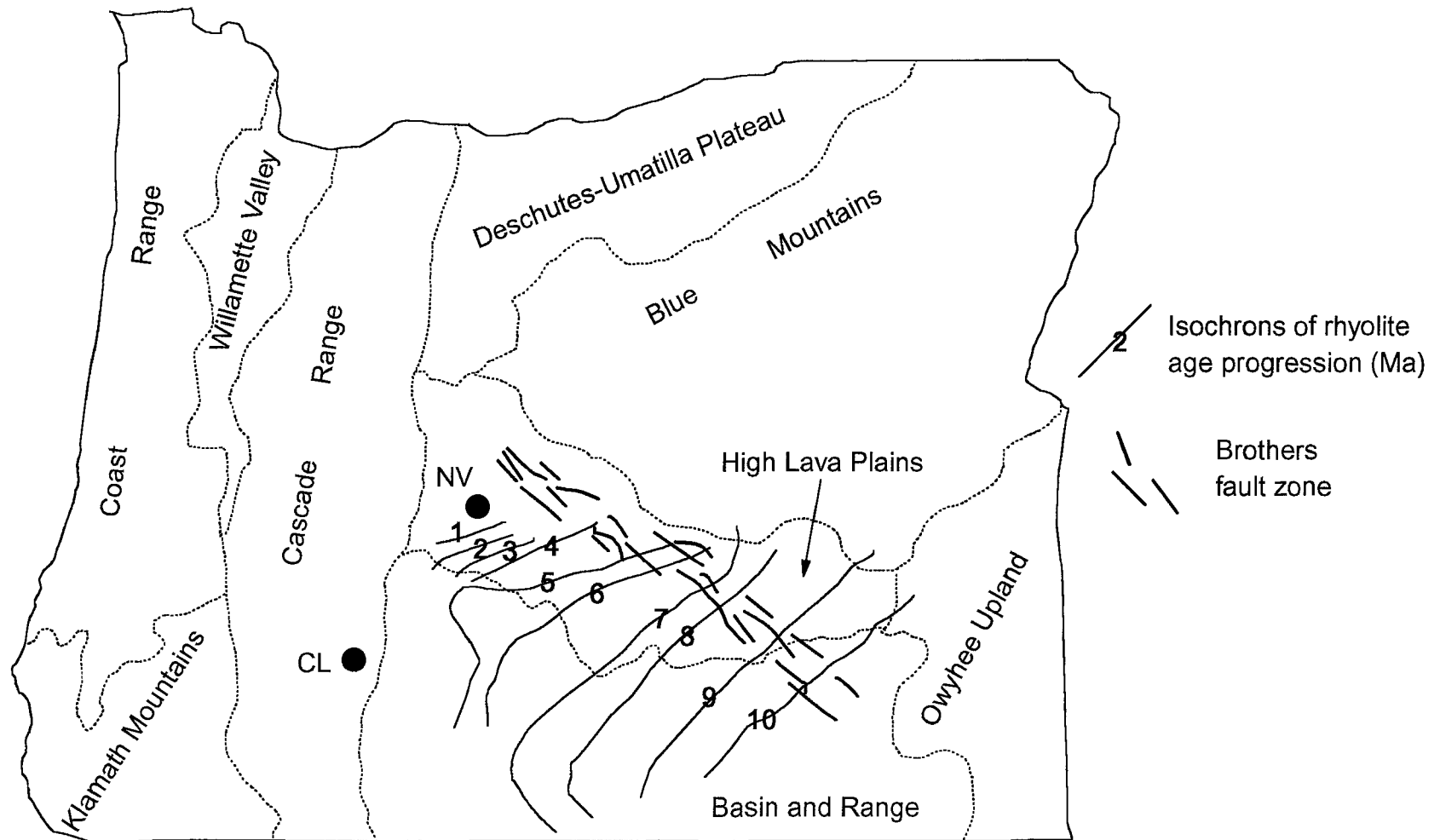


Figure 1.6: Map of physiographic provinces of Oregon showing Brothers fault zone and isochrons for rhyolite age progression in southeastern Oregon. NV=Newberry Volcano. CL=Crater Lake. (Adapted from MacLeod and Sherrod, 1988)

Table 1.1. Decrease in age across Harney Basin and ending at Newberry Volcano.

Name of Outcrop	Rock Type	Material Dated	Date
Duck Butte	rhyodacite	plagioclase, biotite	10 Ma (million years)
Burns Butte	rhyodacite	whole rock	7.8 ± 0.26 Ma
Palomino Butte	rhyolite	whole rock	slightly > 6 Ma
Glass Buttes	rhyolite	obsidian	4.9 Ma
Frederick Butte	rhyodacite	plagioclase	3.6 Ma
Ash-flow tuff (between Hampton Butte and Grassy Butte)	basal vitrophyre	plagioclase and glass separates	3.6 Ma
Squaw Butte	rhyolite	obsidian	3.6 Ma
Quartz Mountain	rhyolite	obsidian	1.1 Ma
East Butte	rhyolite	obsidian	0.85 ± 0.4 Ma
China Hat	rhyolite	obsidian	0.76 ± 0.1
Newberry Caldera	rhyolite	obsidian	7,000 to 1,400 years

Notes: All dates from Walker (1974) except for Newberry Caldera from Friedman (1977). All dates are in potassium-argon years (K-Ar) except for Newberry Caldera. Newberry Caldera dates are in calendar years before present recalculated from carbon-14 years by MacLeod *et al.* (1995).

Previous Work in Oregon

As shown above, the volcanism of Oregon was both voluminous and highly variable. The large amounts of silicic volcanism favored the formation of obsidian. As a result, there are a large number of obsidian sources located in Oregon. According to Skinner (1983), the number of sources is estimated to be about 75. If some of these are multi-compositional sources, the number of obsidian compositional groups could be much higher.

Several of Oregon's obsidian sources have been previously characterized by different methods of compositional analysis. Toepel and Sappington (1982) used x-ray fluorescence (XRF) to analyze source samples from Obsidian Cliff, South Sister, Newberry Caldera, Cougar Mountain, Yamsay Mountain, Frog Mountain, Glass Buttes, Poverty Basin (same as Horse Mountain), Buck Spring, Tucker Hill, Riley, Burns, Seneca, Beatys Buttes, Gregory Creek, and Skull Springs.

In a major study by Hughes (1986a), XRF was used to analyze samples from the obsidian sources at Surveyor Spring, Spodue Mountain, Silver Lake, Sycan Marsh, McComb Butte, Tucker Hill, Hager Mountain, Cogan Buttes, Witham Creek, Cougar Mountain, Beatys Butte, Glass Buttes, Riley, Horse Mountain, Quartz Mountain, and Drews Creek/Butcher Flat. In subsequent studies, he used XRF to analyze obsidian from Dog Hill and Burns Butte (Hughes, 1986b) and obsidian from Obsidian Cliff (Hughes, 1993).

Skinner (1983) also used XRF to analyze obsidian from a number of sources in Oregon. However, he only analyzed samples from confirmed Native American quarrying sites and did not completely characterize each source. Skinner and Winkler (1994)

summarized previous XRF analyses of obsidian from sources at Cougar Mountain, Devil Point, Horse Mountain, Inman Creek, McKay Buttes, Newberry Caldera, Obsidian Cliffs, Quartz Mountain, Salt Creek, Silver Lake, Sycan Marsh, the Siuslaw River, and Spodue Mountain.

There have been other studies of obsidian sources by x-ray fluorescence, but these were generally small (see Skinner, 1983, Table IV-1, p. 279). A very limited number of sources have been characterized by neutron activation analysis (NAA) (see Skinner, 1983, *ibid.*).

Several other studies of Oregon obsidian have not been concerned with chemical characterization. For example, Friedman (1977) examined obsidian specimens from Newberry Caldera in an attempt to establish a hydration dating scheme for the flows there. Ericson (1981) also performed hydration dating experiments on obsidian sources in Oregon, in this case, on Beatys Butte, Glass Mountain, and Glass Buttes. MacLean (1994) analyzed obsidian from Juniper Ridge, Horsehead Mountain, and Burns Butte using several techniques, including XRF, in order to examine some of the underlying geological reasons for the age progression of the High Lava Plains.

Research Goals

Although there have been sporadic efforts to characterize obsidian from Oregon, as yet no comprehensive analysis of sources has been performed, especially by NAA. The current study is intended to amend this situation through a systematic sampling and analysis by NAA of as many Oregon obsidian sources as possible. It is the goal of this study to create a database that contains as much element and spatial information about each source as possible. Although it is important to characterize sources thoroughly, it is

also important to be able to make use of this characterization and to source obsidian artifacts. Thus, this study will also demonstrate the usefulness of the new database by assigning a small assemblage of obsidian artifacts to their sources. An abbreviated method of neutron activation analysis developed at the Missouri University Research Reactor (Glascok, *et al.*, 1994) has been extremely successful when used on obsidian from Mesoamerica. One goal of the present study is to assess the feasibility of determining sources of obsidian from Oregon by a similar, abbreviated procedure.

CHAPTER 2 BACKGROUND

Although it is not certain that glassy rocks (obsidian in particular) represent the pristine composition of a volcanic magma, they provide the best evidence for the composition and types of early crystalline phases, the temperatures at which they equilibrate, and variables such as pressure or fugacity of volatiles (Carmichael, 1979). Obsidian retains most of its pristine chemical composition without changes due to crystallization. It can, therefore, be used as a reference with which to compare its crystallized equivalents (Hughes and Smith, 1993). Elemental analysis of obsidian can also provide other distinctions. If obsidian from temporally- or spatially-related volcanic units is analyzed and compared, fine-scale chemical distinctions can be made which provide insight into the processes and rates of evolution of specific genetic sequences. The geochemistry of obsidian also allows the comparison of petrological areas on a regional or global scale. Tracing these comparisons over distance and time can contribute to a deeper understanding of the tectonics and crustal evolution of the earth (Hughes and Smith, 1993).

Geologists use obsidian composition to investigate magma evolution over time and geographical area. Archaeologists also employ elemental analysis of obsidian to make comparisons over large areas and through time, monitoring not magma but human interaction patterns. By locating and analyzing all sources of artifact-quality obsidian, it should be possible to analyze artifacts in the same way and to identify the sources from which they originated. Obsidian characterization studies then allow archaeologists to develop hypotheses about source-use patterns, trade and exchange between groups or

regions, and the movement of prehistoric humans (Hughes and Smith, 1993). Obsidian is ideal for these kinds of studies because sources are usually homogeneous and unique in chemical composition, are geographically localized and relatively few in number, and the manufacture of artifacts does not result in a change in chemical composition of the obsidian (Williams-Thorpe, 1995; Bowman, *et al.*, 1973a).

It has generally been assumed that an obsidian source is the byproduct of a single homogeneous magma and that geochemical analyses on a small number of source rocks represent the elemental “profile” of the entire source (Hughes and Smith, 1993).

Unfortunately, this is not always true. There are sources where significant variation exists between the individual flows and domes of the same system, although individual domes or flows may be homogeneous. One of the earliest reported examples of within-source variation was described by Bowman *et al.* (1973a & b) for the Borax Lake area of California. They found a series of linear relations between the element compositions for obsidian and dacite samples suggesting variable mixing of different proportions of magma from two chemically dissimilar homogeneous bodies. Large variations between obsidian domes and flows were also discovered in the Medicine Lake Highlands (Hughes, 1982) and the Coso Volcanic Field (Hughes, 1988), both in California. More recently, Hughes (1994) resampled the Casa Diablo source in California and found three different chemical fingerprints where originally it was believed only a single compositional group existed.

The above examples illustrate the importance of delineating the geographical boundaries of a particular source and sampling the source thoroughly in order to characterize all possible intrasource variability. An ability to identify distinct geochemical

varieties of glass provides archaeologists with the capability of tracking the spatial, temporal, and production histories of specific glass types (Hughes, 1994). The following sections will describe the locations, formation, attributes, and analyses of obsidian. The information discussed will provide a background for further understanding of this study.

Formation and Emplacement

Petrologically, obsidian is typically of rhyolitic composition. The melt from which it is erupted is extremely polymerized and viscous (Middlemost, 1985). A rhyolitic melt is very likely formed in part by the partial melting of a wide range of crustal materials. The melt is generally extruded or intruded at high temperatures and pressures from very shallow depths within the crustal interior (Ericson *et al.*, 1975).

Obsidian lavas tend to form at depths where the temperatures are on the order of 1000-1200 degrees Celsius (Shackley, 1990; Bakken, 1977). As pressure increases, the magma begins to move upward. Obsidian lava sometimes erupts explosively, a behavior that is dependent on two factors, the silica content and the content of water and other volatiles. The more silica a melt contains the more viscous it will become (Bakken, 1977). Higher water content decreases the viscosity of a melt because it stops the polymerization of silica. Less water in a melt increases viscosity. As we shall see later, most obsidian contains very little water. A highly siliceous magma also normally contains small amounts of other volatiles such as CO₂, CO, H₂S, and NH₃. At first, these gases help the magma rise to the surface, but as they do so, the volatiles tend to escape. This helps to increase the viscosity of the magma as well as increase the melting point. The magma arrives at the surface with a temperature less than its crystallization temperature and, because it does not have enough energy to crystallize, it becomes a

supercooled liquid or glass (Bakken, 1977).

The extrusion of obsidian can occur in a number of ways. Rhyolite domes and flows are usually composed of glass on the outside but have crystalline interiors (Hughes and Smith, 1993). The outermost layer of glass is typically vesicular and porous (due to gas bubbles) and it grades into a more dense (i.e., pore free) material. At the contact zone between the porous material and the crystalline interior, the highest quality glass (i.e., artifact-quality obsidian) forms (Figure 2.1). Most rhyolite flows will produce at least some obsidian, but the glass is often crystallized by the time erosion later exposes the deposit. Once a deposit has crystallized to perlite, the only obsidian-like materials remaining are small pieces known as marekanites.

Artifact-quality obsidian can also be found in pyroclastic deposits. Pyroclastic deposits are consolidations of volcanic material that were ejected from a volcano during explosive activity (Philpotts, 1990). Obsidian of this type can introduce chemical inhomogeneity to a source in either of two ways. It may be a cogenetic forerunner of a lava flow or a dome that follows a separate eruption. Or, it could be material from an earlier deposit that is disturbed by the new eruption. In the latter, the composition of the obsidian may or may not be chemically related to other obsidians found in the area.

One type of pyroclastic deposit is called a rhyolitic agglutinate. These are formed by the accumulation of larger fragments of ejected material. Such deposits may contain artifact-quality obsidian but, because they are pyroclastic, they tend to be heterogeneous in composition. In North America, rhyolitic agglutinates are typically the product of high temperature rhyolitic magmas and are generally associated with basaltic or andesitic magmas, which may be a source of physical and chemical contamination (Hughes and

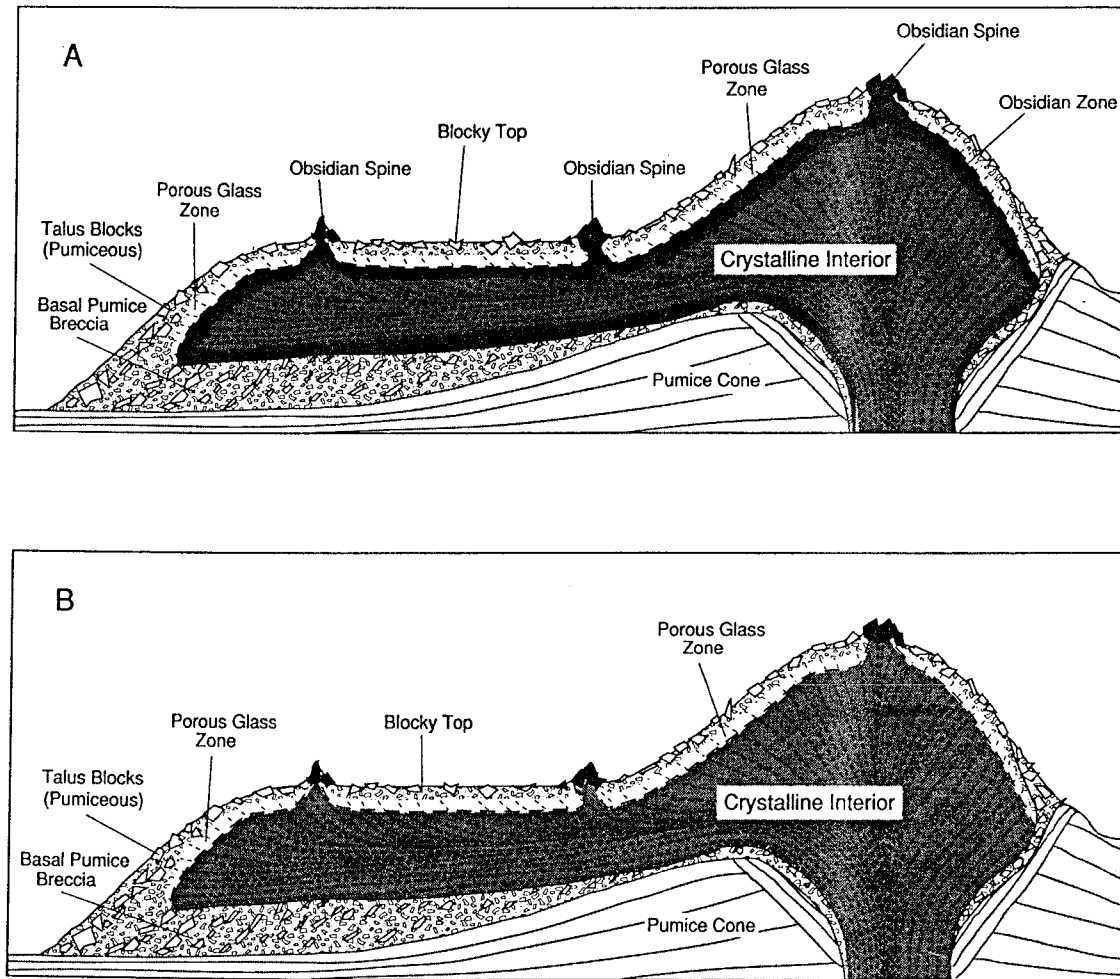


Figure 2.1: Obsidian zones in domes and flows. A shows a cross section of the position of a typical obsidian zone of artifact quality obsidian in a rhyolite flow/dome structure. B shows a cross section of a rhyolite flow/dome structure in which a zone of artifact quality obsidian is absent. (From Hughes and Smith, 1993)

Smith, 1993).

An ash-flow tuff containing obsidian is the product of a large volcanic pyroclastic eruption and is part of more extensive ash-flow sheets (Hughes and Smith, 1993).

Obsidian from ash-flow tuffs tends to exhibit considerable variation in composition. The variation can occur in several ways. Vertical variation occurs when an eruption systematically taps a chemically-zoned magma chamber. The material from the top of the chamber erupts first and the chemical gradation is inverted from the chamber to the deposit. It is also possible to have variable composition both horizontally and vertically. This occurs when there is mixing of material from different levels within a zoned chamber or material from above the chamber and/or material from the earth's surface mixes with the magma (e.g., wall and roof rock contamination). Obsidian is also formed by the reheating and compaction of underlying glassy ash or pumice at the base of high-temperature, welded ash-flow sheets. This latter type of obsidian is rare and inherits the chemical characteristics that the glassy material had before fusion (Hughes and Smith, 1993).

Primary vs. Secondary Deposits

Any discussion of the origins of obsidian used prehistorically must also describe the differences between primary and secondary sources. A primary source is located at or near the vent at which the lava was extruded (usually a dome or flow). A secondary source is spatially removed from the primary source (Skinner, 1983).

Secondary sources can be created by a variety of processes. For example, a minor cause of movement is mass wasting due to rockfalls and avalanches. Another mode is glacial transport which occurs when a glacier moves over a primary source, picks up the

obsidian rocks, and deposits them in another location.

Fluvial transport is probably the most common method by which secondary deposits are created. Streams and rivers passing close to a source may erode material from the source. The eroded material can sometimes be found long distances from the original source area (see Shackley, 1988). Transport by water may also result in a deposit of obsidian downstream from primary sources that contains a mixture of obsidian from a number of upstream sources (Skinner, 1983). Volcanic transport of obsidian as tephra, lahars, or ash-flows is also possible. Tephra are ejecta that normally would be found not farther than a few kilometers from the source. Lahars are mudflows or volcanic material mixed with water and laid down on land. Ash-flows, mentioned earlier, cover very large areas so the obsidian can be found at some distance from the source vent. Humans may also transport obsidian; this is the basis of most archaeological investigations of obsidian (Skinner, 1983).

Location of Obsidian

Geological Environment

MacDonald *et al.* (1992) describe five types of geological environments capable of producing obsidian. The first type includes the early stages of arc development, which occur in regions of subcontinental and relatively young crust. Two examples of this are the Hawaiian Islands and the Caribbean arc. The second type involves regions developing into mature island arcs such as Japan and Indonesia. This type is composed of crust that is transitional between oceanic and continental. The third type occurs near the continental margins like the western coast of North America, where the crust is thicker than the previously mentioned regions. The fourth type includes the continental

interiors, where the obsidian is emplaced within stable continental cratonic regions. This type is also represented in parts of western North America (i.e., Yellowstone). The fifth type is that of islands overlying regions of high heat flow (i.e., hot spots) or near spreading areas of relatively thin oceanic crust such as Iceland and Papua New Guinea.

Geographical Environment

Obsidian deposits are found in many regions of the world. Although obsidian gradually hydrates to become perlite, the process is slow enough that an obsidian deposit will usually exist for several million years and there is no need for geologically recent volcanic activity in areas where obsidian exists. The Pacific Rim region contains many obsidian sources, including the islands of Japan and the Kamchatka Peninsula and Siberia in Russia. To the south, but still within the Pacific Rim, obsidian is found throughout the South Pacific islands, including, but not limited to, Indonesia, Papua New Guinea, Fiji, Easter Island, and New Zealand (Middlemost, 1985; Skinner, 1983). In Africa, obsidian deposits occur in Ethiopia, near the Red Sea, in the Great Rift Valley of Kenya, and in northern Chad (Skinner, 1983).

Obsidian is also found in the Near East. Large obsidian deposits are found in Turkey, Iran, and the Caucasus region of Russia, Armenia, Georgia, and Azerbaijan. Islands in the Aegean with obsidian include Melos, Antiparos, and Griali. Islands near Italy with obsidian include Lipari, Pantelleria, Palmarola, and Sardinia. The continent of Europe contains areas of obsidian in Czechoslovakia, Hungary, and the Ukraine. Islands in the Atlantic containing obsidian include Iceland, Tenerife (Canary Islands), and San Miguel (Azores). Obsidian is also found on the island of Guadeloupe in the West Indies (Skinner, 1983; Williams-Thorpe, 1995).

In the New World, obsidian deposits are found in several areas of North America including the Aleutian Arc and British Columbia, Canada. The western United States contains large deposits of obsidian in Alaska, Arizona, California, Colorado, Idaho, Nevada, New Mexico, Oregon, Utah, and Wyoming. In Central America, obsidian sources are located in Mexico, Guatemala, Nicaragua, El Salvador, and Honduras. In South America, obsidian is located in Colombia, Ecuador, Peru, Bolivia, Chile, and Argentina (Skinner, 1983). A map of regions containing obsidian is shown in Figure 2.2.

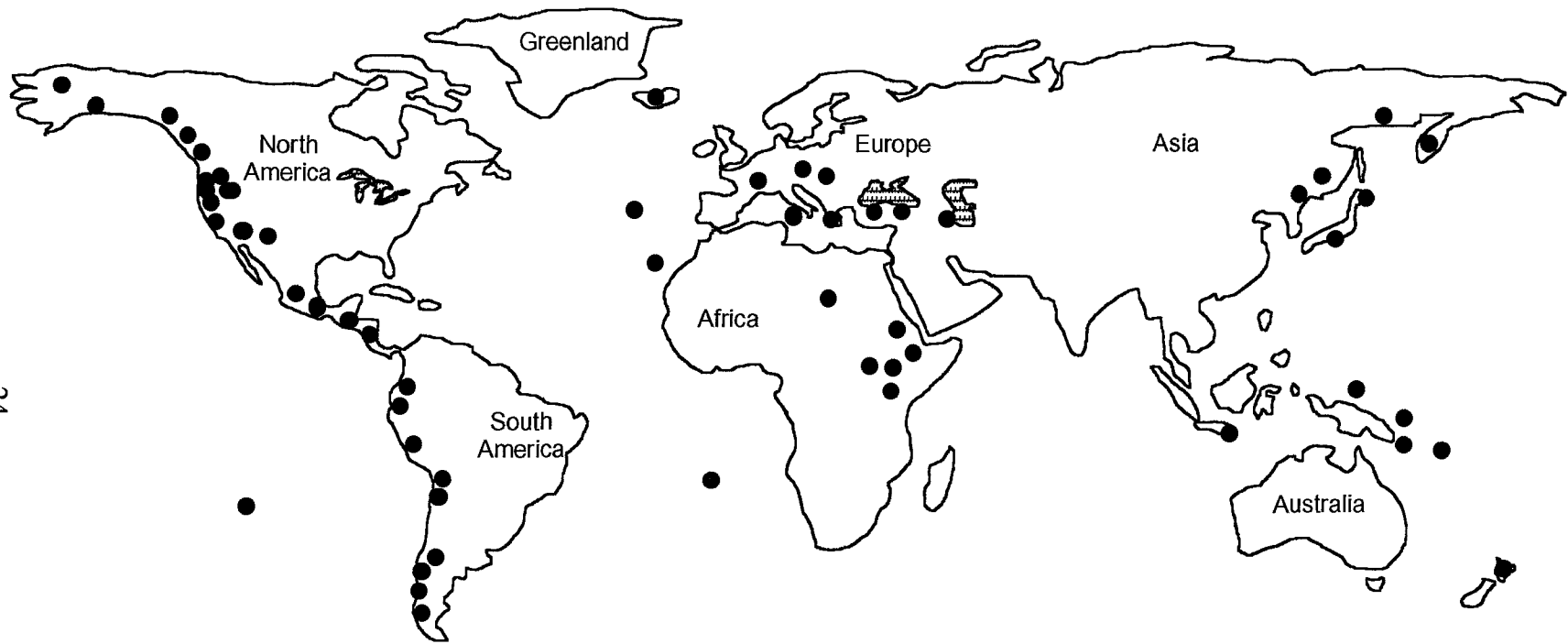
Characteristics of Obsidian

Chemistry of Obsidian

The general chemical makeup of obsidian is not debated though there is some debate over what exactly constitutes obsidian. The most common way of distinguishing rhyolitic obsidian from other natural glasses is by the amount of silica (i.e., SiO₂) present in the glass. Although at least one source identified obsidian as having a silica content of 80% or higher (Middlemost, 1985), obsidian is more generally considered to have a silica content of 70% to 77% (Bouska *et al.*, 1993; Friedman and Long, 1984; MacDonald, *et al.*, 1992). The bulk geochemistry (besides silica) is also generally agreed upon: Al₂O₃ (12-14%), K₂O (3-5%), Na₂O (3-5%), CaO + MgO (0.5-2%), and Fe₂O₃ + FeO (1%) (Bouska *et al.*, 1993). The bulk chemistry can also be used to subdivide obsidians according to a strict chemical classification rather than a geochemical classification [MacDonald, *et al.*, 1992], as follows:

peralkaline	$(\text{Na}_2\text{O} + \text{K}_2\text{O}) \geq \text{Al}_2\text{O}_3$
subalkaline	$(\text{Na}_2\text{O} + \text{K}_2\text{O}) \leq \text{Al}_2\text{O}_3$
peraluminous	$\text{Al}_2\text{O}_3 \geq \text{CaO} + (\text{Na}_2\text{O} + \text{K}_2\text{O})$
metaluminous	$(\text{Na}_2\text{O} + \text{K}_2\text{O}) < \text{Al}_2\text{O}_3 < \text{CaO} + (\text{Na}_2\text{O} + \text{K}_2\text{O})$.

Other classifications include calc-alkaline (high CaO and alkali relative to SiO₂), alkaline



- = non-ocean water
- = area containing obsidian

Figure 2.2: Map showing worldwide distribution of obsidian sources.

(high alkali and low Ca relative to SiO₂), and calcic (high Ca and low alkali) [Williams-Thorpe, 1995].

Obsidian also contains a number of trace elements that are present at the parts per million and parts per billion levels. The amount of trace elements present in a particular obsidian is dependent on both the type of crust into which the obsidian is emplaced and the geological processes that occurred while the obsidian was still a magma. All of the following elements can be found in obsidian, though not every one will be found in every obsidian: titanium, phosphorus, manganese, chlorine, fluorine, barium, cobalt, chromium, cesium, niobium, tantalum, lead, rubidium, antimony, scandium, strontium, thorium, uranium, zinc, zirconium, hafnium, yttrium, and the rare earth elements (MacDonald, *et al.*, 1992). The water content of obsidian is usually low, on the order of 0.1% to 1% by weight (Friedman and Long, 1984).

Obsidian as Glass

Glass is defined as an amorphous solid substance without an ordered structure (Bouska *et al.*, 1993). It is a supercooled liquid in a metastable state (i.e., a melt that was cooled below the liquidus point without crystallization occurring). The factor controlling whether a vitreous state will be formed is kinetic, i.e., the rate of cooling relative to the bond energies involved, and determines the state (vitreous vs. crystalline) [Pollard and Heron, 1996]. The stronger the chemical bonds are, the more resistant to rearrangement the liquid will be. For example, the Si-O bond has an energy of 368 kJ/mol and SiO₂ is very amenable to the formation of glass (including obsidian).

The disordered atomic structure of obsidian gives it the property of having no preferred direction of fracture. This gives obsidian its excellent flaking properties and

results in conchoidal-shaped fractures with very sharp edges (Shackley, 1990; Williams-Thorpe, 1995). These attributes make obsidian an ideal material for tools and other uses. Some obsidian materials are of better quality for making artifacts than others. For example, the obsidian found in most areas of Arizona has been degraded and is found as very small pieces known as marekanites or “Apache tears” (Shackley, 1990). In contrast to obsidian, hydrated glasses such as perlite and pitchstone have preferred planes of cleavage and are therefore less useful as tools (Shackley, 1990).

Obsidian does have some structure: an unperiodical grouping of SiO_4 tetrahedra bonded at the corners by strong covalent Si-O bonds (Figure 2.3) [Bouska *et al.*, 1993]. The structure of obsidian glass is similar to that of crystalline SiO_2 . They both have the same basic type of polyhedron structure. The Si-O-Si angle is between 120 and 180 degrees (average is 144°) and the bond length between Si and O (in all directions) is 1.62 Å; the distance between tetrahedral oxygen atoms is about 2.65 Å (Mozzi and Warren, 1969). The real differences between the natural glasses and the crystalline form are periodicity, symmetry, and ordering of the basic structural units over long distances (Bouska *et al.*, 1993). In general, in obsidian glass there is a random orientation about the Si-O bond directions except when discussing closest neighbors (Mozzi and Warren, 1969).

Glass is composed of three “parts.” Network formers exist in the glass as the pure substance (i.e., they can form glass structure on their own) and include SiO_2 , B_2O_3 , GeO_2 , P_2O_5 , and As_2O_5 (Pollard and Heron, 1996). In obsidian, the (only) network former is SiO_2 . Network modifiers disrupt the continuity of the network and change the chemical and physical properties of the glass. In obsidian, these are normally the alkali and

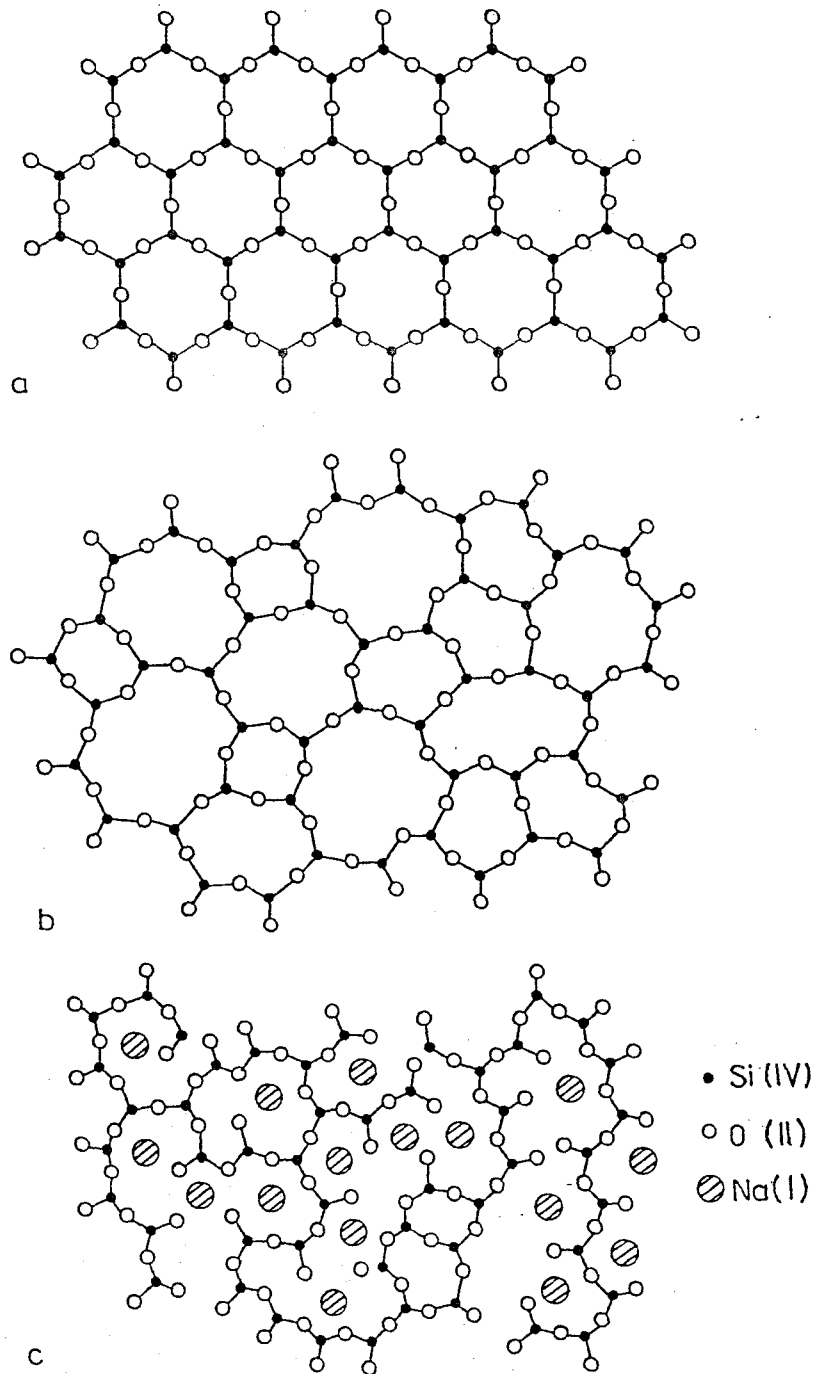


Figure 2.3: Planar depiction of the structure of (a) crystalline silica, (b) quartz glass, and (c) sodium silicate glass, according to the Zachariasen theory. (From Bouska et al., 1993)

alkaline earth oxides such as Na_2O , K_2O , CaO , and MgO . Modifiers of low positive charge and large size can fit into the holes between the tetrahedra to compensate for the excess negative charge created by non-bridging oxygen atoms (Ericson *et al.*, 1976). Other possible network modifiers include gases such as CO_2 and water (Bouska *et al.*, 1993).

Intermediates are oxides which can enter the glass as either network formers or network modifiers but they cannot form glasses by themselves (Pollard and Heron, 1996). The most common intermediate in obsidian is Al_2O_3 . It usually acts as a modifier because it cannot isomorphically replace silicon (Bouska *et al.*, 1993). However, oxides of +1 and +2 metals enable aluminum to enter the tetrahedral lattice and replace part of the silicon. The charge deficits are compensated by MAIO_2 and MAI_2O_4 groups where possible M's include Na and K (Figure 2.4).

Obsidian is not the only type of volcanic glass. The other volcanic glasses are less voluminous than obsidian mainly because they are lower in silica content and a high silica content is needed to easily form glass. Basaltic glass is not very common but is often found at volcanic vents at the ocean bottom where the lava is cooled very quickly by the cold ocean water (Bouska *et al.*, 1993). Volcanic basaltic glasses are found in Iceland and Hawaii (where it is sometimes called Pelee's hair or Pelee's tears) and as thin glassy chill margins on surface flows. Basaltic glass is sometimes mistaken for obsidian (Bouska *et al.*, 1993). The differences between obsidian and basaltic glasses are easily shown through a comparison of their bulk chemistries: basaltic glasses have SiO_2 (45-50%), Al_2O_3 (10-20%), $\text{K}_2\text{O} + \text{Na}_2\text{O}$ (3-5%), $\text{FeO} + \text{Fe}_2\text{O}_3$ (5-10%), $\text{CaO} + \text{MgO}$ (15-20%) (Friedman and Long, 1984; Middlemost, 1985; Bouska *et al.*, 1993). In obsidian,

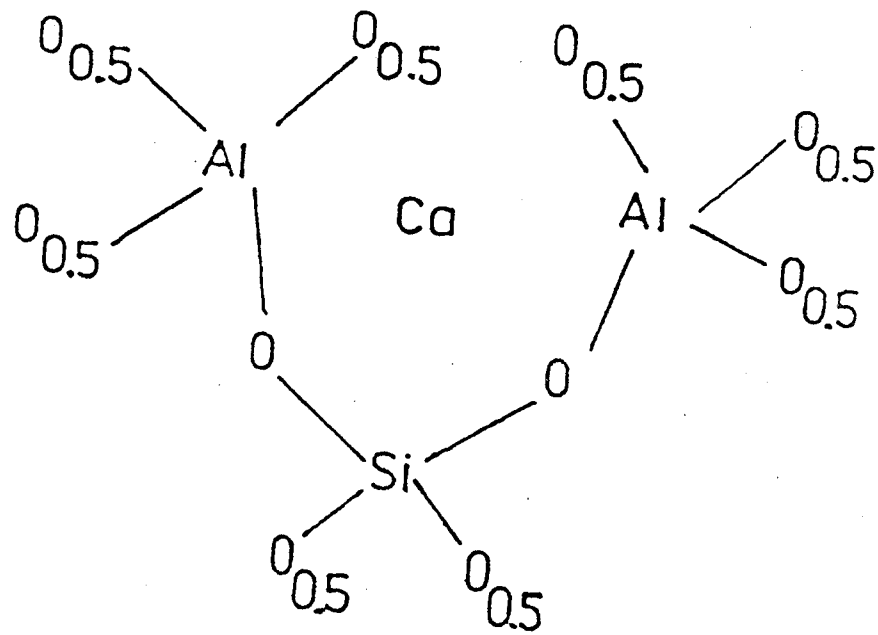


Figure 2.4: Depiction of the bonding of aluminum in aluminosilicate glasses. (From Bouska et al., 1993)

the silica content is much greater (i.e., 70%+) while the $\text{FeO} + \text{Fe}_2\text{O}_3$ and the $\text{CaO} + \text{MgO}$ contents are much less (i.e., 0.5-2%). Basaltic lava is very fluid and much less viscous; such that when it forms a glass it is normally very thin. This contrasts with obsidian flows, which can be several meters thick (Friedman and Long, 1984).

A volcanic glass intermediate in composition between basalts and obsidians is andesite. The silica content of andesites is usually about 60% and the alumina content is relatively high at about 17% (Middlemost, 1985). Andesites are frequently found along with high alumina basalts, dacites, and rhyolites. Another silica type rock includes trachyte-syenites, which are not necessarily glass, and have a SiO_2 content of about 56-66% along with a high alumina and high alkali content. Next in order of silica content are the dacites and rhyolites. Dacites have higher percentages of elements such as iron, magnesium, calcium, titanium, and alumina while the rhyolites have higher silica and potassium concentrations (Middlemost, 1985). Figure 2.5 helps illustrate the distinctions between different silica-type rocks.

Other rocks can sometimes be mistaken for obsidian. Perlite is a volcanic rock with mostly vitreous structure but it has a water content of about 1-6% by weight. Perlite is thought to be a product of the hydration of obsidian (Friedman and Smith, 1958). This has been shown through experiments that compared the deuterium content of the water in obsidian to the deuterium content of the water in perlite. The deuterium content of the water in perlite matched the deuterium content of local waters but the deuterium content of the intrinsic water in the obsidian did not. Therefore, it is believed that the water in obsidians is magmatic in origin while the water in perlite is due to a secondary source, namely hydration by interaction with local waters (Friedman and Smith, 1958; Stewart,

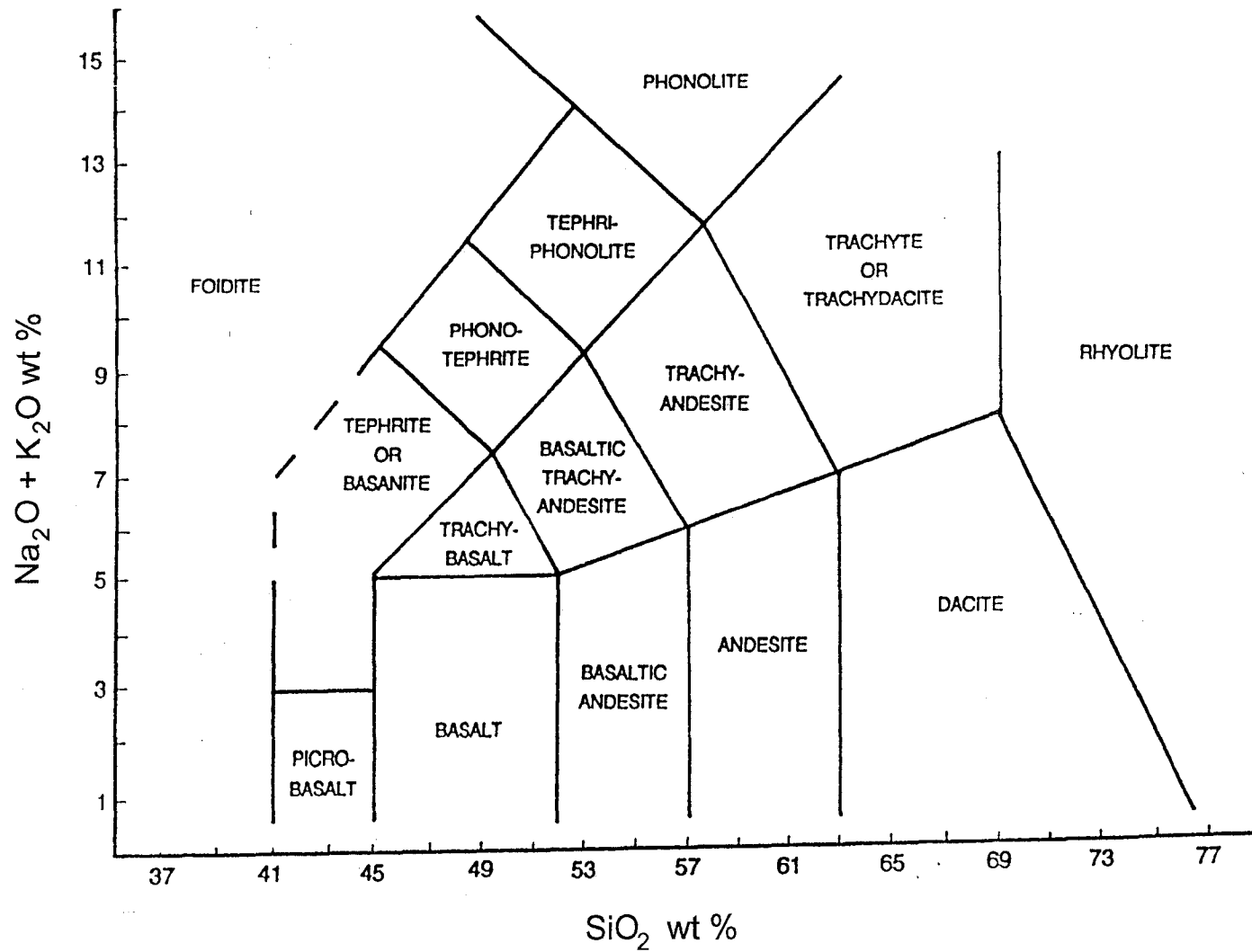


Figure 2.5: Chemical classification of volcanic rocks using the total alkali-silica diagram. (From LeBas et. al, 1986)

1979).

Pitchstone is yet another type of volcanic rock with a resinous pitch-like luster and a relatively high water content (6-16%) [Bouska *et al.*, 1993]. Although it was originally thought possible that pitchstone was also a result of the hydration of obsidian, it is more probable that pitchstones are the result of glass that hydrated under elevated water pressures (Friedman *et al.*, 1966). Pitchstone deposits in northwest Scotland and Ireland were used for tool manufacture during the Neolithic and Bronze Ages (Williams-Thorpe and Thorpe, 1984).

There are other natural glasses which have sometimes been mistaken for obsidian. One type is called a fulgurite. Fulgurites are formed when lightning strikes the ground, melting and vaporizing it. Fulgurites are commonly found in the form of glassy tubes in soils and sands and glassy crusts in crystalline rocks (Bouska *et al.*, 1993).

Another type of glass is formed from the impact of extra-terrestrial bodies on the earth. Larger meteorites enter the earth's atmosphere at high speed, and when they impact on the earth they are slowed quickly and produce enough heat and pressure to melt and vaporize the earth they impact and thus form glass (Bouska *et al.*, 1993). These glasses are found within impact crater interiors and are generally termed impactites. Impactites have the chemical composition of the target rocks and can be distinguished both from other impact glasses and from obsidian.

Yet another natural glass is tektite. These are rounded, acidic silicate glasses with a high melting point. Tektites are found in very large strewn fields in several regions of the world. Tektites come in many different shapes and sizes, and their origins are not completely known although they are not thought to be volcanic in origin. Tektites

contain lechatelierite (i.e., pure silica) and do not contain any crystallites; both characteristics are the opposite in volcanic glasses. There are several other ways by which to distinguish tektites from obsidian including chemical composition and water content (e.g., tektite composition is quite similar to that of terrestrial rocks and tektites have a water content of about 0.02%, which is about 10-100 times lower than most obsidians). Tektites are probably the result of the melting of sedimentary rocks caused by impact of extra-terrestrial objects such as pieces of asteroids or comets. However, they are a different fraction of the melt than that of impactites and their compositions are recognizably different.

Although meteorites are more commonly thought of as the objects that formed glass by impacting with the earth, they themselves may contain glass. This glass was formed on the original meteorite body or by an impact in space. Both impact glass and volcanic glass are found on the moon.

Properties of Obsidian

Obsidian comes in a large variety of colors. The most common color is black due to the presence of magnetite particles. If the magnetite oxidizes, a red/red-brown colored glass containing hematite is formed (Skinner, 1983). Other colors of obsidian include, but are not limited to, blue, green, orange, clear, snowflake, and rainbow.

The density of obsidian glass ranges from 2.22 to 2.46 g/cm³ with the average being about 2.37 g/cm³ (Ericson *et al.*, 1975). Density can be influenced by a number of factors including the presence of crystals, air bubbles, water content, and chemical composition (Skinner, 1983). Stevenson *et al.* (1996) suggest that a correlation between density and intrinsic water content may be used to calculate hydration rates for dating.

The physical properties of obsidian were investigated extensively by Ericson *et al.* (1975). The structure was examined by several methods. The thermal expansion curve for obsidian was found to approximate that of annealed glass, which indicates little or no strain in the structure. X-ray diffraction has found obsidian to be amorphous. Mossbauer spectroscopy reveals that both Fe²⁺ and Fe³⁺ are in 4-fold and 6-fold coordination number environments. Infrared spectroscopy shows a Si-O-Si stretch at 8-16 μm, which places obsidian between silica glass and window glass (Ericson *et al.*, 1975). Physically, obsidian is stable to corrosion from 5% NaOH and 15% HF. Compared to Pyrex glass, it is highly chemically resistant. Its hardness is comparable to that of fused silica, and its Vickers hardness is 500-900 kg/m² (Ericson *et al.*, 1975). Obsidian is intermediate in resistivity between soda lime glass and 96% silica glass; and its refractive index varies between 1.480 and 1.493 (Bouska *et al.*, 1993).

The microscopic and petrographic properties of obsidian differ depending on the thermal history and chemical composition. Small crystalline areas and other inconsistencies are usually present (Skinner, 1983). Bubbles and vesicles (which vary in size from μm to cm) are created as the lava cools and gases exsolve. Spherulites and lithophysae are crystalline objects of various compositions (e.g., feldspars) present due to early stage devitrification that occurred after solidification. Xenoliths present in obsidian are fragments of rock torn from the walls of the magma chamber or conduit that the lava passed through. Obsidian also contains microphenocrysts (plagioclase feldspars), microlites (crystals that polarize light), and crystallites (crystals that don't polarize light) (Skinner, 1983). However, most of these crystals are microscopic and are present at only about 10 ± 18% by volume (Ericson *et al.*, 1975).

Hydration of Obsidian

Obsidian, like other natural glasses, is thermodynamically unstable and has a tendency to undergo chemical alteration into more stable crystalline forms. The process of hydration causes the obsidian to become completely devitrified (i.e., crystallized). Eventually, these processes along with weathering destroy the obsidian. This explains why obsidian older than 65 million years (a relatively short time on a geological scale) is not found (Bouska *et al.*, 1993).

The interaction of obsidian with water causes the eventual breakdown of the glass surface. At first, the water, in the form of H_3O^+ , exchanges with ions in the glass, most notably the alkalis: $-\text{Si-O-Na} + \text{H}_2\text{O} \rightarrow -\text{Si-OH} + \text{Na}^+ + \text{OH}^-$ (Bouska *et al.*, 1993; Pollard and Heron, 1996). The next stage leads to the creation of more non-bridging oxygens: $\text{Si-O-Si-} + \text{OH}^- \rightarrow -\text{Si-OH} + -\text{Si-O}^-$. As a result, non-bridging oxygen atoms are available to react with the hydrogen in water to form silanol bonds on the surface of the glass and another hydroxyl ion which can go on to attack yet another siloxane bond: $-\text{Si-O}^- + \text{H}_2\text{O} \rightarrow -\text{Si-OH} + \text{OH}^-$. If the pH is greater than nine then the silicon is removed from the glass as $\text{Si}(\text{OH})_4$. Eventually the obsidian devitrifies into zeolites and other clay minerals. The process takes many thousands to millions of years and is strongly affected by the presence of crystals in the obsidian, the amounts of certain elements such as aluminum and iron, the initial concentration of water, and the temperature of the environment (Friedman *et al.*, 1966; Ericson *et al.*, 1976; Bouska *et al.*, 1993).

Archaeologists have investigated the hydration of obsidian artifacts as a potential archaeological clock. If the hydration rate is known or can be estimated and the amount of hydration can be measured, then, in principle, the age of an obsidian artifact can be

determined. The age would pertain to the time when the obsidian artifact was made and a fresh surface was exposed in the flaking process. Once an adequate period of time has passed, a hydration layer is visible under magnification and can be measured. The thickness of the layer together with the rate at which the obsidian hydrated provide the information necessary to calculate an age for the artifact.

Friedman and Smith (1960) first recognized the potential of the above approach and developed a formula describing the relations between the hydration rind width, time and hydration rate. Their formula for the rate of diffusion of water into obsidian is as follows:

$$x^2 = kt \tag{1}$$

where:

x = depth of penetration in microns;
 t = time in years; and
 k = a constant for a given temperature.

The parameter k is highly dependent on both the temperature and the water content of the glass (incorporated into both A and E) and can be defined as follows:

$$k = Ae^{-E/RT} \tag{2}$$

where:

k = the rate of hydration;
 A = a constant;
 E = the activation energy (calculated);
 R = the universal gas constant (8.314); and
 T = the temperature in Kelvin (Friedman *et al.*, 1966).

Based on various correlations of obsidian hydration dates with radiocarbon dates, different forms of Equation (1) have been suggested. The equation now more commonly used is $x = kt^y$ (in the case of the original values y would equal 1/2) [Friedman and Long,

1984). Other researchers have found different values for y depending on the obsidian analyzed. For example, Friedman and Smith found a value of 0.5, Clark found a value of 0.75 (Kimberlin, 1976), and Meighan found a value of 1 (Kimberlin, 1976). Hydration dating equations do not always follow the original pattern. Findlow *et al.* (1975), in examining hydration data from Government Mountain-Sitgreaves Peak, Arizona, found that the equation that best fit the data was a negative parabolic with the general form $y = x^2 - x$. Variations in the equations show that the hydration rate of obsidian as well as the functional equation relating hydration to time appear to be source specific and likely dependent on composition and structure. As Ericson *et al.* (1976; p. 43) stated:

“[I]f the structure of obsidian appreciably influences the diffusion kinetics of water in the diffusion process, then as a logical result, it will be necessary to determine the individual hydration rate for each obsidian extrusion and to determine the source of each obsidian sample prior to dating.”

Recent research by Anovitz *et al.* (n. d.) has resulted in the proposal that the hydration process is not a simple diffusion process as previously thought. They suggest that much more work is needed to fully characterize and model the hydration process before accurate and precise obsidian hydration data can be collected.

Eventually a database may be created that could make the dating of artifacts easier and more reliable. This database will contain trace element composition data, intrinsic water content (percent H₂O and OH⁻), density (related to intrinsic water content), hydration rates (as calculated from induced hydration experiments), and descriptive information for each source of obsidian. These data could be used once a reasonably accurate model of the hydration process is developed.

Previous Methods Used to Examine Obsidian

Another reason archaeologists are interested in obsidian is that it is an ideal archaeological material to study cultural interaction and population movement because artifacts made of obsidian can be linked to specific sources. In order to study trade, for example, archaeologists can examine artifacts for stylistic attributes. However, these attributes can be subjective and open to different interpretations. Therefore, the idea of comparing artifacts with source material has become a common way to learn more about how past peoples moved materials across the landscape. In order to successfully link an obsidian artifact to an obsidian source, two things must be accomplished. First, there must be something measurable about the source that makes it unique, and second, it must be possible to measure that unique attribute in the artifact in order to correlate it unequivocally with the source. Over the past thirty years there have been a number of attempts to measure different properties of sources in order to characterize each. The following are examples of several different methods, each of which attempts to characterize, identify, and differentiate between obsidian sources and to link artifacts to those sources.

Physical Methods

Reeves and Armitage (1973) attempted to use density to distinguish between obsidian sources in New Zealand. One advantage of density is that its determination can be done non-destructively. Although these investigators were able to measure the density to $\pm 0.0004 \text{ g/cm}^3$, the technique was unsuccessful. They discovered that density was a more variable property within a source than chemical composition. Although some differences were detected, the technique is more useful as a screening procedure for

initial or tentative identification only.

Sato and Sato (1977) collected obsidian samples and measured gamma-ray spectra for the naturally decaying elements Th, U, and K. They used ratios to form graphs that showed distinctions between volcanoes in Japan but did not analyze any artifacts similarly. Leach *et al.* (1978) also investigated the possibility of using the natural radioactivity present in obsidian to distinguish sources. They detected β emissions from the uranium, thorium, and rubidium present in obsidian samples from New Zealand. Although the method was not completely successful at discriminating among sources because some had significantly higher concentrations of U, Th, and Rb, the method could be used as a preliminary screening method so some artifacts did not have to undergo more rigorous geochemical analyses. This method is also limited by the usually small amount of naturally radioactive elements, which would require extremely long counting times and result in lower overall precision.

Huntley and Bailey (1978) employed thermoluminescence (TL) to characterize obsidian sources from British Columbia and Oregon. They measured both natural thermoluminescence and radiation-induced thermoluminescence in source material. They were able to discriminate between sources by comparing the glow curves of one or both types of TL. Although the authors felt that the technique would not replace x-ray fluorescence, they also felt it was a viable option of characterization. Its main advantage was its non-destructiveness.

McDougall *et al.* (1983) attempted to discriminate between sources in the Mediterranean, central Europe, and the Near East by studying the magnetic properties of obsidian. The method is based on the iron particles present in obsidian; differences in

iron reflect differences in magnetic properties between sources. The magnetic properties studied did not yield source discrimination comparable to geochemical analyses.

However, McDougall *et al.* concluded that it is a good preliminary screening tool that is low cost, high speed, and non-destructive, and that it could reduce the number of geochemical analyses required.

Spectrographic Methods

Cann and Renfrew (1964) were among the first to recognize that obsidian artifacts could be correlated with obsidian sources. They investigated a variety of methods to identify and separate sources from one another, including macroscopic appearance, thin section characterization, refractive index, density, and major elemental constituents. None of the methods provided definitive differentiation, and so they used optical emission spectroscopy (OES) to measure the amounts of several trace elements. They were able to measure 16 elements and to separate sources effectively within the western and eastern Mediterranean and Egypt. In addition, they successfully assigned artifacts to those sources.

Nielson *et al.* (1976) used proton-induced x-ray emission (PIXE) spectroscopy to analyze artifacts from Mexico. They measured 11 elements for each artifact, and although they had anomalous results attributable to variations in sample thickness, their artifacts did fall into groups. These groups somewhat corresponded to data previously reported for sources in Guatemala. Duerden *et al.* (1979) used PIXE to analyze seven elements in source samples and artifacts from the Southwest Pacific. They compared the results of analyses on samples that were carefully prepared to those whose only treatment was washing and found that precision was less for the latter but the separation between

sources was still acceptable. They also attempted to use mounting techniques to minimize variations caused by the angle between the surface and the incident beam and the emergent x-rays.

Bird *et al.* (1978) measured the spectrum of gamma rays emitted during irradiation by proton-induced gamma-ray emission (PIGME). They detected three elements (F, Na, and Al). They were able to achieve about 1% precision and to assign artifacts to sources in the Southwest Pacific area with 95% accuracy. Ambrose *et al.* (1981) used both PIXE and PIGME to analyze artifacts from Melanesia. Using a combination of both techniques, they collected data on 21 elements. Like Duerden *et al.*, they found that the precision was less when using unprepared solid samples than carefully prepared samples; however, this did not affect the final interpretation of their results.

Wheeler and Clark (1977) used flame atomic absorption spectrophotometry (AAS) to analyze both source material and obsidian artifacts from Alaska. They collected data for five elements (Na, Mn, Fe, K, and Zn). They were able to distinguish four groups within their data and to confidently assign artifacts to sources, but they concluded that it is desirable to analyze as many elements as possible when attempting to distinguish between multiple source groups. The AAS technique has a great disadvantage in that the sample preparation is totally destructive. Michels (1982) used AAS to analyze obsidian from the El Chayal source system in Guatemala. He explored the possibility that bulk element composition could substitute for trace element composition when distinguishing between sources. Bulk element composition would be an advantage because of ease of determination. The method assigned only 70% of

samples correctly while trace element data from neutron activation analysis assigned 97% correctly (Michels, 1982).

Merrick and Brown (1984) used an electron microprobe to analyze source samples and artifacts from central Kenya. The electron microprobe looks at very small portions of a mineral at the level of 0.5 μm to 100's of μm , depending on the size of the electron beam. It is a fast, low cost, non-destructive technique but it can only detect major and minor elements with concentrations of 0.03% or greater, and the method only examines a small portion of the surface of a sample. It also measures only a few elements, which may not necessarily be the most discriminating. The method was successful in distinguishing among sources but again it was not as good a technique as trace element analysis and is most useful as a preliminary screening tool.

Burton and Krinsley (1987) used back-scattered electron (BSE) imaging in their study of obsidian provenance. Rather than being a method that uses trace element data to distinguish between sources, BSE looks at the chemical and textural relations among and within minerals and other inorganic material (on a micrometer to centimeter scale). The BSE image visualizes compositional variations but does not indicate the specific elements involved. Therefore, an energy dispersive x-ray analyzer was used in conjunction with the BSE image. Both source samples and artifacts from the southwest United States were examined. They were successful in separating sources as well as correctly assigning obsidian artifacts to sources.

Kilikoglou *et al.* (1997) compared neutron activation analysis and inductively coupled plasma emission spectrometry (ICPES) in the analysis of Aegean and Carpathian obsidian sources. ICPES provides data on the major and some of the trace elements

present in obsidian. The ICPES was quite successful at discriminating sources but it involves very destructive sample preparation, a disadvantage for artifacts. Also, it was not completely successful at separating geochemically related sources (e.g., two sources from the same island).

X-ray Fluorescence

Although the methods discussed previously were sometimes successful in identifying obsidian sources, separating those sources from one another, and assigning artifacts to those sources, they are not being routinely used in provenance studies of obsidian. On the other hand, x-ray fluorescence (XRF) has progressed steadily over the past 25 years to become one of the favorite methods of analysis for obsidian sources and artifacts. There are two main reasons for this: one is the ability to analyze artifacts without altering or destroying them in any way and the other is the fact that XRF has become increasingly easy and quick to use and is relatively inexpensive compared to other methods.

In XRF, the sample is irradiated with x-rays of a shorter wavelength and higher energy than the x-rays that are emitted from the elements. The source is usually a tungsten target x-ray tube, but some studies reported use of a radioactive source. The x-rays strike the surface, and if they are of high enough energy they will induce vacancies in the inner shells of the atoms. As these vacancies are filled x-rays are emitted with wavelengths in the range of 0.1-10 Å. These wavelengths are specific to each element and can be used to identify the element (Goffe, 1980; Giauque *et al.*, 1993). The elements Rb, Sr, Zr, and Ba can be measured with good precision by XRF. The elements Y, Nb, Fe, Mn, Zn, La, Th, and Ce can be measured with lower precision. The intensity

of the x-rays gives a quantitative measure of the elements (Giauque *et al.*, 1993).

There are two approaches to XRF. In wavelength dispersive XRF (WD-XRF) a crystal is used to separate the wavelengths of the emitted x-rays. The crystal can be rotated relative to the direction of the incident beam to select the wavelength (i.e., element) desired (Goffer, 1980). However, wavelength dispersive XRF is now less commonly used than the alternative technique, energy dispersive XRF (ED-XRF). ED-XRF has several advantages over the other method. With ED-XRF it is possible to analyze a greater number of elements simultaneously and the data can be obtained more quickly because it is an automated rather than manual method. Other advantages include lower cost and lower energy requirements (Shackley, 1990).

A common method of analysis is through a semi-quantitative XRF method. By this method, the net intensity counts for three elements are selected and the intensity data is changed to intrinsic proportions of the three elements through data reduction (Shackley, 1990). The ratios, usually of the elements Rb, Zr, and Sr, are commonly plotted on ternary graphs. There are two problems associated with this method. Because data are collected on only three elements, there is more of a chance that two sources will overlap when they are actually different. Also, because the data are in ratio form they cannot be compared to quantitative data collected by other labs (Shackley, 1990). Depending on the goals of the particular study, most data analysis today is performed such that the data are reported in parts per million (ppm) or percent.

Stevenson *et al.* (1971) used WD-XRF to analyze source material from the West Coast and Central America. They used chromium radiation as the source for some elements and tungsten radiation for the remainder. In their experiment, they analyzed

both ground powders of the obsidian and the flat surface of obsidian nodules. They determined that the difference between the two was insufficient to warrant the labor and possible contamination from the grinding process. It is interesting to note that they could not correlate any of the artifacts with the source materials they analyzed. This confirms the need for extensive source sampling, as discussed earlier.

Nelson *et al.* (1975) chose XRF as their analytical method because they wanted a rapid and efficient technique. They studied the effects of sample geometry and surface contamination. They concluded that sample geometry is critical only if quantitative concentrations are required. Because the characterization was based on source-to-source variation of relative intensities for peaks in the spectra they did not concern themselves with the geometry. Unfortunately this makes interlaboratory comparisons very difficult. Their study of how surface contamination and natural weathering processes affect the analysis was important because x-rays do not penetrate very far into a sample (e.g., for Nb, only 2 mm; for Fe, only 100 μm). They concluded that these were not serious problems. Their final conclusions indicated that the technique worked very well for characterization of sources and association of artifacts with those sources. With the help of a computer, several hundred artifacts could be analyzed in a week.

Robie and Preiss (1984) studied the Zr, Rb, and Sr content in obsidian using ED-XRF. To examine how thickness might effect the data, they measured the angle at which a minimum in the variation of intensity occurred and placed the irregularly shaped artifacts in such a way that the path lengths for the primary and analyte x-rays were constant. This helped to improve reproducibility and accuracy. They also examined the obsidian on very a small scale and found inhomogeneities. This prompted them to

recommend sample powdering or smoothing. Unfortunately the need to powder an artifact nullifies one of the key advantages of XRF, namely its non-destructiveness.

Giauque *et al.* (1993) developed a high-precision and non-destructive method of ED-XRF. They were able to improve the technique such that their method was good for both thick and thin samples and were also able to keep sample preparation to a minimum (this was accomplished by brushing the samples with strong bristles to remove dirt). They concerned themselves first with improving sensitivity by trying to reduce the spectral signal-to-background ratio. They also used a collimator to ensure that detector efficiencies would be nearly constant for any x-ray energy and not vary with sample position. Finally, they used an intensive six-step approach to calibrate the entire spectrometer system. This allowed them to measure concentrations for 16 different elements, 13 of which were trace elements, with a high degree of precision. The method developed is useful for analyzing and provenancing obsidian artifacts with great success.

X-ray fluorescence has several advantages and disadvantages. The advantage that is most often highlighted is that it is a non-destructive technique. This is an important selling point for archaeologists because their sample may be from a museum collection and cannot be destroyed, or there just may not be enough sample material to sacrifice in a destructive analysis. Several papers (including some mentioned above) have compared results between powdered and pressed samples and unmodified glass samples. They have universally concluded that the differences detected are not significant and thus little or no sample preparation should be required. Another advantage is that it is considered to be a relatively simple technique to perform, especially with the help of a computer, and yields results fairly quickly and inexpensively.

As with any analytical technique, XRF also has some disadvantages. One of the limitations is due to the nature of the technique itself. Because air absorbs the radiation of certain wavelengths, elements with an atomic number of less than 22 cannot be determined (Goffer, 1980). A number of elements with atomic number greater than 22 cannot be determined either, at least not with any precision. X-ray fluorescence is also a surface rather than a bulk technique: for one thing, the soft radiation used has shallow penetration into matter, and second, XRF radiation is also absorbed by solid matter on the way out (Goffer, 1980).

Another problem involves the samples themselves. Artifacts vary greatly in size and shape. This results in lower precision results for three reasons (Bouey, 1991). Firstly, the x-ray path lengths will vary from point to point in the specimen. Secondly, the surface features of an artifact can prevent a primary x-ray from reaching the specimen and analyte x-rays from leaving. Thirdly, the surface can alter the distance between the x-ray tube and the specimen. X-ray/detector geometry is also affected if the artifact sample does not fit comfortably in the sample holder. These problems can be lessened somewhat by using ratios rather than absolute concentrations, but this solution does not always work well and precludes interlaboratory comparisons.

Despite its problems, XRF remains one of the most frequently used techniques for obsidian provenance studies. At this point, the advantages of non-destructive analysis and low cost are benefits that many archaeologists feel outweigh the disadvantages.

Neutron Activation Analysis

Another technique that has been developed over the past 25 years is neutron activation analysis (NAA). One of the first papers on this topic (Gordus *et al.*, 1967)

reported on the use of NAA at the University of Michigan to examine a number of obsidian artifacts excavated from Hopewell sites in the Midwest. The study used a pneumatic tube system to place the samples in the reactor for a short irradiation. A sodium iodide detector coupled to a single-channel analyzer was subsequently used to detect the radiation for sodium and manganese in the samples. The results were compared to data for source samples from the western United States, Mexico, and Alaska. This comparison showed that the artifacts were most similar in composition to Obsidian Cliff in Wyoming, a source in Idaho, or a source in Mexico. The samples then underwent a long irradiation and were analyzed for another 15 elements. The results showed unequivocally that the artifacts were made of obsidian from the Obsidian Cliff source in Yellowstone National Park.

Gordus *et al.* (1968) followed their earlier work with a more detailed study of sources in the western United States. They analyzed source samples using both short and long irradiations. They found that most flows were homogeneous but that each flow was different from the others, sometimes by as much as 1000%. They concluded that neutron activation analysis was indeed a viable technique to match obsidian artifacts with obsidian sources.

The information gained from the University of Michigan studies was used by Frison *et al.* (1968) to analyze artifacts excavated from six sites in north-central Wyoming. The irradiation method that measured Na and Mn (the pneumatic tube or “short” irradiation) was used unless unambiguous separation of flows was not possible in which case they employed the long irradiation. They were able to assign each artifact to a group that corresponded to a source. One group of artifacts could not be correlated to

any known source at the time of analysis. This analysis showed yet again how NAA could be used quite successfully in obsidian provenancing studies.

Neutron activation analysis, like XRF, has both advantages and disadvantages. The most obvious disadvantage stems from the need for a nuclear reactor and experience with irradiation procedures. Because there are very few reactors around the country it is likely that a person seeking neutron activation analysis would have to travel to a reactor and ask permission to “use” some of the neutrons. Neutron activation analysis can also be very expensive, ranging from \$100 to \$150 per sample or possibly more. A third disadvantage stems from the nature of the technique. The analysis requires a piece of the artifact, and this piece becomes radioactive which usually prohibits its return to the archaeologist after analysis.

The advantages of NAA often outweigh the disadvantages. Unlike x-ray fluorescence, NAA is a bulk technique. This means that it obtains data from throughout the sample and not just the surface. Neutron activation analysis can measure a greater number of elements than XRF. Usually, more than twice as many elements can be determined. The data retrieved are also highly reproducible and the errors are small. Another advantage is that samples as small as five milligrams can be analyzed, which means that an artifact could be analyzed with a minimum of destruction.

In recent years, the possible expense of analysis has been tempered. Most of the cost came from the need to use two different irradiations to feel confident in the assignment of artifacts to sources. Work conducted at the Missouri University Research Reactor has shown that two irradiations on obsidian artifacts are not always necessary (Glascock *et al.*, 1994). The paper by Glascock *et al.* on obsidian sources in

Mesoamerica showed a success rate of greater than 90% when assigning artifacts to sources using only sodium and manganese, and occasionally the element barium, which is also determined by the short analysis. The need to perform only one irradiation greatly decreases time and cost.

The techniques mentioned above all attempt to correlate obsidian artifacts with obsidian sources. No matter which technique is used, it is essential that obsidian sources be sampled extensively. It is important to sample and analyze as many sources as possible in order to compile a large database to assist in the differentiation between sources and to make a confident assignment of artifacts to those sources.

As previously stated in Chapter 1, the creation of a large chemical database on the obsidian sources in Oregon is the main goal of this work. This database should provide a reference for archaeologists seeking information about artifacts from sites within Oregon.

CHAPTER 3 MATERIALS AND METHODS

Neutron activation analysis (NAA) is a commonly employed analytical technique in chemistry. In neutron activation analysis, a sample is bombarded by neutrons; some of the atoms in the sample absorb these neutrons. The absorption results in a nuclear reaction and formation of an excited intermediate nucleus. This intermediate nucleus emits gamma rays, called prompt gamma rays because they are emitted less than 10^{-14} seconds after the intermediate nucleus is formed (Ehmann and Vance, 1991). The result is usually production of a radioactive product nucleus that decays by emission of beta particles and gamma rays (Figure 3.1). In the vast majority of NAA work, the sample is monitored for the emission of characteristic gamma rays which help to identify the original target nucleus (i.e., element). The use of a high-resolution, high-purity germanium (HPGe) detector, a multi-channel analyzer, and spectrum analysis software help to identify the energy of each gamma ray detected and therefore the identity and quantity of the elements present in the sample.

It is possible to use different energies of neutrons to activate a sample, depending on the needs of the analysis (Figure 3.2). Thermal neutrons, which have a mean energy of 0.025 eV and induce neutron capture or (n, γ) reactions, are most commonly used. This is because the capture cross sections for thermal neutrons are quite large and provide good sensitivity for about two-thirds of the elements in the periodic table when these elements occur at very low concentrations. Thermal neutrons have been used to analyze samples coming from a number of disciplines in which data on trace elements are relevant. These include geochemistry, cosmochemistry, biology, environmental science,

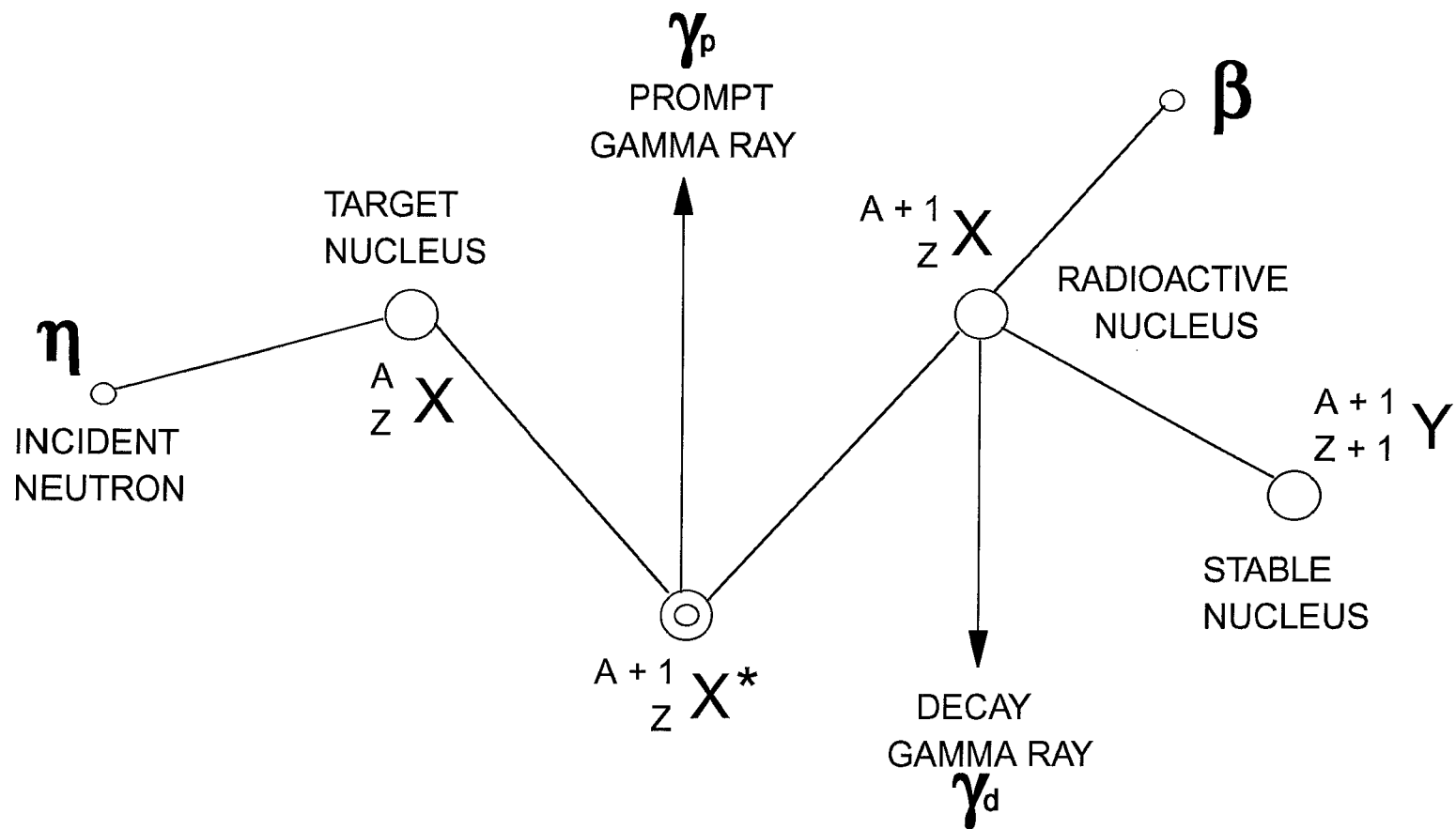


Figure 3.1: Activation of a nucleus by an incident neutron and the prompt and decay gamma rays which are emitted following neutron capture. (Adapted from Glascock, 1992)

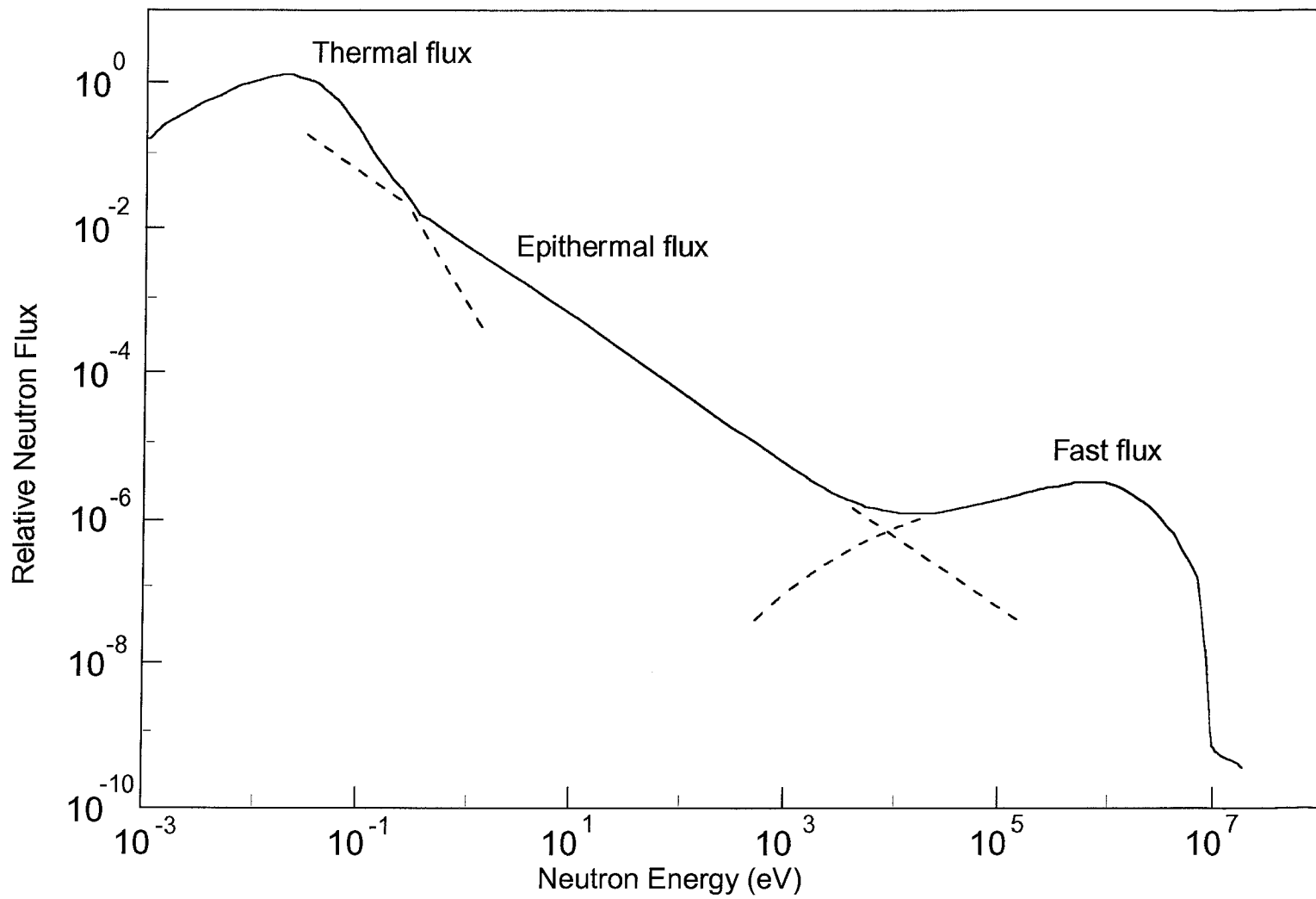


Figure 3.2: Graph showing energies of different neutron fluxes.

forensics, art, and archaeology (Ehmann and Vance, 1991).

Epithermal neutrons, those ranging in energy from 0.1 to 1 eV, also induce (n, γ) reactions. These neutrons are used to activate elements that might have higher cross sections for these more energetic neutrons relative to thermal neutrons and would normally be swamped by other elements well activated by thermal neutrons. Fewer than 25 elements can be enhanced by the use of epithermal neutrons only.

When performing neutron activation analysis, the cross sections and fluxes for both thermal and epithermal neutrons are used in all equations, unless otherwise noted. Fast neutrons, with energy of greater than 0.5 MeV, are rarely used for trace-element analysis (Ehmann and Vance, 1991).

Once the elements within a sample are identified by their gamma rays, it is possible to use a peak fitting program to determine peak area. Peak area is used to determine the amount of an element in the sample. The full standard equation used in neutron activation analysis is

$$C = \frac{WA\theta\sigma(E_n)\phi(E_n)\gamma(1 - e^{-\lambda t_i})e^{-\lambda t_d}(1 - e^{-\lambda t_c})\varepsilon(E_\gamma, g)}{M\lambda} \quad (1)$$

where:

C = counts registered;
 W = weight of target element;
 A = Avogadro's number;
 θ = abundance of target isotope;
 $\sigma(E_n)$ = reaction cross-section;
 $\phi(E_n)$ = flux of neutrons;
 E_n = energy of neutrons;
 γ = gamma-ray branching factor;
 t_i = irradiation time;
 t_d = decay time;
 t_c = counting time;
 $\varepsilon(E_\gamma, g)$ = detector efficiency;

g = counting geometry factor;
 E_γ = gamma-ray energy;
 M = atomic weight of element;
 λ = decay constant ($\ln(2/T_{1/2})$); and
 $T_{1/2}$ = half-life of product radioisotope.

The energies, fluxes, and cross-sections shown in Equation 1 combine the numbers for both the thermal and epithermal neutrons in the following manner:

$$\sigma(E_n)\phi(E_n) = [\sigma_{th}\phi_{th} + I_o\phi_{epi}] \quad (2)$$

where:

σ_{th} = capture cross-section for thermal neutrons
 ϕ_{th} = thermal neutron flux
 I_o = resonance (epithermal neutron) cross-section
 ϕ_{epi} = epithermal neutron flux.

Most analyses for trace elements do not use the activation equation to calculate concentration. It is much more common to use a standard comparator method. In the standard comparator method, a standard containing known amount(s) of the element(s) of interest is irradiated with the sample. Element concentrations in the unknown sample are determined by ratioing the decay-corrected activities per unit weight in the unknown sample to those for the reference standard.

In general, it is required that variables such as the irradiation position, neutron flux, and irradiation time be the same for both the sample and the standard. The laboratory at the Missouri University Research Reactor (MURR) makes several assumptions which greatly simplify Equation 1. The same isotope of an element is measured in both the sample and the standard. This allows for a number of cancellations of variables in Equation 1 because those variables are the same for both sample and standard. These variables are θ , λ , A , M , γ , and $\sigma(E_n)$. Other variables will be cancelled

out because the sample and the standard undergo the same irradiation and counting parameters. These variables are $\phi(E_n)$, $(1-e^{-\lambda t_i})$, $(1-e^{-\lambda t_c})$, and $\varepsilon(E_\gamma, g)$. The final equation is as follows:

$$\frac{R_{std}}{R_{sam}} = \frac{W_{std} (e^{-\lambda t_{d1}})_{std}}{W_{sam} (e^{-\lambda t_{d2}})_{sam}} \quad (3)$$

where:

R = counting rate for a characteristic peak in sample or standard;

W = mass of element in sample or standard; and

$t_{d\#}$ = decay time (Ehmann and Vance, 1991).

When t_{d1} is equal to t_{d2} , as in the short irradiation (see below), those parameters of the equation cancel out. They do not cancel out in the long irradiation because the samples are counted at different times.

Neutron activation analysis has several advantages that make it useful for trace element analysis. NAA can provide very high sensitivity for many elements; NAA based on thermal neutrons can determine the amounts of elements at or below the ppm level. It is also possible to change certain parameters, e.g., the energy and flux of the neutrons and the times of irradiation and decay, in order to selectively increase the sensitivity for particular elements. NAA also saves time because it can perform simultaneous multi-element analysis. The data provided are independent of the matrix and sample preparation is kept to a minimum (e.g., no need to powder or dissolve samples). Because there is much less sample handling there is much less chance of contamination, which is important for trace element work (Ehmann and Vance, 1991). Finally, neutron activation analysis is an instrumental method which helps improve accuracy and precision and reduces labor.

All of the advantages above are also criteria that must be filled by any analytical method applied to archaeometry (Kuleff and Djingova, 1990). The ability to analyze up to 30 elements is very important because it is not known *a priori* which elements will give the best separation between sources of obsidian. The larger the number of elements determined the easier it is to look for and see a separation between sources.

Archaeologists operate under the assumption that the obsidian from one source is most likely homogeneous within but different from all other sources. However, the differences in the content of many elements between sources is often small and therefore the high sensitivity, accuracy, and precision of neutron activation analysis are beneficial.

Laboratory Methods Employed at MURR

Obsidian samples analyzed in this study were obtained from a number of people. Source rocks from several sources were collected by people outside the laboratory at MURR. Craig Skinner, Tom Jackson, Dorothy Freidel, and James Woods all contributed source material. Other source material was collected by the author on a sampling trip in June of 1996. Table 3.1 lists each obsidian source, its approximate location in Oregon, the number of samples analyzed, and the person who provided samples from that source. The artifacts from the Robins Spring site were provided by John Zancanella of the Oregon Bureau of Land Management.

After samples arrived in the lab they are inventoried and washed with a brush and distilled water to remove surface dirt and contamination. A minimum of six pieces was chosen from those collected to represent each sampling location, or in the case where there was only one sampling location at a source, that source. If variability was suspected, additional samples were prepared. Each sample was given a 5

Table 3.1. List of Oregon obsidian sources analyzed and their approximate locations.

Source Name	Source Group	USGS Map	Location	Number of Samples	Person(s) Collecting Sam.
Auger Creek	HGMOR	Hager Mountain 7.5	Lake County T30S, R14E, Sec. 9	12	Skinner, Jackson
Big Obsidian Flow (Newberry Caldera)	BOFOR	East Lake 7.5	Deschutes County T22S, R12E, Sec. 1	8	Jackson
Brooks Canyon	BRCOR	Benjamin Lake 7.5	Lake County T23S, R20E, Sec. 13	12	Skinner, Ambroz, Glascock
Buck Springs	BSOR	Buck Springs 7.5	Harney County T20S, R25E, Sec. 33 T21S, R25E, Sec. 3	12	Skinner, Ambroz, Glascock
Buried Obs. Flow (Newberry Caldera)	BUFOR	East Lake 7.5	Deschutes County	12	Jackson
Burns Area	BUOR	Burns Butte 7.5	Harney County T23S, R30E, Sec. 20	12	Jackson
Burns- Rimrock	BRROR	Burns Butte 7.5	Harney County T22S, R30E, Sec. 32	6	Jackson
Burns- Willow Flat	BUOR, BSOR, DLORB	Burns Butte 7.5	Harney County T23S, R29E, Sec. 1	6	Jackson
Burns Butte	BUOR	Burns Butte 7.5	Harney County T23S, R30E, Sec. 20	12	Skinner
Chickahominy Reservoir	CHYOR	Riley 7.5	Harney County T23S, R26E, Sec. 28	12	Skinner, Ambroz, Glascock
Cougar Mountain	CGMOR	Cougar Mtn. 7.5	Lake County T25S, R15E, Sec. 14	17	Freidel, Jackson

Table 3.1 continued

Source Name	Source Group	USGS Map	Location	Number of Samples	Person(s) Collecting Sam.
Deer Creek	DCOR	Chemult 7.5	Klamath County T27S, R7E, Sec. 13	6	Skinner
Delintment Lake	DLORA DLORB BSOR	Delintment Lk. 7.5 Big Mowich Mtn. 7.5 Donnelly Butte 7.5	Harney County Ochoco Nat'l Forest T19S, R25E, Sec. 26 T19S, R26E, Sec. 33 T20S, R26E, Sec. 4	24	Skinner, Ambroz, Glascock
Dog Hill	DHOR	Holmes Canyon 7.5	Harney County T22S, R29E, Sec. 17/7	6	Ambroz, Glascock
East Lake Flow (Newberry Crater)	ELOR	East Lake 7.5	Deschutes County T21S, R13E, Sec. 28/32	12	Jackson
Game Hut Flow (Newberry Crater)	GHFOR	East Lake 7.5	Deschutes County T21S, R13E, Sec. 31/32	8	Jackson
Glass Buttes	GBORA-GBORG	Glass Butte 7.5 Hat Butte 7.5 Round Top Butte 7.5	Lake County NE corner	203	Skinner, Ambroz, Glascock
Hager Mountain	HGMOR	Hager Mountain 7.5	Lake County T30S, R14E, Sec. 11	10	Skinner, Jackson
Holmes Canyon	BSOR DLORB	Holmes Canyon 7.5	Harney County Ochoco Nat'l Forest T21S, R28E, Sec. 26/35	15	Ambroz, Glascock
Horse Mountain	HMOR	Horse Mountain 7.5	Lake County T28S, R22E, Sec. 18	16	Woods, Jackson
Inman Creek	INCORA INCORB	Veneta 7.5	Lane County T17S, R6W, Sec. 1	12	Skinner
Interlake Flow (Newberry Crater)	GHFOR	East Lake 7.5	Deschutes County T21S, R12E, Sec. 25	8	Jackson

Table 3.1 continued

Source Name	Source Group	USGS Map	Location	Number of Samples	Person(s) Collecting Sam.
Juniper Springs	GBORA, GBORC TO GBORE, GBORG, BSOR	G. I. Ranch 7.5	Crook County T21S, R22E, Sec. 1	12	Skinner
Nicoll Creek	BSOR	Camp Currey Spring 7.5	Harney County Ochoco Nat'l Forest T21S, R25E, Sec. 32	12	Ambroz, Glascoek
Parish Cabin Campground	PCCA, PCCB, WWR	Big Canyon 7.5	Grant County T16S, R33E, Sec. 16	15	Jackson
Plumber Spring	BSOR DLORA DLORB	Donnelly Butte 7.5	Harney County Ochoco Nat'l Forest T20S, R26E, Sec. 23/26	14	Ambroz, Glascoek
Quartz Mountain	QMOR	Firestone Butte 7.5	Deschutes County T22S, R15E, Sec. 26	9	Jackson
Riley	RIOR	Capeheart Lake 7.5	Harney County T24S, R27E, Sec. 19	18	Skinner, Ambroz, Glascoek, Jackson
Rough Creek	BSOR	Camp Currey Spring 7.5	Harney County Ochoco Nat'l Forest T21S, R25E, Sec. 21/28	12	Skinner, Ambroz, Glascoek
Sawmill Creek	BSOR	Buck Spring 7.5	Harney County Ochoco Nat'l Forest T20S, R25E, Sec. 22/26	12	Skinner, Ambroz, Glascoek
Silver Lake	SVLOR	Partin Butte 7.5 or Sycan Marsh West 7.5	Lake County T30S, R13E, Sec. 1	6	Jackson
Surveyor Spring	SSOR	Collins Rim 7.5 or May Lake 7.5	Lake County T41S, R23E, Sec. 11/14	9	Jackson

Table 3.1 continued

Source Name	Source Group	USGS Map	Location	Number of Samples	Person(s) Collecting Sam.
Sycan Marsh	SVLOR	Partin Butte 7.5 or Sycan Marsh West 7.5	Lake County T31S, R13E, Sec. 34	6	Jackson
Tucker Hill	THOR	Tucker Hill 7.5	Lake County T34S, R19E, Sec. 25/36	22	Freidel
Venator	VENOR	McEwen 7.5	Malheur County T24S, R37E, Sec. 16	6	Skinner
Whitewater Ridge	WWROR WCOR	Jump-Off Joe Mtn. 7.5 Big Canyon 7.5	Grant County T17S, R33E, Sec. 6/8, T17S, R32E, Sec. 12	20	Skinner
Wolf Creek	WCOR	Jump-Off Joe Mtn. 7.5 Magpie Table 7.5	Grant County T17S, R33E, Sec. 26/27	6	Skinner
Yreka Butte	YBOR	Benjamin Lake 7.5	Lake County T23S, R20E, Sec. 4 Deschutes County, T22S, R20E, Sec. 33	30	Ambroz, Glascock

or 6 character ID. The first two or three characters are letters corresponding to the name of the source (e.g., AC to indicate Auger Creek). The three remaining characters are numbers, starting with 001 for each source and continuing to 006 or higher, as needed.

Source rocks chosen for analysis were wrapped in a paper towel and crushed into smaller pieces between two steel plates in order to obtain clean interior fragments. Only interior fragments were used for the irradiations. Artifacts were washed in distilled water and a small portion was removed with a trim saw. This piece was also crushed into smaller fragments for irradiation.

Samples were analyzed by two irradiations and three counts. The first irradiation is termed the “short” irradiation. Short irradiation samples were prepared by weighing approximately 100 mg of obsidian pieces into a 2/5-dram high-density polyethylene vial. Pieces were fixed to the bottom using clean styrofoam plugs and the vial was capped. Vials were placed into rabbits two at a time and irradiated sequentially in the pneumatic tube system at the Missouri University Research Reactor. They were irradiated for five seconds at a neutron flux of 8×10^{13} n/cm²/s. This was followed by a 25-minute decay and a 12-minute count using a high-purity germanium detector with 25% efficiency and standard counting software. Uniform counting geometry was ensured by a special sample holder. The sample holder allowed placement of a magnetic stir bar and a magnetic stirrer under the sample to provide continuous rotation during measurement. Elements measured in the short irradiation are Ba, Cl, Dy, K, Mn, and Na. Figure 3.3 shows an example of a gamma spectrum from the short irradiation.

The second irradiation is termed the “long” irradiation. Long irradiation samples of approximately 300 mg were placed in high-purity quartz vials and sealed by an oxygen

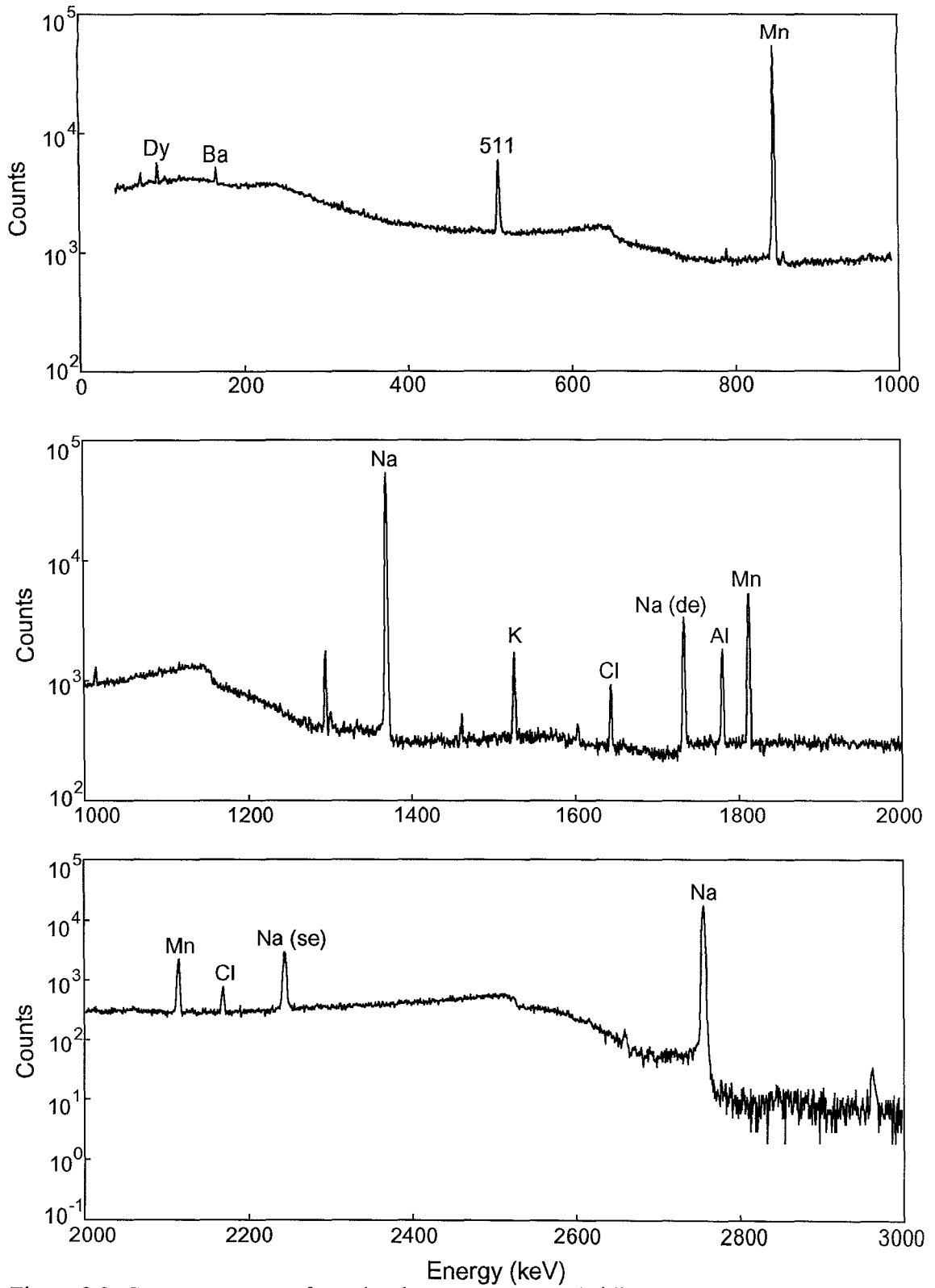


Figure 3.3: Gamma spectrum from the short count on an obsidian specimen showing peaks for various elements. The vertical scale is logarithmic.

torch under vacuum. Thirty samples and six standards were rolled up in aluminum foil bundles and two bundles were placed in an aluminum can. The cans were irradiated near the core for 70 hours in a neutron flux of 5×10^{13} n/cm²/s and rotated continuously to reduce the effects of the reactor's radial flux gradient across the bundles. After 7-8 days of decay, the sample vials were washed in aqua regia to remove surface contamination. Sample vials were then placed in test tubes and loaded on an automatic sample changer coupled to a high-purity germanium detector with 20% efficiency and multi-channel analyzer. The samples were counted a first time for 2,000 seconds each. The elements measured in this "mid-count" are Ba, La, Lu, Nd, Sm, U, and Yb. Figure 3.4 shows an example of a gamma spectrum from the "middle count." Another count was made after about 4-5 weeks decay for 10,000 seconds. Elements measured in the "long count" are Ce, Co, Cs, Eu, Fe, Hf, Rb, Sb, Sc, Sr, Ta, Tb, Th, Zn, and Zr. Figure 3.5 shows an example of a gamma spectrum from the "long count." Table 3.2 lists the nuclear parameters for all elements measured following short and long irradiations.

After the data are collected, the standard comparator method, as described above, was used to determine the concentrations of the elements present in the samples. Standards used for the short irradiation were SRM-278 Obsidian Rock as a primary standard and SRM-1633a Flyash as a secondary standard. Standards used in the long irradiation were the same. See Glascock and Anderson (1993) for a more complete description of the standards. Also see Table 3.3 for a list of elemental concentrations in the standard reference materials.

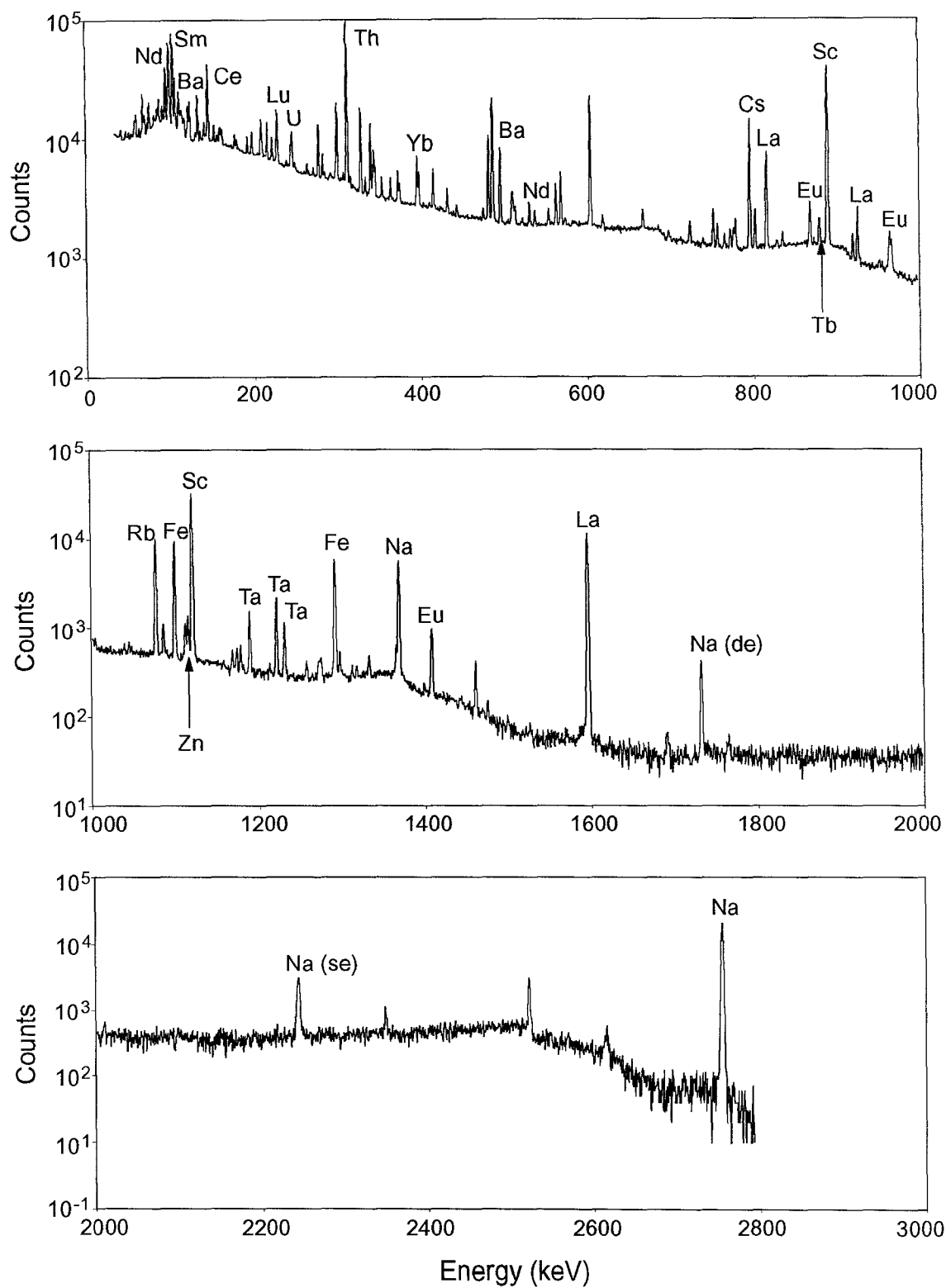


Figure 3.4: Gamma spectrum from the middle count on an obsidian specimen showing peaks for various elements. The vertical scale is logarithmic.

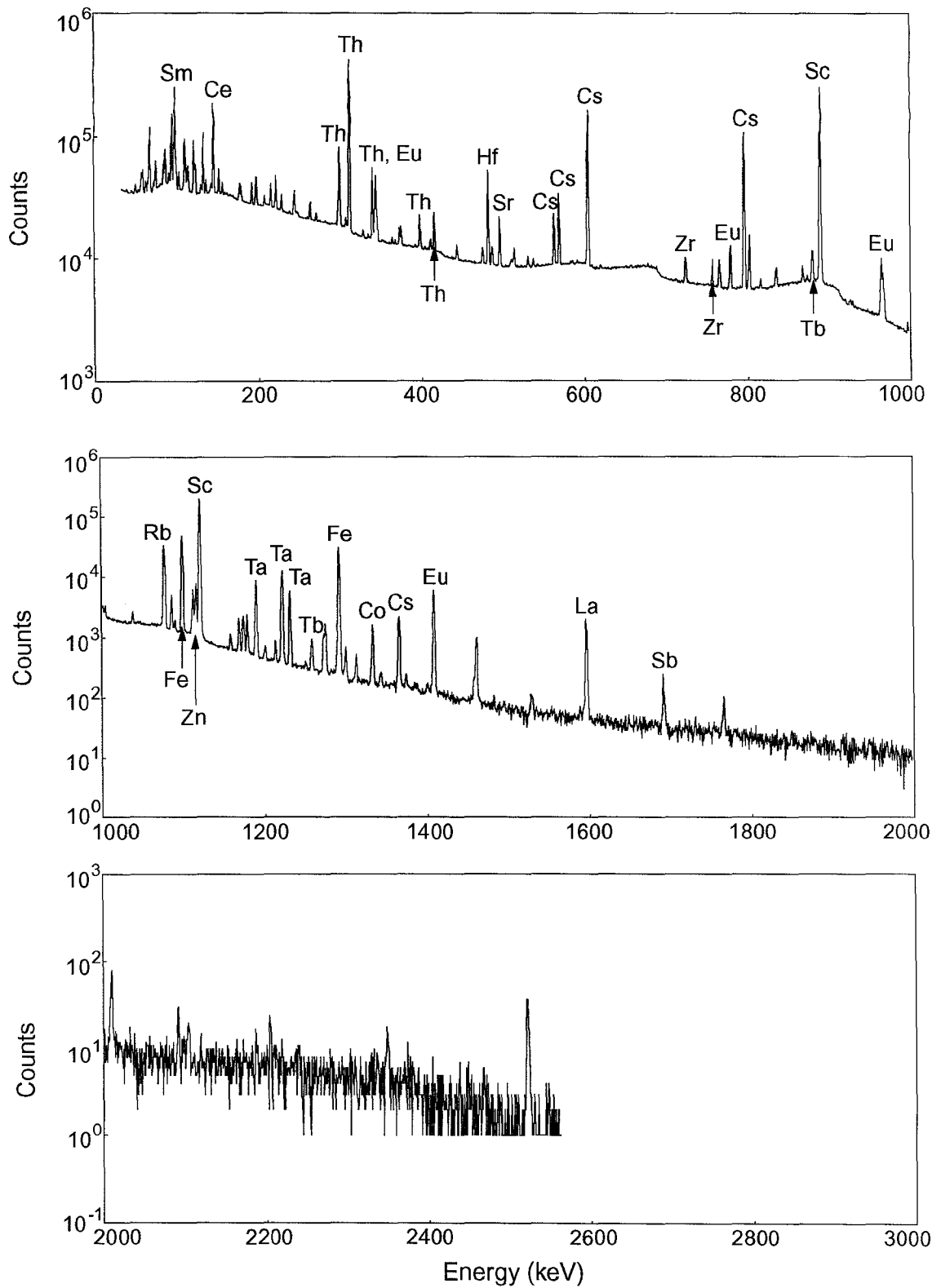


Figure 3.5: Gamma spectrum from the long count on an obsidian specimen showing peaks for various elements. The vertical scale is logarithmic.

Table 3.2: Nuclear Parameters for Radionuclides used at MURR in the Analysis of Obsidian by Neutron Activation Analysis

Element	Radionuclide	Measured Half-life	Gamma Energy (keV)
Barium	Ba-139	84.6 m	165.8
Cerium	Ce-141	32.5 d	145.4
Chlorine	Cl-38	37.24 m	1642.7
Cobalt	Co-60	5.27 y	1332.5
Cesium	Cs-134	2.06 y	795.8
Dysprosium	Dy-165	2.33 h	94.7
Europium	Eu-152	13.3 y	1408.0
Iron	Fe-59	44.5 d	1099.2
Hafnium	Hf-181	42.4 d	482.2
Potassium	K-42	12.4 h	1524.6
Lanthanum	La-140	40.3 h	1596.2
Lutetium	Lu-177	6.71 d	208.4
Manganese	Mn-56	2.58 h	846.8
Sodium	Na-24	15.0 h	1368.6
Neodymium	Nd-147	11.0 d	91.1
Rubidium	Rb-86	18.7 d	1076.6
Antimony	Sb-124	60.2 d	1691.0
Scandium	Sc-46	83.8 d	889.3
Samarium	Sm-153	46.3 h	103.2
Strontium	Sr-85	64.8 d	514.0
Tantalum	Ta-182	114. d	1221.4
Terbium	Tb-160	72.3 d	879.4
Thorium	Pa-233	27.0 d	312.0
Uranium	Np-239	2.36 d	228.2
Ytterbium	Yb-175	4.19 d	396.3
Zinc	Zn-65	244. d	1115.6
Zirconium	Zr-95	64.0 d	756.7

Table 3.3: Element concentrations in standards used in NAA procedures at MURR. All values in parts per million unless otherwise noted.

Element	Conc. in SRM-278 (obsidian rock)	Conc. in SRM-1633a (fly ash)	Counting Procedure
Barium	881	1320	short
Chlorine	640	----	short
Dysprosium	6.27	14.6	short
Potassium (%)	3.45	1.89	short
Manganese	401	190	short
Sodium (%)	3.52	0.165	short
Barium	881	1320	mid
Lanthanum	30.1	79.1	mid
Lutetium	0.682	1.075	mid
Neodymium	25.4	75.7	mid
Samarium	5.80	16.83	mid
Uranium	4.46	10.3	mid
Ytterbium	4.50	7.50	mid
Cerium	61.4	168.3	long
Cobalt	1.44	44.1	long
Cesium	5.10	10.42	long
Europium	0.766	3.58	long
Iron (%)	1.398	9.38	long
Hafnium	8.09	7.29	long
Rubidium	126	134	long
Antimony	1.60	6.15	long
Scandium	4.96	38.6	long
Strontium	64.0	835	long
Tantalum	1.24	1.93	long
Terbium	0.951	2.53	long
Thorium	11.65	24.0	long
Zinc	54.0	220	long
Zirconium	290	240	long

CHAPTER 4 RESULTS AND DISCUSSION

Data collected using the techniques outlined in the previous chapter were tabulated and organized using the LOTUS 1-2-3 spreadsheet program. The spreadsheet data were converted into dBase format, which allowed incorporation of descriptive data for each specimen. This dBASE file was converted into GAUSS data sets, which are compatible with GAUSS language statistical programs written by Dr. Hector Neff of MURR.

Subgroup structure in the data was identified primarily by examining a series of bivariate plots within the GAUSS environment. In these bivariate plots, confidence ellipses are drawn at a constant Mahalanobis distance from the group centroids. In most cases, the confidence ellipse indicates the Mahalanobis distance corresponding to a p-value of 5% for membership in the group.

The examination found that the incompatible elements (i.e., K, Rb, Sr, Zr, Cs, Ba, the REE's, Hf, Th, and U) usually best reveal structure in the data set. The incompatibles are elements which do not substitute into the structures of early crystallizing minerals. This is usually because their ionic radii are too large or they are too highly charged to enter the crystal structure (Philpotts, 1990). Therefore, as the magma is evolving the incompatible elements are preferentially concentrated in the liquid phase.

The distribution of the trace elements between phases is described by the partition coefficient, K_D (Rollinson, 1993). If the K_D is greater than one, the element gets concentrated in the mineral structure (i.e., compatible), but if the K_D is less than one, the element gets concentrated in the melt (i.e., incompatible). The K_D is influenced by a

number of variables, including composition, temperature, pressure, oxygen activity, crystal chemistry, and the water content of the melt. Trace elements are useful to a geological study because their distribution is controlled in a fairly predictable way by geological processes such as partial melting or crystal fractionation.

Geologists employ trace elements in many studies of geological processes. Trace elements have an advantage over the major elements when modeling or tracing processes (e.g., fractional crystallization) because they are partitioned more strongly into either phase than the major elements (Drake and Weill, 1975). This makes the trace elements more sensitive as indicators of the degree and mechanism of differentiation. Geologists devote a significant portion of research to the investigation of the partition coefficients of the trace elements and how they are affected by the factors mentioned above (e.g., Blundy and Wood, 1991; Drake and Weill, 1975; Green and Pearson, 1983; Green and Pearson, 1985; Hildreth, 1981).

The processes studied by geologists are important to the formation of obsidians. Because different conditions and processes can change the K_D of elements, the concentrations of the incompatible and other trace elements may be changed with each eruption resulting in flows/domes with slightly to extremely different concentrations. Because no two volcanic centers will likely have the same conditions, such differences in concentrations explain why archaeologists can successfully use chemical analysis to distinguish between sources as well as compare artifacts to sources with successful attribution.

Each of the following sections is devoted to examining and discussing the data produced from the analysis of the source samples. The divisions made between sections

are based generally on geographical boundaries. Each section will begin with an introduction to the general area and then move on to a discussion of the results.

Malheur National Forest

Introduction

Three areas within the Malheur National Forest (MNF) were sampled. The areas fall mainly within the southeastern portions of Grant County but can be slightly extended to include northeastern Harney County (for a map of the general area see Figure 4.1a). The geology of the Malheur National Forest is dominated by the "Strawberry Volcanics" zone as described by Brown and Thayer (1966). The Strawberry Volcanics zone is named for Strawberry Mountain and covers a fairly large range. The lava flows associated with it erupted from a number of vents in the area of Strawberry and Lookout Mountains. Apparently an ash-flow tuff, Brown and Thayer (1966) described the Strawberry Volcanics as "...mostly medium to pale gray basaltic andesite. Ranges from olivine basalt at the base to dacite and rhyolite at the top." It is this rhyolite, in the form of obsidian, which was sampled.

Results and Discussion

Samples were obtained from Whitewater Ridge, Wolf Creek, and Parish Cabin Campground (for a map of the sampling areas see Figure 4.1b). Data are shown in Tables 4.1-4.4. The Parish Cabin Campground collection site is a secondary source locale, i.e., source samples were collected from stream gravels and valley alluvial fill. The Whitewater Ridge and Wolf Creek collection sites are primary source locales. Samples collected from these three areas resulted in four different chemical groups as shown in Figures 4.2a (Th vs. Eu) and 4.2b (Eu vs. Rb). The Whitewater Ridge chemical group consists of 18 samples from the Whitewater Ridge area and 7 samples from Parish Cabin Campground. The Wolf Creek chemical group consists of six samples from Wolf

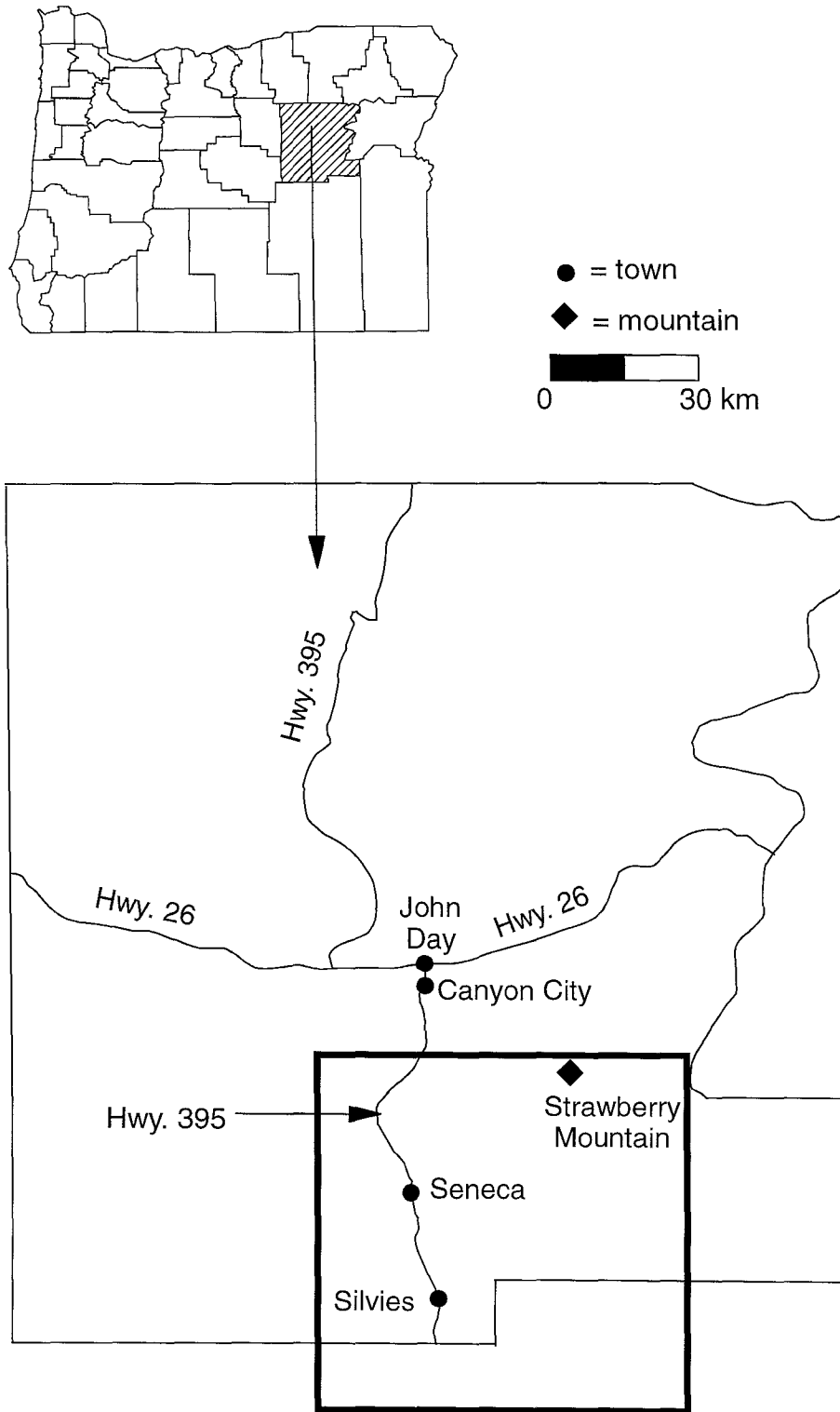


Figure 4.1a: Map showing Grant County, Oregon. See Figure 4.1b for enlargement of area in rectangle.

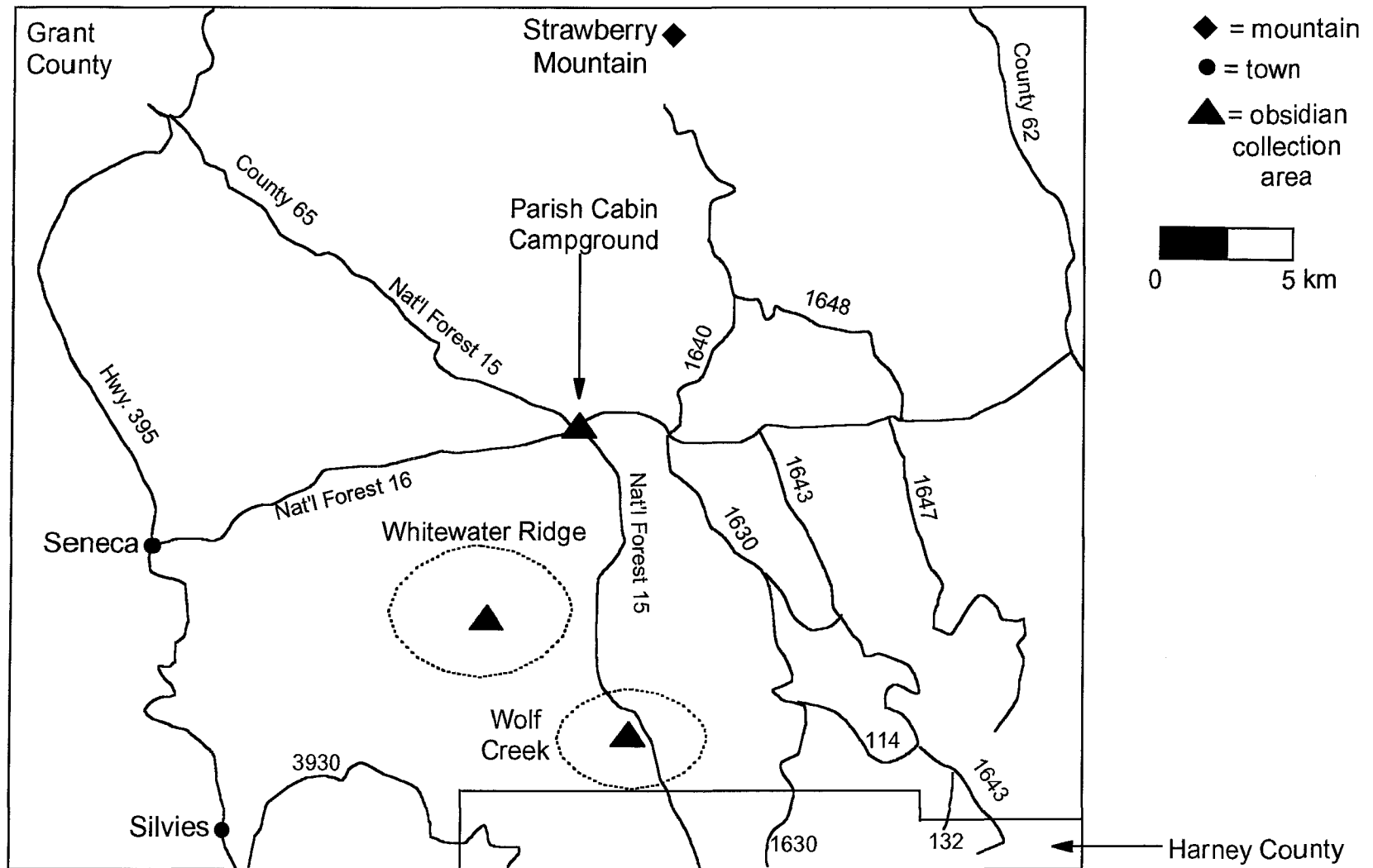


Figure 4.1b: Enlargement of rectangle in Figure 4.1a showing obsidian collection areas in the Malheur National Forest.

Table 4.1: Descriptive Statistics for Whitewater Ridge, Malheur National Forest.

Element	Mean	St. Dev.	% St. Dev.	No. Obs.	Minimum	Maximum
BA	1480	60.	4.36	25	1340	1580
LA	25.6	1.0	4.13	25	24.2	27.1
LU	0.378	0.010	2.52	25	0.360	0.395
ND	24.3	5.7	23.4	25	11.0	32.9
SM	3.75	0.12	3.06	25	3.59	3.92
U	5.25	1.40	26.6	25	3.50	9.34
YB	2.28	0.12	5.08	25	2.11	2.49
CE	48.6	1.7	3.55	25	45.6	50.8
CO	0.545	0.174	32.0	25	0.338	0.788
CS	5.35	0.06	1.10	25	5.25	5.48
EU	0.476	0.037	7.76	25	0.414	0.524
FE	6970	700	9.98	25	6110	7970
HF	3.90	0.22	5.57	25	3.61	4.26
RB	113	2	1.80	25	109	118
SB	0.677	0.037	5.42	25	0.616	0.749
SC	3.32	0.16	4.96	25	3.01	3.55
SR	75.9	15.8	20.9	25	44.1	104
TA	0.786	0.026	3.31	25	0.753	0.837
TB	0.589	0.071	12.1	25	0.463	0.694
TH	9.17	0.20	2.18	25	8.80	9.48
ZN	39.2	7.3	18.6	25	17.7	47.9
ZR	141	13	9.18	25	118	167
CL	201	28	14.0	25	155	265
DY	3.52	0.25	7.15	25	3.18	4.12
K	35300	1600	4.58	25	33100	38400
MN	234	11	4.62	25	217	253
NA	27600	460	1.66	25	26800	28300

ANIDs of specimens included:

PCC002	PCC004	PCC006	PCC008	PCC010	PCC012	PCC013	WWR001
WWR002	WWR003	WWR004	WWR005	WWR006	WWR007	WWR008	WWR009
WWR010	WWR011	WWR012	WWR013	WWR014	WWR017	WWR018	WWR019
WWR020							

Note: Element concentration values available for individual samples upon request. This applies to all following data tables.

Table 4.2: Descriptive Statistics for Wolf Creek, Malheur National Forest.

Element	Mean	St. Dev.	% St. Dev.	No. Obs.	Minimum	Maximum
BA	1030	5	0.48	8	1020	1040
LA	27.8	0.3	1.13	8	27.3	28.2
LU	0.409	0.008	1.95	8	0.395	0.421
ND	25.5	3.6	14.2	8	19.1	32.1
SM	4.11	0.06	1.49	8	4.05	4.21
U	4.75	0.60	12.6	8	3.90	5.67
YB	2.33	0.05	2.28	8	2.27	2.41
CE	52.7	0.90	1.71	8	51.7	54.2
CO	0.224	0.010	4.34	8	0.210	0.235
CS	5.75	0.05	0.80	8	5.68	5.80
EU	0.344	0.007	2.02	8	0.334	0.352
FE	5570	50.	0.91	8	5510	5670
HF	3.49	0.04	1.18	8	3.44	3.57
RB	120.	1	1.00	8	119	123
SB	0.727	0.014	1.95	8	0.704	0.753
SC	3.13	0.04	1.22	8	3.09	3.20
SR	33.9	8.9	26.2	8	21.8	46.5
TA	0.861	0.010	1.16	8	0.848	0.875
TB	0.580	0.078	13.4	8	0.518	0.716
TH	10.0	0.1	1.09	8	9.88	10.2
ZN	34.7	1.2	3.52	8	33.3	36.8
ZR	116	5	4.07	8	109	124
CL	206	29	14.1	8	158	236
DY	3.97	0.25	6.30	8	3.65	4.38
K	37500	950	2.54	8	36100	39300
MN	236	5	2.14	8	230.	246
NA	27700	260	0.96	8	27200	28100

ANIDS of specimens included:

WWR015 WWR016 WC001 WC002 WC003 WC004 WC005 WC006

Table 4.3: Descriptive Statistics for Parish Cabin Campground A, Malheur National Forest

Element	Mean	St. Dev.	% St. Dev.	No. Obs.	Minimum	Maximum
BA	886	5	0.58	3	881	891
LA	24.5	0.2	0.84	3	24.3	24.7
LU	0.385	0.024	6.17	3	0.358	0.404
ND	17.3	0.5	3.09	3	17.0	18.0
SM	4.19	0.05	1.12	3	4.14	4.24
U	0.790	0.705	89.3	3	0.364	1.60
YB	2.05	0.03	1.45	3	2.02	2.08
CE	47.2	0.4	0.78	3	46.9	47.6
CO	15.3	0.1	0.70	3	15.2	15.4
CS	1.09	0.04	3.52	3	1.05	1.12
EU	1.16	0.01	1.10	3	1.15	1.18
FE	39600	420	1.06	3	39100	39900
HF	4.38	0.03	0.65	3	4.35	4.41
RB	39.6	0.59	1.48	3	38.9	40.0
SB**				0		
SC	14.9	0.2	1.65	3	14.7	15.2
SR	427	14	3.36	3	415	443
TA	0.606	0.042	6.89	3	0.569	0.651
TB	1.15	0.07	5.83	2	1.10	1.20
TH	3.20	0.04	1.28	3	3.18	3.25
ZN	80.7	0.6	0.70	3	80.3	81.3
ZR	174	10.	5.48	3	164	183
CL	187	63	33.8	3	131	255
DY	3.96	0.41	10.2	3	3.62	4.41
K	17200	870	5.05	3	16200	17900
MN	850.	5	0.58	3	844	854
NA	28000	190	0.69	3	27800	28200

ANIDs of specimens included:

PCC001 PCC003 PCC007

**Values not available because element concentrations below detection limit.

Table 4.4: Descriptive Statistics for Parish Cabin Campground B, Malheur National Forest

Element	Mean	St. Dev.	% St. Dev.	No. Obs.	Minimum	Maximum
BA	831	9	1.13	2	824	838
LA	20.0	0.1	0.52	2	19.9	20.0
LU	0.441	0.030	6.71	2	0.420	0.462
ND	15.4	0.02	0.11	2	15.4	15.4
SM	4.19	0.02	0.37	2	4.18	4.20
U**				0		
YB	1.98	0.03	1.42	2	1.96	2.00
CE	38.9	0.5	1.39	2	38.5	39.3
CO	14.9	0.2	1.30	2	14.8	15.1
CS	1.01	0.003	0.27	2	1.01	1.01
EU	1.27	0.01	0.98	2	1.26	1.28
FE	48000	170	0.36	2	47900	48100
HF	3.66	0.08	2.12	2	3.60	3.71
RB	38.6	0.1	0.18	2	38.5	38.6
SB	0.207	0.047	22.7	2	0.174	0.241
SC	17.5	0.5	2.97	2	17.2	17.9
SR	517	88	17.1	2	454	579
TA	0.458	0.018	3.89	2	0.445	0.470
TB**	1.237			1	1.24	1.24
TH	2.67	0.01	0.53	2	2.66	2.68
ZN	92.7	2.2	2.37	2	91.1	94.2
ZR	147	11	7.44	2	140.	155
CL	134	11	8.25	2	126	142
DY	3.88	0.06	1.41	2	3.84	3.92
K	14600	2070	14.2	2	13200	16100
MN	946	25	2.66	2	928	964
NA	27200	150	0.55	2	27100	27300

ANIDs of specimens included:

PCC009 PCC011

**Values not available because element concentrations below detection limit.

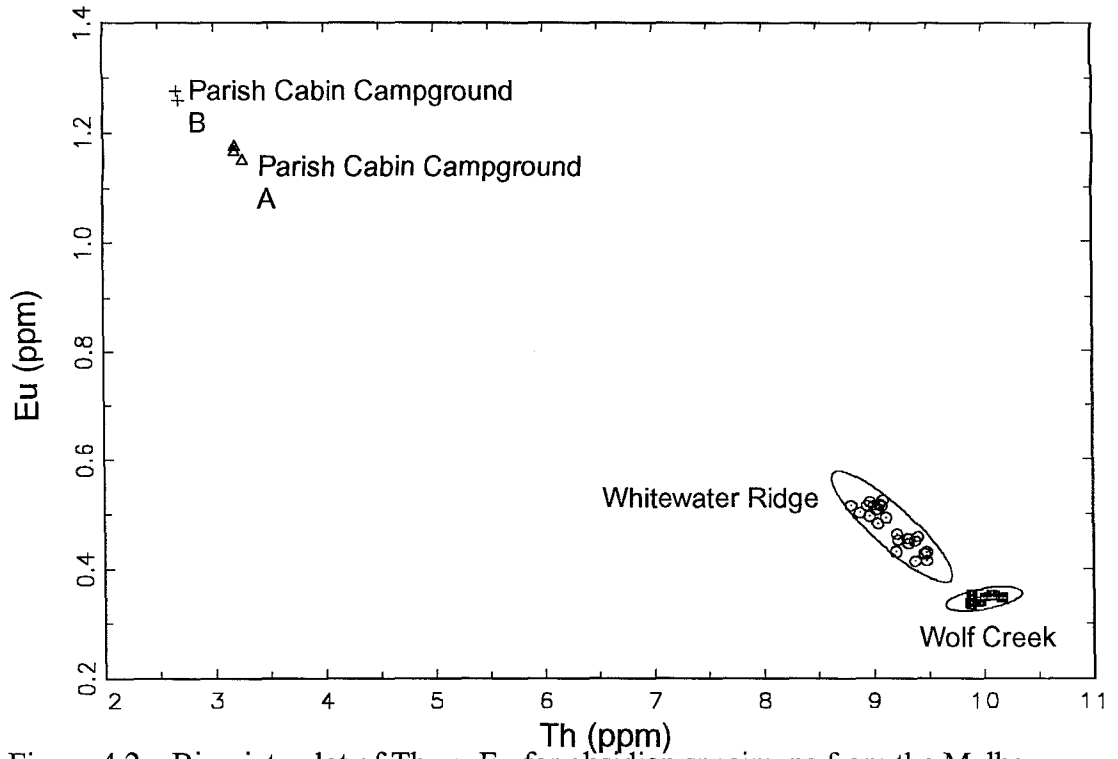


Figure 4.2a: Bivariate plot of Th vs. Eu for obsidian specimens from the Malheur National Forest.

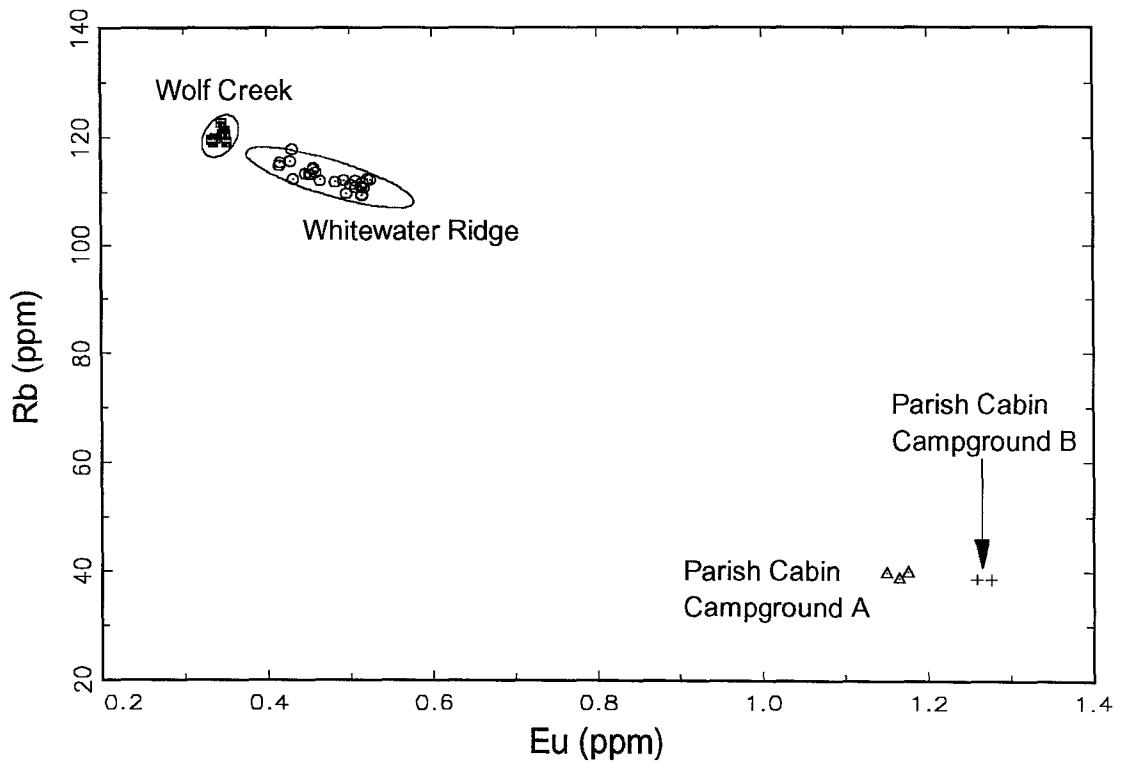


Figure 4.2b: Bivariate plot of Eu vs. Rb for obsidian specimens from the Malheur National Forest.

Creek and two samples from Whitewater Ridge. The Parish Cabin Campground A (PCCA) chemical group consists of three samples from Parish Cabin Campground. The Parish Cabin Campground B (PCCB) chemical group consists of two samples from Parish Cabin Campground. Three samples from Parish Cabin Campground did not fall into any of the other chemical groups, nor did they group together, and until further sampling is undertaken they have been classified as outliers. An outlier is a solo sample with no apparent chemically similar mates.

It is possible that the two Parish Cabin Campground chemical groups are actually part of a single larger group. An examination of the NAA data does show elemental differences between the two groups. For example, elemental data for PCCB are significantly lower (e.g., Ba, Ce, Hf, Th) than the data for PCCA, but some elemental data of PCCB (especially Fe and Mn) are significantly higher than the data for PCCA. Because there are only two members in one group and three members in the other it is difficult to say for certain that the differences are “real.”

It is interesting to note that although some samples from Parish Cabin Campground correlate readily with the Whitewater Ridge chemical group the samples that form their own chemical groups are very different chemically from Whitewater Ridge. For example, the concentration values for iron are almost a factor of six higher in the Parish Cabin Campground groups compared to the Whitewater Ridge group. Other elements do not show such a dramatic difference but the distinction is clear. The differences encountered here may be because the Parish Cabin Campground area is a secondary source and may consist of obsidian washed down from an as yet unsampled

primary source. On the other hand, a comparison of Whitewater Ridge and Wolf Creek shows that they are possibly related.

It is also interesting to examine Figure 4.3a. In this bivariate plot of Rb vs. Fe, the outlying samples have been included with the four chemical groups. It is possible to see a linear pattern extending from Wolf Creek to Whitewater Ridge to the outliers of the Parish Cabin Campground samples. Other element pairs (i.e., Th and Cs, Cs and Fe, Rb and Fe) also show linear patterns. If europium is not one of the elements used, the linear pattern move from the Whitewater Ridge and Wolf Creek groups to the Parish Cabin Campground outliers to the two Parish Cabin Campground groups (Figure 4.3b). If hafnium is used as one of the elements, then the linear pattern extends through the Parish Cabin Campground outliers and groups and does not include the Whitewater Ridge and Wolf Creek groups (Figure 4.3c). These plots indicate the possibility of a systematically varying ash-flow tuff that extends throughout the Malheur National Forest. This would obviously have to be confirmed with a much more intensive collection of samples. This will be attempted in the future.

Finally, an attempt was made to separate the four chemical groups based on data from the abbreviated-NAA method. The results are shown in Figures 4.4a (Mn vs. Na) and 4.4b (Ba vs. Mn). The plot based on sodium and manganese fails to provide adequate separation between Whitewater Ridge and Wolf Creek. However, these two chemical groups are sufficiently different in barium concentration that the plot of barium vs. manganese successfully shows differentiation.

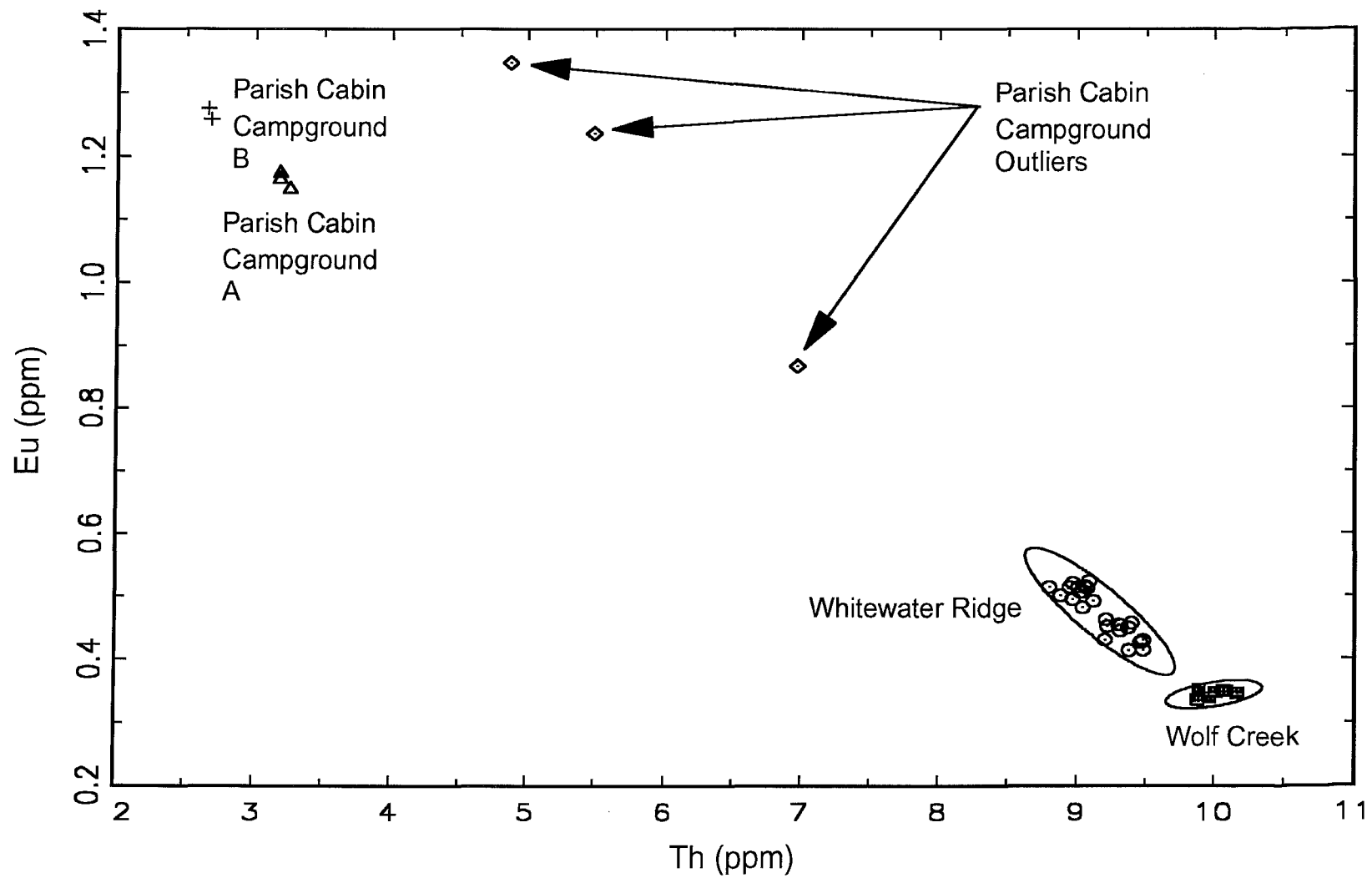


Figure 4.3a: Bivariate plot of Th vs. Eu for obsidian specimens from the Malheur National Forest. Plot shows possible trend from Whitewater Ridge through the Parish Cabin Campground outliers.

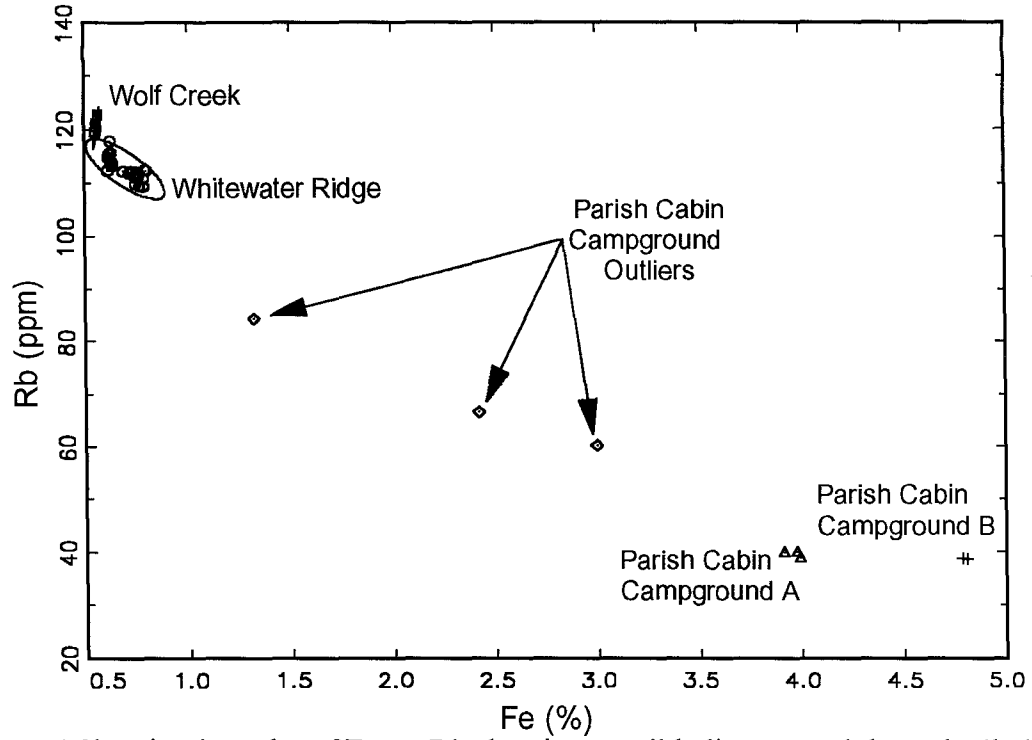


Figure 4.3b: Bivariate plot of Fe vs. Rb showing possible linear trend through all obsidian samples from the Malheur National Forest.

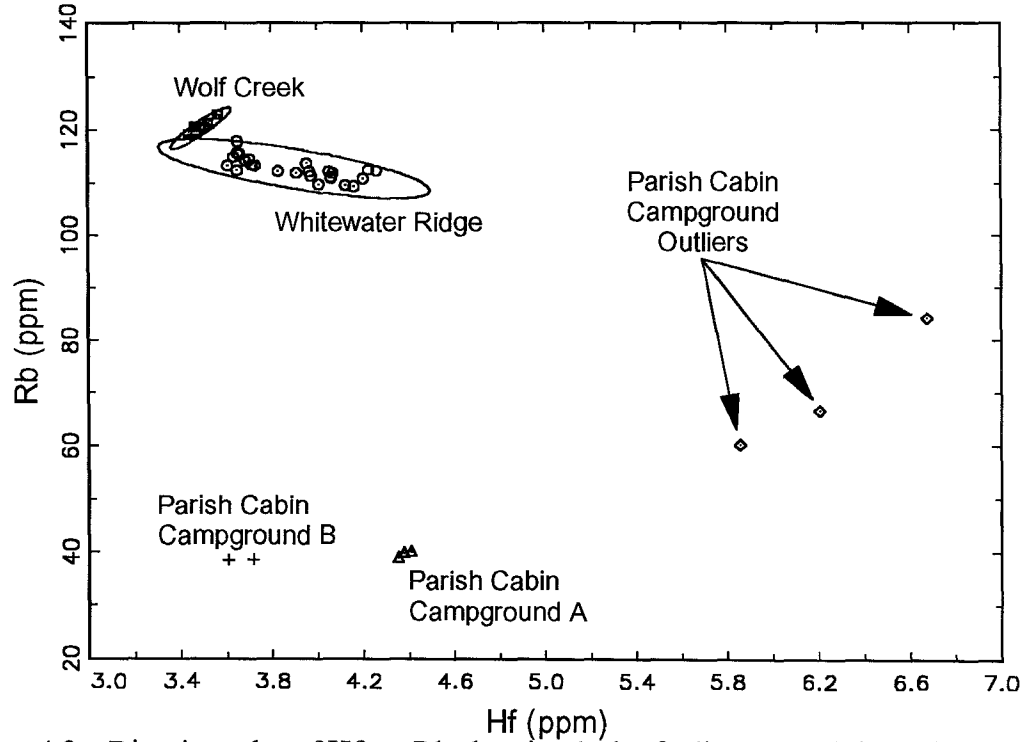


Figure 4.3c: Bivariate plot of Hf vs. Rb showing lack of a linear trend through all obsidian samples from the Malheur National Forest.

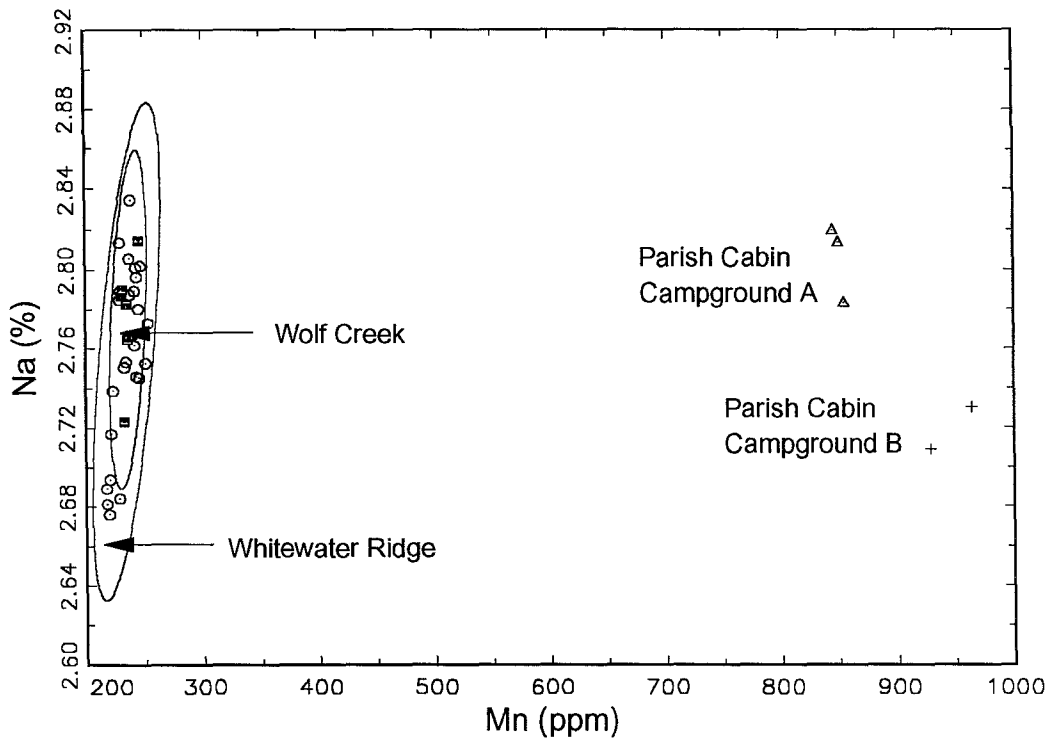


Figure 4.4a: Bivariate plot of Mn vs. Na for obsidian specimens from the Malheur National Forest.

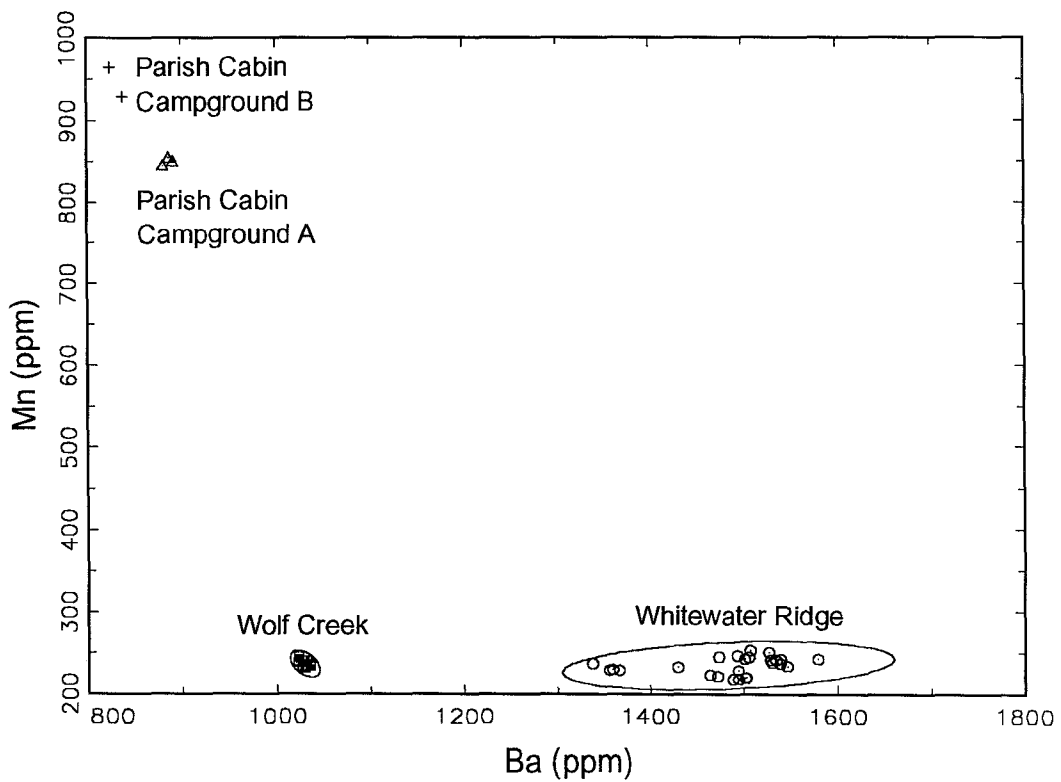


Figure 4.4b: Bivariate plot of Ba vs. Mn for obsidian specimens from the Malheur National Forest.

Harney County

Introduction

Harney County, Oregon is partly dissected by the High Lava Plains and is the site of numerous rhyolitic vent areas, many of which produced high quality obsidian. In the present study, obsidian from sites in the northern half of the county has been analyzed, especially from areas around the city of Burns (for a map of Harney County see Figure 4.5a; Figure 4.5b shows an enlargement of the sampling areas around Burns). The Venator source is farthest away from the others, almost in Malheur County.

The underlying geology for Harney County appears to be composed of a base of basalt and andesite although there is also a unit of rhyodacite (Greene *et al.*, 1972). The geologic map is very generalized and does not show the locations of obsidian. The geologic mapping of the Chickahominy Reservoir area also does not indicate any outcrops of obsidian. There is rhyolite and rhyodacite shown across Highway 20 from Chickahominy. It is possible that these units could have eroded to expose the obsidian found at Chickahominy. Although the map does not indicate obsidian in the Riley area, Hughes (1986a) describes abundant evidence for prehistoric reduction of nodules. The Dog Hill sampling locale was not shown on the map though Hughes (1986b) also described this area as containing evidence for prehistoric use. Although the geologic map by Greene *et al.* (1972) does not show it, these areas are well known for their obsidian outcrops.

Burns Butte is the best known site of obsidian in the Burns area. The entire area is underlain by the welded ash-flow tuff of the Double-O Ranch, which is thought to be the source of the obsidian in the Ochoco National Forest. However, the main part of

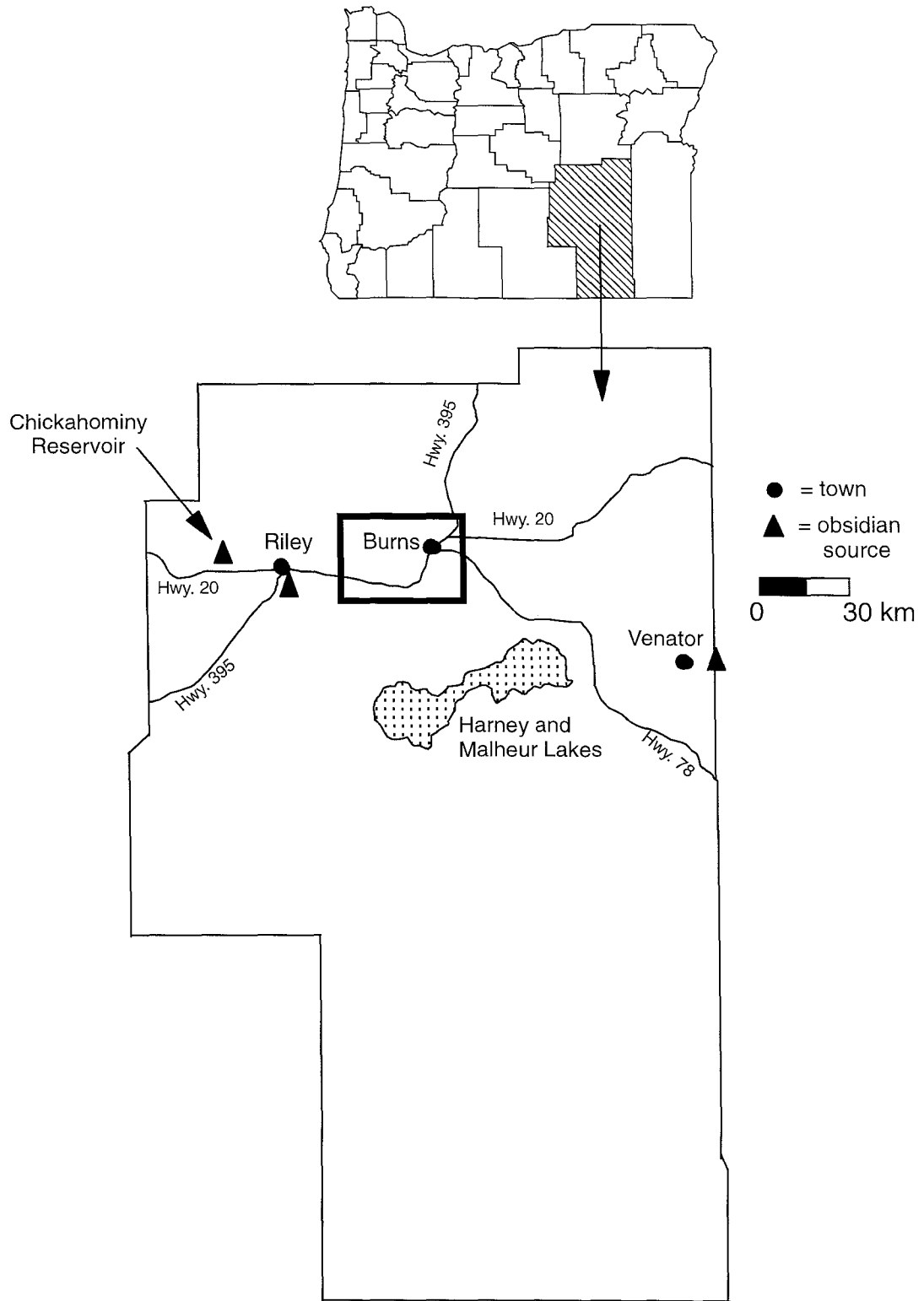


Figure 4.5a: Map of Harney County, Oregon showing location of obsidian sources discussed in the text. Please see Figure 4.5b for enlargement of rectangle.

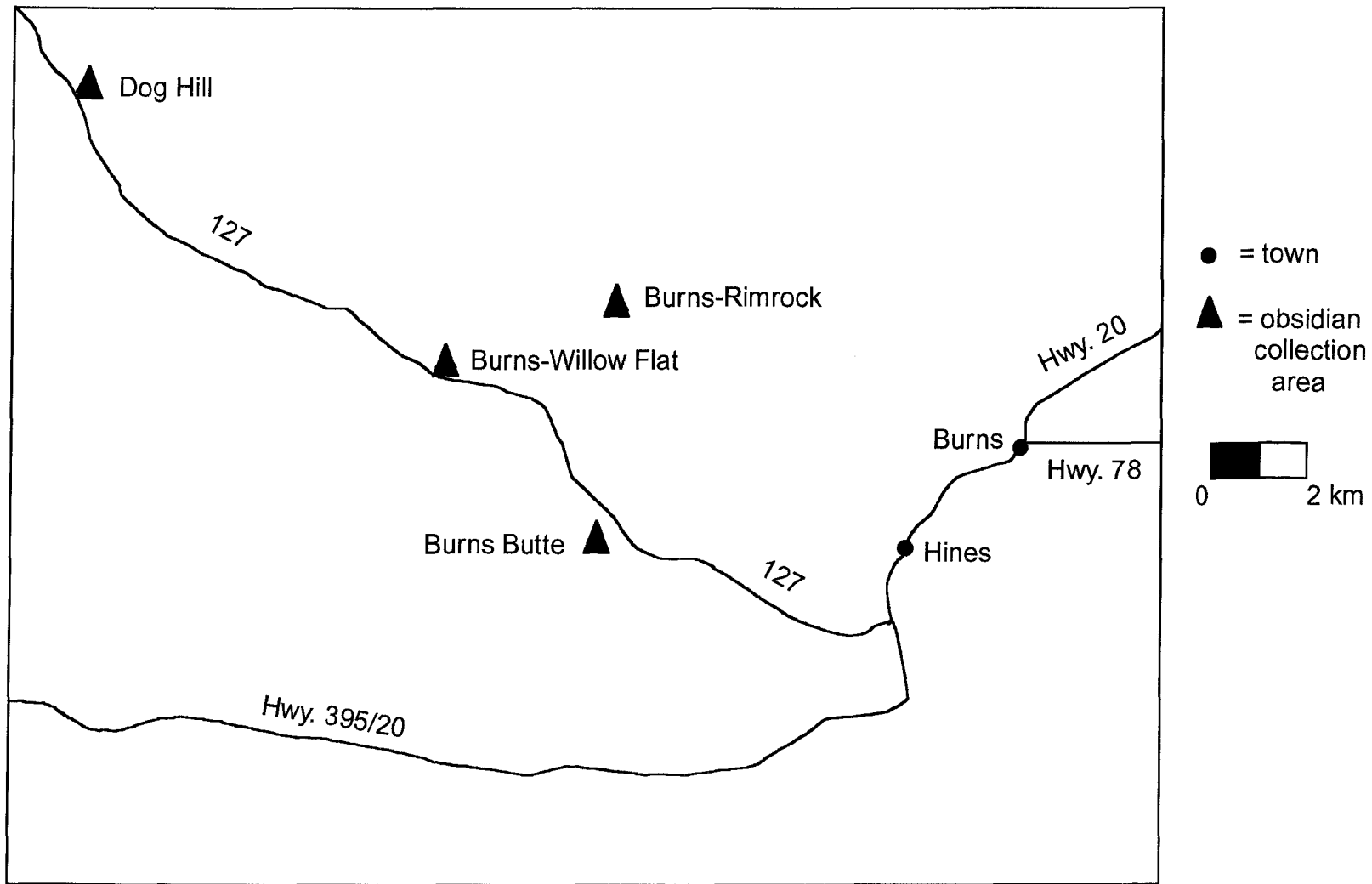


Figure 4.5b: Enlargement of rectangle around Burns (in Figure 4.5a) showing obsidian sampling zones in the Burns area.

Burns Butte and the surrounding area appears to be rhyodacite (Greene *et al.*, 1972). Obsidian was also found at the surface of the butte and the area is known as a place of high quality glass (Hughes, 1986b). The sample sites of Burns-Rimrock and Burns-Willow Flat are included in the same general geographic area.

Native Americans occupied areas in Harney County and the Harney Basin at least as far back as 8700 years B. P. (Gehr and Newman, 1978). Although obsidian artifacts were found at sites around Harney and Malheur Lakes (near Burns), they were not analyzed to determine which source they came from. Data presented here will likely prove helpful in determining where the Native Americans that were living on the shores of the lakes obtained the raw materials for their tools.

Results and Discussion

Compositional data for the six chemical groups identified by this study are shown in Tables 4.5-4.10. Venator, Chickahominy Reservoir, Riley, and Dog Hill are four chemical groups that separated quite nicely and all are chemically homogeneous.

Obsidian from Burns and Burns Butte fell into the same chemical group as shown by Figures 4.6a (Hf vs. Eu) and 4.6b (Fe vs. Cs). This group is termed the Burns Area Obsidian group. The samples from Burns Rimrock also form their own unique and homogeneous chemical group.

The samples from the Burns-Willow Flat sampling locale are very interesting. One sample from Burns-Willow Flat fell into the Burns chemical group. Three samples from Burns-Willow Flat were originally assigned to their own chemical group and appeared to be related to the other chemical groups in the Burns area (see Figures 4.6a and 4.6b). However, upon further consideration and comparison, they correlated with the

Table 4.5: Descriptive Statistics for Burns Area Obsidian, Harney County.

Element	Mean	St. Dev.	% St. Dev.	No. Obs.	Minimum	Maximum
BA	580.	25	4.28	19	527	616
LA	39.4	0.7	1.88	19	38.2	41.0
LU	0.739	0.014	1.88	19	0.715	0.758
ND	29.3	1.3	4.50	19	27.3	31.4
SM	5.95	0.08	1.40	19	5.80	6.12
U	3.35	0.44	13.2	19	2.49	3.89
YB	4.83	0.24	4.92	19	4.50	5.41
CE	76.0	1.6	2.13	19	73.2	78.7
CO	0.905	0.054	5.98	19	0.839	1.10
CS	3.34	0.08	2.42	19	3.23	3.53
EU	0.396	0.015	3.85	19	0.366	0.423
FE	11200	200	1.95	19	10800	11600
HF	7.93	0.18	2.21	19	7.56	8.27
RB	116	2	1.82	19	112	120.
SB	0.921	0.033	3.54	19	0.843	0.987
SC	3.69	0.08	2.12	19	3.53	3.83
SR	25.6	7.6	29.8	6	14.8	37.0
TA	1.89	0.04	2.02	19	1.82	1.96
TB	0.962	0.031	3.21	19	0.878	1.00
TH	10.1	0.2	2.19	19	9.72	10.5
ZN	40.1	4.6	11.5	19	28.5	44.6
ZR	254	13	5.23	19	233	272
CL	1090	80	7.19	19	933	1300
DY	6.69	0.36	5.43	19	6.08	7.41
K	42100	1300	3.13	19	39800	44300
MN	333	5	1.56	19	325	348
NA	31800	390	1.23	19	31200	32400

ANIDs of specimens included:

BWF004	BUB001	BUB002	BUB003	BUB004	BUB005	BUB006	BUB007
BUB008	BUB009	BUB010	BUB011	BUB012	BU001	BU002	BU003
BU004	BU005	BU006					

Table 4.6: Descriptive Statistics for Burns-Rimrock Obsidian, Harney County.

Element	Mean	St. Dev.	% St. Dev.	No. Obs.	Minimum	Maximum
BA**	0	0	0	0	0	0
LA	61.6	0.3	0.52	6	61.1	62.0
LU	1.29	0.02	1.26	6	1.27	1.31
ND	54.6	6.2	11.3	6	50.4	66.6
SM	11.2	0.1	0.99	6	11.0	11.3
U	4.33	0.98	22.7	6	2.41	5.07
YB	9.13	0.09	0.96	6	9.03	9.22
CE	123	2	1.40	6	122	126
CO	0.032	0.006	17.9	6	0.023	0.037
CS	2.93	0.02	0.77	6	2.90	2.96
EU	0.251	0.004	1.59	6	0.246	0.256
FE	16200	200	1.17	6	16000	16500
HF	14.5	0.2	1.30	6	14.3	14.8
RB	104	1	1.37	6	102	106
SB	0.748	0.017	2.21	6	0.720	0.772
SC	0.566	0.006	1.12	6	0.560	0.576
SR**				0		
TA	2.79	0.04	1.55	6	2.72	2.85
TB	1.97	0.02	1.27	6	1.95	2.02
TH	9.16	0.12	1.37	6	9.04	9.40
ZN	103	2	1.55	6	101	105
ZR	473	10.	2.16	6	462	489
CL	1120	30.	2.51	6	1090	1170
DY	13.2	0.5	3.80	6	12.7	13.8
K	36800	1600	4.40	6	34800	38600
MN	402	4	0.97	6	395	406
NA	34900	260	0.75	6	34500	35200

ANIDs of specimens included:

BRR001 BRR002 BRR003 BRR004 BRR005 BRR006

**Values not available because element concentrations below detection limit.

Table 4.7: Descriptive Statistics for Dog Hill Obsidian, Harney County.

Element	Mean	St. Dev.	% St. Dev.	No. Obs.	Minimum	Maximum
BA	70.2	7.2	10.3	6	58.4	79.5
LA	67.2	0.7	1.11	6	66.3	68.2
LU	1.42	0.02	1.48	6	1.39	1.44
ND	59.4	2.2	3.70	6	56.0	61.4
SM	13.4	0.1	0.98	6	13.2	13.6
U	2.84	0.14	4.96	6	2.70	3.08
YB	10.1	0.2	1.49	6	9.86	10.3
CE	136	1	0.66	6	135	137
CO	0.048	0.006	11.4	6	0.041	0.056
CS	4.99	0.04	0.74	6	4.93	5.03
EU	0.895	0.005	0.52	6	0.889	0.902
FE	17800	130	0.74	6	17600	18000
HF	16.4	0.1	0.51	6	16.2	16.5
RB	109	1	0.73	6	108	110.
SB	1.84	0.01	0.78	6	1.82	1.86
SC	0.290	0.004	1.33	6	0.286	0.296
SR**				0		
TA	2.71	0.02	0.69	6	2.69	2.74
TB	2.38	0.02	0.79	6	2.37	2.42
TH	8.99	0.05	0.58	6	8.93	9.07
ZN	132	2	1.50	6	129	134
ZR	594	11	1.89	6	579	608
CL	717	30.	4.18	6	675	752
DY	15.7	0.4	2.49	6	15.1	16.2
K	35800	1700	4.62	6	33300	37600
MN	439	4	0.88	6	435	445
NA	34000	260	0.75	6	33600	34400

ANIDS of specimens included:

DHA001 DHA002 DHA003 DHA004 DHA005 DHA006

**Values not available because element concentrations below detection limit.

Table 4.8: Descriptive Statistics for Riley Obsidian, Harney County.

Element	Mean	St. Dev.	% St. Dev.	No. Obs.	Minimum	Maximum
BA	1080	20.	1.71	18	1050	1110
LA	35.4	0.5	1.40	18	34.2	36.4
LU	1.01	0.01	1.41	18	0.982	1.03
ND	32.4	2.8	8.78	18	28.1	38.0
SM	8.03	0.10	1.28	18	7.86	8.20
U	3.57	0.69	19.3	18	2.82	5.14
YB	6.95	0.26	3.81	18	6.32	7.51
CE	73.8	1.0	1.42	18	72.0	75.7
CO	0.376	0.030	7.97	18	0.349	0.488
CS	4.70	0.05	0.99	18	4.65	4.79
EU	1.07	0.02	1.46	18	1.03	1.10
FE	16400	200	1.17	18	16100	16800
HF	12.2	0.1	1.11	18	11.9	12.4
RB	105	2	1.64	18	102	108
SB	0.599	0.040	6.75	18	0.529	0.677
SC	6.63	0.11	1.65	18	6.47	6.87
SR**				0		
TA	1.50	0.02	1.57	18	1.45	1.53
TB	1.53	0.30	19.6	18	1.36	2.42
TH	8.92	0.09	1.05	18	8.77	9.06
ZN	89.0	7.2	8.06	18	82.0	106
ZR	427	15	3.61	18	406	460.
CL	661	48	7.33	18	569	753
DY	9.52	0.49	5.16	18	8.54	10.4
K	38400	2100	5.47	18	34600	41900
MN	705	14	2.00	18	684	742
NA	36900	500	1.37	18	36	38100

ANIDs of specimens included:

RI007	RI008	RI009	RI010	RI011	RI012	RI001	RI002
RI003	RI004	RI005	RI006	RI013	RI014	RI015	RI016
RI017	RI018						

**Values not available because element concentrations below detection limit.

Table 4.9: Descriptive Statistics for Chickahominy Reservoir Obsidian, Harney County.

Element	Mean	St. Dev.	% St. Dev.	No. Obs.	Minimum	Maximum
BA	1300	20.	1.73	12	1260	1330
LA	33.6	0.4	1.26	12	32.8	34.2
LU	0.890	0.029	3.24	12	0.837	0.951
ND	30.9	1.6	5.22	12	29.3	34.4
SM	7.30	0.04	0.58	12	7.23	7.36
U	3.29	0.42	12.9	12	2.66	3.77
YB	5.96	0.24	3.96	12	5.55	6.25
CE	70.3	0.4	0.62	12	69.4	70.9
CO	0.511	0.038	7.40	12	0.485	0.626
CS	6.26	0.05	0.81	12	6.19	6.35
EU	0.734	0.010	1.32	12	0.714	0.747
FE	11500	80.	0.73	12	11300	11600
HF	8.66	0.08	0.96	12	8.51	8.84
RB	102	2	1.74	12	99.6	106
SB	2.59	0.04	1.70	12	2.52	2.65
SC	7.10	0.06	0.84	12	7.00	7.19
SR**				0		
TA	1.20	0.02	1.68	12	1.16	1.23
TB	1.29	0.08	5.85	12	1.19	1.43
TH	7.55	0.08	1.03	12	7.39	7.68
ZN	68.6	13.7	20.0	12	53.8	90.6
ZR	280.	12	4.40	12	248	292
CL	450.	45	10.2	12	360.	505
DY	8.57	0.39	4.53	12	7.78	9.18
K	36600	1600	4.37	12	34600	39300
MN	429	13	2.99	12	403	443
NA	32400	870	2.69	12	30300	33400

ANIDs of specimens included:

CHY007 CHY008 CHY009 CHY010 CHY011 CHY012 CHY001 CHY002
 CHY003 CHY004 CHY005 CHY006

**Values not available because element concentrations below detection limit.

Table 4.10: Descriptive Statistics for Venator Obsidian, Harney County.

Element	Mean	St. Dev.	% St. Dev.	No. Obs.	Minimum	Maximum
BA	867	22	2.48	6	847	906
LA	16.8	0.2	1.46	6	16.5	17.1
LU	0.384	0.007	1.70	6	0.377	0.391
ND	15.1	1.2	7.91	6	13.8	17.3
SM	3.50	0.07	2.01	6	3.37	3.57
U	2.18	0.17	7.61	6	2.03	2.48
YB	2.47	0.17	6.78	6	2.35	2.70
CE	32.2	0.5	1.47	6	31.4	32.8
CO	0.878	0.205	23.3	6	0.777	1.30
CS	2.99	0.03	0.86	6	2.97	3.04
EU	0.528	0.011	2.02	6	0.515	0.547
FE	7370	650	8.78	6	7030	8680
HF	3.33	0.04	1.18	6	3.28	3.39
RB	98.8	0.6	0.64	6	97.8	99.7
SB	0.425	0.018	4.28	6	0.398	0.454
SC	3.44	0.11	3.28	6	3.37	3.66
SR	154	26	17.0	6	107	187
TA	0.850	0.016	1.87	6	0.829	0.865
TB	0.658	0.092	13.9	6	0.566	0.835
TH	4.36	0.09	2.12	6	4.28	4.50
ZN	46.8	5.2	11.0	6	37.5	52.2
ZR	97.8	9.0	9.21	6	81.9	108
CL	246	42	16.9	6	173	294
DY	4.15	0.52	12.5	6	3.46	5.01
K	38200	1200	3.07	6	36500	39300
MN	654	5	0.78	6	645	659
NA	28400	166	0.59	6	28200	28600

ANIDs of specimens included:

VENOR01 VENOR02 VENOR03 VENOR04 VENOR05 VENOR06

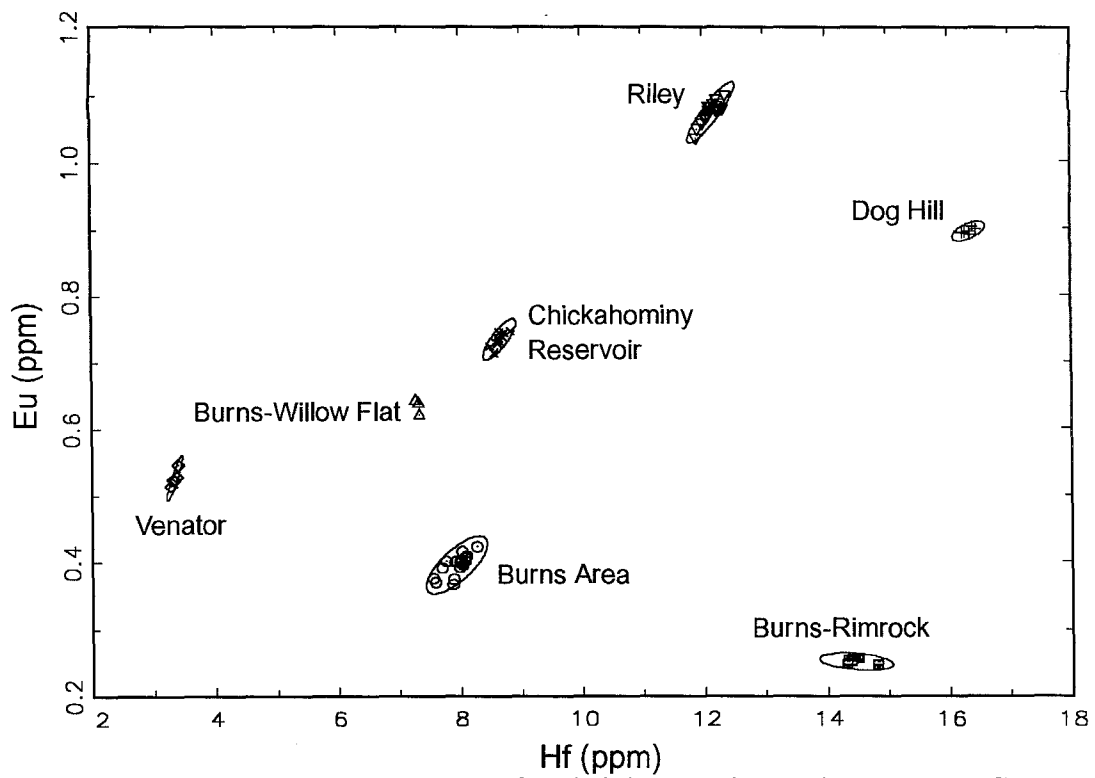


Figure 4.6a: Bivariate plot of Hf vs. Eu for obsidian specimens from Harney County.

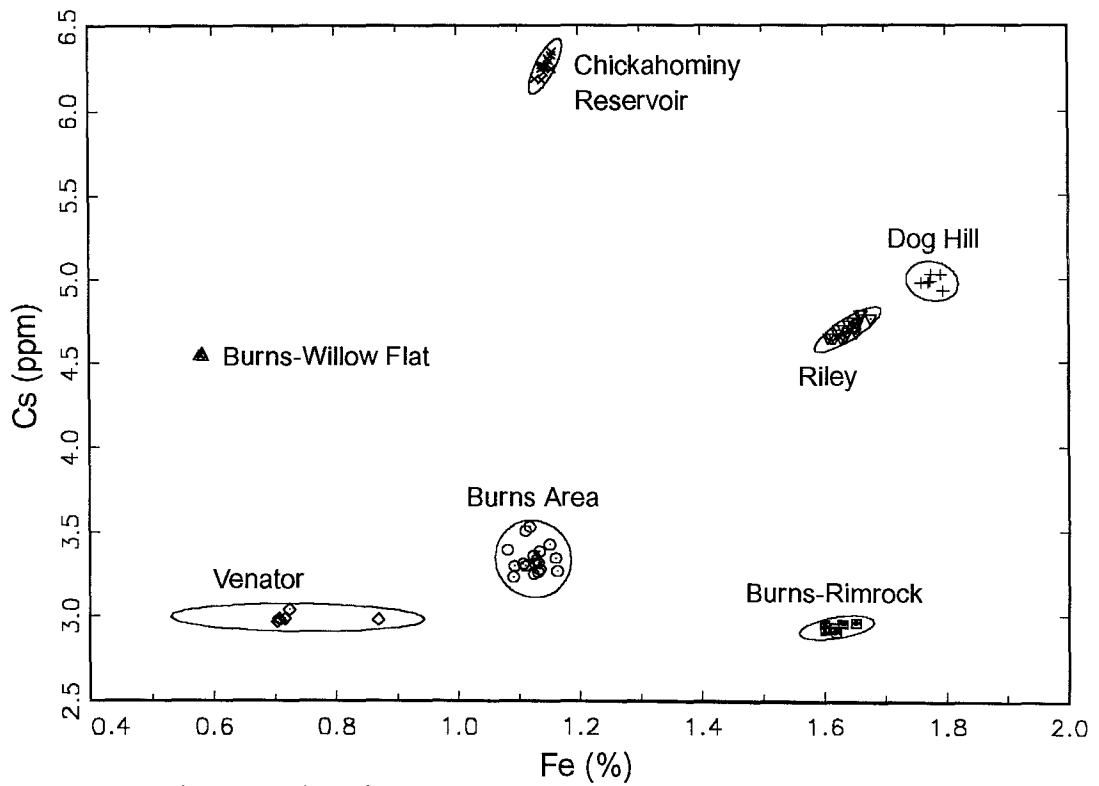


Figure 4.6b: Bivariate plot of Fe vs. Cs for obsidian specimens from Harney County.

Buck Springs group of the Ochoco National Forest (see next section).

The remaining two samples from Burns-Willow Flat (BWF005 and BWF006) are labeled outliers because they do not match any of the chemical groups around Burns. When the data from the two outliers from Burns-Willow Flat were examined and compared to data from the Ochoco National Forest, both fell into the chemical groups from that area. BWF005 falls into the Buck Springs Chemical Group. BWF006 falls into the Delintment Lake B Chemical Group. Figure 4.7 (Th vs. Cs) illustrates the grouping of the Burns-Willow Flat samples in the chemical groups of the Ochoco National Forest.

The results for the samples from Burns-Willow Flat are not an unlikely scenario for two reasons. Firstly, the Burns area is relatively close to the Ochoco National Forest in distance (e.g., Dog Hill is actually within the national forest boundaries). Secondly, and more importantly, the Burns area is underlain by the same welded ash-flow tuff as the Ochoco National Forest. Therefore, it is possible that additional samples from the Burns area would also be included in the chemical groups of the Ochoco National Forest.

It is also possible to successfully distinguish among the sources in Harney County using only the abbreviated-NAA method. Figure 4.8a shows a bivariate plot of sodium versus manganese. In this case, the Dog Hill and Chickahominy Reservoir chemical groups cannot be separated. However, as Figure 4.8b shows, a plot of manganese versus barium is very useful in separating those two groups. The Burns-Rimrock source is not shown in Figure 4.8b because the element concentration data for barium were below our detection limit.

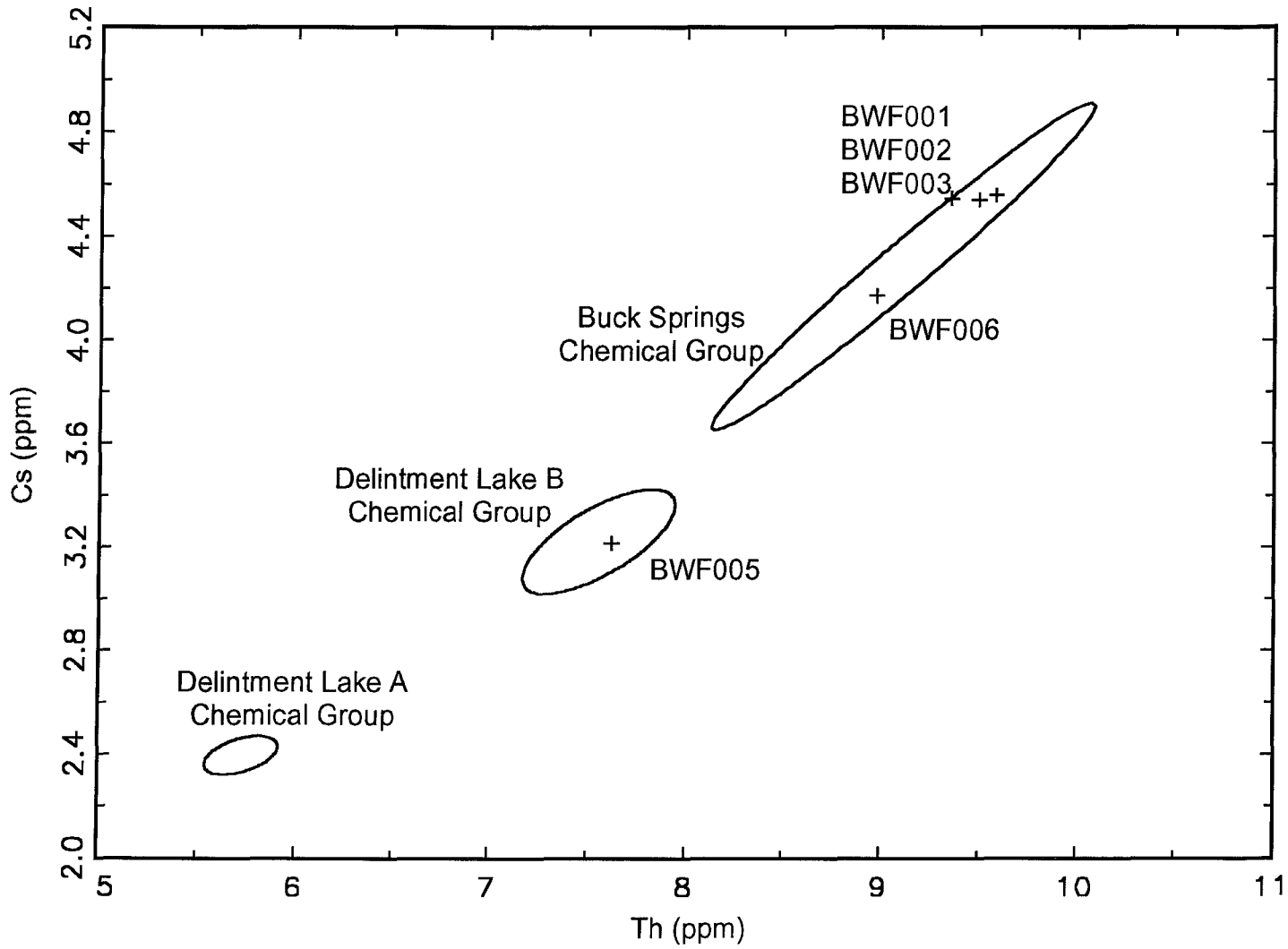


Figure 4.7: Bivariate plot showing five obsidian samples from Burns-Willow Flat projected against the 95% confidence ellipses of the chemical groups in the Ochoco National Forest.

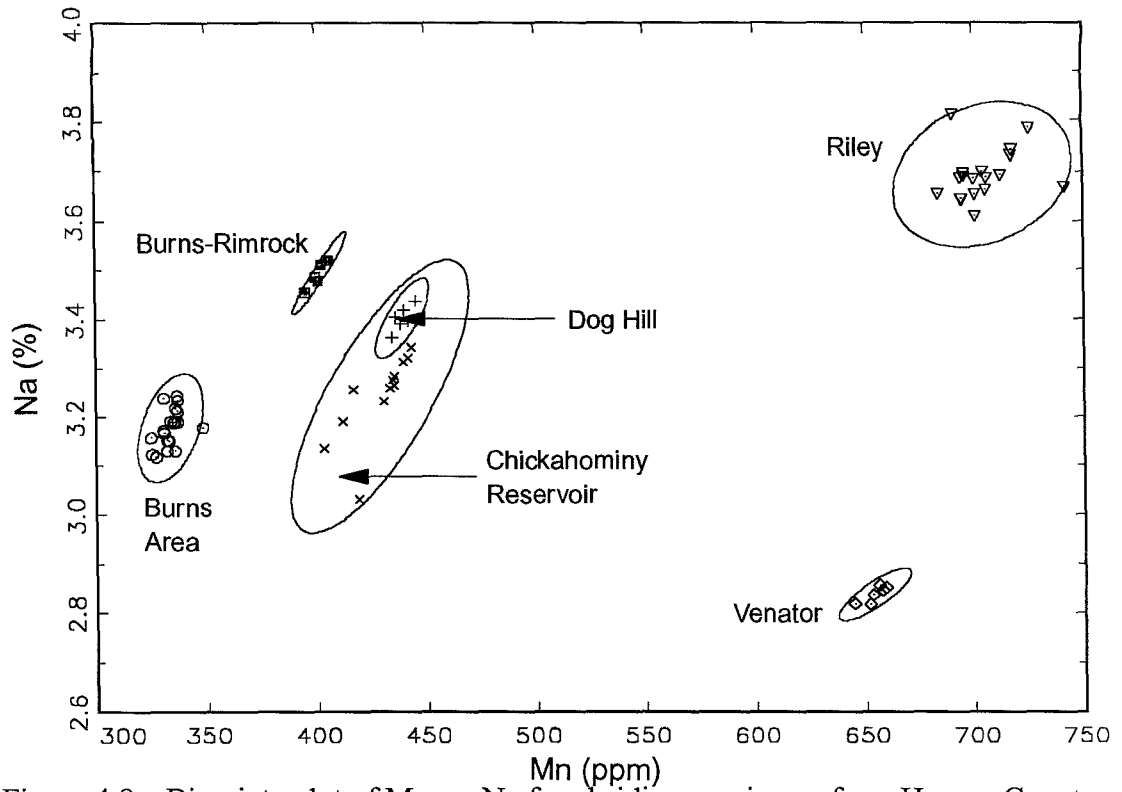


Figure 4.8a: Bivariate plot of Mn vs. Na for obsidian specimens from Harney County.

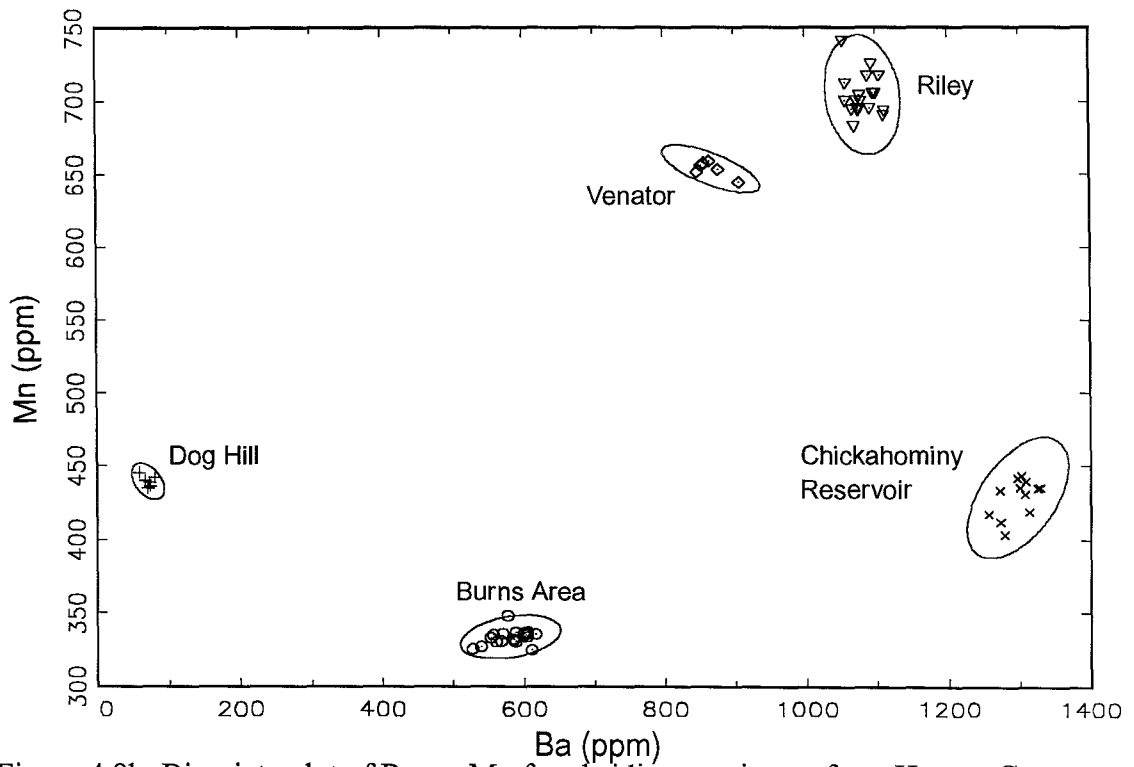


Figure 4.8b: Bivariate plot of Ba vs. Mn for obsidian specimens from Harney County.

Burns-Rimrock is not shown because its Ba concentration is below the detection limit.

Hughes (1986b) performed XRF analyses on obsidian from the Dog Hill and Burns Butte outcrops. He determined that both sources were geochemically homogeneous and that they were distinguishable from one another. The elements analyzed in common are the following: Th, Nd, Ce, La, Ba, Zr, Sr, Rb, and Zn. In comparing Hughes (1986b) data with the data from this thesis (for the Burns Area and Dog Hill groups) most of the data match fairly well. The data agree least well for the element thorium. However, Hughes states that Th is not one of the best elements to use to distinguish sources by XRF because it is so variable and so the disagreement is not unexpected. Thorium is one of the best elements for NAA in terms of precision.

MacLean (1994) also analyzed several types of rocks, including obsidian, from Burns Butte. The data presented in this study matched most closely to the NAA data on aphyric low-silica rhyolite (low-silica means 72-75.5% SiO₂). The elements compared are Sc, Co, Cs, Sb, La, Ce, Nd, Sm, Eu, Tb, Yb, Lu, Hf, Ta, Th, and U.

Ochoco National Forest

Introduction

The Ochoco National Forest is an area dominated geologically by the ash-flow tuff of the Double-O Ranch (Greene *et al.*, 1972). This ash-flow tuff is part of a larger volcanic outcrop dominating the Harney Basin that is called the Rattlesnake Formation. The Rattlesnake Formation is exposed over approximately 9000 km² from the Blue Mountain Province in the north to the northern Basin and Range in the south. It is also part of the age progression of the High Lava Plains, with a K-Ar date of about 7.05 million years. Chemical analysis by NAA has shown that the Rattlesnake Formation includes the Double-O Ranch Tuff and Twelvemile Tuff (Streck and Grunder, 1995). The Rattlesnake Formation has also been identified as part of the Danforth Formation (Lund, 1966; Walker, 1969; Enlows, 1973).

Early work on the ash-flow tuff(s) in the Harney Basin was concerned mainly with the descriptive geology. Lund (1966) describes three ash-flow tuffs of the Danforth Formation exposed on Highway 395 north of Highway 20 including pumice, other rocks, vitric particles, and crystal fragments. The base of the uppermost unit is not welded but welding increases as one goes from the lower to upper part of the tuff (Figure 4.9). The welded area grades into a perlitic structure and then into an area of spherulites and lithophysae. In the lower part of the spherulitic zone are masses of obsidian-like glass which are either areas where the tuff completely melted and resolidified or are actual obsidian inclusions.

Walker (1969) was interested in identifying a possible vent for the youngest of three ash-flow tuffs of the Danforth Formation (equivalent to the Rattlesnake Formation).

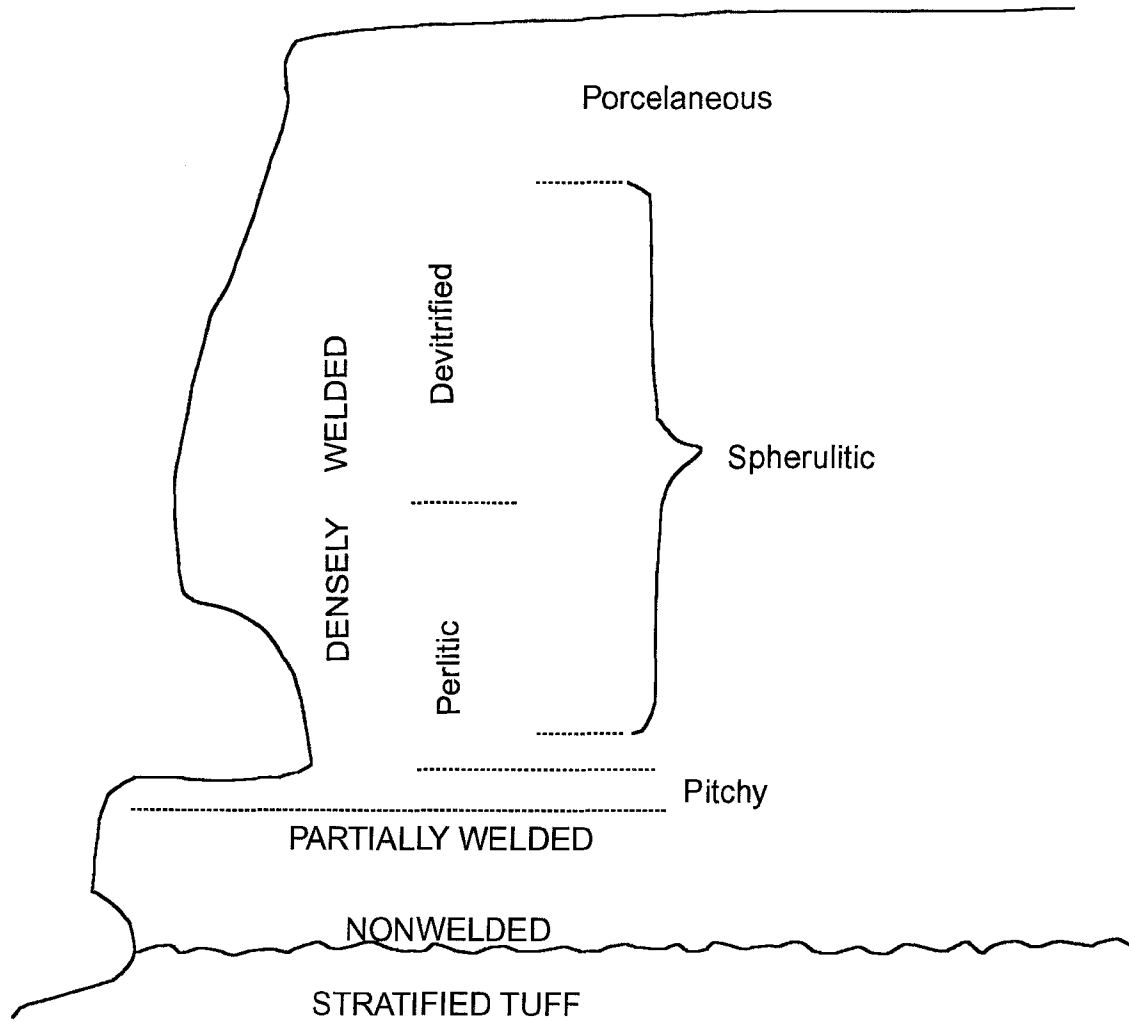


Figure 4.9: Diagram showing zones in upper ash flow of Rattlesnake Formation. (Adapted from Lund, 1966)

This outcrop covered some 7700 km² in the Harney Basin and originally contained more than 98% glass in the form of shards, pumice lapilli, and blocks. A graben that contains a possible vent for the tuff was identified in the Buzzard Creek area although that vent may be only one of several fissure zones from which the ash-flow tuff emerged. The graben was considered to be spatially and possibly genetically related to the Brothers Fault Zone.

Enlows and Parker (1973) describe the Rattlesnake Formation as a Pliocene sequence consisting of two sedimentary members of fluvial origin separated by thin ignimbrite (i.e., a felsic pyroclastic and rhyolitic rock) rich in pumice and without a large amount of minerals. Like Lund and Walker, they describe the ash-flow as grading upward from a basal zone of no welding to a vitrophyric densely welded zone to a top partially welded zone. Enlows (1976) expands on this information, comparing the chemical compositions of the clear and brown glass shards found in the formation. According to its chemistry, he identifies the tuff as a "leuco-sodaclase-rhyolite."

Work in more recent years has concentrated on the actual chemistry of the formation. The chemical composition has been used to identify the limits of the formation and possible vent areas. Today, the Rattlesnake Formation is semi-continuously exposed over the area it covers, with fairly uniform thickness (Streck and Grunder, 1995). Originally, the tuff may have covered up to 35,000 km² (and possibly more) [Figure 4.10]. The large area and fairly uniform thickness are probably due to low topographic relief at the time of the eruption. Streck and Grunder also tried to identify a vent area for the flow. After examining their data, they concluded that the source area best fitting the data was Capeheart Lake (18 km SSW of Riley). Although the eruption

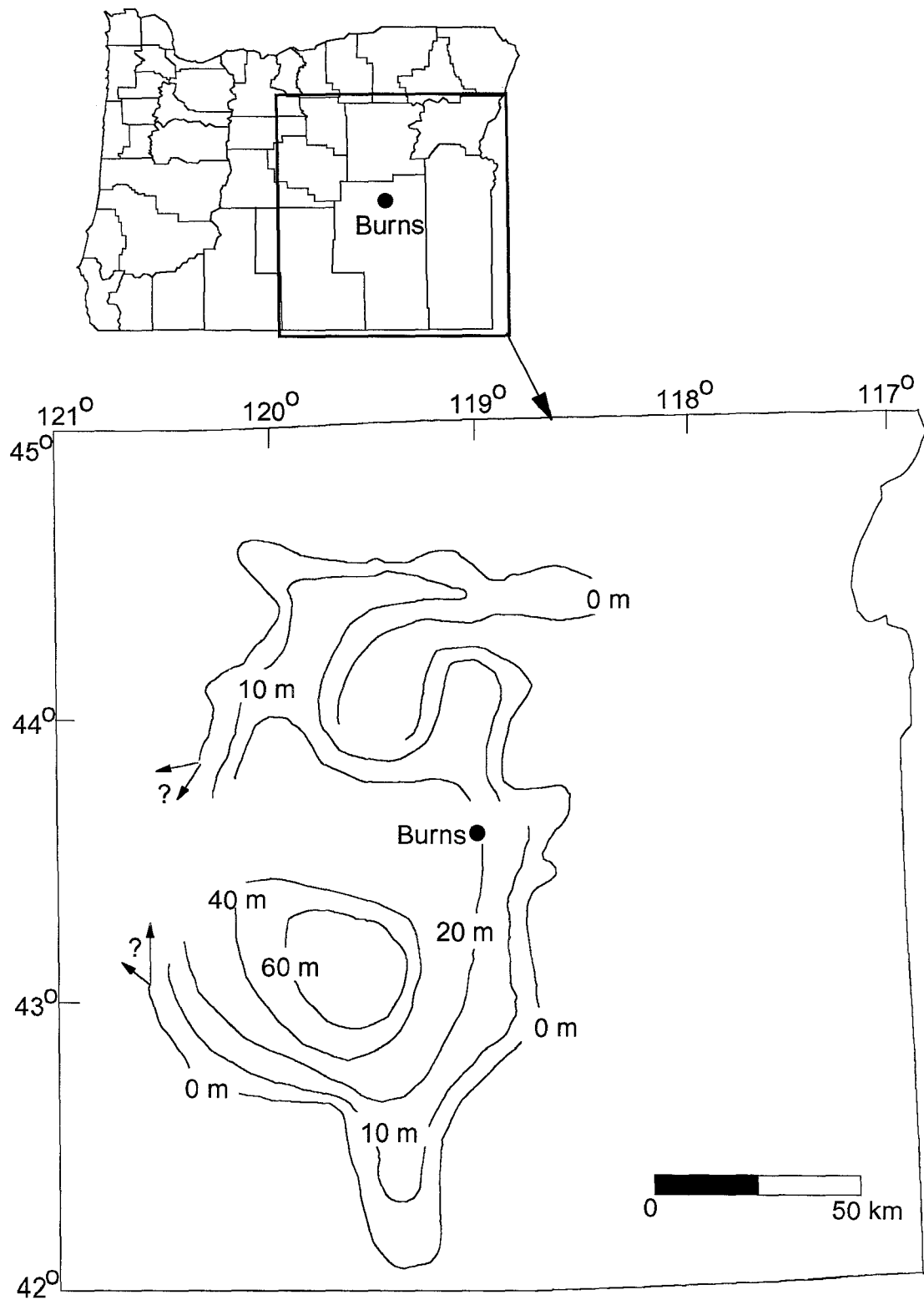


Figure 4.10: Isopach map showing pre-erosion distribution of the Rattlesnake Ignimbrite Tongue. (Adapted from Parker, 1974)

was very large (332 km³) it was apparently short lived and if a caldera formed it is now covered by the tuff.

As noted previously, the geology varies within the tuff area from non-welded to welded zones. From within the non-welded to the welded zones the density goes from <1.5 to 2.34 g/cm³ (Streck and Grunder, 1995). The color also changes from white/gray to black and dull to vitreous and glassy. This dense welding produced tuff that is an obsidian-like vitrophyre. In fact, most of the glassy shards are high silica rhyolite (SiO₂ of 75-77.5%) and these probably make up about 99% of the entire tuff. Some basalt and basaltic andesite inclusions exist but these and other phenocryst inclusions are minimal.

The Rattlesnake Formation probably erupted as multiple high-energy ash-flows though it did cool as a single unit (Streck and Grunder, 1995). In fact, the geological variations, both vertical and lateral, indicate that the eruption was probably the result of the tapping of successively deeper levels of a zoned magma chamber. This is further complicated by both the actual deposition and subsequent erosion. Examining the chemical composition of the tuff shows that this is possible. According to Streck (1992), there exist some continuous trends in elemental compositions that support a direct daughter-parent relationship between high-silica rhyolites and dacites. There are also compositional gaps in the concentrations of Fe, Ti, Ca, Mn, Sr, Sc, and Cu between the rhyolites and dacites that may indicate possible fractionation processes.

Results and Discussion

Figures 4.11a and 4.11b are maps showing the locations in the Ochoco National Forest where 102 obsidian samples were collected for analysis. The data are presented in Tables 4.11-4.13. At first, examination of the data collected did not show a pattern.

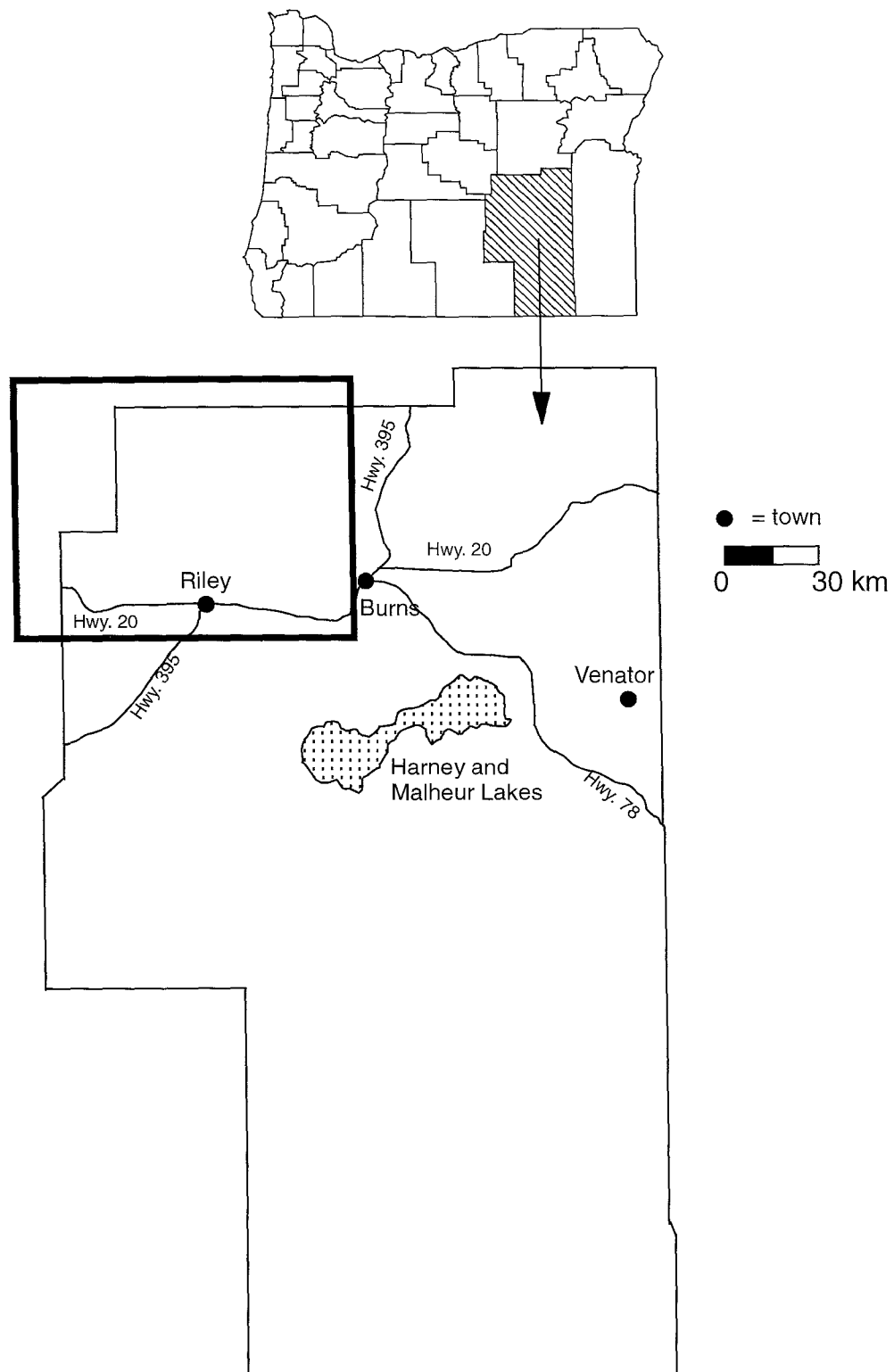


Figure 4.11a: Map of Harney County, Oregon. Rectangle encloses area of the Ochoco National Forest that was sampled for obsidian. Please see Figure 4.11b for enlargement of rectangle.

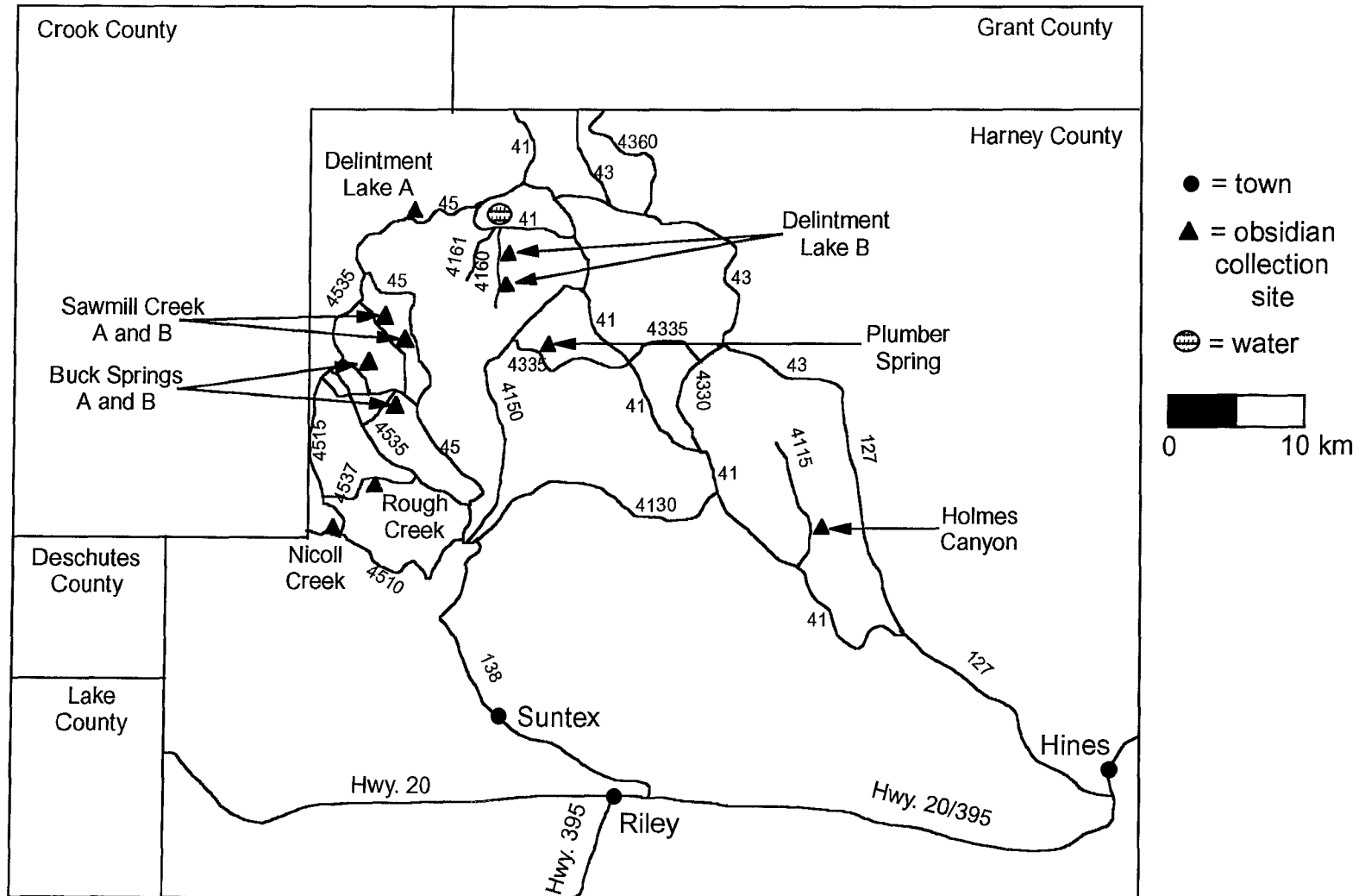


Figure 4.11b: Enlargement of rectangle in Figure 4.11a showing obsidian collection sites in the Ochoco National Forest.

Table 4.11: Descriptive Statistics for Buck Springs Obsidian, Ochoco National Forest.

Element	Mean	St. Dev.	% St. Dev.	No. Obs.	Minimum	Maximum
BA	94.8	66.7	70.3	85	21.1	314
LA	24.0	3.9	16.5	91	19.4	35.9
LU	1.54	0.04	2.36	91	1.45	1.61
ND	29.4	5.2	17.6	91	20.1	41.9
SM	9.68	0.72	7.41	91	8.76	11.7
U	3.65	0.70	19.0	91	1.59	5.41
YB	10.9	0.4	4.04	91	9.51	12.6
CE	60.3	8.3	13.8	91	50.2	83.8
CO	0.191	0.310	162	90	0.029	2.89
CS	4.28	0.25	5.84	91	3.61	4.59
EU	0.760	0.123	16.1	91	0.620	1.12
FE	6840	980	14.4	91	5660	11300
HF	7.76	0.48	6.17	91	7.12	9.04
RB	117	7	5.82	91	99.2	131
SB	1.38	0.06	4.27	91	1.24	1.53
SC	3.98	0.28	7.07	91	3.52	5.84
SR**				0		
TA	2.10	0.09	4.41	91	1.82	2.25
TB	2.21	0.11	4.89	91	2.02	2.54
TH	9.11	0.39	4.27	91	7.93	9.62
ZN	99.4	22.6	22.7	91	59.9	168
ZR	208	24	11.5	91	167	274
CL	472	51	10.9	91	342	578
DY	15.6	0.8	5.09	91	14.2	17.8
K	40000	3200	8.10	91	29700	48600
MN	672	20.	3.04	91	646	779
NA	29100	1600	5.60	91	24600	30900

ANIDS of specimens included:

BSA001 BSA002 BSA003 BSA004 BSA005 BSA006 BSOR01 BSOR02
 BSOR03 BSOR04 BSOR05 BSOR06 BWF001 BWF002 BWF003 BWF005
 DLA001 DLA002 DLA003 DLA004 DLA005 DLA006 DLB001 DLB002
 DLB003 DLB008 DLB009 DLB010 DLB011 DELOR01 DELOR03 DELOR04
 DELOR05 DELOR06 HCB001 HCB002 HCB003 HCB004 HCB005 HCB006
 HCB007 HCB009 HCB010 HCB013 HCB014 HCB015 JRB002 NCA001
 NCA002 NCA003 NCA004 NCA005 NCA006 NCA007 NCA008 NCA009
 NCA010 NCA011 NCA012 PSA002 PSA005 PSA007 PSA008 PSB001
 PSB002 PSB004 PSB006 RCA001 RCA002 RCA003 RCA004 RCA005
 RCA006 RCROR01 RCROR02 RCROR03 RCROR04 RCROR05 RCROR06 SCB001
 SCB002 SCB003 SCB004 SCB005 SCB006 SAWOR01 SAWOR02 SAWOR03
 SAWOR04 SAWOR05 SAWOR06

**Values not available because element concentrations below detection limit.

Table 4.12: Descriptive Statistics for Delintment Lake A Obsidian, Ochoco National Forest.

Element	Mean	St. Dev.	% St. Dev.	No. Obs.	Minimum	Maximum
BA	1840	50	2.84	4	1770	1900
LA	51.6	0.4	0.72	4	51.3	52.1
LU	1.19	0.01	1.14	4	1.17	1.20
ND	62.6	2.7	4.29	4	58.6	64.2
SM	13.0	0.1	0.64	4	13.0	13.2
U	1.57	0.62	39.6	4	1.19	2.49
YB	8.19	0.17	2.12	4	8.06	8.44
CE	116	1	1.25	4	114	118
CO	0.089	0.013	14.6	4	0.072	0.104
CS	2.40	0.02	0.97	4	2.36	2.42
EU	2.46	0.04	1.64	4	2.41	2.49
FE	14900	600	4.24	4	14400	15800
HF	11.4	0.2	1.37	4	11.2	11.6
RB	63.6	1.0	1.55	4	62.9	65.0
SB	1.18	0.02	1.73	4	1.17	1.21
SC	4.08	0.14	3.43	4	3.89	4.20
SR**				0		
TA	1.31	0.01	0.93	4	1.30	1.33
TB	1.94	0.03	1.38	4	1.91	1.97
TH	5.73	0.06	1.02	4	5.67	5.80
ZN	105	14	13.6	4	84.0	116
ZR	445	22	5.07	4	422	476
CL	440.	33	7.49	4	411	487
DY	13.0	0.1	1.02	4	12.9	13.2
K	37100	3000	8.18	4	33500	40400
MN	759	8	1.06	4	753	770.
NA	29800	2200	7.53	4	27500	32800

ANIDS of specimens included:

DLB004 PSA003 PSA004 PSA006

**Values not available because element concentrations below detection limit.

Table 4.13: Descriptive Statistics for Delintment Lake B Obsidian, Ochoco National Forest.

Element	Mean	St. Dev.	% St. Dev.	No. Obs.	Minimum	Maximum
BA	140.	28	19.9	12	105	215
LA	39.2	1.8	4.56	12	37.7	44.2
LU	1.44	0.02	1.11	12	1.41	1.48
ND	43.7	5.0	11.4	12	36.0	49.8
SM	13.0	0.3	2.21	12	12.5	13.5
U	2.19	0.84	38.5	12	1.62	4.55
YB	10.1	0.2	1.87	12	9.82	10.4
CE	94.8	3.6	3.76	12	91.0	104
CO	0.062	0.015	24.0	12	0.035	0.085
CS	3.22	0.06	1.96	12	3.08	3.31
EU	1.14	0.04	3.99	12	1.10	1.27
FE	9330	410	4.39	12	8790	10100
HF	9.84	0.34	3.42	12	9.28	10.4
RB	91.6	3.7	4.01	12	88.4	102
SB	1.30	0.06	4.56	12	1.21	1.40
SC	3.66	0.16	4.30	12	3.47	3.93
SR**				0		
TA	1.73	0.02	1.29	12	1.70	1.77
TB	2.47	0.07	2.87	12	2.34	2.56
TH	7.56	0.12	1.60	12	7.32	7.73
ZN	111	22	20.0	12	78.3	164
ZR	294	18	6.17	12	264	325
CL	498	103	20.7	12	386	738
DY	16.6	0.7	4.44	12	15.3	17.8
K	40100	2600	6.38	12	35900	43600
MN	697	66	9.51	12	648	898
NA	28700	1600	5.55	12	25900	30600

ANIDs of specimens included:

BWF006 DLB005 DLB006 DLB007 DLB012 DELOR02 HCB008 HCB011
HCB012 PSA001 PSB003 PSB005

**Values not available because element concentrations below detection limit.

However, as illustrated by Figures 4.12a (Th vs. Cs) and 4.12b (Hf vs. Rb), further analysis has indicated the existence of three highly distinctive chemical groups. The Buck Springs Chemical Group contains samples from Buck Springs, four samples from Burns-Willow Flat (recall the section on Harney County), Delintment Lake, Holmes Canyon, one sample from Juniper Ridge (see Glass Buttes), Nicoll Creek, Plumber Spring, Rough Creek, and Sawmill Creek (91 samples total). The Delintment Lake B Chemical Group contains one sample from Burns-Willow Flat (recall the section on Harney County), five samples from Delintment Lake, three from Holmes Canyon, and three from Plumber Spring. The Delintment Lake A Chemical Group contains three samples from Plumber Spring and one sample from Delintment Lake.

The correlations among the chemical groups are highly indicative of their origin in an ash-flow tuff. Bowman *et al.* (1973b) first identified a trend in an ash-flow tuff at Borax Lake, California. They used graphs of several different element concentrations versus the iron concentration to present their results and found that the data produced correlation lines with different slopes for each element being compared with iron. Based upon these linear relationships, they hypothesized that compositions of the rocks were due to differential mixing of different proportions of two homogeneous bodies. The data from the current investigation have been graphed in the same way using the elements Ta, Zr, Lu, and Eu versus Fe (Figures 4.13a, b, c, and d). There is a clear linear progression of the chemical groups. The Buck Springs and Delintment Lake B groups tend to overlap together because of the large range in Fe concentrations for the Buck Springs group while Delintment Lake A is an entirely separate group.

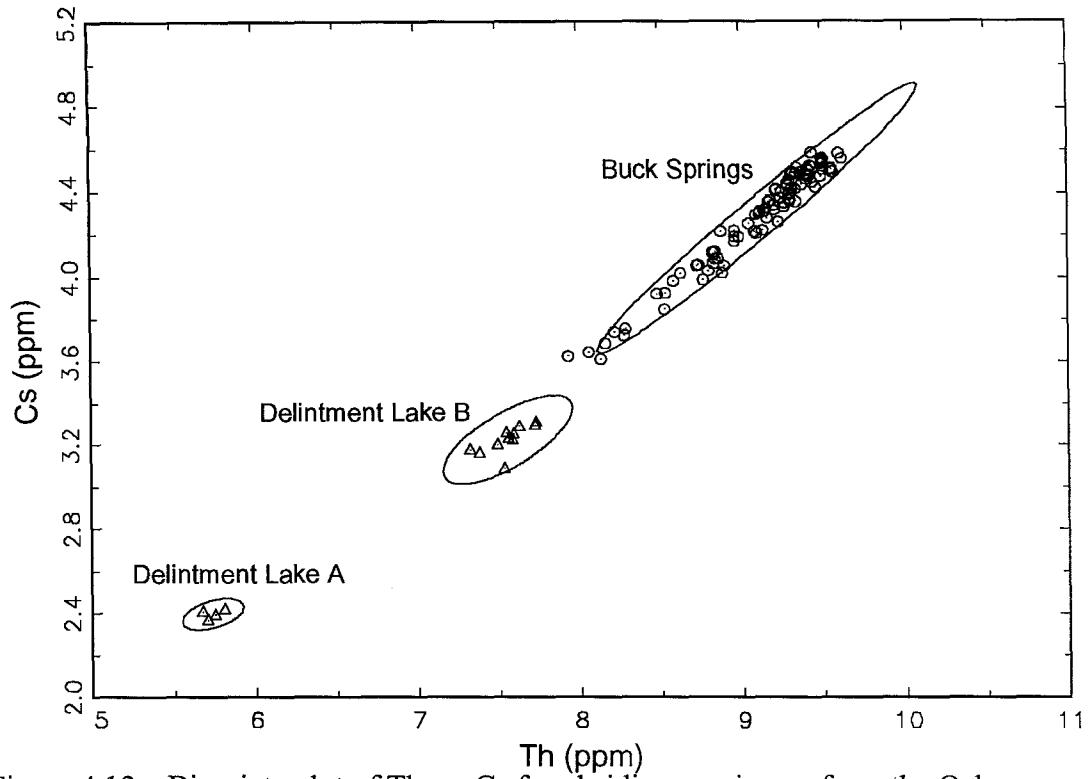


Figure 4.12a: Bivariate plot of Th vs. Cs for obsidian specimens from the Ochoco National Forest.

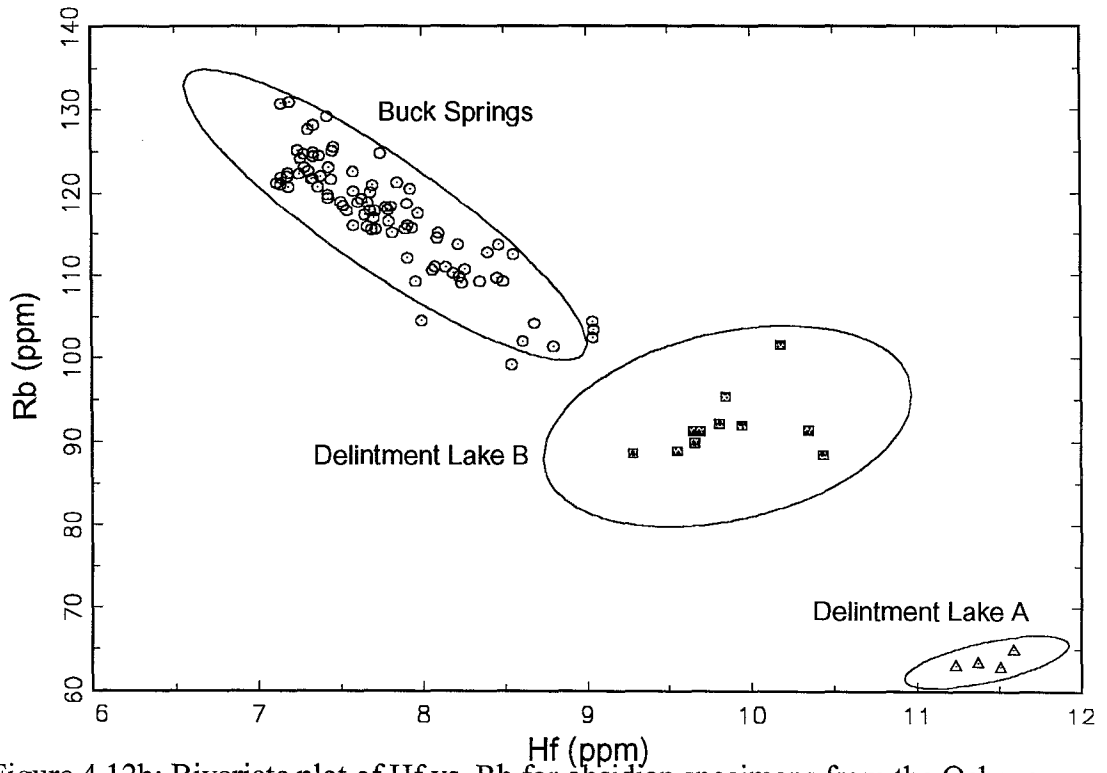


Figure 4.12b: Bivariate plot of Hf vs. Rb for obsidian specimens from the Ochoco National Forest.

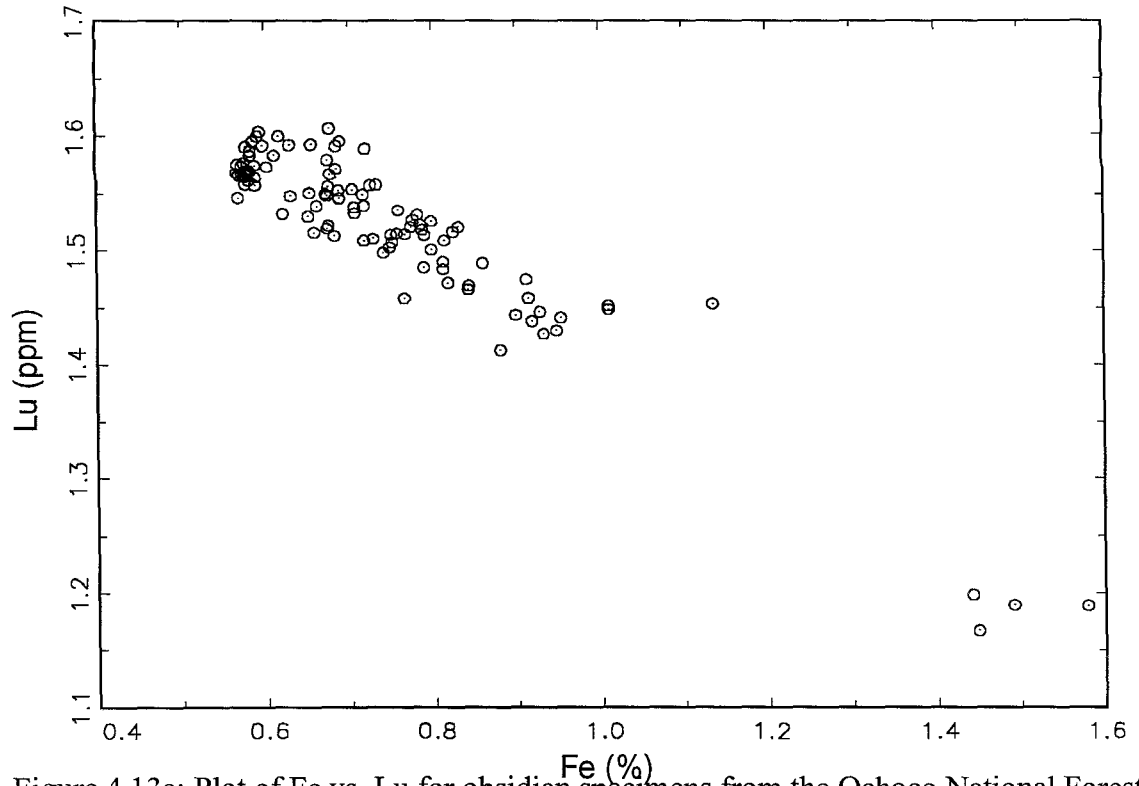


Figure 4.13a: Plot of Fe vs. Lu for obsidian specimens from the Ochoco National Forest showing possible linear trend.

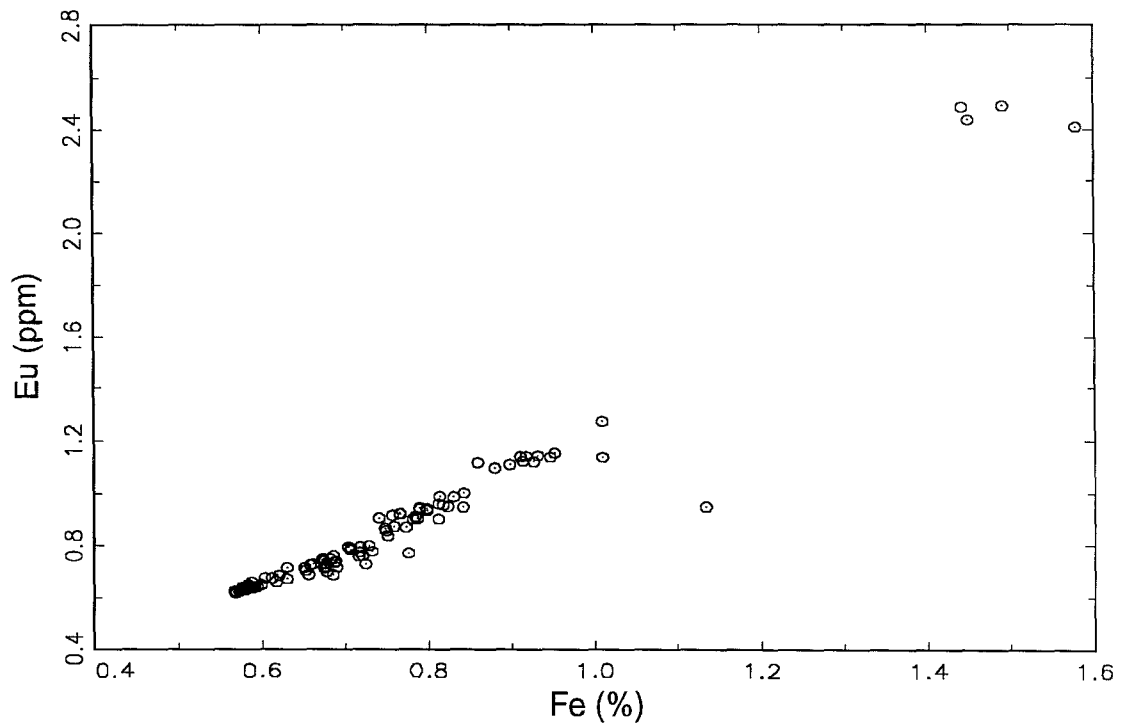


Figure 4.13b: Plot of Fe vs. Eu for obsidian specimens from the Ochoco National Forest showing possible linear trend.

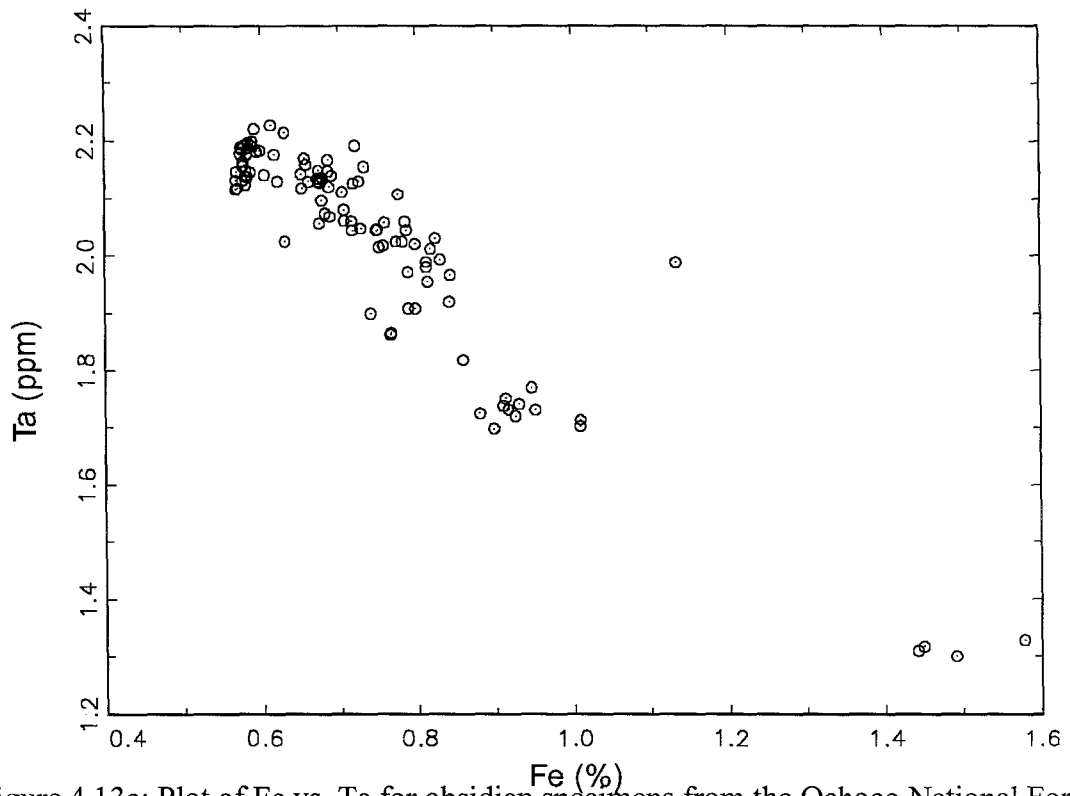


Figure 4.13c: Plot of Fe vs. Ta for obsidian specimens from the Ochoco National Forest showing possible linear trend.

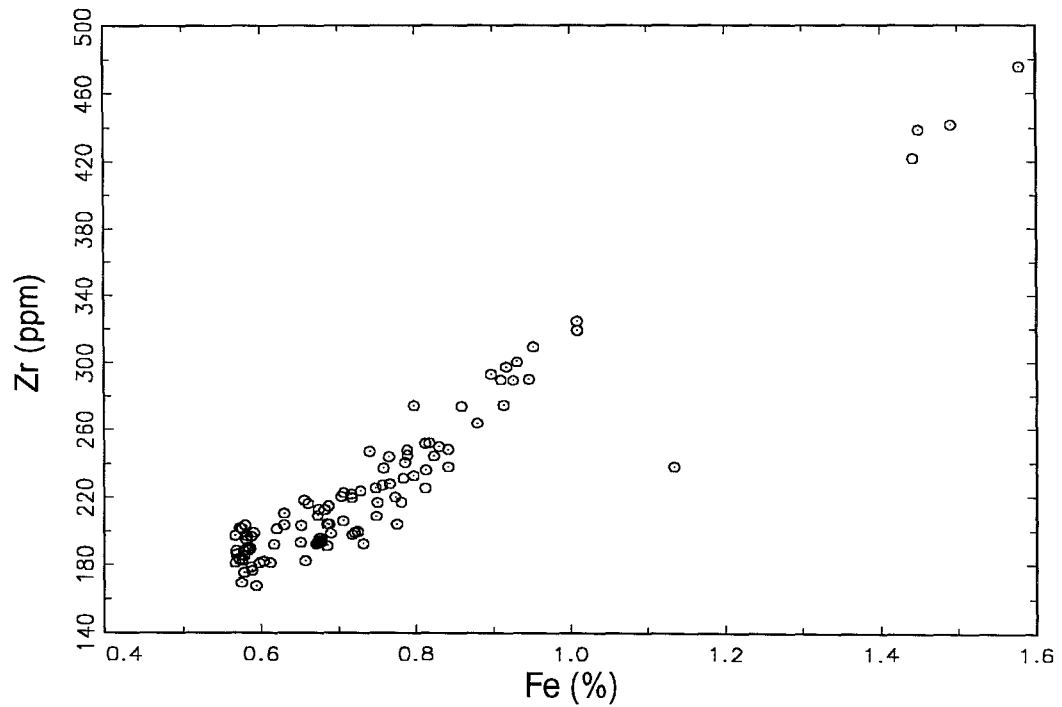


Figure 4.13d: Plot of Fe vs. Zr for obsidian specimens from the Ochoco National Forest showing possible linear trend.

Bowman *et al.* observed a compositional gradation between dacites and rhyolites. Whether the trends shown by the data in this paper are due to grading between dacites and rhyolites is at this time uncertain. Without data on the silica content of the samples analyzed it is impossible to comment one way or another. This type of compositional grading has also been observed at the Mullimica source in Ecuador (Asaro *et al.*, 1981). The Mullimica source was also used to test the possibility of elemental compositions linearly related to Fe abundances. The results were not completely confirmatory. In fact, they ran into a similar problem as this investigation, i.e., that the mixing hypothesis is not secure unless the linearity is observed on measurements of source samples with wider variations in iron abundance (Asaro *et al.*, 1994). Collection of more samples from the Rattlesnake Formation from both inside and outside of the Ochoco National Forest is recommended to provide a better understanding of how this ash-flow tuff was formed.

A largely unsuccessful attempt to separate the chemical groups of the Ochoco National Forest using the short irradiation technique is illustrated in Figure 4.14a (Mn vs. Na). Additionally, the two groups of Buck Springs and Delintment Lake B are not separable using Ba, mainly because of the large range in values. However, Ba does provide a better discrimination between Delintment Lake A and the other two groups (Figure 4.14b). Therefore the short irradiation data can be used in a limited fashion to source artifacts from these sources.

While the area within the Ochoco National Forest is extremely complex and interesting, it is only the tip of the iceberg. The entire geographic extent of the Rattlesnake Formation is not known. As recently as 1984, new outcrops were found as far west as north and south of the town of Prineville in Crook County (Smith *et al.*,

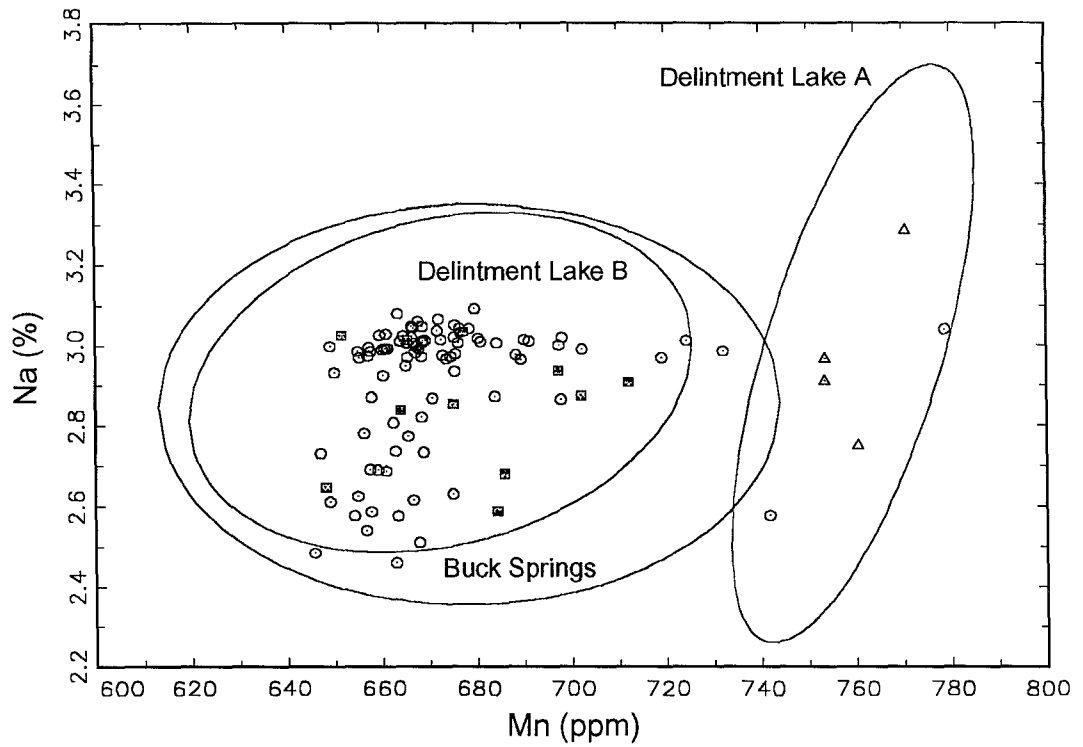


Figure 4.14a: Bivariate plot of Mn vs. Na for obsidian specimens from the Ochoco National Forest.

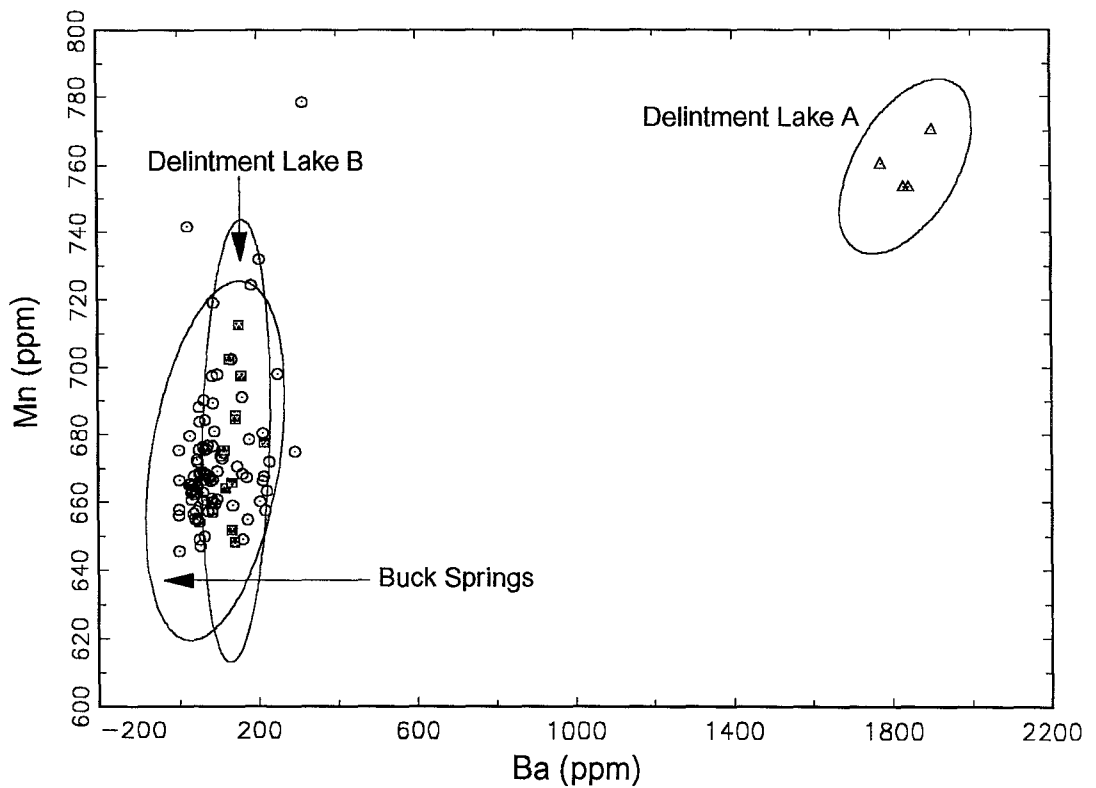


Figure 4.14b: Bivariate plot of Ba vs. Mn for obsidian specimens from the Ochoco National Forest.

1984). It will likely require a much larger number of collection sites and samples before a clearer picture emerges. It is quite possible that with more sampling the areas between the chemical groups identified here will “fill in” until only one large but varied chemical group exists.

Comparison of artifacts to the source groups known from the Rattlesnake Formation should be challenging. Archaeologists must be aware that there is currently no definite correlation between a geographical sampling site and the chemical group a sample may fall into (e.g., samples from Delintment Lake and Plumber Spring fell into all three chemical groups). This means that instead of pinpointing a single outcrop as having been exploited the archaeologist may have to include a much broader geographical obsidian procurement area in his/her discussion. Also, until more sampling of the entire formation is completed, some artifacts may fall into the unknown source category that may fall in between the groups as they are known now or even outside them. The geology of the Rattlesnake Formation guarantees that any work done there, whether geological or archaeological, will not be boring.

Glass Buttes

Introduction

Glass Buttes is a large rhyolitic complex located approximately 80 km west of Burns, Oregon and just south of U.S. Highway 20 in the northeast corner of Lake County, Oregon. A map is shown in Figure 4.15. The complex is approximately 20 km long and 10 km wide and trends generally to the southeast. It is situated in the physiographic province of the High Lava Plains as defined by Dicken (1950). Glass Buttes is a part of the westward progression of complexes with decreasing age discussed earlier and intersects the Brothers Fault Zone. Obsidian from Little Glass Buttes (a small peak to the southeast of Glass Buttes proper) has been dated by K-Ar to an approximate age of 4.9 ± 0.3 million years (Walker, 1974).

Waters (1927) conducted the first significant geological study of Glass Buttes. He identified three periods of extrusion of both basalts and andesites. He described the obsidian as boulders in dry stream channels and as loose blocks in pumiceous sand but these were rarely found in place. Since that time, Glass Buttes has been explored for its geothermal potential, its cinnabar (i.e., mercury) deposits, and its precious metal content (Berri, 1982; Johnson, 1984). For some time, Glass Buttes was mined for its cinnabar deposits, but at the present time all mining activity has ceased. Berri (1982) studied the petrography of part of Glass Buttes, from its easternmost edge to Little Glass Buttes. She found that the rhyolitic volcanism began between about 9 million years ago and 5 million years ago.

With the exception of the basalts, all the rocks at Glass Buttes are highly glassy or completely glassy. A typical obsidian dome consists of a black obsidian core with an

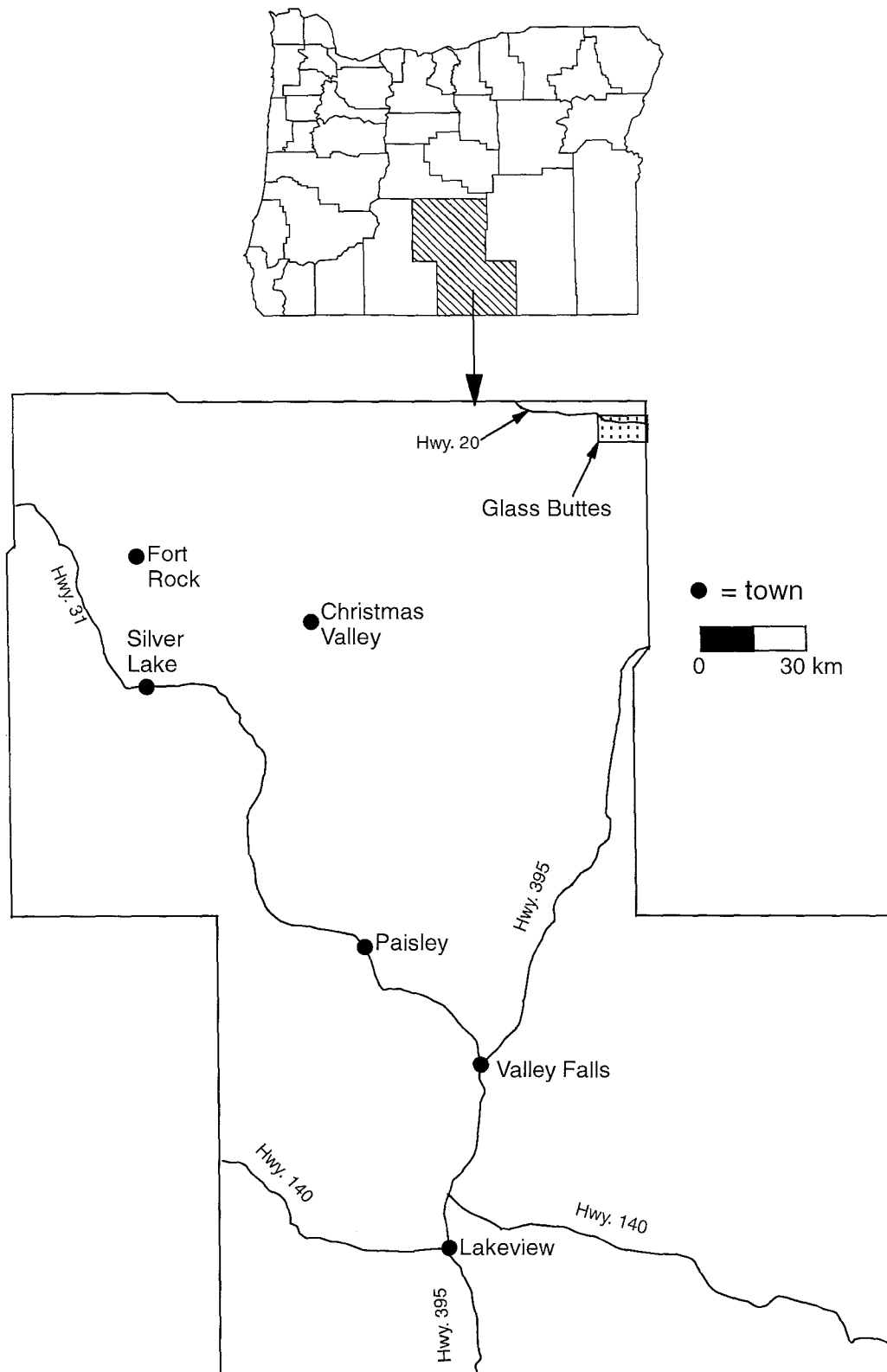


Figure 4.15: Map of Lake County, Oregon showing location of Glass Buttes. See Figure 4.17 for enlargement of the rectangle.

outer layer of gray glass (Cummings, 1985). These two layers together make up about 80% of the volume of the dome. Above the gray glass is a layer of gray glass with obsidian inclusions. The final three layers are part of a glass breccia that grades from gray glass clasts in a brown glass matrix to stretched brown glass clasts in a brown glass matrix to the final layer of fused stretched brown glass clasts.

The stratigraphy at Glass Buttes is very complicated because the complex was built by successive eruptions of small volume (Berri, 1982). Berri mentions obsidian only when discussing the Little Glass Buttes area. She identified three separate units around Little Glass Buttes and Obsidian Hills (to the north) which overlap and are overlapped by basalts. Although it is difficult to separate them, they contributed to her theory of bimodal volcanism at Glass Buttes (i.e., there are no volcanic rocks of intermediate composition between the basalts and the rhyolite/obsidian) (Berri, 1982). Although Johnson (1984) continued some of the work started by Berri, he concentrated mainly on the hydrothermal alteration that took place at Glass Buttes. Roche (1987) also built on the work of Berri. He performed a greater number of analyses on the obsidian but only analyzed samples from the eastern areas.

Glass Buttes obsidian is typically of extremely high quality. It is found in a large variety of colors including black, mahogany, snowflake, and rainbow. The glass is highly prized by gem collectors and flintknappers. During the summer months it is quite common to find large numbers of people collecting glass from the various outcrops.

Obsidian from Glass Buttes was also widely used by Native Americans. There are several springs on the complex, each with an associated archaeological site (Zancanella, 1997). Glass Buttes obsidian was also used at sites distant from the source

area. For example, Hughes (1990) found some of the large bifaces at the Gold Hill site (about 300 km from Glass Buttes) in Oregon were made from Glass Buttes obsidian.

Glass Buttes obsidian has also been found at the Gunther Island site in northwestern California (Hughes, 1978). Certain varieties (e.g. red-colored) may have been highly prized and traded great distances for ceremonial purposes (Zancanella, 1997).

Undoubtedly, there are many other sites that have not been studied yet that contain Glass Buttes obsidian.

Results and Discussion

As illustrated in Figures 4.16a (Cs vs. Eu) and 4.16b (Rb vs. Th), seven different chemical groups of Glass Buttes obsidian were identified in this study. A map detailing the sampling sites and the geographical areas of the groups at Glass Buttes is shown in Figure 4.17. The data are presented in Tables 4.14-4.20. X-ray fluorescence data (Skinner, unpubl. data) was almost as successful at separating the groups as NAA. Using Sr and Rb, Skinner distinguished six of the seven chemical groups found by NAA (Figure 4.18). Glass Buttes A, by far the largest chemical group at Glass Buttes, consists of 110 source samples from 20 different sampling sites. It includes the main peak of Glass Buttes as well as a significant number of areas surrounding the peak. The other chemical groups are small by comparison. The three smallest groups each contain samples from only one collection site each. The areas around these collection sites will be sampled in the future to better determine the geographical limits of their respective chemical groups.

Some of the chemical groups contain samples that belong to them but were collected from areas other than Glass Buttes. For example, Juniper Springs is a secondary deposit of obsidian located north of Glass Buttes across Highway 20 at the

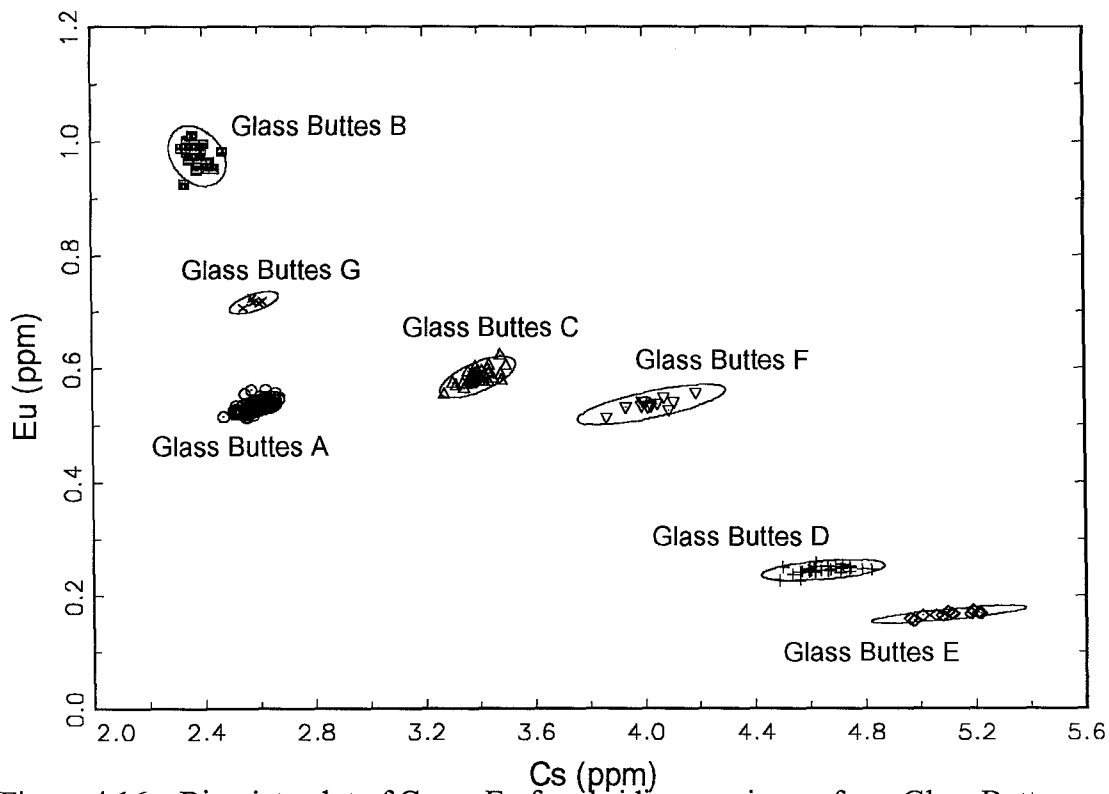


Figure 4.16a: Bivariate plot of Cs vs. Eu for obsidian specimens from Glass Buttes.

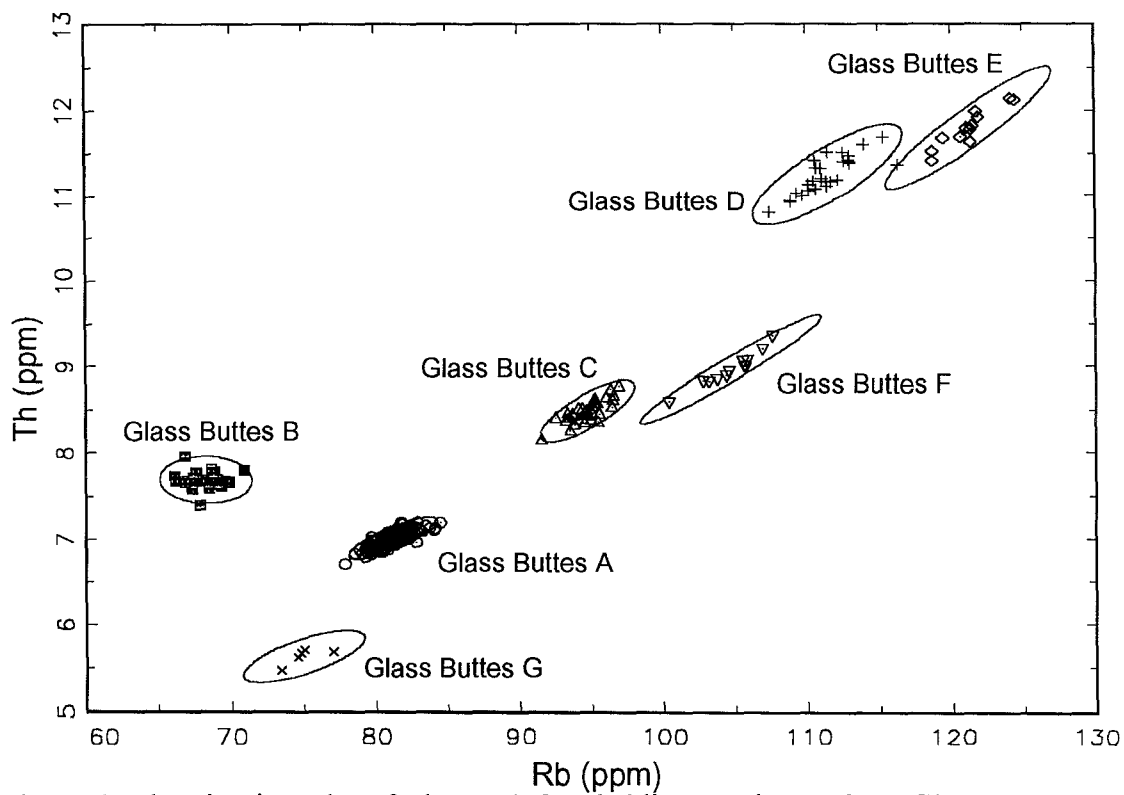


Figure 4.16b: Bivariate plot of Rb vs. Th for obsidian specimens from Glass Buttes.

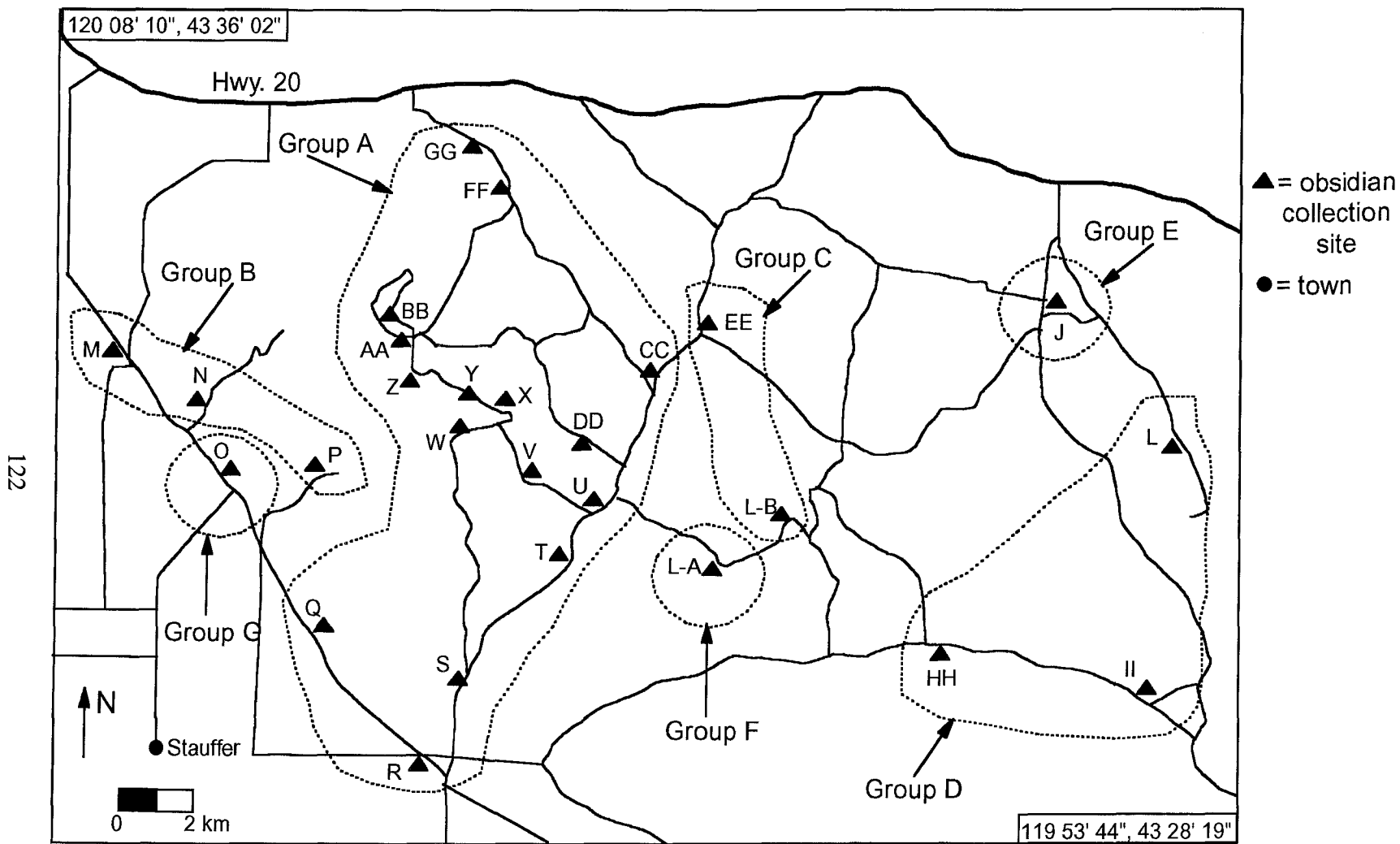


Figure 4.17: Map showing sampling areas within Glass Buttes and estimated limits of the chemical groups as determined by NAA. This map is an enlargement of the rectangle shown in Figure 4.15.

Table 4.14: Descriptive Statistics for Glass Buttes A Obsidian, Lake County.

Element	Mean	St. Dev.	% St. Dev.	No. Obs.	Minimum	Maximum
BA	1110	20	1.47	110	1070	1160
LA	24.2	0.7	3.02	110	23.3	30.9
LU	0.810	0.016	2.01	110	0.778	0.848
ND	22.8	3.3	14.4	110	16.2	32.0
SM	5.85	0.09	1.53	110	5.61	6.12
U	3.07	0.52	17.1	110	1.51	4.34
YB	5.54	0.18	3.17	110	5.06	5.85
CE	52.2	1.5	2.92	110	49.5	65.2
CO	0.180	0.016	9.04	110	0.153	0.234
CS	2.59	0.04	1.58	110	2.47	2.67
EU	0.536	0.010	1.82	110	0.514	0.564
FE	5580	80	1.38	110	5390	5780
HF	4.05	0.08	2.11	110	3.85	4.36
RB	81.2	1.2	1.52	110	77.8	84.5
SB	0.423	0.018	4.31	110	0.387	0.464
SC	3.63	0.08	2.31	110	3.49	4.28
SR	18.2	5.8	32.1	39	6.62	38.2
TA	0.825	0.014	1.64	110	0.794	0.854
TB	1.12	0.08	6.66	110	0.903	1.46
TH	7.01	0.10	1.41	110	6.71	7.20
ZN	39.0	6.5	16.6	110	26.1	52.9
ZR	110.	8	7.34	110	95.6	135
CL	204	32	15.7	110	133	340.
DY	7.55	0.34	4.47	110	6.48	8.38
K	34300	1500	4.36	110	31100	38300
MN	314	11	3.48	110	301	414
NA	30800	470	1.53	110	28800	31900

ANIDS of specimens included:

GBAA01	GBAA02	GBAA03	GBAA04	GBAA05	GBAA06	GBBB01	GBBB02
GBBB03	GBBB04	GBBB05	GBBB06	GBCC01	GBCC02	GBCC03	GBCC04
GBCC06	GBDD01	GBDD02	GBDD03	GBDD04	GBDD05	GBDD06	GBFF01
GBFF02	GBFF03	GBFF04	GBFF05	GBFF06	GBGG01	GBGG02	GBGG03
GBGG04	GBGG05	GBGG06	GBO006	GBO011	GBO012	GBQ001	GBQ002
GBQ003	GBQ004	GBQ005	GBQ006	GBR001	GBR002	GBR003	GBR004
GBR006	GBS001	GBS002	GBS003	GBS004	GBS005	GBS006	GBT001
GBT002	GBT003	GBT004	GBT005	GBT006	GBU001	GBU002	GBU003
GBU004	GBU005	GBU006	GBV001	GBV002	GBV003	GBV004	GBV005
GBV006	GBW001	GBW002	GBW003	GBW004	GBW005	GBW006	GBX001
GBX002	GBX003	GBX004	GBX005	GBX006	GBY001	GBY002	GBY003
GBY004	GBY005	GBY006	GBZ001	GBZ002	GBZ003	GBZ004	GBZ005
GBZ006	GB006	JRB011	WT001	WT002	WT003	WT004	WT005
WT006	YBC001	YBC005	YBC006	YBC007	YBC008		

Table 4.15: Descriptive Statistics for Glass Buttes B Obsidian, Lake County.

Element	Mean	St. Dev.	% St. Dev.	No. Obs.	Minimum	Maximum
BA	1250	20	1.35	26	1220	1280
LA	37.2	0.7	1.93	26	36.0	38.5
LU	0.725	0.016	2.16	26	0.682	0.748
ND	31.1	4.0	12.8	26	26.5	37.1
SM	6.66	0.12	1.75	26	6.40	6.86
U	2.42	0.67	27.6	26	1.19	3.51
YB	5.05	0.20	3.96	26	4.59	5.41
CE	74.7	1.4	1.81	26	70.6	78.0
CO	0.338	0.017	4.98	26	0.309	0.391
CS	2.38	0.04	1.59	26	2.32	2.47
EU	0.975	0.019	1.98	26	0.924	1.01
FE	6490	110	1.75	26	6230	6720
HF	4.50	0.06	1.33	26	4.37	4.60
RB	68.2	1.2	1.70	26	66.1	70.9
SB	0.335	0.024	7.01	26	0.288	0.374
SC	3.52	0.05	1.37	26	3.41	3.66
SR	44.6	9.5	21.3	26	25.8	73.1
TA	0.751	0.014	1.92	26	0.720	0.777
TB	1.08	0.09	8.60	26	0.890	1.34
TH	7.69	0.10	1.28	26	7.40	7.95
ZN	41.9	4.9	11.7	26	30.2	55.8
ZR	140.	12	8.79	26	115	163
CL	192	32	16.7	26	133	268
DY	7.07	0.29	4.08	26	6.45	7.63
K	30200	1250	4.15	26	28000	33000
MN	318	7	2.33	26	303	328
NA	32200	330	1.03	26	31600	32700

ANIDs of specimens included:

GBCC05	GBM001	GBM002	GBM003	GBM004	GBM005	GBM006	GBN001
GBN002	GBN003	GBN004	GBN005	GBN006	GBO003	GBO005	GBO008
GBO009	GBO010	GBO013	GBP001	GBP002	GBP003	GBP004	GBP005
GBP006	GBR005						

Table 4.16: Descriptive Statistics for Glass Buttes C Obsidian, Lake County.

Element	Mean	St. Dev.	% St. Dev.	No. Obs.	Minimum	Maximum
BA	1270	20	1.29	32	1230	1310
LA	25.8	0.4	1.50	32	25.2	26.6
LU	0.441	0.013	2.88	32	0.429	0.487
ND	18.7	4.9	26.3	32	12.4	31.8
SM	3.66	0.05	1.42	32	3.54	3.76
U	4.09	0.63	15.5	32	3.32	5.63
YB	2.77	0.10	3.67	32	2.63	2.97
CE	48.4	1.0	1.98	32	46.4	50.2
CO	0.389	0.013	3.44	32	0.365	0.423
CS	3.40	0.05	1.52	32	3.27	3.50
EU	0.585	0.013	2.30	32	0.556	0.623
FE	6200	100	1.58	32	5940	6480
HF	3.67	0.06	1.64	32	3.53	3.79
RB	94.7	1.2	1.29	32	91.5	96.9
SB	0.205	0.011	5.41	32	0.181	0.230
SC	2.81	0.05	1.83	32	2.69	2.94
SR	77.6	20.5	26.5	32	48.0	169
TA	0.659	0.012	1.80	32	0.634	0.678
TB	0.549	0.033	6.07	32	0.499	0.642
TH	8.48	0.13	1.58	32	8.15	8.77
ZN	30.9	7.1	23.0	32	20.0	47.8
ZR	118	7	5.62	32	103	130.
CL	113	29	26.0	32	79.2	186
DY	3.62	0.27	7.49	32	2.84	4.02
K	35200	1650	4.70	32	32000	38700
MN	327	6	1.81	32	314	339
NA	28400	600	2.15	32	25700	29200

ANIDs of specimens included:

LGB001	LGB002	LGB003	LGB004	LGB005	LGB006	GBEE01	GBEE02
GBEE03	GBEE04	GBEE05	GBEE06	LGBA09	LGBB01	LGBB02	LGBB03
LGBB04	LGBB05	LGBB06	LGBB07	LGBB08	LGBB09	GB001	GB002
GB003	GB004	GB005	GB007	GB008	JRB005	JRB006	JRB008

Table 4.17: Descriptive Statistics for Glass Buttes D Obsidian, Lake County.

Element	Mean	St. Dev.	% St. Dev.	No. Obs.	Minimum	Maximum
BA	259	15	5.73	28	231	289
LA	18.3	0.4	2.03	28	17.6	19.7
LU	1.06	0.02	2.03	28	1.01	1.10
ND	21.8	7.3	33.6	28	15.5	45.0
SM	6.98	0.12	1.69	28	6.79	7.11
U	6.83	0.50	7.26	28	5.85	7.98
YB	7.22	0.31	4.35	28	6.64	7.65
CE	44.6	1.5	3.45	28	41.9	48.2
CO	0.071	0.009	12.2	28	0.056	0.087
CS	4.65	0.08	1.78	28	4.49	4.82
EU	0.245	0.007	2.76	28	0.227	0.258
FE	4710	99.9	2.12	28	4460	4860
HF	4.27	0.10	2.34	28	4.08	4.48
RB	111	2	1.72	28	107	116
SB	0.470	0.033	6.98	28	0.410	0.531
SC	6.40	0.10	1.51	28	6.16	6.55
SR**				0		
TA	1.00	0.02	1.88	28	0.973	1.05
TB	1.54	0.07	4.62	28	1.44	1.66
TH	11.2	0.2	1.94	28	10.8	11.7
ZN	55.1	5.9	10.8	28	42.7	76.1
ZR	114	8	7.36	28	94.3	129
CL	166	26	15.6	28	114	232
DY	10.1	0.4	3.75	28	9.38	10.6
K	37100	1660	4.48	28	33300	40600
MN	416	5	1.27	28	405	426
NA	30300	500	1.71	28	29000	31000

ANIDs of specimens included:

GBHH01	GBHH02	GBHH03	GBHH04	GBHH05	GBHH06	GBII01	GBII02
GBII03	GBII04	GBII05	GBII06	GBL001	GBL002	GBL003	GBL004
GBL005	GBL006	GBL007	GBL008	GBL009	GBL010	GBL011	GBL012
JRB001	JRB003	JRB004	JRB009				

**Values not available because element concentrations below detection limit.

Table 4.18: Descriptive Statistics for Glass Buttes E Obsidian, Lake County.

Element	Mean	St. Dev.	% St. Dev.	No. Obs.	Minimum	Maximum
BA	62.4	13.2	21.1	11	41.2	86.7
LA	14.8	0.2	1.32	12	14.4	15.2
LU	1.15	0.02	1.60	12	1.12	1.18
ND	19.0	2.2	11.4	12	16.6	24.7
SM	7.19	0.10	1.34	12	7.02	7.35
U	7.72	0.85	11.0	12	6.97	10.2
YB	8.11	0.16	2.02	12	7.84	8.44
CE	37.8	1.0	2.57	12	36.2	40.1
CO	0.049	0.010	20.9	12	0.035	0.070
CS	5.10	0.09	1.74	12	4.96	5.22
EU	0.167	0.005	2.95	12	0.157	0.174
FE	4770	100	2.02	12	4600	4910
HF	4.48	0.11	2.52	12	4.18	4.62
RB	121	2	1.49	12	119	124
SB	0.506	0.029	5.70	12	0.435	0.537
SC	6.77	0.13	1.96	12	6.52	6.97
SR**				0		
TA	1.09	0.02	1.76	12	1.05	1.12
TB	1.58	0.04	2.40	12	1.48	1.62
TH	11.8	0.2	1.90	12	11.4	12.1
ZN	57.6	5.4	9.39	12	52.0	68.8
ZR	108	10	9.22	12	86.9	122
CL	178	24	13.6	12	144	214
DY	11.0	0.5	4.21	12	10.3	11.9
K	37900	2300	6.16	12	33600	43600
MN	447	4	0.79	12	442	453
NA	30900	310	0.99	12	30400	31400

ANIDs of specimens included:

GBJ001 GBJ002 GBJ003 GBJ004 GBJ005 GBJ006 GBJ007 GBJ008
 GBJ009 GBJ010 JRB010 JRB012

**Values not available because element concentrations below detection limit.

Table 4.19: Descriptive Statistics for Glass Buttes F Obsidian, Lake County.

Element	Mean	St. Dev.	% St. Dev.	No. Obs.	Minimum	Maximum
BA	1040	20	1.85	12	1000	1070
LA	24.1	0.4	1.56	12	23.5	24.6
LU	0.477	0.009	1.82	12	0.457	0.489
ND	24.2	5.4	22.2	12	14.5	32.8
SM	3.80	0.06	1.69	12	3.68	3.87
U	5.10	0.64	12.5	12	4.19	6.30
YB	3.02	0.17	5.68	12	2.78	3.24
CE	47.5	1.2	2.54	12	45.6	49.1
CO	0.290	0.011	3.65	12	0.274	0.307
CS	4.03	0.08	2.11	12	3.86	4.19
EU	0.536	0.011	2.07	12	0.514	0.557
FE	5660	120	2.05	12	5410	5890
HF	3.54	0.08	2.16	12	3.40	3.69
RB	105	2	1.88	12	100.	108
SB	0.219	0.011	4.93	12	0.199	0.232
SC	3.10	0.09	2.83	12	2.98	3.27
SR	48.6	10.7	22.1	12	36.4	66.3
TA	0.770	0.015	1.89	12	0.747	0.802
TB	0.611	0.036	5.84	12	0.572	0.668
TH	8.97	0.20	2.22	12	8.59	9.35
ZN	32.3	5.5	17.1	12	23.6	41.6
ZR	119	8	6.43	12	106	133
CL	111	37	33.5	12	71.9	182
DY	4.10	0.20	5.00	12	3.70	4.46
K	37200	1600	4.24	12	34400	40200
MN	368	6	1.63	12	359	376
NA	28800	400	1.36	12	28200	29200

ANIDs of specimens included:

LGBA01 LGBA02 LGBA03 LGBA04 LGBA05 LGBA06 LGBA07 LGBA08
 LGBA10 LGBA11 LGBA12 JRB007

Table 4.20: Descriptive Statistics for Glass Buttes G Obsidian, Lake County.

Element	Mean	St. Dev.	% St. Dev.	No. Obs.	Minimum	Maximum
BA	1000	30	2.73	5	956	1030
LA	20.8	0.6	2.87	5	19.8	21.4
LU	0.881	0.032	3.62	5	0.838	0.914
ND	19.8	1.9	9.78	5	17.8	22.8
SM	5.87	0.18	3.02	5	5.56	6.01
U	2.67	0.38	14.3	5	2.18	2.98
YB	6.16	0.40	6.41	5	5.64	6.55
CE	46.3	1.0	2.16	5	45.0	47.8
CO	0.172	0.011	6.54	5	0.161	0.188
CS	2.58	0.03	1.06	5	2.54	2.62
EU	0.717	0.006	0.88	5	0.707	0.724
FE	5350	70	1.29	5	5240	5430
HF	4.04	0.07	1.62	5	3.93	4.08
RB	75.0	1.3	1.76	5	73.4	77.0
SB	0.420	0.036	8.48	5	0.379	0.453
SC	3.94	0.06	1.43	5	3.85	4.00
SR	16.8	2.7	16.2	2	14.8	18.7
TA	0.895	0.005	0.60	5	0.889	0.902
TB	1.18	0.14	11.5	5	1.01	1.30
TH	5.63	0.09	1.67	5	5.47	5.71
ZN	48.7	3.6	7.33	5	44.1	53.2
ZR	104	9	8.61	5	95.0	115
CL	170.	21	12.1	5	139	191
DY	8.63	0.39	4.47	5	8.27	9.25
K	32500	1300	4.07	5	30800	34100
MN	424	2	0.57	5	421	426
NA	32800	200	0.68	5	32500	33100

ANIDs of specimens included:

GB0001 GB0002 GB0004 GB0007 GB0014

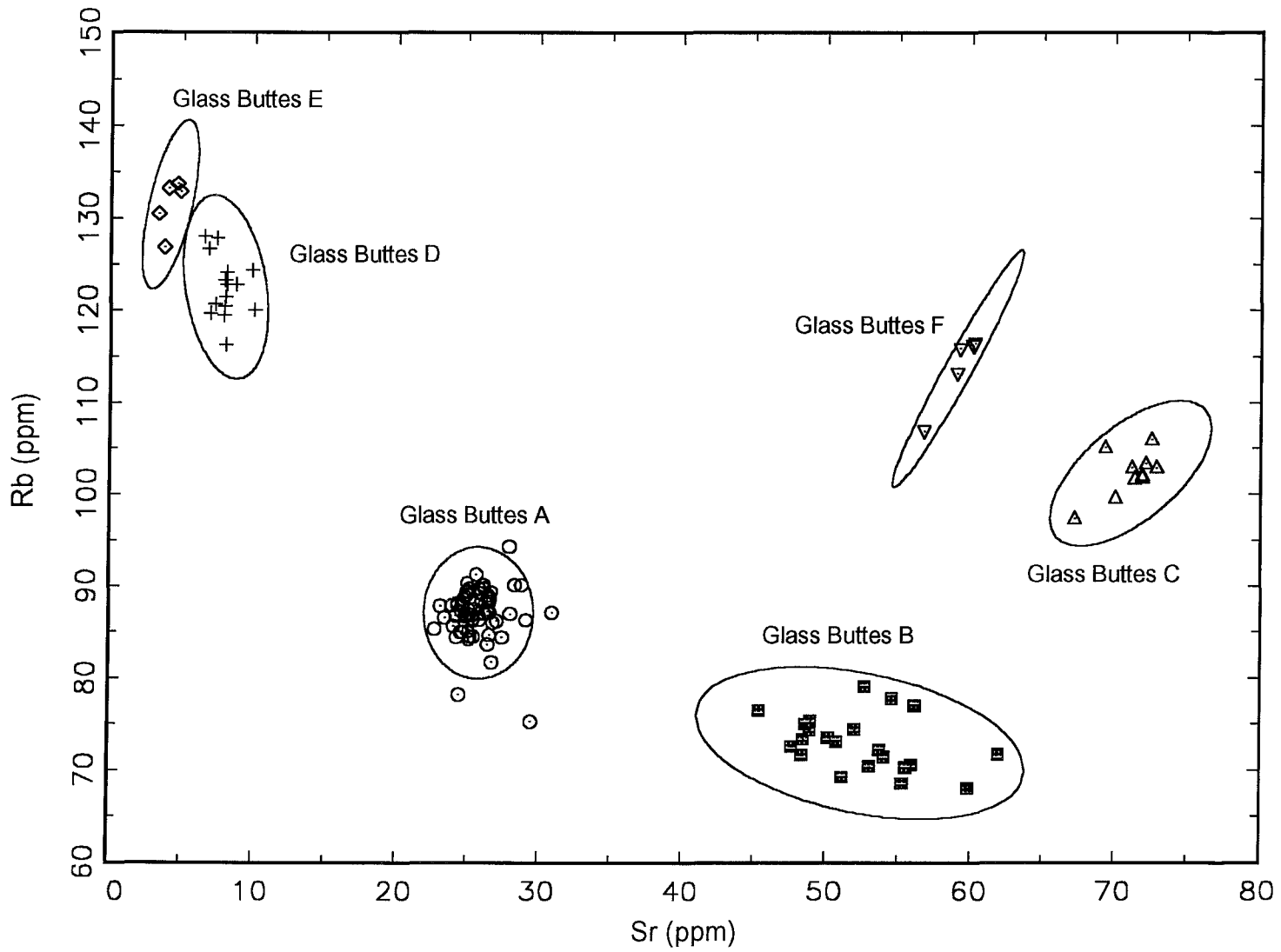


Figure 4.18: Bivariate plot of Sr vs. Rb for obsidian specimens from Glass Buttes using XRF data.

junction of Juniper Springs and G. I. Ranch road. One sample from Juniper Springs fell into the Glass Buttes A chemical group, three fell into the Glass Buttes C group, four fell into the Glass Buttes D group, two fell into the Glass Buttes E group, and one fell into the Glass Buttes F group.

One possible explanation for the occurrence of Glass Buttes obsidian at Juniper Springs is that the eruptions that produced the chemical groups mentioned were somewhat explosive and therefore blocks of obsidian were thrown some distance. Juniper Springs is also interesting because one sample from there fell into the Buck Springs chemical group of the Ochoco National Forest. There is an ash-flow tuff located only a few miles east of Juniper Springs. It is possible that the tuff is part of the Rattlesnake Formation and the sample was washed down from there. According to Skinner (pers. commun.), the Juniper Springs sampling locale is in a basin and acts somewhat like a “bowl” that has collected obsidian from the many sources that surround it. More sampling in this area should provide insight into the mechanisms of the secondary deposition.

Analysis of obsidian from a water tank near Glass Buttes showed it to also be a secondary deposit. In this case, six samples analyzed from the water tank area were shown to belong to the Glass Buttes A chemical group. Apparently, someone had loaded their truck with obsidian from one of the ubiquitous deposits on Glass Buttes and dumped it near a water tank to provide some kind of base. This explanation is analogous to the explanation given above concerning the Juniper Springs sample from the Rattlesnake Formation. This discovery illustrates how the influence of modern man must be taken into account when locating and identifying outcrops of obsidian. The influence of

modern man is also a possibility when trying to explain the occurrence of five samples from Yreka Butte that fell into Glass Buttes A. Explosive volcanism provides another possible explanation.

The abbreviated-NAA method was also successful in separating the seven chemical groups of Glass Buttes. In Figure 4.19a, a plot of Mn versus Na shows an overlap of groups A and B. However, as illustrated in Figure 4.19b, Ba can be used to differentiate between the two chemical groups.

It is very interesting to note that the geochemical fingerprints that are closest to one another geochemically are typically closest to one another geographically (e.g., groups D and E, groups C and F, and groups A, B, and G). Cummings and Roche (1989) identified two separate geographic trends. From east to west they found that the elemental concentrations of Sc, Rb, Cs, Tb, Yb, Lu, U, and Th decreased while the elemental concentrations of Mg, Ca, Ti, Ba, La, Ce, and Eu increased. The results of this study show some similar trends. For example, from east to west (i.e., group E to D to F to C to groups A, B, and G), the elemental concentrations of Cs, Rb, U, and Th decrease while Eu, La, and Ce concentrations increase.

However, because this study analyzed samples from the western part of Glass Buttes (i.e., groups A, B, and G) while Cummings and Roche did not, other trends have been identified. For example, Cummings and Roche (1989) determined the elements Sc, Tb, Yb, and Lu to decrease in concentration from east to west. However, the results of the current investigation indicate that the concentrations of these elements increase from C to A to B to G. The elements Sm, Ta, and Hf also follow the same pattern. These trends may indicate two different volcanic sequences, perhaps influenced by the

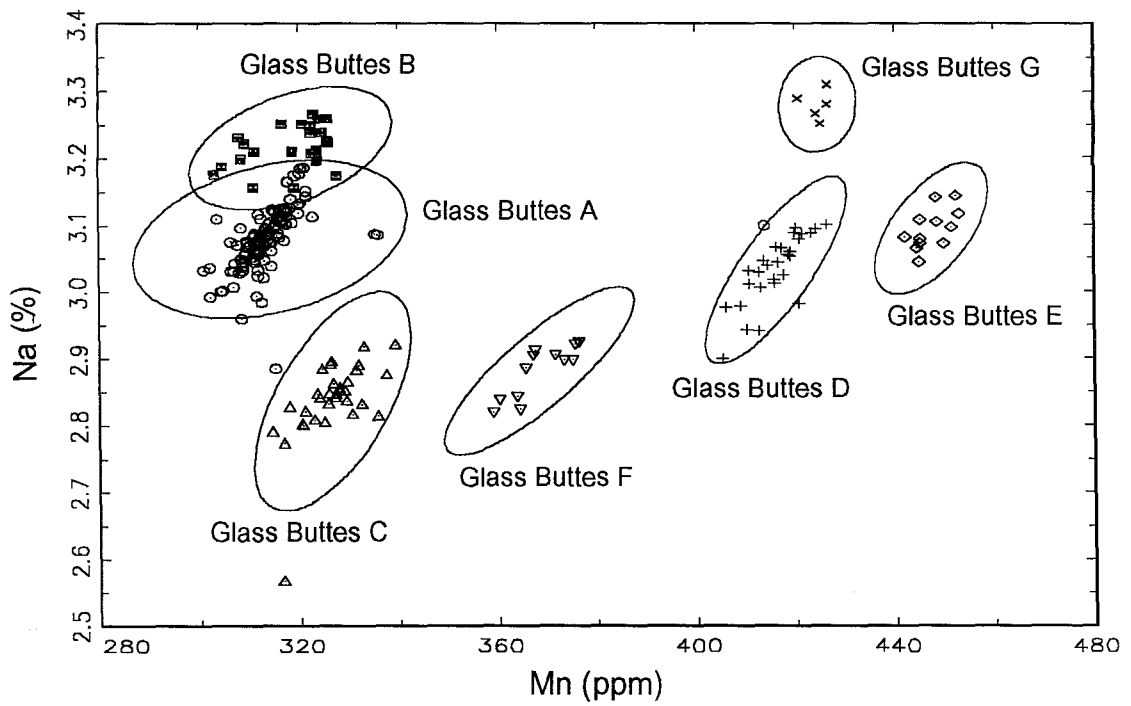


Figure 4.19a: Bivariate plot of Mn vs. Na for obsidian specimens from Glass Buttes.

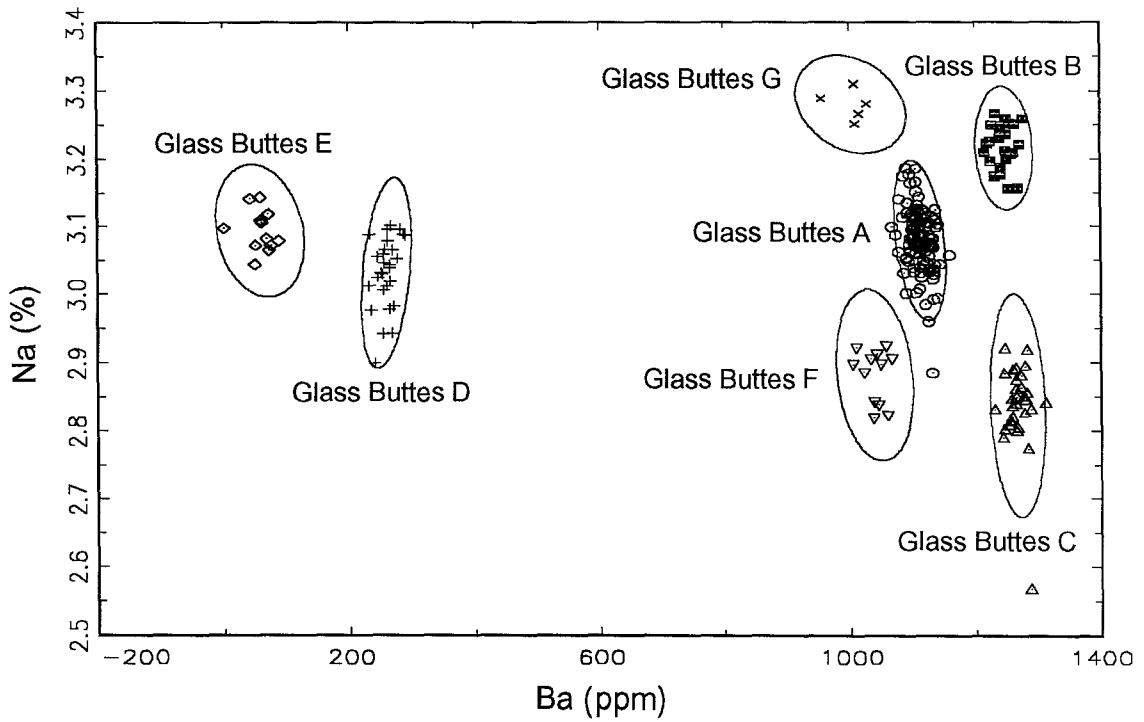


Figure 4.19b: Bivariate plot of Ba vs. Na for obsidian specimens from Glass Buttes.

propagation of the Brothers Fault Zone. Additional sampling and analysis of samples for both major and trace elements is necessary to explore these trends further.

Glass Buttes covers a very large area and remains incompletely sampled. Hopefully future sampling will further delineate the geographic boundaries of the chemical groups already identified as well as identify any remaining new chemical signatures within the complex.

Lake County

Introduction

Lake County, like Harney County, is partially overlaid by the High Lava Plains (see Figure 4.20 for a map of Lake County). This accounts for most, but not all, of the volcanic activity that produced several of the rhyolitic flows and domes that dominate the landscape. Despite the large number of silicic vents, the geology of Lake County is highly variable. It includes considerable amounts of basalt as well as alluvial deposits, sedimentary rocks, playa deposits, and ash-flow tuffs, among others (Walker *et al.*, 1967). The areas from which obsidian was sampled were identified in a geologic map as rocks of silicic vents: “Dikes, plugs, and complex exogenous domes, including related flows and flow breccias, of dacitic to rhyolitic composition....”

There is little available information about the silicic vents examined in this paper. Tucker Hill has been investigated thoroughly for the economic value of its perlite deposit (Wilson and Emmons, 1985). Given a potassium-argon (K-Ar) date of about 7.41 ± 0.9 million years, it is not unconceivable that much of the obsidian would have been hydrated to perlite. This perlite, possibly able to replace commercial perlite for a variety of applications, attracted the geologists who performed the study of Tucker Hill. Tucker Hill follows the standard pattern for zonation of a rhyolitic dome. The core is rhyolitic glass that is surrounded by an inner glass envelope of poorer quality, which is surrounded, by an outer glass envelope. This chill margin originally was obsidian but has been hydrated to perlite. Hughes (1986a) found large cobbles and nodules at Tucker Hill, as well as a “staggering amount of obsidian tool manufacturing debris.”

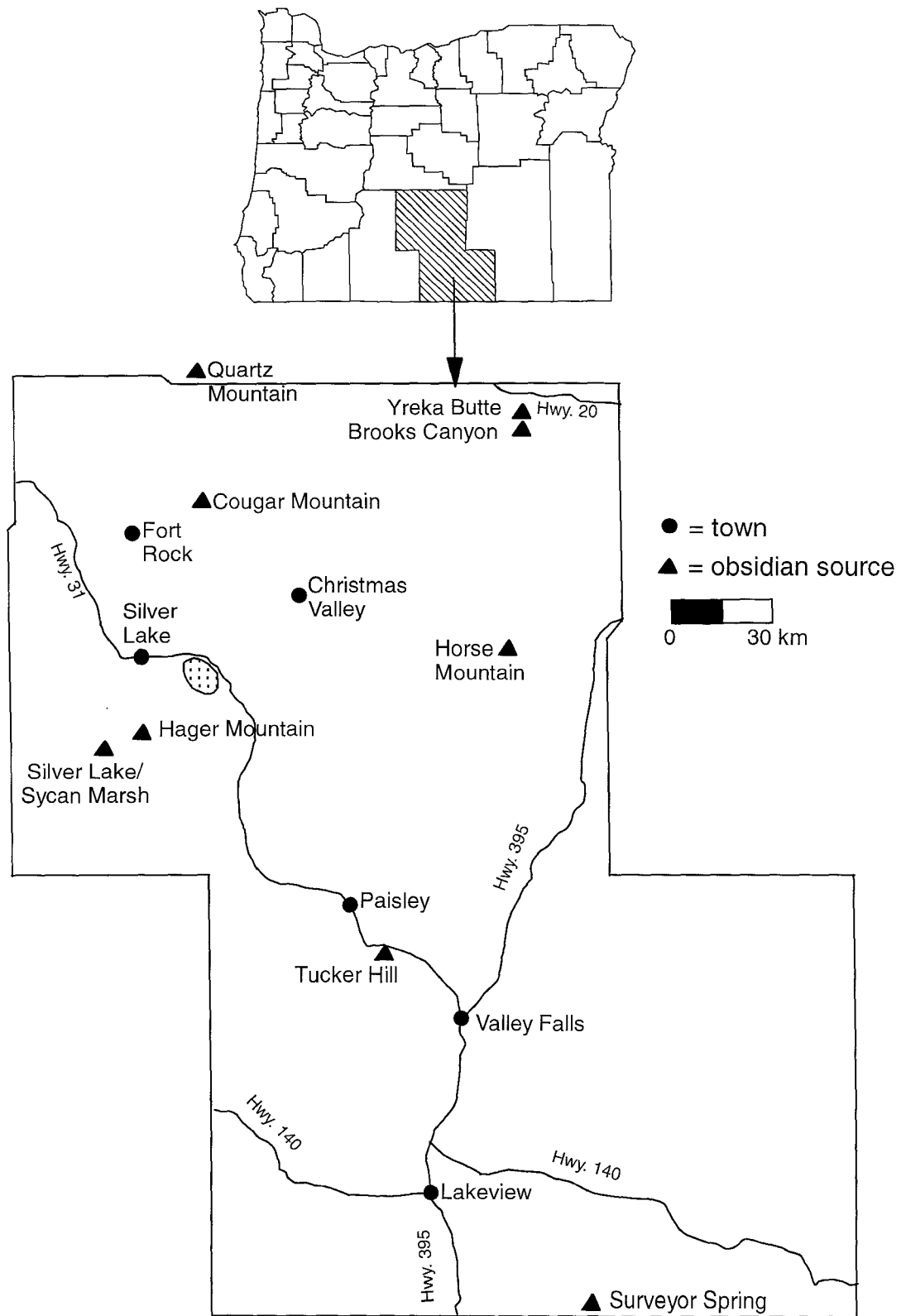


Figure 4.20: Map showing locations of obsidian sources in Lake County, Oregon.

Archaeological investigations have been performed at a site near the Cougar Mountain obsidian source. An amateur originally excavated the site of Cougar Mountain Cave and therefore the chronology and stratigraphy were somewhat unknown. Layton (1972) attempted to use obsidian hydration dating to shed light on this problem. He was able to identify 10 types of projectile points and date them in such a way as to describe a long duration of occupation beginning about 13,000 radiocarbon years B.P. Since compositional analysis was not made to determine the source of the artifacts (though Cougar Mountain itself is likely), the data from this paper could be used in a future study of the points. Hughes (1986a) describes cobbles and nodules of obsidian on a west trending slope near the top of Cougar Mountain, evidence for prehistoric tool manufacture. A K-Ar date of Cougar Mountain was given as 4.31 ± 0.34 million years (this date and the following K-Ar dates were reported by McKee *et al.*, 1976).

Hughes (1986a) identified other sources analyzed in this study as prehistoric exploitation sites. At Silver Lake and Sycan Marsh, he found biface fragments, cores, and biface reduction debris, all evidence of prehistoric quarrying. Hager Mountain, given a K-Ar date of 5.90 ± 0.09 million years, and Auger Creek showed evidence for limited prehistoric use. Horse Mountain, given a K-Ar date of 6.91 ± 0.14 million years, has a dense cover of obsidian nodules over a large area and abundant evidence for prehistoric use of those nodules. Quartz Mountain, given a K-Ar date of 1.10 ± 0.05 million years, shows evidence of biface manufacture. Finally, Surveyor Spring shows a small amount of evidence for some prehistoric use.

The prehistoric use of obsidian from some of these areas has been validated by archaeological studies. For example, a study of the Gold Hill site by Hughes (1990)

identified some of the obsidian artifacts as coming from sources within Lake County. Using XRF analyses, Hughes matched the artifacts to source samples from Glass Buttes, Silver Lake/Sycan Marsh, Spodue Mountain, Horse Mountain, and Quartz Mountain. This was an interesting study because it showed the exploitation of obsidian sources that were relatively distant. It is likely that excavation of more sites in the future will reveal that the obsidian sources in Lake County as well as other areas of Oregon were indeed used during the prehistoric period.

Results and Discussion

In Lake County, obsidian from 11 different sampling locations yielded nine different chemical groups (Figure 4.20). The data are summarized in Tables 4.21-4.29. The nine chemical groups are Yreka Butte, Brooks Canyon, Horse Mountain, Cougar Mountain, Tucker Hill, Hager Mountain, Silver Lake/Sycan Marsh, and Quartz Mountain. All of the sources are homogeneous single composition sources except for Yreka Butte, which contained one outlier. The Hager Mountain chemical group includes samples from Auger Creek. The Silver Lake/Sycan Marsh chemical group includes samples from Sycan Marsh. The Quartz Mountain chemical group is actually in Deschutes County and has sometimes been included in discussions of Newberry Volcano but for the purposes of this discussion it was placed into this chapter.

All nine chemical groups were easily separated as shown in Figures 4.21a (Eu vs. Rb) and 4.21b (Cs vs. Fe). The chemical groups are also separated easily using sodium and manganese from the short irradiation (Figure 4.22a). However, data on barium are required to separate Yreka Butte from Silver Lake/Sycan Marsh and to provide a more definitive separation between Quartz Mountain and Cougar Mountain (Figure 4.22b).

Table 4.21: Descriptive Statistics for Yreka Butte Obsidian, Lake County.

Element	Mean	St. Dev.	% St. Dev.	No. Obs.	Minimum	Maximum
BA	1180	20	1.34	24	1140	1200
LA	36.5	0.4	1.08	24	35.5	37.0
LU	1.04	0.01	1.15	24	1.02	1.06
ND	38.3	3.5	9.19	24	31.3	45.2
SM	9.14	0.13	1.39	24	8.92	9.41
U	1.83	0.50	27.4	23	1.08	3.21
YB	7.17	0.16	2.31	24	6.87	7.46
CE	78.4	1.1	1.42	24	75.7	80.6
CO	0.505	0.030	5.95	24	0.466	0.609
CS	3.85	0.06	1.44	24	3.75	3.98
EU	1.45	0.02	1.41	24	1.41	1.48
FE	16000	200	1.33	24	15600	16400
HF	10.6	0.1	1.17	24	10.4	10.8
RB	82.3	1.3	1.58	24	79.9	85.0
SB	1.17	0.03	2.71	24	1.09	1.22
SC	6.50	0.10	1.57	24	6.30	6.68
SR	67.1	25.0	37.4	23	33.5	109
TA	1.03	0.02	1.46	24	1.01	1.06
TB	1.65	0.28	16.9	24	1.40	2.27
TH	7.91	0.12	1.46	24	7.69	8.11
ZN	84.3	9.93	11.8	24	62.0	104
ZR	373	11	2.96	24	356	394
CL	489	47	9.54	24	405	561
DY	11.1	0.3	2.73	24	10.4	11.6
K	29100	1600	5.61	24	26100	33200
MN	590.	12	1.96	24	566	631
NA	37100	500	1.32	24	36300	37800

ANIDs of specimens included:

YBC002	YBC003	YBC004	YBC009	YBC010	YBC011	YBC012	YBD001
YBD002	YBD003	YBD004	YBD005	YBD006	YBE001	YBE002	YBE003
YBE005	YBE006	YBF001	YBF002	YBF003	YBF004	YBF005	YBF006

Table 4.22: Descriptive Statistics for Brooks Canyon Obsidian, Lake County.

Element	Mean	St. Dev.	% St. Dev.	No. Obs.	Minimum	Maximum
BA	1100	14	1.32	12	1080	1120
LA	34.9	0.4	1.17	12	34.2	35.6
LU	1.00	0.01	1.14	12	0.978	1.02
ND	34.2	1.9	5.53	12	31.7	38.0
SM	8.28	0.10	1.21	12	8.09	8.42
U	3.04	0.56	18.6	12	2.39	4.31
YB	7.05	0.15	2.08	12	6.86	7.34
CE	74.7	1.0	1.33	12	72.7	76.5
CO	1.14	0.02	1.41	12	1.12	1.17
CS	3.76	0.05	1.21	12	3.68	3.84
EU	1.05	0.01	1.18	12	1.02	1.07
FE	14100	160	1.14	12	13800	14400
HF	10.8	0.1	1.14	12	10.6	11.0
RB	87.2	1.4	1.66	12	85.1	90.4
SB	1.11	0.03	2.62	12	1.07	1.16
SC	7.11	0.07	1.03	12	6.98	7.21
SR	39.9	10.8	27.2	9	28.0	58.5
TA	1.05	0.01	1.31	12	1.03	1.07
TB	1.51	0.05	3.24	12	1.44	1.61
TH	8.16	0.08	1.03	12	8.06	8.32
ZN	62.4	7.7	12.4	12	49.8	74.8
ZR	355	10.	2.84	12	340.	372
CL	407	48	11.9	12	329	488
DY	10.4	0.4	3.85	12	9.76	11.2
K	33900	1800	5.19	12	31400	36900
MN	452	7	1.50	12	432	459
NA	35300	300	0.90	12	34400	35700

ANIDS of specimens included:

BRC007 BRC008 BRC009 BRC010 BRC011 BRC012 BRCOR01 BRCOR02
 BRCOR03 BRCOR04 BRCOR05 BRCOR06

Table 4.23: Descriptive Statistics for Quartz Mountain Obsidian, Deschutes County.

Element	Mean	St. Dev.	% St. Dev.	No. Obs.	Minimum	Maximum
BA	895	13	1.44	9	883	925
LA	26.7	0.3	1.21	9	26.3	27.2
LU	0.643	0.008	1.32	9	0.628	0.657
ND	36.3	10.7	29.5	9	19.2	52.5
SM	5.46	0.08	1.41	9	5.36	5.58
U	4.20	0.32	7.55	9	3.77	4.60
YB	4.44	0.26	5.78	9	4.30	5.10
CE	53.8	0.8	1.42	9	52.0	54.7
CO	0.334	0.007	2.23	9	0.324	0.349
CS	5.86	0.08	1.36	9	5.68	5.93
EU	0.685	0.009	1.38	9	0.669	0.704
FE	10900	160	1.44	9	10600	11200
HF	5.70	0.07	1.18	9	5.56	5.80
RB	128	2	1.18	9	124	129
SB	0.651	0.007	1.07	9	0.643	0.666
SC	3.46	0.08	2.24	9	3.34	3.63
SR	52.0	10.2	19.7	9	37.3	68.7
TA	0.864	0.016	1.81	9	0.839	0.885
TB	0.859	0.028	3.29	9	0.819	0.924
TH	11.1	0.1	1.22	9	10.8	11.2
ZN	48.8	2.9	5.95	9	41.6	51.3
ZR	193	6	3.07	9	186	204
CL	454	14	3.16	9	434	477
DY	6.49	0.34	5.20	9	5.75	6.83
K	33400	1100	3.27	9	31900	35400
MN	297	2	0.75	9	292	300.
NA	33200	260	0.77	9	32700	33500

ANIDs of specimens included:

QM001 QM002 QM003 QM004 QM005 QM006 QM007 QM008
 QM009

Table 4.24: Descriptive Statistics for Cougar Mountain Obsidian, Lake County.

Element	Mean	St. Dev.	% St. Dev.	No. Obs.	Minimum	Maximum
BA	1180	26	2.22	17	1120	1220
LA	17.5	0.4	2.08	17	16.6	18.1
LU	0.788	0.029	3.67	17	0.740	0.841
ND	22.8	4.7	20.6	17	19.3	37.6
SM	6.19	0.13	2.12	17	5.87	6.38
U	2.84	0.24	8.56	17	2.49	3.48
YB	5.51	0.19	3.51	17	5.22	5.86
CE	40.1	0.7	1.65	17	38.6	41.1
CO	0.144	0.017	12.1	17	0.127	0.194
CS	3.47	0.08	2.34	17	3.32	3.59
EU	0.730	0.018	2.43	17	0.703	0.761
FE	7940	150	1.86	17	7630	8130
HF	5.08	0.11	2.15	17	4.85	5.25
RB	88.8	1.9	2.18	17	83.9	92.2
SB	0.411	0.027	6.50	17	0.356	0.444
SC	4.04	0.08	1.92	17	3.88	4.16
SR	38.8	11.2	28.8	10	23.0	57.8
TA	0.805	0.023	2.81	17	0.756	0.835
TB	1.23	0.04	3.10	17	1.16	1.29
TH	6.69	0.14	2.04	17	6.41	6.91
ZN	65.5	4.2	6.44	17	59.4	73.8
ZR	136	13	9.74	17	115	164
CL	419	40.	9.60	17	343	482
DY	8.38	0.28	3.30	17	7.93	8.78
K	31300	1800	5.79	17	27200	34600
MN	312	7	2.19	17	294	320.
NA	32800	700	2.18	17	31300	34000

ANIDs of specimens included:

CGM012 CGM013 CGM014 CGM015 CGM016 CGM017 CGMOR01 CGMOR02
 CGMOR03 CGMOR04 CGMOR05 CGMOR06 CGMOR07 CGMOR08 CGMOR09 CGMOR10
 CGMOR11

Table 4.25: Descriptive Statistics for Horse Mountain Obsidian, Lake County.

Element	Mean	St. Dev.	% St. Dev.	No. Obs.	Minimum	Maximum
BA	61.9	8.5	13.7	16	45.3	76.2
LA	57.4	0.9	1.48	16	56.4	59.0
LU	1.61	0.02	1.23	16	1.57	1.64
ND	59.8	1.9	3.26	16	57.2	64.4
SM	14.3	0.2	1.21	16	14.0	14.7
U	4.69	0.59	12.6	16	3.92	5.68
YB	11.4	0.7	5.92	16	11.0	13.8
CE	124	3	2.13	16	120.	130.
CO	0.024	0.008	34.5	2	0.018	0.029
CS	5.71	0.11	1.90	16	5.47	5.94
EU	1.15	0.02	2.04	16	1.11	1.20
FE	19900	300	1.71	16	19300	20600
HF	16.6	0.3	2.03	16	16.0	17.4
RB	122	2	1.75	16	117	126
SB	2.46	0.07	2.63	16	2.38	2.60
SC	0.527	0.009	1.79	16	0.509	0.548
SR**				0		
TA	2.08	0.03	1.34	16	2.02	2.13
TB	2.56	0.05	1.79	16	2.44	2.62
TH	11.8	0.2	1.59	16	11.4	12.2
ZN	155	11	7.22	16	145	176
ZR	585	20.	3.49	16	559	626
CL	778	66	8.48	16	698	931
DY	17.2	0.6	3.72	16	16.0	18.3
K	38100	2200	5.77	16	35300	44500
MN	570.	7	1.29	16	555	580.
NA	34300	400	1.10	16	33500	34800

ANIDs of specimens included:

HM001	HM002	HM003	HM004	HM005	HM006	HM007	HM008
HM009	HM010	HM011	HM012	HMOR01	HMOR02	HMOR03	HMOR04

**Values not available because element concentrations below detection limit.

Table 4.26: Descriptive Statistics for Silver Lake/Sycan Marsh Obsidian, Lake County.

Element	Mean	St. Dev.	% St. Dev.	No. Obs.	Minimum	Maximum
BA	756	14	1.82	12	732	774
LA	35.5	0.4	1.11	12	34.9	36.1
LU	0.845	0.015	1.79	12	0.810	0.871
ND	33.2	5.6	16.8	12	29.7	50.0
SM	7.80	0.14	1.80	12	7.56	8.13
U	4.37	0.60	13.8	12	3.15	5.39
YB	5.70	0.12	2.14	12	5.60	5.95
CE	73.0	1.2	1.63	12	71.0	75.0
CO	0.137	0.014	10.3	12	0.119	0.164
CS	5.77	0.10	1.78	12	5.58	5.94
EU	0.709	0.014	2.00	12	0.684	0.736
FE	12800	220	1.76	12	12300	13200
HF	9.31	0.12	1.31	12	9.06	9.45
RB	113	2	1.51	12	110.	115.
SB	0.980	0.031	3.12	12	0.940	1.03
SC	8.33	0.11	1.36	12	8.09	8.51
SR**				0		
TA	1.04	0.02	2.30	12	1.00	1.09
TB	1.29	0.17	13.4	12	1.21	1.83
TH	11.2	0.2	1.41	12	10.9	11.4
ZN	88.4	10.8	12.2	12	60.4	101
ZR	316	12	3.77	12	300.	338
CL	646	41	6.35	12	596	740.
DY	8.08	0.36	4.49	12	7.59	8.72
K	33900	3000	8.94	12	25300	37400
MN	624	7	1.07	12	616	641
NA	37500	260	0.70	12	37000	37900

ANIDs of specimens included:

SVL001 SVL002 SVL003 SVL004 SVL005 SVL006 SM001 SM002
 SM003 SM004 SM005 SM006

**Values not available because element concentrations below detection limit.

Table 4.27: Descriptive Statistics for Hager Mountain Obsidian, Lake County.

Element	Mean	St. Dev.	% St. Dev.	No. Obs.	Minimum	Maximum
BA	827	10.	1.22	22	814	850.
LA	22.6	0.2	1.12	22	22.3	23.1
LU	0.530	0.010	1.98	22	0.516	0.565
ND	18.6	0.9	4.71	22	17.3	20.5
SM	4.43	0.04	0.89	22	4.36	4.50
U	4.73	0.12	2.53	22	4.54	4.95
YB	3.42	0.08	2.22	22	3.31	3.67
CE	45.1	0.6	1.28	22	44.2	46.2
CO	0.186	0.008	4.03	22	0.174	0.202
CS	4.30	0.04	0.98	22	4.22	4.38
EU	0.483	0.009	1.77	22	0.459	0.499
FE	9490	120	1.26	22	9300	9770
HF	4.92	0.15	3.11	22	4.70	5.20
RB	103	1	1.16	22	101	105
SB	0.916	0.049	5.34	22	0.824	0.982
SC	2.82	0.03	1.10	22	2.77	2.88
SR	60.8	13.6	22.4	22	38.4	89.2
TA	0.845	0.009	1.03	22	0.834	0.866
TB	0.680	0.014	2.11	22	0.654	0.704
TH	10.4	0.1	1.02	22	10.2	10.6
ZN	49.3	1.7	3.53	22	45.6	52.5
ZR	164	9	5.58	22	140.	181
CL	517	45	8.76	22	424	621
DY	4.31	0.41	9.44	22	3.80	5.47
K	34600	1800	5.05	22	32100	38200
MN	693	7	1.03	22	680.	705
NA	35300	340	0.95	22	34400	35800

ANIDs of specimens included:

AC001	AC002	AC003	AC004	AC005	AC006	AC007	AC008
AC009	AC010	AC011	AC012	HGM001	HGM002	HGM003	HGM004
HGM005	HGM006	HGM007	HGM008	HGM009	HGM010		

Table 4.28: Descriptive Statistics for Tucker Hill Obsidian, Lake County.

Element	Mean	St. Dev.	% St. Dev.	No. Obs.	Minimum	Maximum
BA	289	8	2.68	22	274	308
LA	12.5	0.2	1.76	22	12.0	13.0
LU	0.412	0.006	1.57	22	0.402	0.428
ND	15.2	5.4	35.1	22	6.90	26.0
SM	2.82	0.03	1.07	22	2.79	2.89
U	4.39	0.73	16.6	22	3.21	6.18
YB	2.44	0.11	4.38	22	2.35	2.67
CE	24.3	0.3	1.43	22	23.7	25.0
CO	0.171	0.010	5.83	22	0.155	0.197
CS	4.20	0.06	1.38	22	4.11	4.30
EU	0.322	0.005	1.66	22	0.311	0.333
FE	4540	180	3.92	22	4360	5090
HF	3.15	0.08	2.39	22	3.10	3.46
RB	98.1	1.2	1.22	22	95.9	100.
SB	0.309	0.013	4.33	22	0.289	0.333
SC	2.39	0.04	1.57	22	2.32	2.46
SR	47.4	11.4	24.1	21	27.3	78.6
TA	0.988	0.012	1.23	22	0.961	1.01
TB	0.495	0.051	10.3	22	0.443	0.617
TH	7.51	0.08	1.06	22	7.38	7.67
ZN	31.3	6.2	19.7	22	23.5	41.0
ZR	91.8	5.3	5.79	22	80.5	101
CL	385	32	8.40	22	317	452
DY	3.30	0.31	9.40	22	2.90	4.13
K	37600	1200	3.26	22	35000	39600
MN	510.	5	1.01	22	500.	522
NA	29500	500	1.69	22	28300	30400

ANIDs of specimens included:

TH001	TH002	TH003	TH004	TH005	TH006	TH007	TH008
TH009	TH010	TH011	TH012	TH013	TH014	TH015	TH016
TH017	TH018	TH019	TH020	TH021	TH022		

Table 4.29: Descriptive Statistics for Surveyor Spring Obsidian, Lake County.

Element	Mean	St. Dev.	% St. Dev.	No. Obs.	Minimum	Maximum
BA	316	8	2.42	9	306	327
LA	28.5	0.4	1.25	9	28.0	29.2
LU	0.498	0.009	1.74	9	0.482	0.507
ND	21.9	9.0	41.3	9	17.0	44.5
SM	4.18	0.04	0.88	9	4.10	4.22
U	10.8	1.2	11.3	9	9.59	13.2
YB	2.76	0.02	0.80	9	2.72	2.79
CE	54.4	1.5	2.79	9	52.1	56.2
CO	0.558	0.013	2.30	9	0.534	0.572
CS	4.73	0.08	1.66	9	4.60	4.85
EU	0.299	0.005	1.53	9	0.292	0.305
FE	7270	130.	1.85	9	7040	7450
HF	4.66	0.09	1.85	9	4.53	4.78
RB	153	2	1.42	9	149	155
SB	1.00	0.01	1.43	9	0.980	1.02
SC	2.50	0.05	1.85	9	2.43	2.56
SR	26.8	7.9	29.5	8	16.4	39.4
TA	1.14	0.02	1.50	9	1.13	1.17
TB	0.493	0.017	3.41	9	0.467	0.524
TH	17.9	0.4	2.02	9	17.3	18.5
ZN	23.4	4.2	18.2	9	17.3	27.5
ZR	175	9	4.88	9	164	189
CL	962	54	5.68	9	838	1030
DY	3.59	0.29	8.02	9	3.21	4.08
K	42000	1600	3.84	9	39900	45500
MN	283	2	0.74	9	281	288
NA	26500	990	3.75	9	24000	27400

ANIDs of specimens included:

SS001 SS002 SS003 SS004 SS005 SS006 SS007 SS008
 SS009

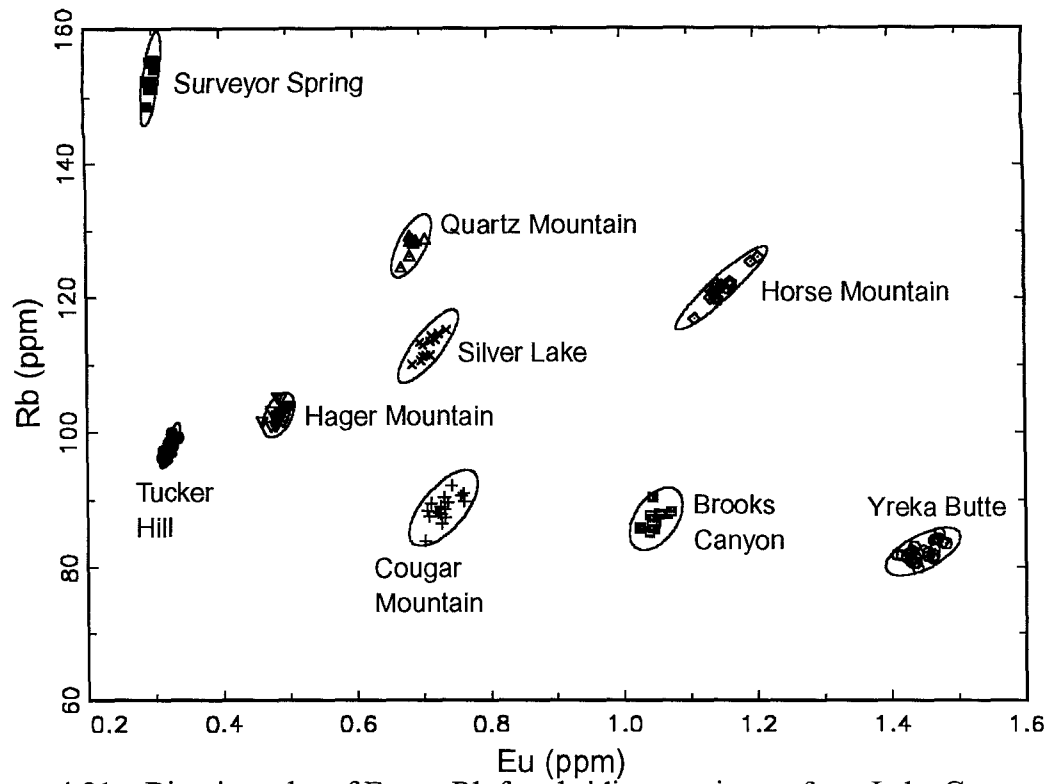


Figure 4.21a: Bivariate plot of Eu vs. Rb for obsidian specimens from Lake County, OR.

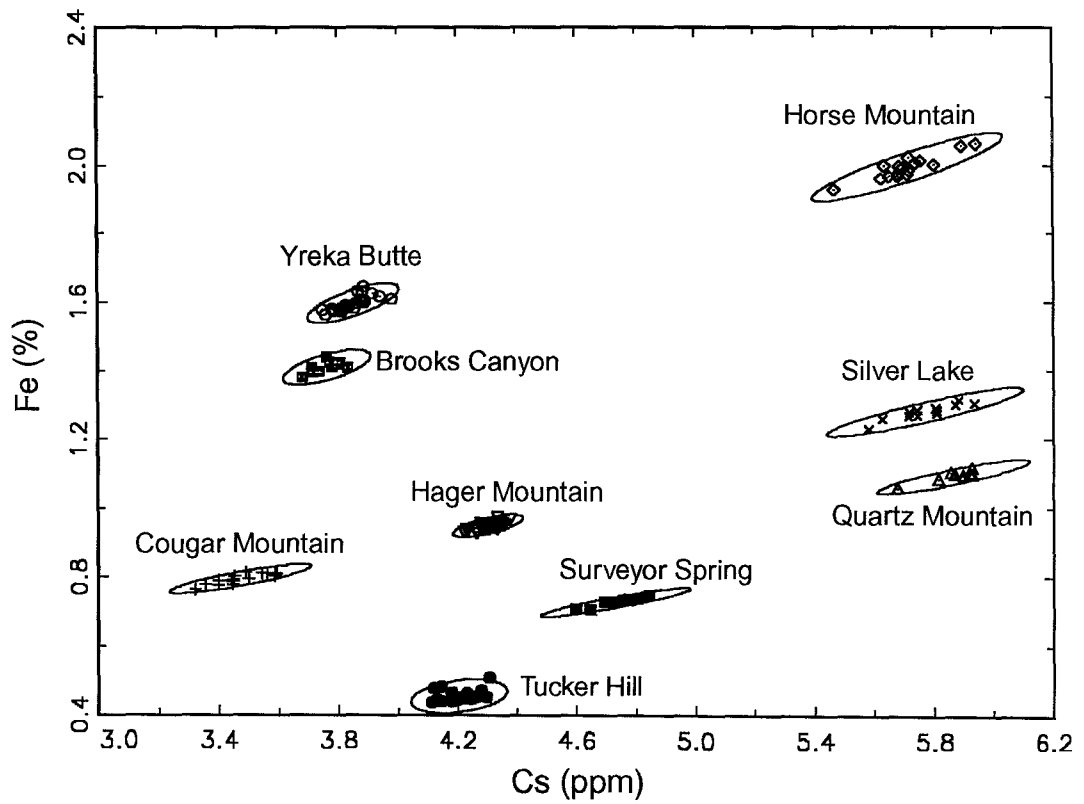


Figure 4.21b: Bivariate plot of Cs vs. Fe for obsidian specimens from Lake County, OR.

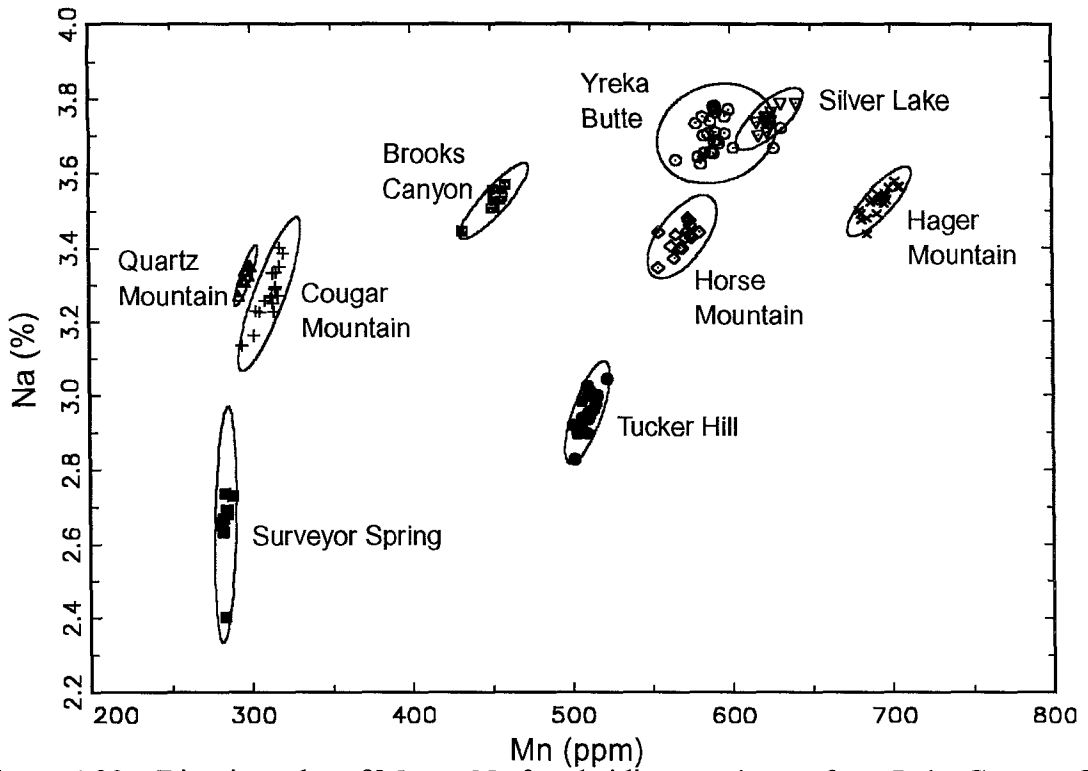


Figure 4.22a: Bivariate plot of Mn vs. Na for obsidian specimens from Lake County, OR.

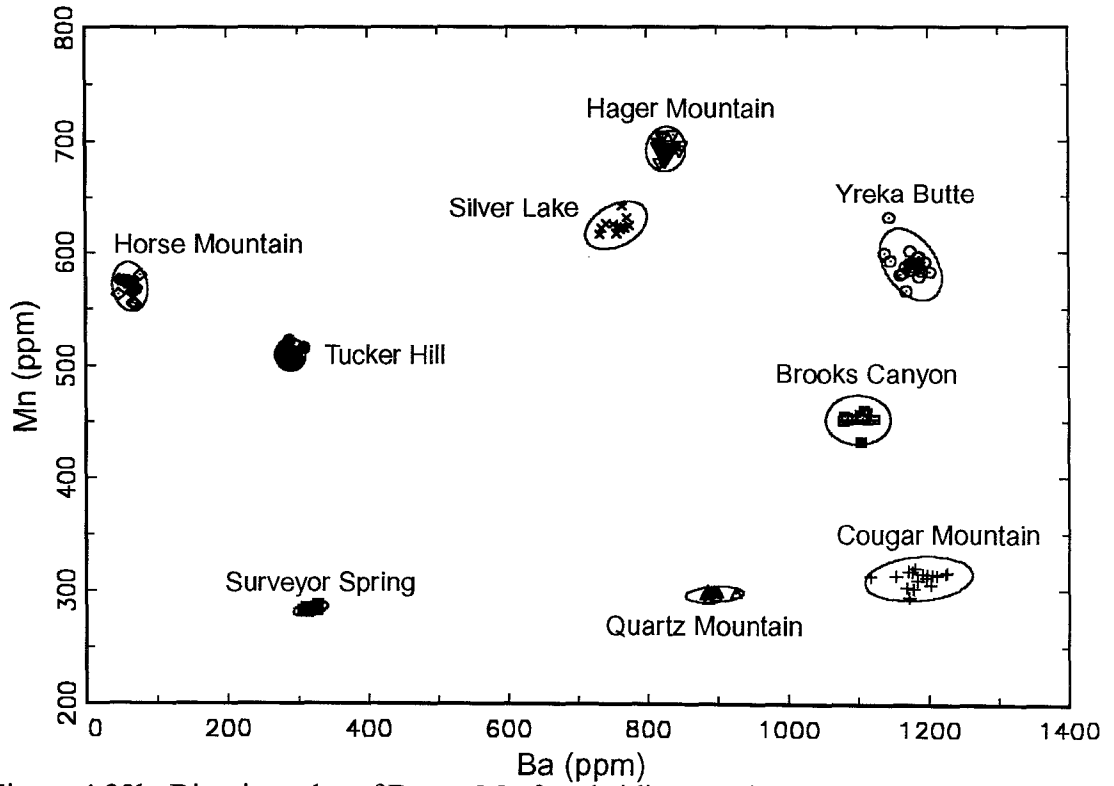


Figure 4.22b: Bivariate plot of Ba vs. Mn for obsidian specimens from Lake County, OR.

Newberry Volcano

Introduction

Newberry Volcano is a large volcanic complex located in Deschutes County, Oregon, about 32 km southeast of Bend. A map of the area is shown in Figure 4.23. The largest Quaternary volcano in the United States, Newberry Volcano covers an area of approximately 1280 km² (MacLeod *et al.*, 1981). The Newberry complex consists of several types of lavas, including basalt flows, andesite, rhyolite, pumice, and obsidian (MacLeod *et al.*, 1995). At its summit is a caldera that is 5 km long from north to south and 7 km wide from east to west with walls from 10's to 100's of meters high (MacLeod and Sherrod, 1988). The caldera encloses Paulina and East Lakes and it was the site for a number of Holocene rhyolitic eruptions, including those that produced the obsidian flows analyzed in this paper. See a map of the caldera in Figure 4.24.

Newberry Volcano sits at the end of the age progression of the High Lava Plains and incorporates features of both the Cascade Range and the Basin and Range Province (MacLeod *et al.*, 1995). It is surrounded by three complex fault systems, the Brothers Fault zone, the Green Ridge Fault zone, and the Walker Rim Fault zone (MacLeod *et al.*, 1981). Though the Brothers Fault zone does not affect the volcano itself, both Green Ridge and Walker Rim cut some flows, on the northwest and south flanks, respectively, and these are likely connected (MacLeod and Sherrod, 1988). The volcano has erupted approximately 25 times over the past one million to half million years.

The eruptions at Newberry have been extremely varied. The north and south flanks consist mainly of basalt and basaltic andesite (MacLeod *et al.*, 1981). The flows are divided into two time spans based on whether they overlie or underlie a layer of

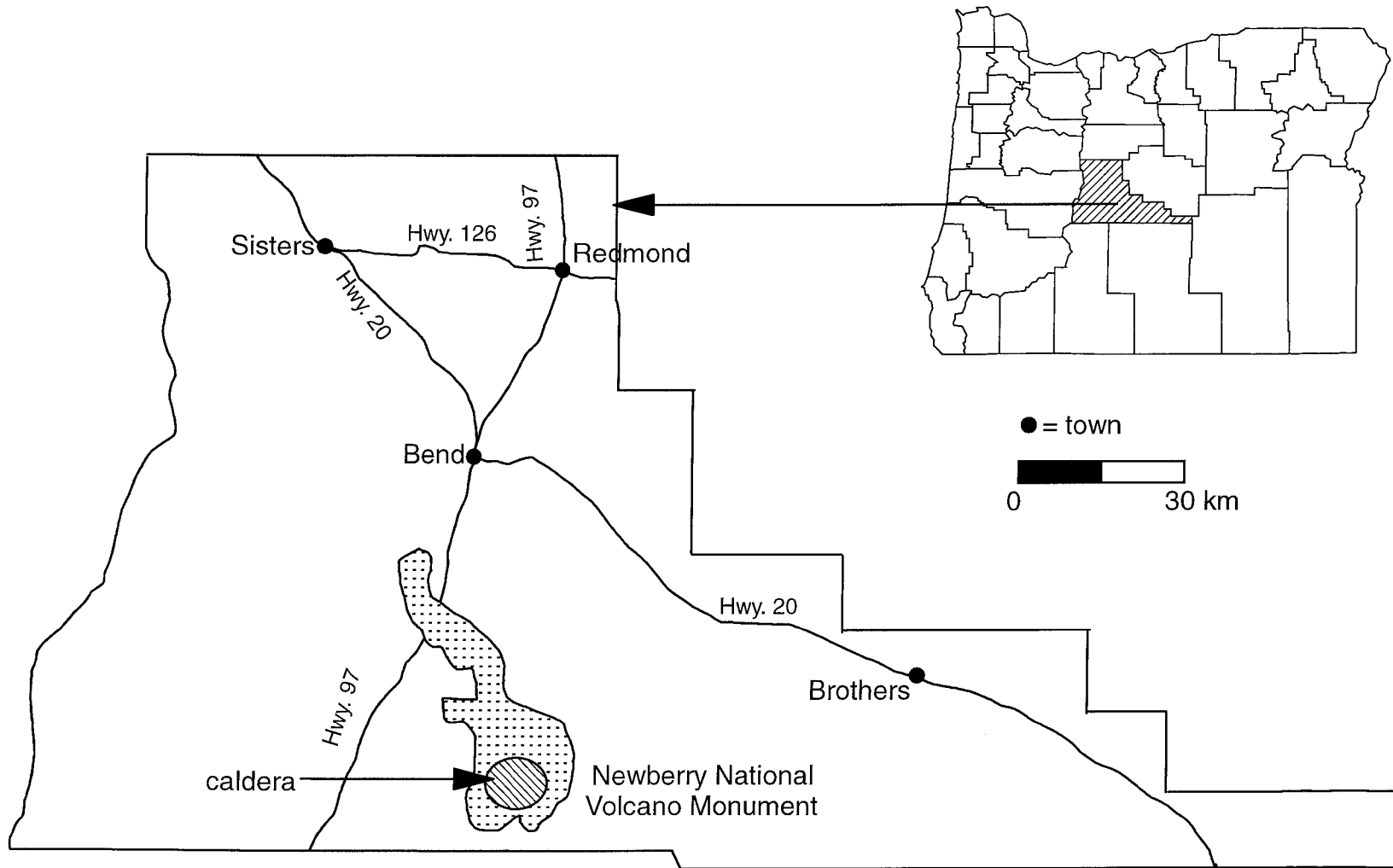


Figure 4.23: Map showing location of Newberry Volcano Obsidian, Deschutes County.

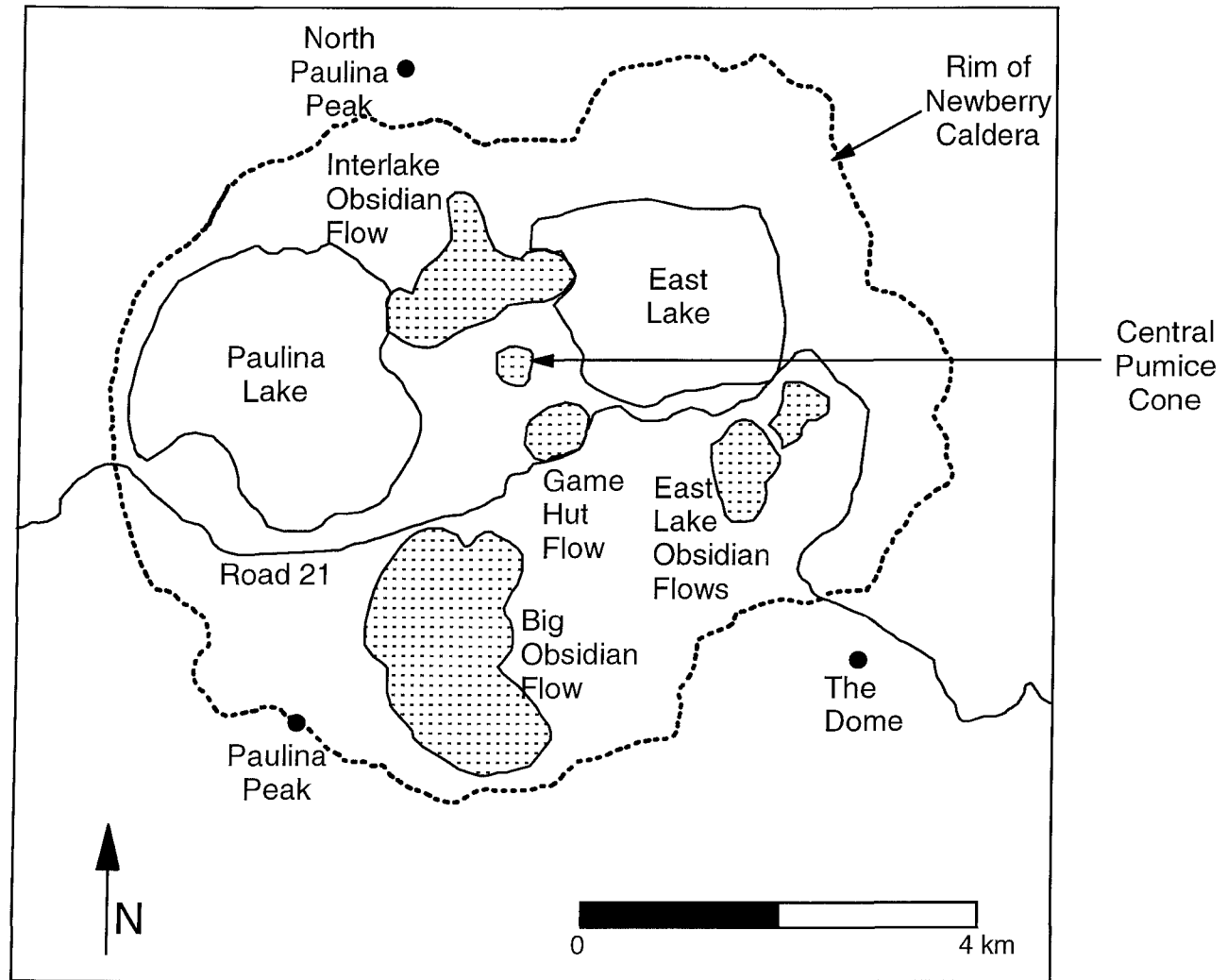


Figure 4.24: Map showing obsidian flows inside Newberry Caldera. (Adapted from Jensen, 1993)

Mazama ash (Mount Mazama is the volcano that formed Crater Lake after its eruption). Also covering the flanks of the volcano are more than 400 cinder cones and fissure vents. The many hills on the flanks are rhyolitic domes. Pumice rings, obsidian flows, and small rhyolitic or obsidian protrusions occur in many places. The west and east flanks are covered with ash-flows, pumice falls, mudflows, and other pyroclastic materials. Outside the rim of the caldera, the uppermost northeast, east, and southern flanks contain pumice and ash deposits from vents within the caldera. Some of the deposits on the flanks may be related to collapse of the caldera.

The geologic history of the caldera is very complicated. It is thought to have collapsed more than once and is interpreted as several nested calderas of different ages (MacLeod *et al.*, 1981; MacLeod and Sherrod, 1988). Eruptions have also been varied with rocks, flows, and domes of both Pleistocene and Holocene age. According to MacLeod and Sherrod (1988), there were six Holocene eruptive episodes within the caldera. The first was an obsidian flow and dome erupted south of East Lake. It is approximately 8,000-10,000 years old. The second was a basaltic andesitic to rhyodacitic flow from the east rim fissure to East Lake. The third eruption was voluminous and rhyolitic. It produced a large tephra deposit, the Central Pumice Cone and an obsidian flow within it, Game Hut Obsidian Flow, Interlake Obsidian Flow, a large pumice ring at the northeastern edge of the Big Obsidian Flow, and other small pumice rings and obsidian flows. Material from this eruption has been dated at 6200 radiocarbon years. The fourth eruption followed the third very closely in time (6100 radiocarbon years) and generated basaltic andesitic flows, cinder cones, and fissure vents on the north and south flanks of the volcano though none erupted in the caldera. The fifth eruption produced

only an obsidian flow and pumice within the caldera southeast of East Lake. The sixth and final eruption (1350 radiocarbon years ago) yielded tephra, then an ash-flow, and finally the Big Obsidian Flow.

Obsidian flows within the caldera have been studied intensively. Laidley and McKay (1971) investigated the Big Obsidian Flow. Because it is quite large (1.5 km long, 2 km²), they tested it for chemical homogeneity and looked for systematic trends or variations related to the sequence of the lava extrusion. Using XRF, atomic absorption (AA), and gamma-ray spectroscopy they found the Big Obsidian Flow to be very chemically homogeneous. They also analyzed other flows, namely the Game Hut Flow, the Interlake Flow, and the East Lake Flow. The other flows were chemically similar to one another and to the Big Obsidian Flow, indicating a common magma source. However, some real differences exist, especially with regard to Rb and Zn. Unfortunately, the authors did not investigate the cause of these differences. Jensen (1993) also found that the obsidian flows within the caldera were chemically similar, mainly citing the small range in silica content of 73-74%.

Analysis of the obsidian flows has also contributed to a theory of the source of the eruptions in the caldera. The rhyolitic rocks less than 10,000 years old are all chemically similar to one another but they are chemically different from older silicic rocks at Newberry (MacLeod and Sherrod, 1985). The differences show that the major and trace elements are more evolved in the younger obsidian flows (e.g., the Rb/Sr ratio is higher). The younger obsidians also contain fewer phenocrysts, indicating either an increase in water or an increase in heat. An increase in heat would likely come from basaltic magma pushing up from underneath a silicic magma chamber. MacLeod and Sherrod (1988)

offer several lines of evidence supporting the existence of a silicic magma chamber underneath the caldera that is periodically affected by an influx of basaltic magma. Two of the strongest indications for this theory are the similar compositions between the different rhyolitic flows indicating a single chamber and the fact that the basalt and rhyolitic flows are mutually exclusive (basalt outside caldera, rhyolite inside caldera).

Geologists are not the only ones who were interested in the obsidian flows at the Newberry Caldera. The obsidian produced in the eruptions was high quality glass that was intensively exploited by early Native Americans (MacLeod *et al.*, 1995). It is possible that groups such as the Tenino and the Northern Paiute moved into the caldera in the summer and fall to gather obsidian to make tools. The caldera may have been used as a source of glass prior to the Mazama ashfall, possibly from the rhyolite flow south of East Lake. (A weighted-mean age for the Mazama eruption, taken from charcoal within or below the ash-flow is given as 6840 ± 50 years B. P. [Sarna-Wojcicki *et al.*, 1983].)

Archaeologists can use the chemical analysis of the obsidians to correlate artifacts and to investigate trade and land-use patterns. Because the flows have also been dated, archaeological deposits within the caldera as well as those outside containing artifacts made from caldera obsidian can also be dated and a series of stratigraphic markers for archaeological studies in Oregon can be created.

Results and Discussion

Previous research by XRF has suggested that the obsidians from Newberry Caldera are chemically similar. At the present time, it is thought that there are only two main chemical groups within the caldera. The Big Obsidian Flow Chemical Group includes obsidian from Big Obsidian Flow and Buried Obsidian Flow. The Newberry

Volcano Chemical Group includes Central Pumice Cone, East Lake Flows, Game Hut Flow, Interlake Flow, and Little Obsidian Flow. For more information, see the following web page: http://www.peak.org/~skinnrcr/s_or.html. Our NAA results (data are shown in Tables 4.30-4.33) indicate that the two chemical groups can be further subdivided to give a total of four distinct chemical groups.

As shown in Figures 4.25a (Cs vs. Fe) and 4.25b (Rb vs. Fe), the Big Obsidian Flow and Buried Obsidian Flow are each a separate homogeneous chemical group. The two groups can be separated from one another by differences in a number of elements besides cesium and rubidium including Lu, Sm, Co, Sb, Ta, and Tb. Enough similarities remain to indicate that they are still related to each other.

Also shown in Figures 4.25a and 4.25b are the results of an analysis of the East Lake, Game Hut, and Interlake Flows. In this case, the data indicated that the Game Hut and Interlake Flows were chemically identical. This confirms what could be expected since they were coincident eruptions. The two East Lake Flows were found to be chemically different enough to form their own chemical group. However, the chemical group is likely highly related to the Game Hut Chemical Group. The fact that the slopes of their ellipses are correlated indicates that they follow the same general trends in the elements.

These two cases highlight an advantage of NAA over XRF. NAA measures several elements that XRF cannot measure and these elements can be used to find differences that XRF misses.

The abbreviated-NAA method was also applied to this set of chemical groups. As shown in Figure 4.26, a plot of sodium versus manganese yields separation between all

Table 4.30: Descriptive Statistics for Big Obsidian Flow Obsidian, Newberry Caldera.

Element	Mean	St. Dev.	% St. Dev.	No. Obs.	Minimum	Maximum
BA	844	18	2.08	8	821	881
LA	31.1	0.5	1.58	8	30.3	31.7
LU	0.737	0.014	1.93	8	0.720	0.763
ND	25.5	1.8	7.01	8	23.3	28.1
SM	6.17	0.09	1.46	8	6.03	6.32
U	3.90	0.28	7.22	8	3.57	4.27
YB	5.02	0.21	4.18	8	4.75	5.34
CE	62.9	0.6	0.95	8	61.9	63.8
CO	0.831	0.020	2.41	8	0.811	0.871
CS	4.54	0.03	0.76	8	4.50	4.60
EU	0.839	0.009	1.08	8	0.827	0.852
FE	15100	190	1.28	8	14900	15500
HF	9.36	0.09	0.10	8	9.26	9.50
RB	112	2	1.48	8	110.	114
SB	0.389	0.016	4.16	8	0.367	0.417
SC	5.72	0.07	1.15	8	5.62	5.81
SR	56.9	11.2	19.6	8	41.2	75.2
TA	1.42	0.02	1.15	8	1.38	1.43
TB	1.03	0.02	2.06	8	0.995	1.06
TH	10.6	0.1	0.79	8	10.4	10.7
ZN	61.4	4.4	7.23	8	54.3	67.2
ZR	334	11	3.41	8	320.	354
CL	819	71	8.71	8	754	963
DY	6.59	0.33	5.05	8	6.05	7.05
K	33500	1600	4.63	8	31600	36000
MN	474	4	0.89	8	469	481
NA	38000	380	0.99	8	37500	38500

ANIDs of specimens included:

BOF001 BOF002 BOF003 BOF004 BOF005 BOF006 BOF007 BOF008

Table 4.31: Descriptive Statistics for Buried Obsidian Flow Obsidian, Newberry Caldera.

Element	Mean	St. Dev.	% St. Dev.	No. Obs.	Minimum	Maximum
BA	814	15	1.83	12	796	838
LA	30.3	0.4	1.28	12	29.3	30.9
LU	0.801	0.012	1.44	12	0.777	0.819
ND	31.0	2.3	7.48	12	26.0	33.6
SM	6.56	0.09	1.34	12	6.40	6.74
U	3.90	0.57	14.6	12	3.42	5.18
YB	5.56	0.34	6.05	12	5.14	5.94
CE	62.3	0.7	1.13	12	61.5	64.2
CO	1.22	0.06	5.18	12	1.12	1.34
CS	4.86	0.06	1.21	12	4.77	4.98
EU	0.863	0.028	3.27	12	0.809	0.890
FE	15000	370	2.45	12	14200	15400
HF	9.60	0.17	1.79	12	9.27	9.82
RB	122	2	1.39	12	119	126
SB	0.575	0.021	3.66	12	0.537	0.620
SC	5.44	0.20	3.71	12	5.17	5.97
SR	55.7	20.3	36.5	11	26.0	94.3
TA	1.26	0.02	1.44	12	1.23	1.30
TB	1.22	0.16	13.6	12	1.08	1.72
TH	10.7	0.1	1.27	12	10.4	11.0
ZN	49.9	7.6	15.3	12	34.9	60.8
ZR	337	13	3.85	12	315	357
CL	703	62	8.81	12	631	829
DY	7.33	0.40	5.42	12	6.64	8.00
K	33700	1300	3.73	12	31900	35700
MN	440.	8	1.71	12	424	452
NA	37000	180	0.50	12	36600	37300

ANIDs of specimens included:

BUF001	BUF002	BUF003	BUF004	BUF005	BUF006	BUF007	BUF008
BUF009	BUF010	BUF011	BUF012				

Table 4.32: Descriptive Statistics for East Lake Obsidian Flows Obsidian, Newberry Caldera.

Element	Mean	St. Dev.	% St. Dev.	No. Obs.	Minimum	Maximum
BA	838	8	0.98	12	826	850.
LA	29.8	0.4	1.42	12	29.1	30.3
LU	0.665	0.009	1.43	12	0.650	0.682
ND	27.8	1.2	4.42	12	25.9	30.0
SM	5.66	0.10	1.71	12	5.50	5.85
U	4.30	0.53	12.3	12	3.58	5.19
YB	4.23	0.28	6.53	12	3.96	4.91
CE	59.7	1.1	1.86	12	57.7	61.8
CO	1.31	0.03	2.19	12	1.26	1.35
CS	5.06	0.09	1.72	12	4.86	5.18
EU	0.763	0.015	1.95	12	0.737	0.795
FE	13700	230	1.68	12	13200	14000
HF	7.90	0.14	1.75	12	7.63	8.15
RB	124	2	1.46	12	120.	125
SB	0.509	0.024	4.68	12	0.477	0.548
SC	4.90	0.08	1.56	12	4.74	5.03
SR	78.3	28.7	36.6	12	41.4	123
TA	1.22	0.02	1.88	12	1.18	1.25
TB	0.949	0.072	7.58	12	0.846	1.09
TH	11.4	0.2	1.76	12	11.0	11.7
ZN	41.3	5.5	13.3	12	31.3	45.9
ZR	281	10.	3.45	12	266	293
CL	610.	49	8.08	12	504	672
DY	6.44	0.31	4.81	12	5.95	7.05
K	35300	1400	4.09	12	32300	37500
MN	382	3	0.87	12	379	388
NA	35400	280	0.80	12	35000	35900

ANIDs of specimens included:

EL001	EL002	EL003	EL004	EL005	EL006	EL007	EL008
EL009	EL010	EL011	EL012				

Table 4.33: Descriptive Statistics for Game Hut Obsidian Flow Obsidian, Newberry Caldera.

Element	Mean	St. Dev.	% St. Dev.	No. Obs.	Minimum	Maximum
BA	845	13	1.52	16	816	869
LA	29.8	0.3	1.02	16	29.4	30.7
LU	0.673	0.013	1.94	16	0.652	0.699
ND	27.5	6.8	24.8	16	18.4	38.4
SM	5.66	0.08	1.34	16	5.55	5.83
U	4.36	0.52	11.9	16	3.39	5.60
YB	4.48	0.28	6.35	16	4.16	5.01
CE	59.8	0.62	1.04	16	58.8	61.0
CO	1.16	0.06	5.07	16	1.11	1.36
CS	5.11	0.05	0.95	16	5.01	5.21
EU	0.734	0.009	1.28	16	0.719	0.750
FE	13000	100.	0.78	16	12800	13200
HF	7.82	0.07	0.92	16	7.71	7.95
RB	126	1	1.08	16	124	129
SB	0.485	0.011	2.19	16	0.454	0.502
SC	4.77	0.16	3.37	16	4.61	5.15
SR	55.8	11.2	20.1	16	27.6	70.1
TA	1.23	0.01	0.97	16	1.20	1.25
TB	1.03	0.09	8.97	16	0.880	1.27
TH	11.6	0.1	0.81	16	11.4	11.7
ZN	53.5	11.7	21.9	16	36.8	73.7
ZR	287	10.	3.35	16	270.	297
CL	616	38	6.16	16	533	674
DY	6.34	0.27	4.30	16	5.90	6.82
K	35000	1400	3.88	16	32200	37700
MN	366	4	1.20	16	359	375
NA	34600	490	1.42	16	34000	35800

ANIDs of specimens included:

GHF001	GHF002	GHF003	GHF004	GHF005	GHF006	GHF007	GHF008
ILK001	ILK002	ILK003	ILK004	ILK005	ILK006	ILK007	ILK008

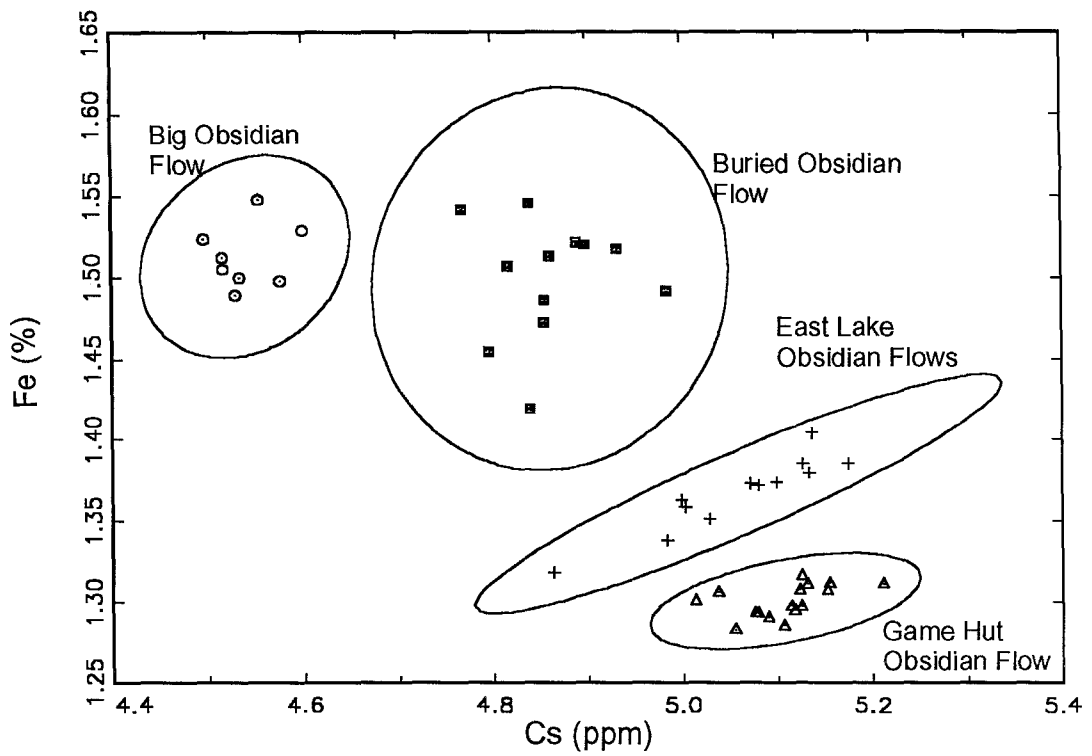


Figure 4.25a: Bivariate plot of Cs vs. Fe for obsidian specimens from Newberry Caldera.

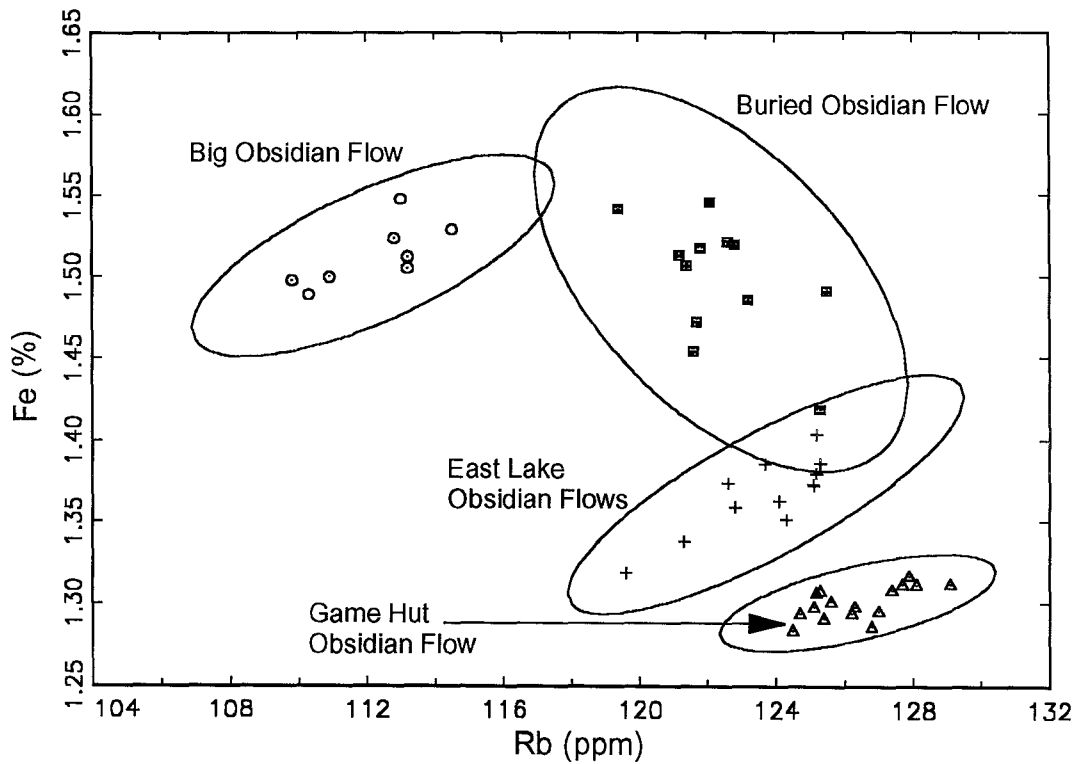


Figure 4.25b: Bivariate plot of Rb vs. Fe for obsidian specimens from Newberry Caldera.

four chemical groups. It is not necessary to use barium as a third element to help prove differentiation. Therefore, it is highly probable that, given a set of artifacts believed to come from the Newberry Caldera, the short irradiation procedure would be successful and economical in identifying the correct flow that the artifacts came from.

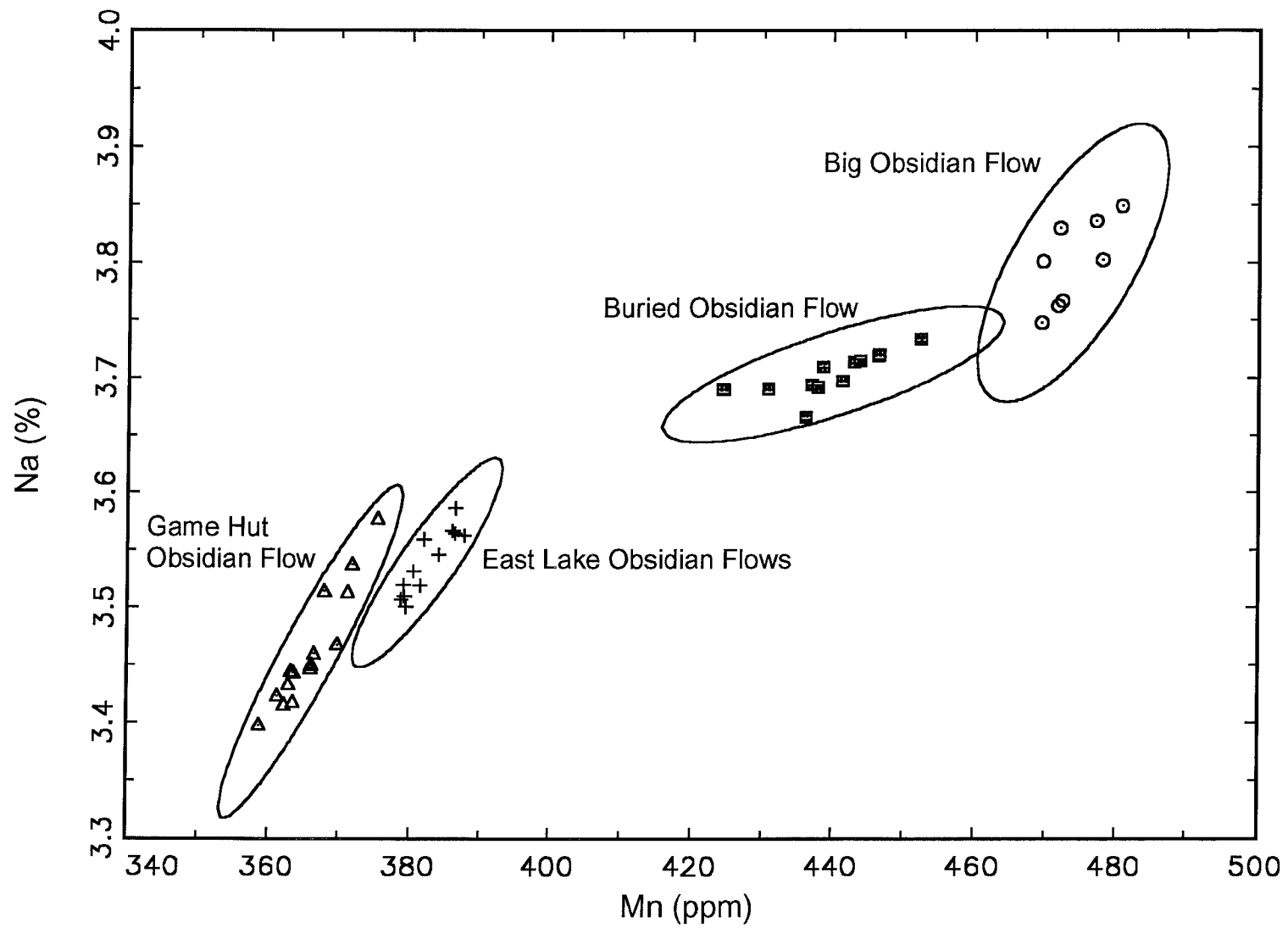


Figure 4.26: Bivariate plot of Mn vs. Na for obsidian specimens from Newberry Caldera.

Miscellaneous

Introduction

The samples discussed in this section are from areas that do not fit neatly into any of the other regions previously discussed. Deer Creek is the only sampling area from Klamath County (Figure 4.27). Inman Creek is the only sampling area from Lane County (Figure 4.28).

There are several other obsidian sources in the western Cascades area that have not been sampled at this point. For example, Crater Lake does have some obsidian but none is of artifact quality (Skinner, pers. commun.). Condon Butte, Upper Winberry Creek, and Rock Mesa are also non-artifact quality glass sources. The Western Cascades are also interesting because of the large number of rivers in which obsidian can be found. River gravel sources include the following: McKenzie River (Obsidian Cliffs), Long Tom River (Inman Creek), Willamette River (Inman Creek and Obsidian Cliffs), Columbia River (sources unknown at this point), and the Clackamas River (sources unknown at this point). Obsidian Cliffs is a very important obsidian source in Oregon and material was used prehistorically throughout northwest and central Oregon. It is expected that in the future the database being created will include source samples from all of these areas.

Deer Creek is a fairly homogeneous chemical group. However, one outlier sample was found and without further sampling it is difficult to discuss whether this is truly an outlier or if there are perhaps other chemical groups in the area. Until more samples are collected from that area, this paper can offer only the raw data and limited speculation.

Inman Creek is more interesting at this point because there has been some earlier

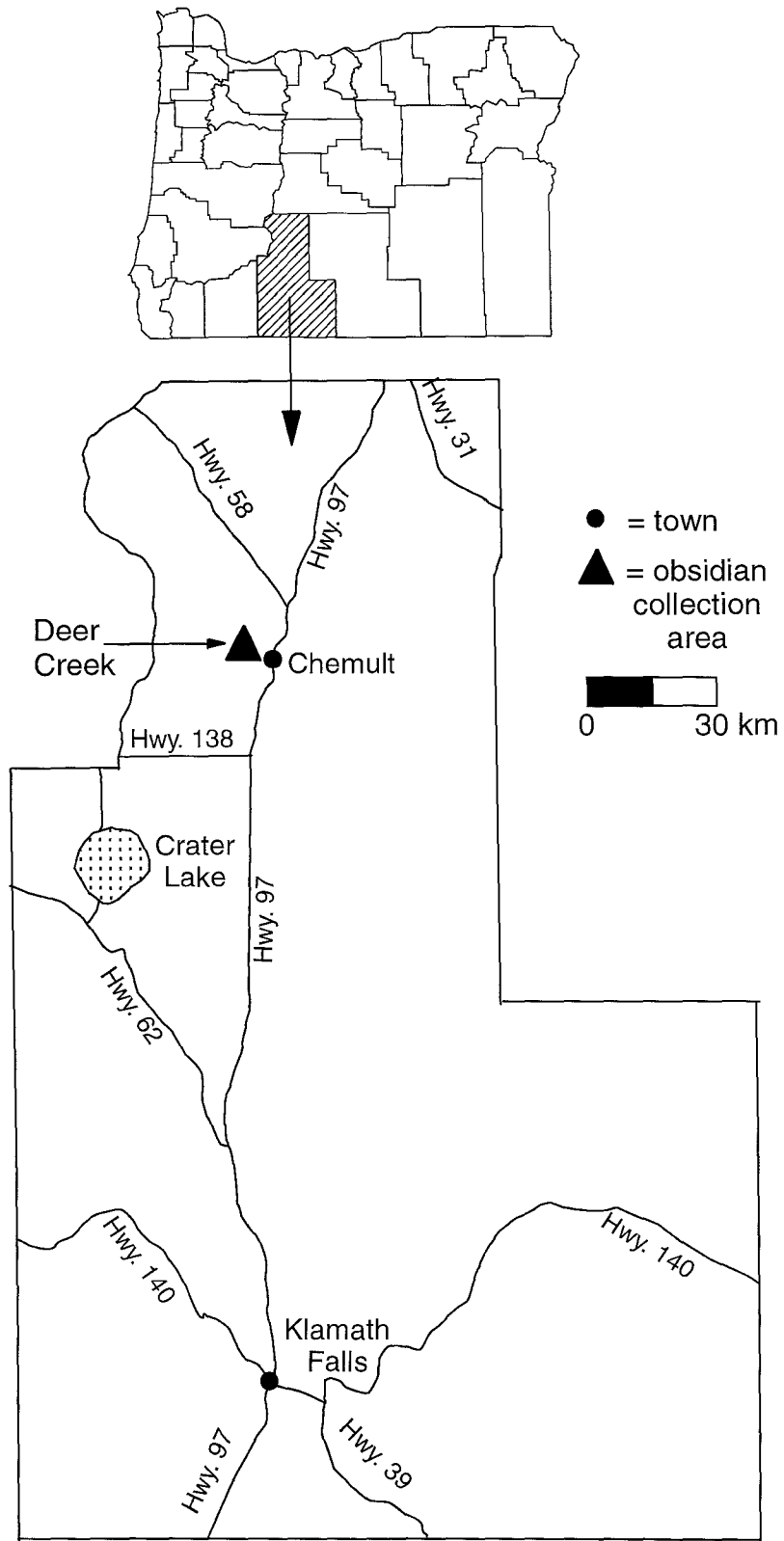


Figure 4.27: Map of Klamath County, Oregon showing obsidian collection areas.

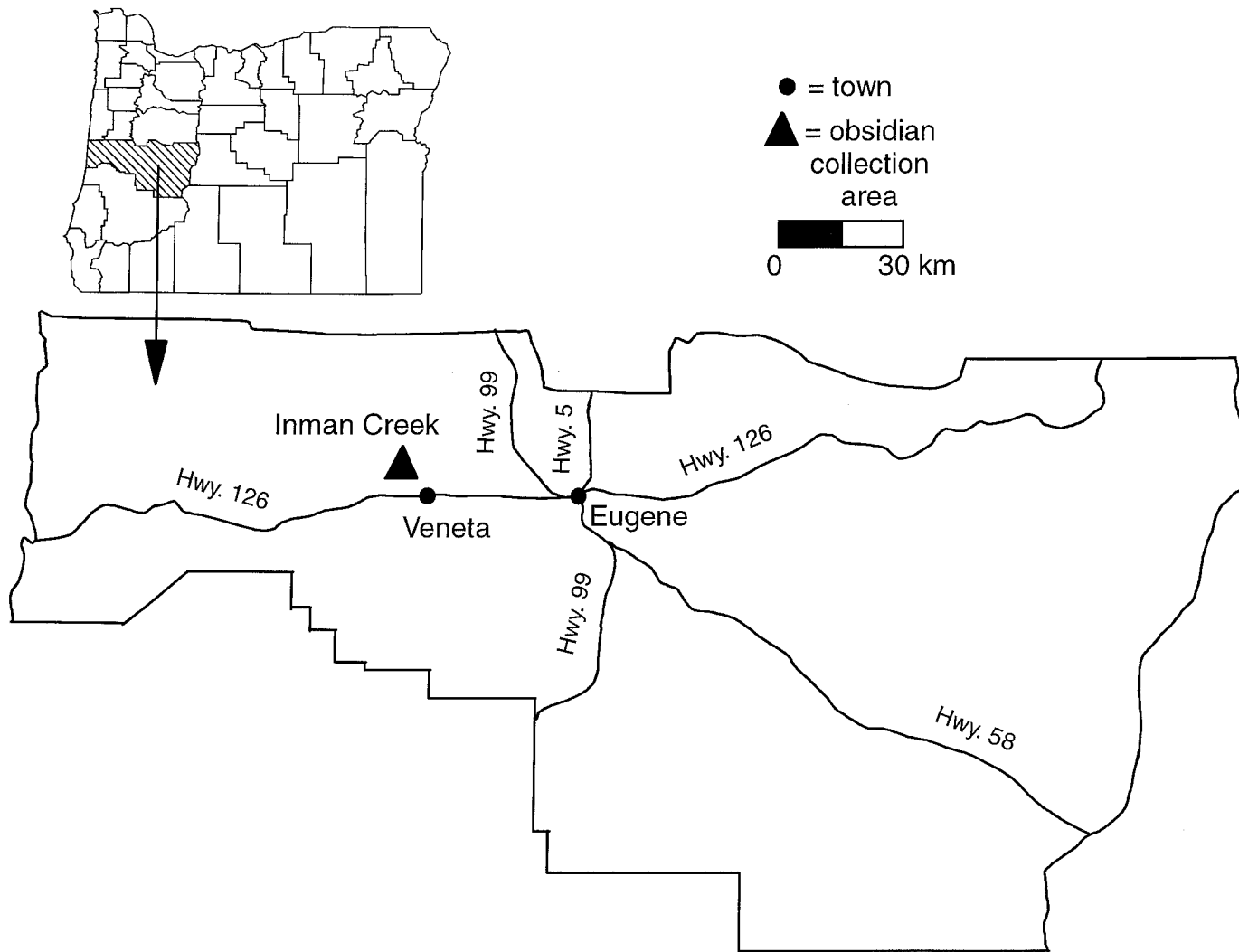


Figure 4.28: Map of Lane County, Oregon showing obsidian collection areas.

work performed in this area. Skinner and Winkler (1994) reported that the Inman Creek area is geochemically similar to Siuslaw River obsidians (which are from alluvial and gravel sources). It is likely that they share the same primary source, a Miocene obsidian flow near Salt Creek in the Middle Fork Willamette sub-basin.

Results and Discussion

The data for the chemical groups is given in Tables 4.34-4.36. As shown in Figures 4.29a (Hf vs. Fe) and 4.29b (Ce vs. Cs) Inman Creek is composed of two chemical groups and all three groups separated from each other very well. This was an expected result, especially considering the distance between the two sampling areas. Interestingly enough, Deer Creek and Inman Creek A overlap on a number of elements that usually provide the best separation between groups, including Cs, Eu, and Th. However, they are distinct on a large enough number of elements so that their separation is easily accomplished.

These three chemical groups can be separated using the elements Na and Mn from the abbreviated-NAA method (Figure 4.30). It is not necessary to use barium.

These two areas definitely need more extensive sampling in the future. Hopefully additional analysis will reveal more about the origins of the two Inman Creek chemical groups as well as illuminate the source of the outlier specimen from the Deer Creek chemical group.

Table 4.34: Descriptive Statistics For Deer Creek Obsidian, Klamath County.

Element	Mean	St. Dev.	% St. Dev.	No. Obs.	Minimum	Maximum
BA	823	12	1.45	5	810.	839
LA	22.5	0.3	1.47	5	22.1	23.0
LU	0.427	0.004	0.88	5	0.422	0.432
ND	20.4	1.0	4.94	5	19.3	21.9
SM	4.74	0.05	1.10	5	4.68	4.81
U	3.16	0.28	8.98	5	2.82	3.52
YB	2.84	0.06	2.28	5	2.76	2.93
CE	46.9	0.8	1.72	5	46.0	47.8
CO	0.684	0.039	5.64	5	0.624	0.721
CS	3.72	0.08	2.21	5	3.63	3.83
EU	0.564	0.020	3.52	5	0.530	0.581
FE	10100	240	2.35	5	9720	10300
HF	6.63	0.08	1.23	5	6.48	6.68
RB	74.8	1.22	1.63	5	72.8	76.1
SB	0.650	0.015	2.37	5	0.624	0.662
SC	5.56	0.05	0.83	5	5.50	5.61
SR	51.0	19.1	37.5	5	19.6	69.0
TA	0.567	0.011	1.93	5	0.554	0.580
TB	0.698	0.016	2.29	5	0.686	0.725
TH	6.50	0.11	1.65	5	6.37	6.61
ZN	44.8	1.4	3.09	5	42.4	45.8
ZR	211	12	5.55	5	191	219
CL	784	88	11.2	5	706	915
DY	4.69	0.68	14.4	5	3.64	5.41
K	29400	1900	6.59	5	26800	31800
MN	304	9	2.91	5	296	317
NA	36200	680	1.88	5	35500	37000

ANIDs of specimens included:

DC002 DC003 DC004 DC005 DC006

Table 4.35: Descriptive Statistics for Inman Creek A Obsidian, Lane County.

Element	Mean	St. Dev.	% St. Dev.	No. Obs.	Minimum	Maximum
BA	792	13	1.62	7	774	808
LA	20.9	0.2	0.96	7	20.6	21.2
LU	0.272	0.004	1.37	7	0.265	0.275
ND	12.9	2.6	20.3	7	10.4	17.0
SM	3.22	0.08	2.39	7	3.05	3.28
U	2.31	0.57	24.7	7	1.83	3.53
YB	1.79	0.16	9.03	7	1.61	2.03
CE	41.9	0.8	1.80	7	40.6	42.8
CO	0.459	0.026	5.59	7	0.420	0.481
CS	3.79	0.08	2.21	7	3.68	3.89
EU	0.503	0.010	1.98	7	0.488	0.520
FE	11000	210	1.88	7	10800	11400
HF	3.36	0.05	1.44	7	3.29	3.43
RB	80.1	1.9	2.39	7	77.0	82.1
SB	0.362	0.011	3.03	7	0.342	0.373
SC	1.51	0.03	2.09	7	1.47	1.56
SR	152	8	5.56	7	141	166
TA	0.644	0.014	2.13	7	0.626	0.661
TB	0.411	0.007	1.80	7	0.405	0.425
TH	6.57	0.15	2.23	7	6.37	6.74
ZN	48.9	0.8	1.70	7	48.0	50.3
ZR	111	8	7.48	7	99.2	122
CL	582	41	7.04	7	503	631
DY	2.48	0.38	15.5	7	2.00	2.96
K	27200	3500	12.84	7	23400	32500
MN	545	5	0.84	7	538	552
NA	35000	360	1.03	7	34500	35500

ANIDs of specimens included:

INC001 INC002 INC003 INC004 INC006 INC007 INC012

Table 4.36: Descriptive Statistics for Inman Creek B Obsidian, Lane County.

Element	Mean	St. Dev.	% St. Dev.	No. Obs.	Minimum	Maximum
BA	774	11	1.39	5	763	790.
LA	18.8	0.2	1.33	5	18.6	19.2
LU	0.265	0.008	3.04	5	0.251	0.270
ND	15.0	6.3	41.7	5	10.3	22.6
SM	3.16	0.04	1.10	5	3.12	3.21
U	3.46	0.88	25.5	5	2.20	4.44
YB	1.71	0.07	3.94	5	1.62	1.80
CE	37.8	0.5	1.35	5	37.1	38.5
CO	0.318	0.005	1.69	5	0.310	0.323
CS	4.15	0.03	0.68	5	4.10	4.17
EU	0.399	0.004	0.91	5	0.393	0.402
FE	8950	50	0.61	5	8890	9020
HF	2.90	0.10	3.39	5	2.83	3.08
RB	85.4	0.3	0.40	5	85.0	85.8
SB	0.372	0.011	2.99	5	0.355	0.385
SC	1.56	0.01	0.76	5	1.55	1.58
SR	119	6	4.82	5	110.	125
TA	0.642	0.009	1.39	5	0.626	0.649
TB	0.425	0.019	4.40	5	0.410	0.457
TH	6.82	0.04	0.65	5	6.78	6.88
ZN	47.1	1.4	3.00	5	45.5	48.8
ZR	94.5	8.7	9.23	5	84.2	104
CL	505	44	8.65	5	449	559
DY	2.53	0.39	15.2	5	2.23	3.18
K	27300	2000	7.32	5	24900	30000
MN	480.	5	1.13	5	473	488
NA	33800	330	0.97	5	33500	34300

ANIDS of specimens included:

INC005 INC008 INC009 INC010 INC011

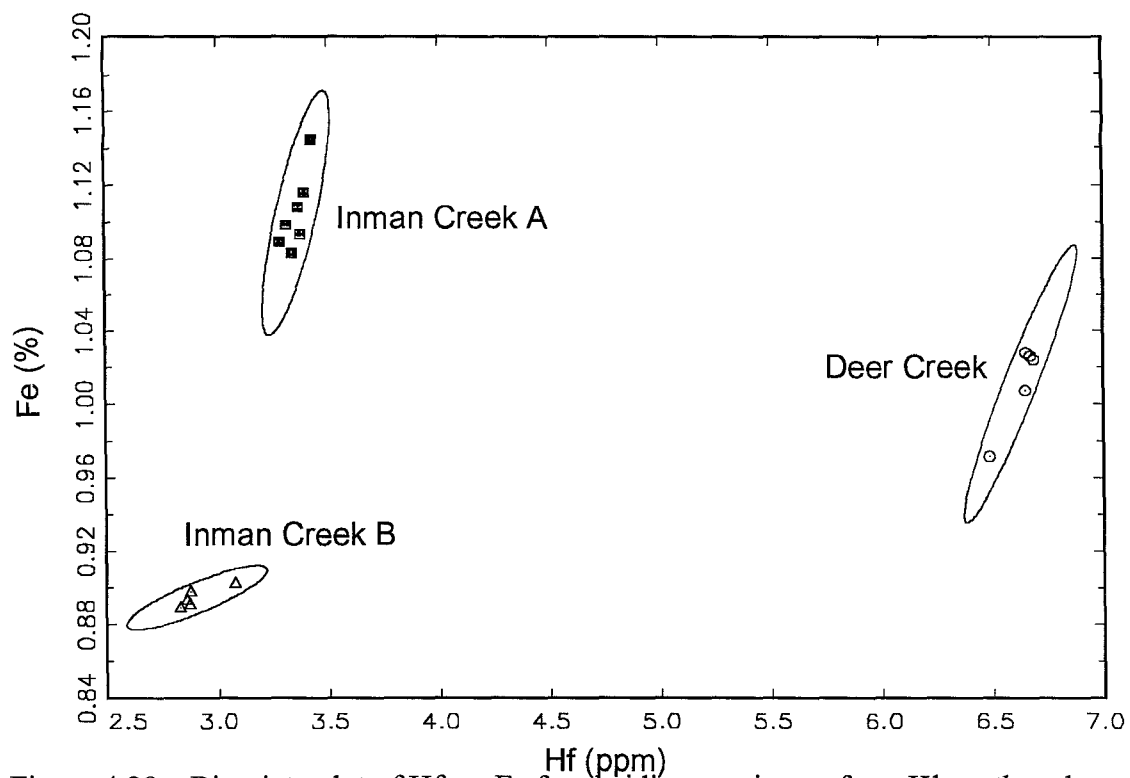


Figure 4.29a: Bivariate plot of Hf vs. Fe for obsidian specimens from Klamath and Lane Counties.

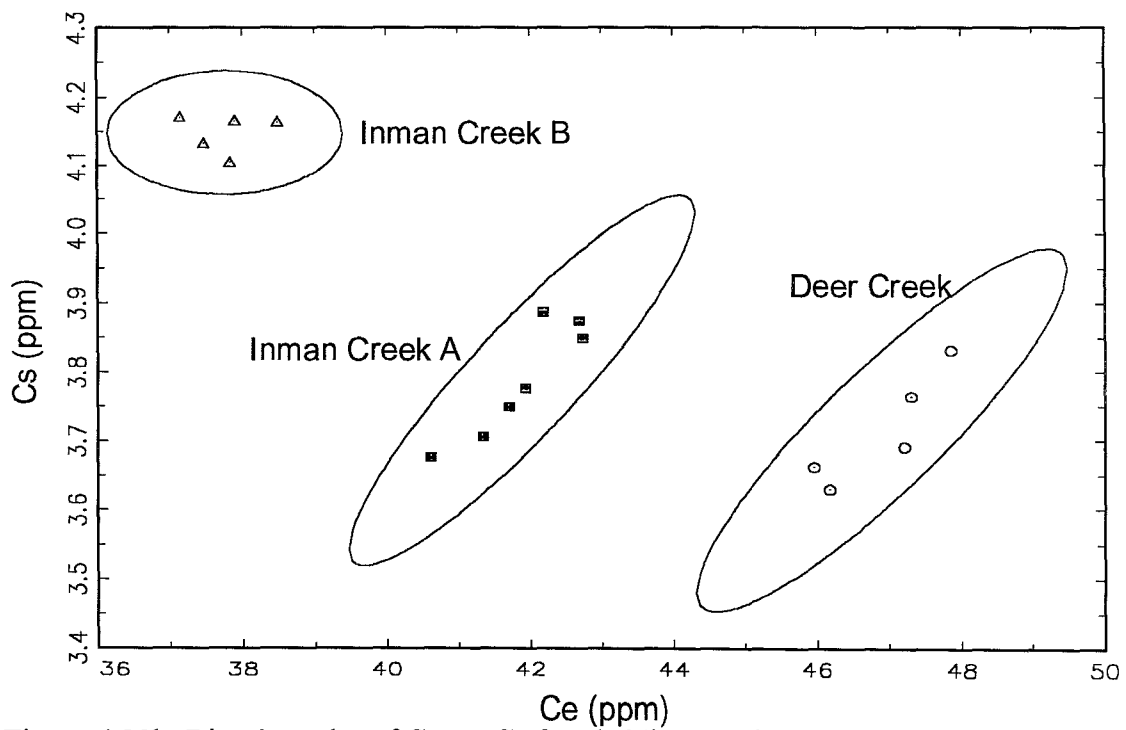


Figure 4.29b: Bivariate plot of Ce vs. Cs for obsidian specimens from Klamath and Lane counties.

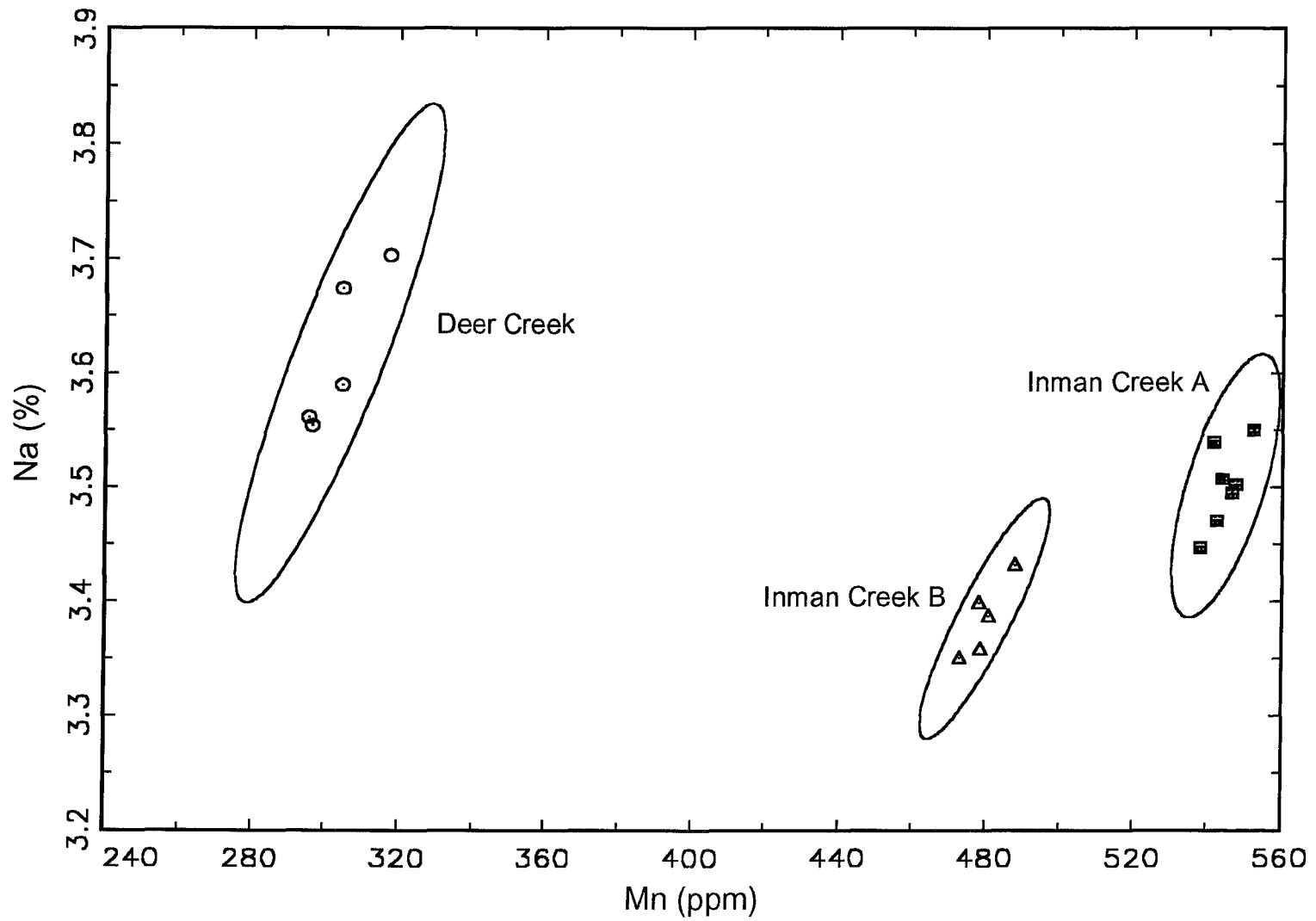


Figure 4.30: Bivariate plot of Mn vs. Na for obsidian specimens from Klamath and Lane Counties.

CHAPTER 5 APPLICATIONS

“Source characterization is a necessary first step in the reconstruction of ancient patterns of exploitation and distribution of obsidian or volcanic glass by humans” (Darling and Hayashida, 1995; p. 245). Previous sections of this thesis have provided that first step, at least partially, for obsidian studies in Oregon. Analysis of the data permitted the recognition of distinct chemical fingerprints for some 36 localized sources. In most cases, the chemically distinct sources are also separated geographically.

When archaeologists recover obsidian artifacts, the origin of the items is not known. Chemical characterization is a way to determine sources and thereby to monitor the interaction patterns of the site’s prehistoric inhabitants. But a problem may arise because the artifacts, when analyzed, may have to be compared to a potentially huge number of obsidian sources (e.g., in Oregon that number could be as high as 100-150). A potential solution to this problem is to group sources together on a regional basis. (In accord with the provenance postulate (Weigand *et al.*, 1977), these regional source groups should contain more variation between regions than within.) The archaeologist can then compare artifacts to these regional groups and discover which regions are most likely to have produced the artifacts. In this way, the archaeologist may be able to reduce the number of sources that must be compared and more rapidly determine the actual source of the artifact. Once regions have been discarded the archaeologist can “zoom in” on the remaining regions and identify which sub-regions or sources within those are the best “matches” to the artifacts. Finally, the archaeologist will be able to compare artifacts to highly specific source groups at the level discussed in the previous chapter.

Due to the large number of sources analyzed in this study, an attempt at organizing the sources on a regional basis was made. The regions were divided as follows. All of the Newberry Caldera groups were included in the "Newberry" regional group. All of the groups from the Ochoco National Forest were included in the "Ochoco" regional group. The groups Whitewater Ridge and Wolf Creek were included in the "Malheur" regional group. The Parish Cabin Campground samples were excluded because of their obvious differences. The groups Chickahominy Reservoir and Riley were included in the "Harney" regional group. Venator was not included in the Harney group because of the distance between it and the other sources. The groups Burns Area, Burns-Rimrock, and Dog Hill were included in the "Burns" regional group. All of the groups from Glass Buttes and all of the groups from Lake County except Surveyor Spring were included in the "Lake" regional group. Surveyor Spring was excluded because of the distance between it and the other sources. Deer Creek and the Inman Creek sources were not placed into regional groups because of their small size and small sampling area.

These regional groups were then graphed on bivariate plots to examine their similarities and differences. Unfortunately, a simple visual separation of the regional groups from one another was not attained. In this case, there tends to be more variation within the regional groups than between them, especially in the Lake, Harney, and Burns groups. This variation is partially due to the way these groupings were assigned. Although each of the three regional groups contains sources which are geographically close to each other, their chemical composition truly varies. This problem might be solved by careful selection of smaller regional groups or different clustering.

Despite the fact that the regional groups could not be separated visually, they were subjected to a posterior classification scheme. In this case, discriminant analysis was used to evaluate the distance between individual points and several centroids hypothesized to exist in the multi-dimensional space or hyperspace defined by the elemental concentrations (Bishop and Neff, 1989). The Mahalanobis distance from an unknown point (i.e., sample) to each of the alternative centroids (i.e., center of a particular regional group) provides criteria for evaluating the relative probabilities of membership of the sample in each of the groups (Bishop and Neff, 1989). The output of such a statistical analysis is in the form of a matrix showing which samples were placed into which groups as well as a list of each individual sample's probability of belonging to any of the groups.

In the analysis of the regional groups the samples were jackknifed. This means that an individual sample was excluded from the group it was in while it was being compared to that group. The groups were classified using concentrations for the following elements: La, Sm, Yb, Ce, Cs, Eu, Fe, Hf, Rb, Sc, Ta, Th, Mn, and Na. As shown in Table 5.1 although the regional groups could not be separated visually when only two dimensions at a time were inspected, they are reasonably well separated on a multivariate basis.

Table 5.1: Posterior classification matrix for regional groups in Oregon using elements from the long irradiation.

Regional Group	n	<i>Lake</i>	<i>Malheur</i>	<i>Burns</i>	<i>Harney</i>	<i>Ochoco</i>	<i>Newberry</i>
Lake	359	358		1			
Malheur	33		33				
Burns	31			31			
Harney	30				30		
Ochoco	107				1	106	
Newberry	48						48

There are two misclassifications. The sample HMOR04 was put into the Burns group from the Lake group and the sample RCROR01 was put into the Harney group from the Ochoco group. These are not serious problems. The probabilities of these samples being in either group were smaller than 0.001. These two samples are likely to simply be samples that differed just enough from their respective groups such that it can be difficult to determine where to put them. Examination of the raw data shows the samples to belong to their groups in spite of the misclassification by posterior classification.

Although the regional groups could not be separated from each other visually, an attempt was made to use bivariate plots to separate all the individual source groups. Figure 5.1 shows a bivariate plot of Cs vs. Hf. An examination of the graph will show separation between almost all of the groups. However, there are some groups which still overlap, including Inman Creek A and Glass Buttes F, Inman Creek B and Tucker Hill, Surveyor Spring and Glass Buttes D, East Lake and Game Hut Flow, Glass Buttes A and G, and Yreka Butte and Brooks Canyon.

A second bivariate plot of Cs vs. Sc eliminates the problem overlapping groups above (Figure 5.2). The Parish Cabin Campground A and B groups were excluded from this plot because their values for Sc are so high as to be “off-scale.” Although the second plot introduces some new groups which overlap (e.g., Riley and Glass Buttes D and

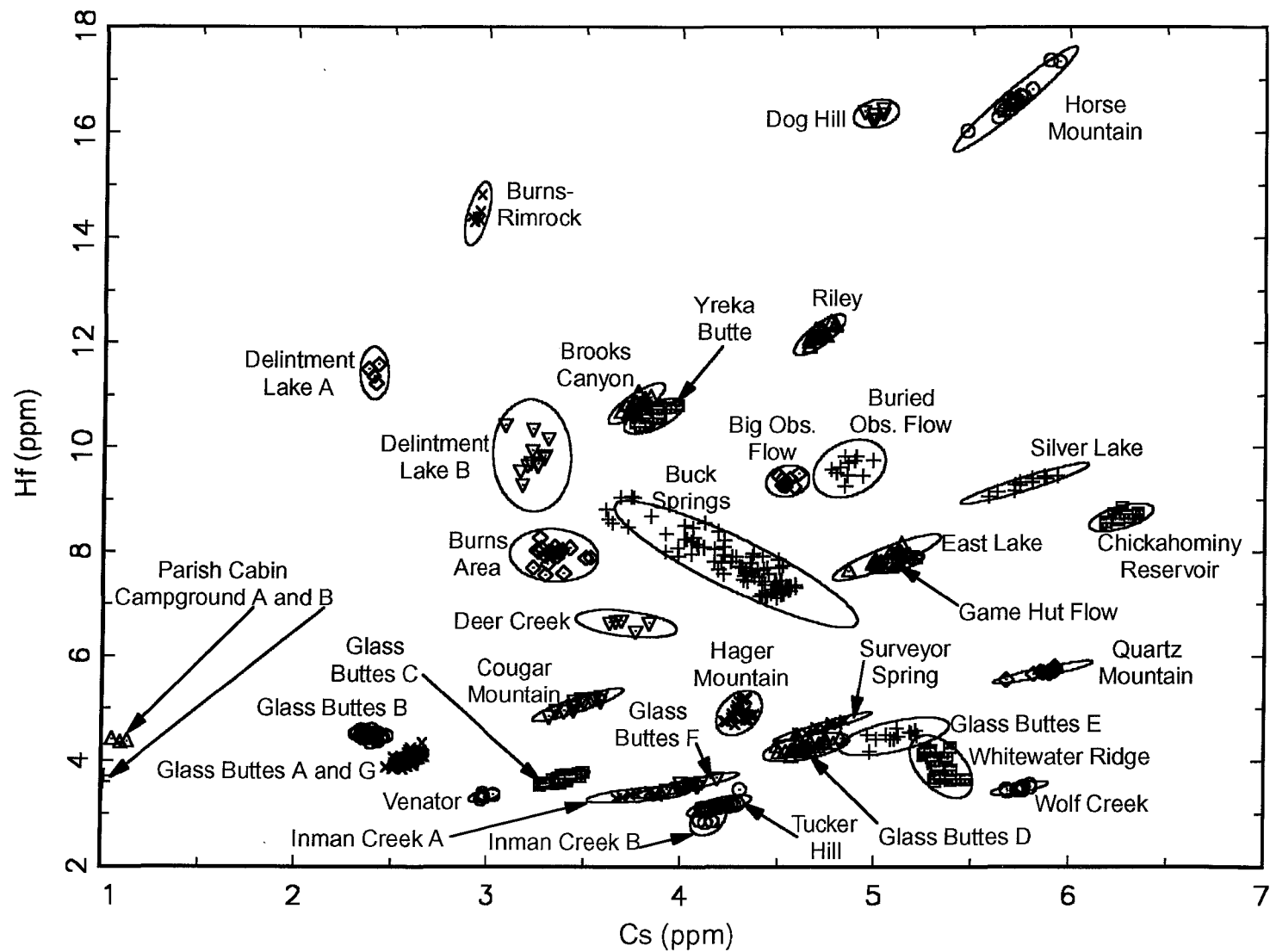


Figure 5.1: Bivariate plot of Cs vs. Hf showing separation of all obsidian sources analyzed in this study.

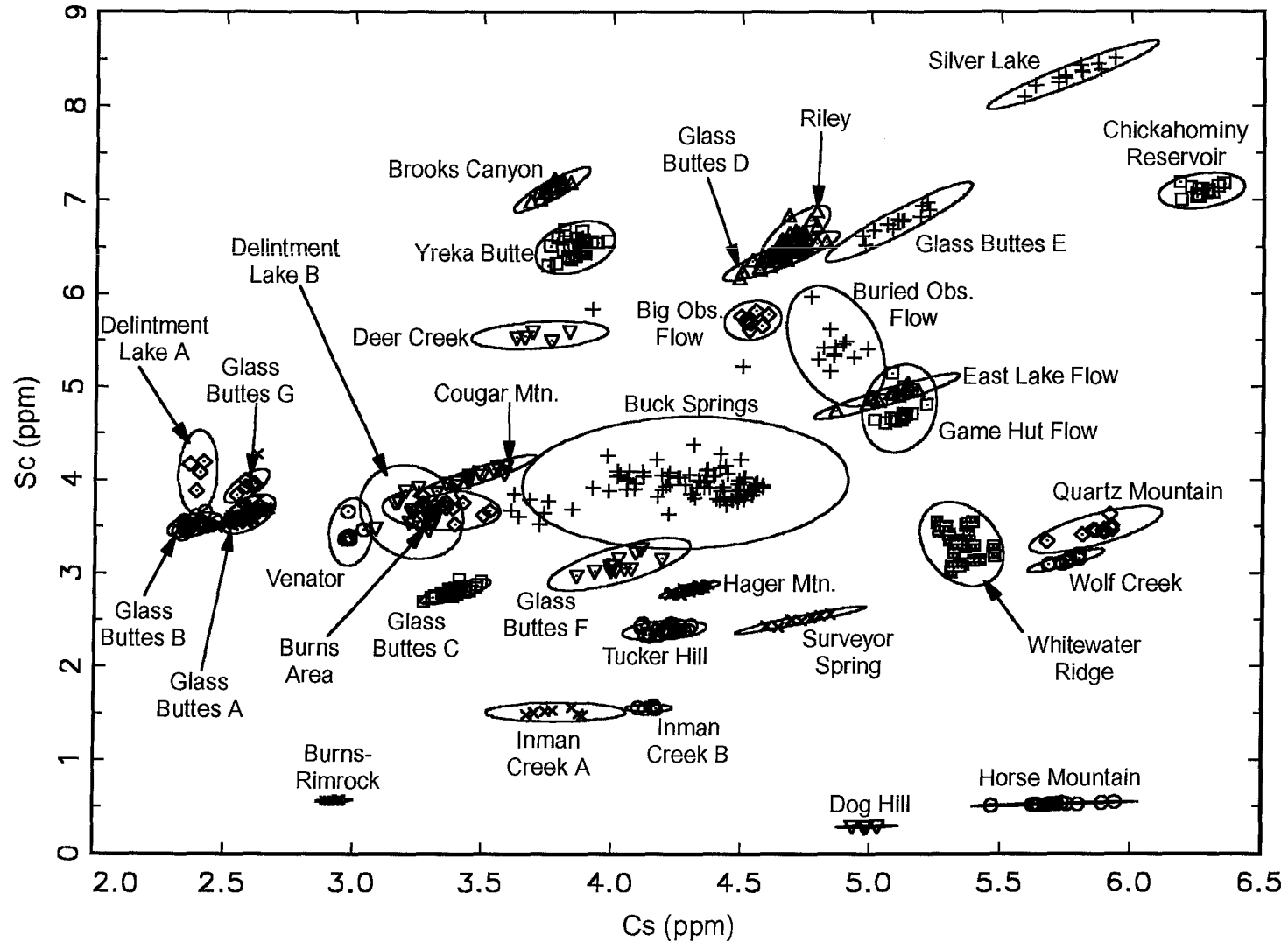


Figure 5.2: Bivariate plot showing separation of obsidian sources analyzed in this study. Parish Cabin Campground A and B are not shown because their element concentrations for Sc are off-scale.

Cougar Mountain, Delintment Lake B, and Burns Area), those groups do not overlap in Figure 5.1.

The only exceptions to the overlapping problem are the East Lake and Game Hut Flow groups. Although they overlap on both plots here they were easily separated in the section on Newberry Volcano (see Figures 4.25a, 4.25b, and 4.26). The East Lake and Game Hut Flow groups were also subjected to the posterior classification scheme that the regional groups were and the results indicated that each sample was in the correct group.

The regional groups were also subjected to analysis using only the elements from the abbreviated-NAA method. In this case, a visual separation of the regional groups could not be attained on the basis of bivariate plots alone. Because the groups could not be distinguished visually they were subjected to the same posterior classification scheme as described above.

Again the samples within the groups were jackknifed and the groups were classified using concentrations for the following elements: Ba, Cl, Dy, K, Mn, and Na. As shown in Table 5.2, although the elements from the short irradiation and count were not useful in separating the regional groups visually when only two dimensions were examined, they are reasonably well-separated by multivariate means.

Table 5.2: Posterior classification matrix for regional groups in Oregon using elements from the abbreviated-NAA method.

Regional Group	n	<i>Lake</i>	<i>Malheur</i>	<i>Burns</i>	<i>Harney</i>	<i>Ochoco</i>	<i>Newberry</i>
Lake	359	359					
Malheur	33	5	28				
Burns	31			31			
Harney	30	2			28		
Ochoco	107	1				106	
Newberry	48						48

The misclassifications in this set are more of a problem than the misclassifications in the previous one. There is one exception. The sample BWF006, which was placed into the Lake group from the Ochoco group, has a probability of less than 0.001 of being in either group. The other misclassifications, all into the Lake group, show probabilities of being in the Lake group ranging from 3.290 to 58.847. (It should be pointed out that their probabilities of belonging to the “correct” group were sometimes almost as high.) Therefore, caution should be used when trying to match artifacts to groups using the short elements, especially when working with the Malheur and Harney groups.

Although the regional groups could not be separated visually using the elements available from the abbreviated-NAA method, an attempt was made to use bivariate plots to separate all the individual source groups. A plot of Mn vs. Na is shown in Figure 5.3. Although it is messy, the degree of separation is fairly high. An attempt to clear up some of the overlapping groups was made with the creation of a plot of Ba vs. Mn (Figure 5.4). In this case all of the overlapping groups from Figure 5.3 were resolved except for Buck Springs and Delintment Lake B (their non-separation has already been discussed in the section on the Ochoco National Forest) and Cougar Mountain, Glass Buttes A, and Glass Buttes B. It is highly probable that elements from the long method would be required for a comparison of artifacts to any of these groups.

Future analysis of obsidian sources in Oregon should make the prospect of separating all the source groups even more interesting, and perhaps more difficult.

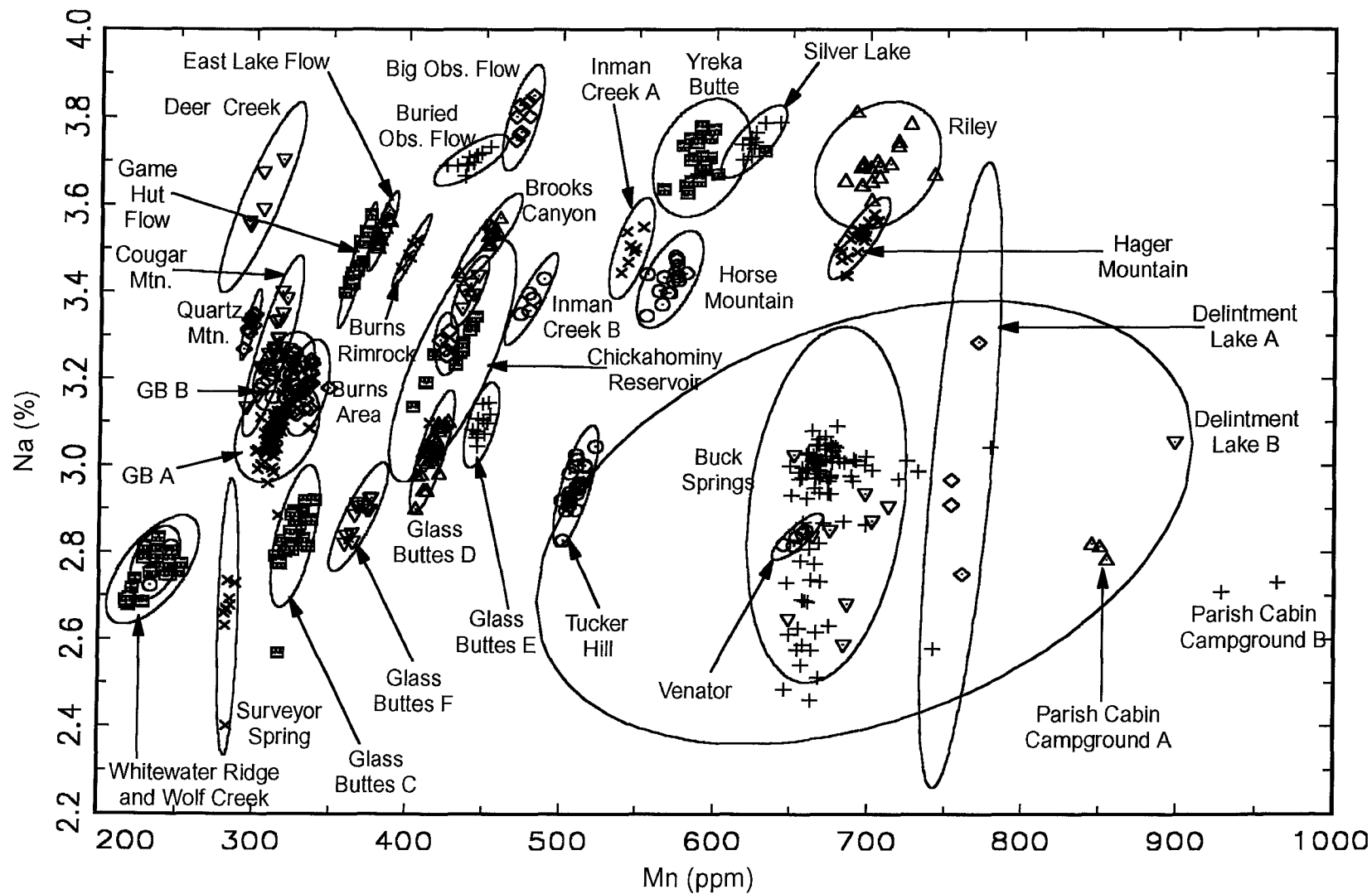


Figure 5.3: Bivariate plot of Mn vs. Na showing separation of obsidian sources analyzed in this study. Dog Hill and Glass Buttes G ellipses are within the Chickahominy Reservoir ellipse. GB = Glass Buttes.

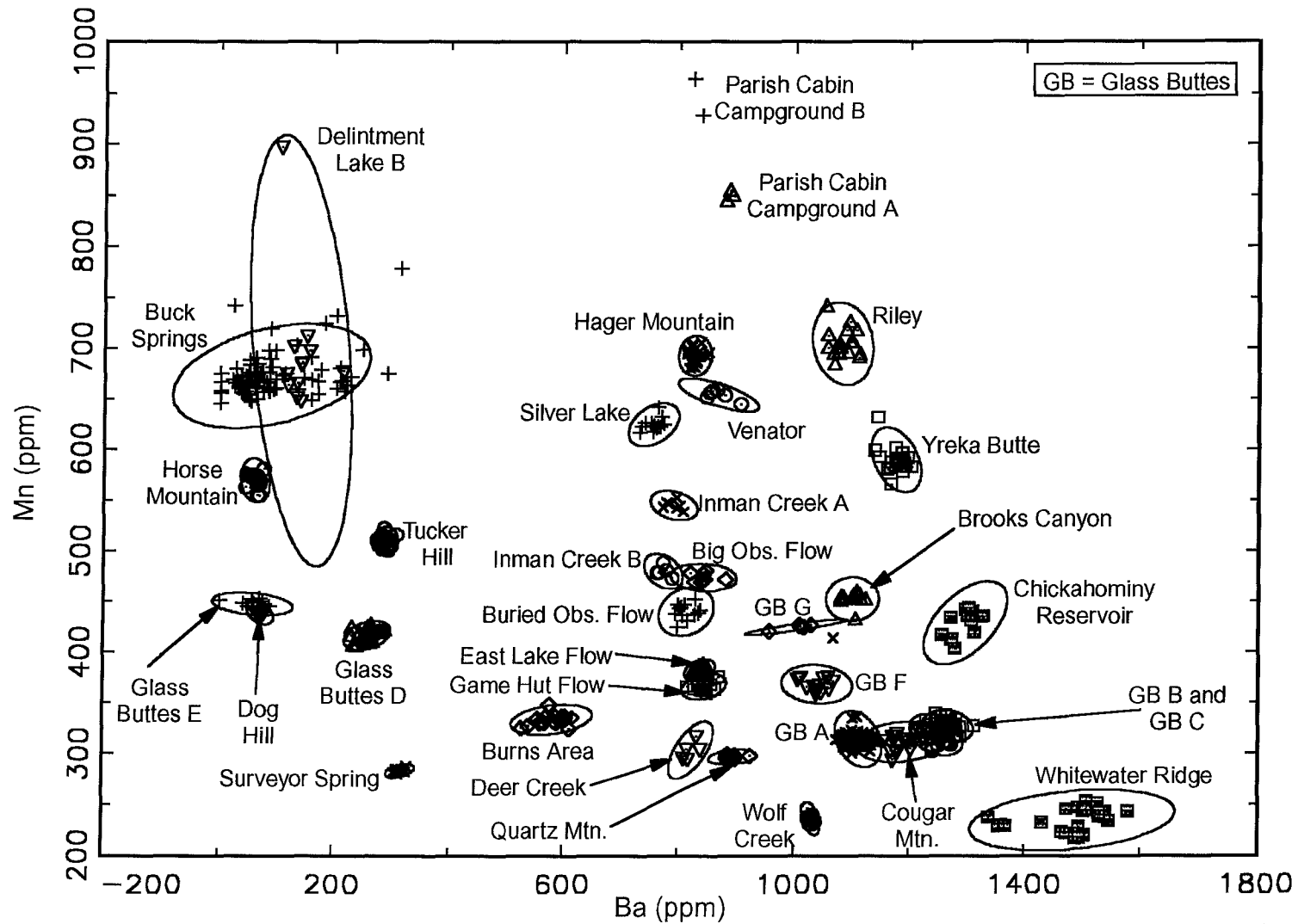


Figure 5.4: Bivariate plot of Ba vs. Mn showing separation of obsidian sources analyzed in this study. Burns-Rimrock is not shown because it is below the detection limit in barium. Delintment Lake A is not shown because it is off-scale in barium.

An Artifactual Case Study: Obsidian from the Robins Spring Site

Introduction

Thirty-one artifacts collected from the Robins Spring site were obtained from John Zancanella of the Oregon Bureau of Land Management. Robins Spring is an archaeological site located within the complex and near Glass Buttes proper as shown in Figure 4.17. The dimensions of the site are about 1.5 km north-south and 0.8 km east-west (Zancanella, 1997). A large hill to the east is the main source of the obsidian. Chipped stone covers most of the site and some ground stone is also present. Certain areas show more advanced production of bifaces; however, no diagnostic artifacts have been found. Unfortunately, the site investigation is still in progress and as yet, no intensive excavations have been undertaken.

The artifacts submitted for analysis comprise a random sample from across the site and were subjected to both short and long neutron activation analysis irradiations as explained earlier.

Results and Discussion

Once the fingerprints of the subsources at Glass Buttes were established, the data from the 31 artifacts were examined and compared with the source groups. In this case the artifacts were not compared to any of the regional groups because they came from a site on Glass Buttes and therefore the most likely area in which to begin a comparison is Glass Buttes. Using the elements Cs and Eu, as shown in Figure 5.5, all of the artifacts were assigned to subgroups from within the Glass Buttes complex, except one artifact which was assigned to the Yreka Butte source (an obsidian outcrop about 5-8 km west of Glass Buttes; see Lake County).

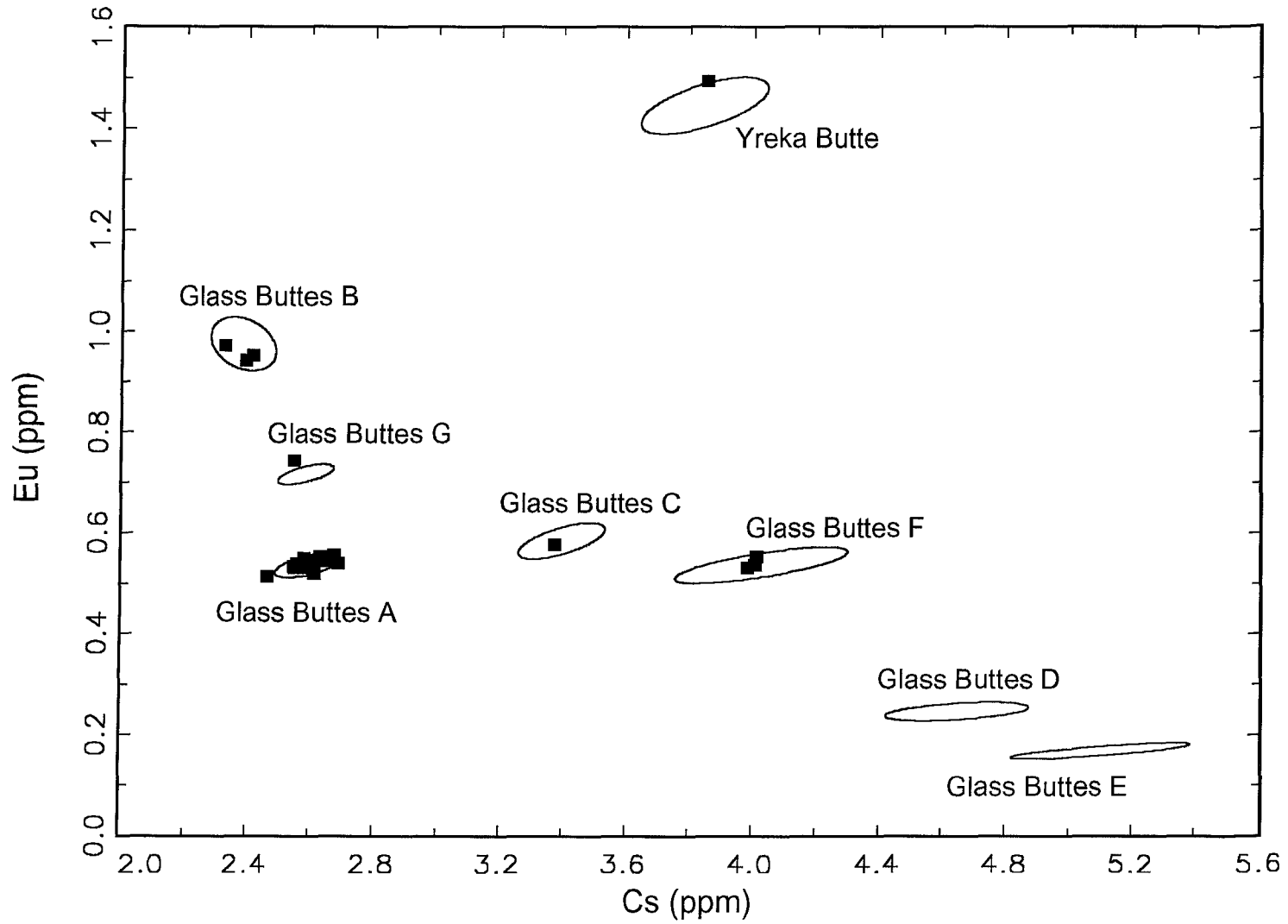


Figure 5.5: Bivariate plot showing projection of obsidian artifacts from the Robins Spring site onto 95% confidence ellipses of Glass Buttes and Yreka Butte chemical groups.

The artifacts were also successfully assigned to sources using the abbreviated-NAA method, i.e., using Mn and Na (see Figure 5.6). Although groups A and B overlap slightly, this is not a problem because, as mentioned earlier, they are significantly different for barium (1110 ppm and 1250 ppm, respectively).

The artifacts were compared to the source groups at Glass Buttes and Yreka Butte using the posterior classification scheme using the element concentrations from Cs, Eu, and Th. The results indicated that the artifact group assignments were mathematically sound and no mis-assignments occurred.

The Robins Spring site is just one small example of the possible application of this database. Hopefully, the database will receive more use in the future and become a valuable resource for archaeologists working in and around Oregon.

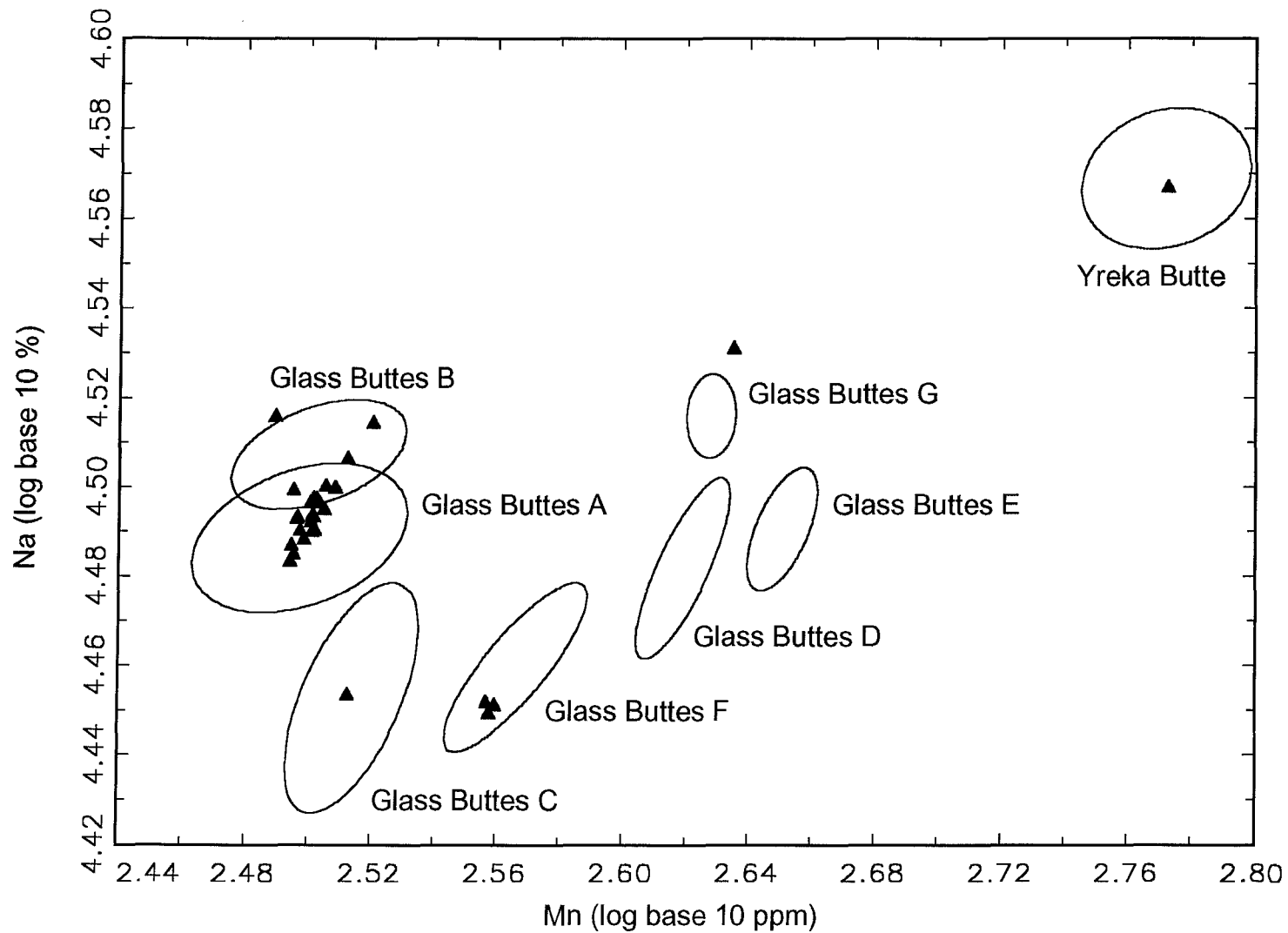


Figure 5.6: Bivariate plot for abbreviated-NAA method showing projection of obsidian artifacts from the Robins Spring site onto 95% confidence ellipses of Glass Buttes and Yreka Butte chemical groups.

CHAPTER 6 CONCLUSIONS

Obsidian is one of the best natural materials with which to make tools and weapons. Therefore, prehistoric people used obsidian extensively when it was available to them. Because each obsidian source is usually chemically homogeneous and geographically distinct, archaeologists can compare obsidian artifacts to obsidian sources to learn more about trade and exchange, raw material acquisition patterns, and interactions between different peoples. Oregon is an ideal area in which to study obsidian because of the large amount of silicic volcanism that has occurred there.

This thesis has presented an analysis of 667 obsidian source samples from throughout the state of Oregon. Using results from neutron activation analysis, the source samples were separated into 36 distinct chemical groups.

The data from the 667 source samples comprise only the beginning of an obsidian database for the state of Oregon. The use of the elemental data from the NAA technique resulted in the successful identification of 36 distinct chemical groups. The NAA technique has been proven to be superior to XRF in that NAA data can separate some chemical groups that are indistinguishable by XRF. The abbreviated-NAA method has also been shown to be useful, especially as a "first cut" before deciding whether to use the more expensive and time-consuming (but more accurate) long procedure.

The obsidian database and the success of the NAA technique lay the groundwork for further study in Oregon. Archaeologists now have the tools to be able to source artifacts made from Oregon obsidian with high accuracy and precision. The creation of a large database allows for a high success rate when trying to compare artifact data to the

possible sources. An archaeologist can now do better archaeology. For example, more accurately tracing patterns of past interaction should now be possible. Great strides have been made in the understanding of Oregon obsidian since this project began and even more progress is expected in the future.

Future Work

Although the 36 source groups identified in this thesis are some of the most important in Oregon, they probably comprise less than fifty percent of all the obsidian sources in Oregon. In order to provide the best source sample database for archaeologists working in Oregon more work needs to be accomplished. There are several areas covered in this thesis that need more intensive sampling due to their complexity or their inadequate sample numbers. The Rattlesnake Formation, from which we sampled only in the Ochoco National Forest, is one example of an extremely complex area. It may take years to understand fully the compositional variations of this ash-flow tuff. The area of the Malheur National Forest (another possible ash-flow tuff?) and Glass Buttes are two other examples of areas requiring more sampling. Glass Buttes is especially important because it is known to have been utilized heavily by prehistoric people. Inadequate sample size was a problem for both the Deer Creek and Inman Creek groups.

The obsidian sources of southeastern Oregon were fairly well covered by the work reported in this thesis. The few remaining obsidian sources in this area should be sampled and characterized. The northeastern and northwestern sections of Oregon are also important areas. Small portions of these sections have already been sampled but large tracts remain. The most important part of Oregon in which to sample obsidian is probably the Cascade Range and the gravel beds of the rivers which originate within the

mountains. The Cascade Range is important because it was a natural barrier between groups of people. An awareness of the obsidian sources in the Cascade Range will aid in an understanding of obsidian use and trade between prehistoric people living on either side.

The Oregon obsidian database is of little use unless it is utilized by the archaeologists for whom it was created. It would be beneficial to work with more archaeological collections in order to test the usefulness of the database. Also, collections containing artifacts that do not match an obsidian chemical group currently in the database could provide ideas as to where to look for more obsidian source areas. The absence of a matching source for an artifact may be due to many factors. For example, a local source may have been overlooked, the primary source of a secondary source has not been found, or the obsidian may have been traded in from an external source not yet known. Knowledge of a possible problem will assist in finding a solution.

The Oregon obsidian database developed by the Archaeometry Group at the Missouri University Research Reactor is the only database known to contain comprehensive neutron activation analysis data for sources in Oregon. The organization and extensiveness of the database should allow it to become a preferred choice for Oregon archaeologists wishing to analyze their obsidian artifacts. Although there is much work to accomplish in order to complete the database, this thesis has provided a good start.

BIBLIOGRAPHY

- Ambrose, W. R.; Duerden, P.; Bird, J. R. An Archaeological Application of PIXE-PIGME Analysis to Admiralty Islands Obsidians. *Nucl. Instrum. Methods* **1981**, *191*, 397-402.
- Anovitz, L. M.; Elam, J. M.; Riciputi, L. R.; Nolan, T. The Failure of Obsidian Hydration Dating: Sources, Implications, and Resolution. To be submitted for publication.
- Asaro, F.; Michel, H. V.; Burger, R. L. Major Sources of Ecuadorian Archaeological Obsidian and Provenience Assignment of Artifacts. *Lawrence Berkeley Laboratory Report LBL-13246*: Berkeley, CA, 1981.
- Asaro, F.; Salazar, E.; Michel, H. V.; Burger, R. L.; Stross, F. H. Ecuadorian Obsidian Sources used for Artifact Production and Methods for Provenience Assignments. *Latin American Antiquity* **1994**, *5*(3), 257-277.
- Bakken, B. Obsidian and its Formation. *Northwest Geology* **1977**, *6*(2), 88-93.
- Berri, D. A. Geology and Geothermal Alteration at Glass Buttes, Southeast Oregon. M. S. Thesis, Portland State University, 1982.
- Bird, J. R.; Russell, L. H.; Scott, M. D.; Ambrose, W. Obsidian Characterization with Elemental Analysis by Proton Induced γ -Ray Emission. *Anal. Chem.* **1978**, *50*(14), 2082-2084.
- Bishop, R. L.; Neff, H. Compositional Analysis in Archaeology. In *Archaeological Chemistry IV*; Allen, R. O., Ed.; American Chemical Society: Washington, DC, 1989; pp 57-86.
- Blundy, J. D.; Wood, B. J. Crystal-chemical Controls on the Partitioning of Sr and Ba between Plagioclase feldspar, Silicate Melts, and Hydrothermal Solutions. *Geochimica et Cosmochimica Acta* **1991**, *55*, 193-209.
- Bouey, P. D. Recognizing the Limits of Archaeological Applications of Non-destructive Energy-dispersive X-ray Fluorescence Analysis of Obsidians. *Mater. Res. Soc. Symp. Proc.* **1991**, *185*, 309-320.
- Bouska, V.; Borovec, Z.; Cimbalnikova, A.; Kraus, I.; Lajcakova, A.; Pacesova, M. *Natural Glasses*; Ellis Horwood: New York, 1993, 354 p.
- Bowman, H. R.; Asaro, F.; Perlman, I. Composition Variations in Obsidian Sources and the Archaeological Implications. *Archaeometry* **1973a**, *15*(1), 123-127.

- Bowman, H. R.; Asaro, F.; Perlman, I. On the Uniformity of Composition in Obsidians and Evidence for Magmatic Mixing. *J. Geology* **1973b**, *81*, 312-327.
- Brown, C. E.; Thayer, T. P. Geologic Map of the Canyon City Quadrangle, Northeastern Oregon. *U. S. Geological Survey Miscellaneous Investigations*; Map I-447; USGS: Denver, CO, 1966.
- Burton, J. H.; Krinsley, D. H. Obsidian Provenance Determination by Back-scattered Electron Imaging. *Nature* **1987**, *326*(9), 585-587.
- Cann, J. R.; Renfrew, C. The Characterization of Obsidian and its Application to the Mediterranean Region. *Proc. Prehistoric Soc.* **1964**, *30*(8), 111-133.
- Carlson, R. W.; Hart, W. K. Crustal Genesis on the Oregon Plateau. *J. Geophys. Res.* **1987**, *92*(B7), 6191-6206.
- Carmichael, I. S. E. Glass and the Glassy Rocks. In *The Evolution of the Igneous Rocks*; Yoder, Jr., H. S., Ed.; Princeton University: Princeton, NJ, 1979; pp 233-244.
- Cummings, M. L. Volcanic Stratigraphy of the Glass Buttes Complex, South-central Oregon. *Geological Society of America Abstracts with Programs* **1985**, *17*, 215.
- Cummings, M. L.; Roche, R. L. Volcanic Evolution of a Silicic Center astride the Brothers Fault Zone, the Glass Buttes Complex, Oregon. *Geological Society of America Abstracts with Programs* **1989**, *21*(5), 70.
- Darling, J. A.; Hayashida, F. M. Compositional Analysis of the Huitzila and La Lobera Obsidian Sources in the Southern Sierra Madre Occidental, Mexico. *J. Radioanal. Nucl. Chem., Articles* **1995**, *196*(2), 245-254.
- Dicken, S.N. *Oregon Geography*; Edwards Brothers: Ann Arbor, MI, 1950; pp 70-76.
- Drake, M. J.; Weill, D. F. Partition of Sr, Ba, Ca, Y, Eu^{2+} , Eu^{3+} , and other REE between Plagioclase feldspar and Magmatic Liquid: an Experimental Study. *Geochimica et Cosmochimica Acta* **1975**, *39*, 689-712.
- Diggles, M. F.; King, H. D.; Plouff, D.; Conrad, J. E.; Sawatzky, D. L.; Benjamin, D. A. Mineral Resources of the Guano Creek Wilderness Study Area, Lake County, Oregon. *U. S. Geological Survey Open-File Report 88-0297*; USGS: Denver, CO, 1988.
- Duerden, P.; Cohen, D. D.; Clayton, E.; Bird, J. R.; Ambrose, W.; Leach, B. F. Elemental Analysis of Thick Obsidian Samples by Proton Induced X-ray Emission Spectrometry. *Anal. Chem.* **1979**, *51*(14), 2350-2354.

- Ehmann, W. D.; Vance, D. E. *Radiochemistry and Nuclear Methods of Analysis*; John Wiley & Sons: New York, 1991, Chapter 9.
- Enlows, H. E. Rattlesnake Formation. In *Geologic Field Trips in Northern Oregon and Southern Washington*; Department of Geology and Mineral Industries Bulletin-Oregon, 1973; Vol. 77, pp 24-28.
- Enlows, H. E.; Parker, D. The Rattlesnake Ignimbrite Tongue. *Geological Society of America Abstracts with Programs* **1973**, 5(1), 38-39.
- Enlows, H. E. Petrography of the Rattlesnake Formation at the Type Area, Central Oregon. *Oregon Dept. of Geology and Mineral Industries* **1976**, 25, 1-34.
- Ericson, J. E. *Exchange and Production Systems in Californian Prehistory*; British Archaeological Reports International Series 110: Oxford, England, 1981.
- Ericson, J. E.; Makishima, A.; Mackenzie, J. D.; Berger, R. Chemical and Physical Properties of Obsidian: A Naturally Occurring Glass. *J. Non-Cryst. Solids* **1975**, 17, 129-142.
- Ericson, J. E.; Mackenzie, J. D.; Berger, R. Physics and Chemistry of the Hydration Process in Obsidians I: Theoretical Implications. In *Advances in Obsidian Glass Studies: Archaeological and Geochemical Perspectives*; Taylor, R. E., Ed.; Noyes: Park Ridge, New Jersey, 1976; pp 25-45.
- Findlow, F. J.; Ericson, J. E.; Bennett, V. C.; DeAtley, S. P. A New Obsidian Hydration Rate for Certain Obsidians in the American Southwest. *American Antiquity* **1975**, 40, 344-348.
- Friedman, I. I.; Smith, R. L. The Deuterium Content of Water in Some Volcanic Glasses. *Geochimica et Cosmochimica Acta* **1958**, 15, 218-228.
- Friedman, I.; Smith, R. L. A New Dating Method Using Obsidian: Part I, the Development of the Method. *American Antiquity* **1960**, 25, 476-522.
- Friedman, I.; Smith, R. L.; Long, W. D. Hydration of Natural Glass and Formation of Perlite. *Geol. Soc. Amer. Bull.* **1966**, 77, 323-328.
- Friedman, I. Hydration Dating of Volcanism at Newberry Crater, Oregon. *J. Res. U. S. Geological Survey* **1977**, 5(3), 337-342.
- Friedman, I.; Long, W. Volcanic Glasses, their Origins, and Alteration Processes. *J. Non-Cryst. Solids* **1984**, 67, 127-133.

- Frison, G. C.; Wright, G. A.; Griffin, J. B.; Gordus, A. A. Neutron Activation Analysis of Obsidian: An Example of its Relevance to Northwestern Plains Archaeology. *Plains Archaeologist* **1968**, *13*, 209-217.
- Gehr, K. D.; Newman, T. M. Preliminary Note on the Late Pleistocene Geomorphology and Archaeology of the Harney Basin, Oregon. *The Ore Bin* **1978**, *40*(10), 165-170.
- Gianque, R. D.; Asaro, F.; Stross, F. H.; Hester, T. R. High-precision Non-destructive X-ray Fluorescence Method Applicable to Establishing the Provenance of Obsidian Artifacts. *X-Ray Spectrometry* **1993**, *22*, 44-53.
- Glascock, M. D. Characterization of Archaeological Ceramics at MURR by Neutron Activation Analysis and Multivariate Statistics. In *Chemical Characterization of Ceramic Pastes in Archaeology*; Neff, H., Ed.; Prehistory: Madison, WI, 1992; pp 11-26.
- Glascock, M. D.; Anderson, M. P. Geological Reference Materials for Standardization and Quality Assurance of Instrumental Neutron Activation Analysis. *J. of Radioanal. Nucl. Chem., Articles* **1993**, *174*(2), 229-242.
- Glascock, M. D.; Neff, H.; Stryker, K. S.; Johnson, T. N. Sourcing Archaeological Obsidian by an Abbreviated NAA Procedure. *J. Radioanal. Nucl. Chem., Articles* **1994**, *180*(1), 29-35.
- Green, T. H.; Pearson, N. J. Effect of Pressure on Rare Earth Element Partition Coefficients in Common Magmas. *Nature* **1983**, *305*, 414-416.
- Green, T. H.; Pearson, N. J. Rare Earth Element Partitioning between Clinopyroxene and Silicate Liquid at Moderate to High Pressure. *Contrib. Mineral. and Petrol.* **1985**, *91*, 24-36.
- Greene, R. C.; Walker, G. W.; Corcoran, R. E. Geologic Map of the Burns Quadrangle, Oregon. *U. S. Geological Society Miscellaneous Investigations*; Map I-680; USGS: Denver, CO, 1972.
- Goffer, Z. *Archaeological Chemistry: A Sourcebook on the Applications of Chemistry to Archaeology*; John Wiley & Sons: New York, 1980; pp 31-53.
- Gordus, A. A.; Fink, W. C.; Hill, M. E.; Purdy, J. C.; Wilcox, T. R. Identification of the Geologic Origins of Archaeological Artifacts: An Automated Method of Na and Mn Neutron Activation Analysis. *Archaeometry* **1967**, *10*, 87-96.
- Gordus, A. A.; Wright, G. A.; Griffin, J. B. Obsidian Sources Characterized by Neutron-Activation Analysis. *Science* **1968**, *161*, 382-384.

- Hart, W. K.; Carlson, R. W. Tectonic Controls on Magma Genesis and Evolution in the Northwestern United States. *J. Volcanology and Geothermal Res.* **1987**, *32*, 119-135.
- Hildreth, W. Gradients in Silicic Magma Chambers: Implications for Lithospheric Magmatism. *J. Geophys. Res.* **1981**, *86*(B11), 10153-10192.
- Hughes, R. E. Aspects of Prehistoric Wiyot Exchange and Social Ranking. *J. California Anthropology* **1978**, *5*, 53-66.
- Hughes, R. E. Age and Exploitation of Obsidian from the Medicine Lake Highland, California. *J. Archaeological Science* **1982**, *9*, 173-185.
- Hughes, R. E. *Diachronic Variability in Obsidian Procurement Patterns in Northeastern California and Southcentral Oregon*; University of California: Berkeley, CA, 1986a; pp 311-322.
- Hughes, R. E. Energy Dispersive X-ray Fluorescence Analysis of Obsidian from Dog Hill and Burns Butte. *Northwest Science* **1986b**, *60*, 73-80.
- Hughes, R. E. The Coso Volcanic Field Reexamined: Implications for Obsidian Sourcing and Hydration Dating Research. *Geoarchaeology* **1988**, *3*(4), 253-265.
- Hughes, R. E. The Gold Hill Site: Evidence for a Prehistoric Socioceremonial System in Southwestern Oregon. In *Living with the Land: The Indians of Southwest Oregon*; Hannon, N.; Olmo, R. K., Eds.; Southern Oregon Historical Society: Medford, OR, 1990; pp 48-55.
- Hughes, R. E. Trace Element Geochemistry of Volcanic Glass from the Obsidian Cliffs Flow, Three Sisters Wilderness, Oregon. *Northwest Science* **1993**, *67*(3), 199-207.
- Hughes, R. E. Intrasource Chemical Variability of Artefact-Quality Obsidians from the Casa Diablo Area, California. *J. Archaeological Science* **1994**, *21*, 263-271.
- Hughes, R. E.; Smith, R. L. Archaeology, Geology, and Geochemistry in Obsidian Provenance Studies. In *Effects of scale on archaeology and geoscientific perspectives*; Stein, J.K.; Linse, A.R., Eds.; Geological Society of America Special Paper 283, 1993; pp 79-91.
- Huntley, D. J.; Bailey, D. C. Obsidian Source Identification by Thermoluminescence. *Archaeometry* **1978**, *20*(2), 159-170.
- Jensen, R. A. Explosion Craters and Giant Gas Bubbles on Holocene Rhyolite Flows at Newberry Crater, Oregon. *Oregon Geology* **1993**, *55*(1), 13-19.

- Johnson, M. Geology, Alteration, and Mineralization of a Silicic Volcanic Center, Glass Buttes, Oregon. M. S. Thesis, Portland State University, 1984
- Kilikoglou, V.; Bassiakos, Y.; Doonan, R. C.; Stratis, J. NAA and ICP Analysis of Obsidian from Central Europe and the Aegean: Source Characterisation and Provenance Determination. *J. Radioanal. Nucl. Chem.* **1997**, *216*(1), 87-93.
- Kimberlin, J. Obsidian Hydration Rate Determination on Chemically Characterized Samples. In *Advances in Obsidian Glass Studies: Archaeological and Geochemical Perspectives*; Taylor, R.E., Ed.; Noyes: Park Ridge, NJ, 1976; pp 63-80.
- Kuleff, I.; Djingova, R. Activation Analysis in Archaeology. In *Activation Analysis*; Alfassi, Z. B., Ed.; CRC: Boca Raton, FL, 1990; Vol. 2, pp 427-489.
- Laidley, R. A.; McKay, D. S. Geochemical Examination of Obsidians from Newberry Caldera, Oregon. *Contrib. Mineral. and Petrol.* **1971**, *30*(1), 336-342.
- Layton, T. N. Lithic Chronology in the Fort Rock Basin. *Tebiwa* **1972**, *15*, 1-21.
- Leach, B. F.; Warren S.; Fankhauser, B. Obsidian from the far north of New Zealand: a Method of Sourcing based on Natural Radioactive Emission. *New Zealand Journal of Science* **1978**, *21*, 123-128.
- Le Bas, M. J.; Le Maitre, R. W.; Streckeisen, A.; Zanettin, B. A Chemical Classification of Volcanic Rocks Based on the Total Alkali-Silica Diagram. *J. Petrology* **1986**, *27*(3), 745-750.
- Lund, E. H. Zoning in an Ash-flow of the Danforth Formation, Harney County, Oregon. *The Ore Bin* **1966**, *28*(9), 161-170.
- Macdonald, R.; Smith, R. L.; Thomas, J. E. Chemistry of the Subalkalic Obsidians. *U. S. Geol. Survey Prof. Paper 1523*; USGS: Denver, Colorado, 1992.
- MacLean, J. W. Geology and Geochemistry of Juniper Ridge, Horsehead Mountain, and Burns Butte: Implications for the Petrogenesis of Silicic Magma on the High Lava Plains, Southeastern Oregon. M. S. Thesis, Oregon State University, 1994.
- MacLeod, N. S.; Sherrod, D. R.; Chitwood, L. A.; McKee, E. H. Newberry Volcano, Oregon. *U. S. Geological Survey Circular 838*; USGS: Denver, CO, 1981.
- MacLeod, N. S.; Sherrod, D. R. The Magmatic System of Newberry Volcano, Oregon. In *Proceedings of the Workshop on Geothermal Resources of the Cascades*; Guffanti, M.; Muffler, L. J. P., Eds.; USGS: Reston, VA, 1985; Open-File Report 85-0521, pp 40-41.

- MacLeod, N. S.; Sherrod, D. R. Geologic Evidence for a Magma Chamber Beneath Newberry Volcano, Oregon. *J. Geophys. Res.* **1988**, *93*(B9), 10,067-10,079.
- MacLeod, N. S.; Sherrod, D. R.; Chitwood, L. A.; Jensen, R. A. Geologic Map of Newberry Volcano, Deschutes, Klamath, and Lake Counties, Oregon. *U. S. Geological Survey Misc. Investigations*; Map I-2455; USGS: Denver, CO, 1995.
- McDougall, J. M.; Tarling, D. H.; Warren, S. E. The Magnetic Sourcing of Obsidian Samples from Mediterranean and Near Eastern Sources. *J. Archaeological Science* **1983**, *10*, 441-452.
- McKee, E. H.; MacLeod, N. S.; Walker, G. W. Potassium-Argon Ages of Late Cenozoic Silicic Volcanic Rocks, Southeast Oregon. *Isochron/West* **1976**, *15*, 37-41.
- Merrick, H. V.; Brown, F. H. Rapid Chemical Characterization of Obsidian Artifacts by Electron Microprobe Analysis. *Archaeometry* **1984**, *26*(2), 230-236.
- Michels, J. W. Bulk Element Composition Versus Trace Element Composition in the Reconstruction of an Obsidian Source System. *J. Archaeological Science* **1982**, *9*, 113-123.
- Middlemost, E. A. K. *Magmas and Magmatic Rocks*; Longman: New York, 1985; pp 117-149.
- Mozzi, R. L.; Warren, B. E. The Structure of Vitreous Silica. *J. Appl. Crystallogr.* **1969**, *2*, 164-172.
- Nelson, D. E.; D'Auria, J. M.; Bennett, R. B. Characterization of Pacific Northwest Coast Obsidian by X-ray Fluorescence Analysis. *Archaeometry* **1975**, *17*(1), 83-97.
- Nielson, K. K.; Hill, M. W.; Mangelson, N. F.; Nelson, F. W. Elemental Analysis of Obsidian Artifacts by Proton Particle-Induced X-ray Emission. *Anal. Chem.* **1976**, *48*(13), 1947-1950.
- Parker, D. J. Petrology of Selected Volcanic Rocks of the Harney Basin, Oregon. Ph.D. Dissertation, Oregon State University, 1974.
- Philpotts, A. R. *Principles of Igneous and Metamorphic Petrology*; Prentice Hall: Englewood Cliffs, NJ, 1990; Chapters 4, 13.
- Pollard, A. M.; Heron, C. *Archaeological Chemistry*; The Royal Society of Chemistry: Cambridge, UK, 1996; Chapters 3, 5.
- Reeves, R. D.; Armitage, G. C. Density Measurements and Chemical Analysis in the Identification of New Zealand Archaeological Obsidians. *New Zealand Journal of Science* **1973**, *16*, 561-572.

- Robie, S. B.; Preiss, I. L. Investigation of Obsidian by Radioisotope X-ray Fluorescence. *Advances in X-ray Analysis* **1984**, *27*, 459-468.
- Roche, R. L. Stratigraphic and Geochemical Evolution of the Glass Buttes Complex, Oregon. M. S. Thesis, Portland State University, 1987.
- Rollinson, H. R. *Using Geochemical Data: Evaluation, Presentation, Interpretation*; Longman Group Limited: Singapore, 1993; Chapters 3, 4.
- Sarna-Wojcicki, A. M.; Champion, D. E.; Davis, J. O. Holocene Volcanism in the Conterminous United States and the Role of Silicic Volcanic Ash Layers in Correlation of Latest-Pleistocene and Holocene Deposits. In *Late-Quaternary Environments of the United States Volume 2: The Holocene*; Wright, Jr., H. E., Ed.; University of Minnesota: Minneapolis, 1983; pp. 52-77.
- Sato, J.; Sato, K. Gamma-ray Spectrometric Characterization of Volcanic Magmas. *Geochemical Journal* **1977**, *11*, 261-266.
- Shackley, M. S. Sources of Archaeological Obsidian in the Southwest: an Archaeological, Petrological, and Geochemical Study. *American Antiquity* **1988**, *53*(4), 752-772.
- Shackley, M. S. Early Hunter-gatherer Procurement Ranges in the Southwest: Evidence from Obsidian Geochemistry and Lithic Technology. PhD. Dissertation, Arizona State University, 1990.
- Skinner, C. E. Obsidian Studies in Oregon. M. A. Thesis, University of Oregon, 1983.
- Skinner, C. E. Northwest Research Obsidian Studies Laboratory, Corvallis, Oregon, unpublished data, 1997.
- Skinner, C. E. Northwest Research Obsidian Studies Laboratory, Corvallis, Oregon, personal communication, 1997.
- Skinner, C. E.; Winkler, C. J. Prehistoric Trans-Cascade Procurement of Obsidian in Western Oregon: A Preliminary Look at the Geochemical Evidence. In *Contributions to the Archaeology of Oregon: 1989-1994*; Baxter, P. W., Ed.; Association of Oregon Archaeologists Occasional Papers No. 5: Eugene, OR, 1994; pp 29-44.
- Smith, G.; Taylor, E.; Thormahlen, D.; Enlows, H. Three Newly Recognized Occurrences of Rattlesnake Ignimbrite in Central Oregon. *Proceedings of the Oregon Academy of Science* **1984**, *20*, 55.

- Stevenson, C. M.; Sheppard, P. J.; Sutton, D. G. Advances in the Hydration Dating of New Zealand Obsidian. *J. Archaeological Science* **1996**, *23*, 233-242.
- Stevenson, D. P.; Stross, F. H.; Heizer, R. F. An Evaluation of X-ray Fluorescence Analysis as a Method for Correlating Obsidian Artifacts with Source Location. *Archaeometry* **1971**, *13*(1), 17-25.
- Stewart, D. B. The Formation of Siliceous Potassic Glassy Rocks. In *The Evolution of the Igneous Rocks*; Yoder, Jr., H. S., Ed.; Princeton University: Princeton, NJ, 1979; pp 339-350.
- Streck, M. J. Element Gradients in the High-silica Rhyolites and Dacites from the Rattlesnake Tuff, Southeastern Oregon. *Geological Society of America Abstracts with Programs* **1992**, *24*(5), 83.
- Streck, M. J.; Grunder, A. L. Crystallization and Welding Variations in a Widespread Ignimbrite Sheet; the Rattlesnake Tuff, Eastern Oregon, USA. *Bull. Volcanol.* **1995**, *57*, 151-169.
- Toepel, K. A.; Sappington, R. L. Obsidian Use in the Willamette Valley: Trace Element Analysis of Obsidian from the Halverson Site. *Tebiwa* **1982**, *19*, 27-40.
- Walker, G. W. Possible Fissure Vent for a Pliocene Ash-flow Tuff, Buzzard Creek Area, Harney County, Oregon. *U. S. Geol. Survey Prof. Paper 650-C* **1969**, C8-C17.
- Walker, G. W. Cenozoic Ash-flow Tuffs of Oregon. *The Ore Bin* **1970**, *32*(6), 97-115.
- Walker, G. W. Some Implications of Late Cenozoic Volcanism to Geothermal Potential in the High Lava Plains of South-central Oregon. *The Ore Bin* **1974**, *36*(7), 109-119.
- Walker, G. W.; Peterson, N. V.; Greene, R. C. Reconnaissance Map of the East Half of the Crescent Quadrangle, Lake, Deschutes, and Crook Counties, Oregon. *U. S. Geological Survey Misc. Investigations*; Map I-493; USGS: Denver, CO, 1967.
- Waters, A. A Structural and Petrographic Study of the Glass Buttes, Lake County, Oregon. *J. Geology* **1927**, *35*, 441-452.
- Weigand, P. C.; Harbottle, G.; Sayre, E. V. Turquoise Sources and Source Analysis: Mesoamerica and the Southwestern U. S. A. In *Exchange Systems in Prehistory*; Earle, T. K.; Ericson, J. E., Eds.; Academic: New York, 1977; pp 15-34.
- Wheeler, M. E.; Clark, D. W. Elemental Characterization of Obsidian from the Koyukuk River, Alaska, by Atomic Absorption Spectrophotometry. *Archaeometry* **1977**, *19*(1), 15-31.

Williams-Thorpe, O.; Thorpe, R. S. The Distribution and Sources of Archaeological Pitchstone in Britain. *J. Archaeological Science* **1984**, *11*, 1-34.

Williams-Thorpe, O. Review Article: Obsidian in the Mediterranean and the Near East: a Provenancing Success Story. *Archaeometry* **1995**, *37*(2), 217-248.

Wilson, J. L.; Emmons, D. L. Tucker Hill Perlite Deposit, Lake County, Oregon. *Mining Engineering* **1985**, *37*(11), 1301-1308.

Zancanella, J. Oregon Bureau of Land Management, Prineville, Oregon, personal communication, 1997.